Davidson Laboratory
Marine Hydrodynamics,
Coastal & Ocean Engineering

STEVENS
INSTITUTE of TECHNOLOGY
THE INNOVATION UNIVERSITY
1870

Castle Point on Hudson,
Hoboken, NJ 07030

TECHNICAL REPORT NO. 325

May, 1947

Model Tests on a Standard Series of Flying-Boat Hulls

by

Albert Strumpf

Prepared For:

Bureau of Aeronautics, Department of the Navy

TR-325

EXPERIMENTAL TOWING TANK
STEVENS INSTITUTE OF TECHNOLOGY

REPORT NO. 325

PART I

MODEL TESTS ON A STANDARD SERIES OF FLYING-BOAT HULLS

by

Albert Strumpf

HOBOKEN, NEW JERSEY
MAY, 1947

Experimental Towing Tank
Stevens Institute of Technology
Hoboken, New Jersey

MODEL TESTS ON A STANDARD SERIES OF FLYING-BOAT HULLS

by

Albert Strumpf

PART I

Prepared for the
Bureau of Aeronautics
Navy Department

May 1947

Report No. 325

TABLE OF CONTENTS

Page

PART I

TABLE OF CONTENTS (continued)

SUMMARY

This report presents data, together with some discussion, on the effects of length-beam ratio, afterbody angle, and deadrise angle upon the main spray, resistance, porpoising and static properties of flying-boat hull models.

Information which was available prior to the outset of the investigation indicated that these hull-shape variables had important effects on most hydrodynamic characteristics. Explorations with radiating patterns of models indicated that main spray, resistance and longitudinal stability were the principal characteristics for which systematic information was most needed. This need was substantiated by full-size experience.

The model tests were made by the "general" methods described in previous reports and included ranges of load and speed which were shown by past analyses to be thoroughly practical.

The test results show that:

1) Increasing length-beam ratio does not materially affect the hydrodynamic characteristics of flying-boat hulls when the hulls are compared with equivalent loading conditions on the basis of constant length^2-beam products.

2) Increasing afterbody angle, for the most part, helps the longitudinal stability characteristics, but is detrimental to the hump speed resistance and to the main spray configuration at moderate displacement speeds. The range of afterbody angles tested embrace an optimum afterbody angle at which minimum spray heights can be obtained at low displacement speeds. The static trims and drafts are increased with afterbody angle, the increase in static trims being approximately equal to one-half the increase in afterbody angle (measured in degrees), and the increase in static draft coefficient being about equal to the increase in afterbody angle (measured in radians).

The best afterbody angle must reflect, essentially, a compromise of these hydrodynamic considerations.

3) Increasing deadrise angle increases the resistance appreciably at planing speeds and lowers the peaks of the main spray blisters at moderate displacement and hump speeds. Both the upper and lower longitudinal stability limits are raised by increasing the deadrise angle from 10° to 30°. Extremely low (0° to 10°) and high (40°) deadrise angles tend to develop regions with no stable trim angles. Increasing deadrise angle increases the static draft, and tends to decrease the static trim. The increase in the static draft coefficient is approximately equal to the number of degrees increase in deadrise divided by 200.

4) There is a close relationship between the effects of afterbody angle and deadrise angle because both variables have a considerable effect on trim. Increasing deadrise angle has little effect on the main spray heights at low displacement speeds, but the higher the afterbody angle, the lower the speed at which a given increase in deadrise angle will cause a reduction in spray height. The effect of deadrise angle on hump resistance is also dependent upon afterbody angle. With low afterbody angles, i.e. 5°, the hump resistance increases with increase in deadrise angle; with high afterbody angles, i.e. 9°, the hump resistance decreases with increase in hull deadrise. Low afterbody angles combined with either low or high deadrise angles intensify the tendency of these deadrise angles to develop completely unstable trim regions.

INTRODUCTION

The principal objective of this investigation was to establish a broad background of fundamental information relating to the design of flying-boat hulls by means of experiments utilizing a Standard Series of models. The Series was developed and the model hulls tested at the Stevens Experimental Towing Tank in accordance with Contract NOa(s)-560 with the Bureau of Aeronautics, Navy Department.

Over a period of several years, work had been done on limited series of hull models (some of which is reported in References 1, 2, 3, 4, 5, and 6) in order to arrive at a point in development where there would be reasonable assurance that a Standard Series program on flying-boat hulls would produce useful results. In general, these investigations were either concerned with the effect of only one shape variable or only one hydrodynamic performance characteristic. Each series usually had a different parent and a different method of altering the hull lines. By July 1943, it was believed that sufficient progress had been made to justify a start on a Standard Series program.

Since the outstanding characteristic of a Standard Series lies in the fact that changes of different variables are combined to make a multi-dimensional model "grid" pattern, it can easily be seen that if the variables are not severely limited, the number of models necessary would make the series prohibitive in extent. It is apparent that corresponding limitations must also be made of the hydrodynamic properties to be investigated. Accordingly, in the current Standard Series of flying-boat hull models, the investigation is made of the effect of three hull shape variables on four hydrodynamic characteristics. The hull shape variables are length-beam ratio, afterbody angle and deadrise angle; the hydrodynamic characteristics are main spray, resistance, longitudinal stability, and static properties.

In this report, the more obvious conclusions are enumerated without too much elaboration. Further analysis of the test results would undoubtedly reveal additional trends.

- - - - - - - - - - - - - -

The report is presented in two parts, bound separately. Part One contains all final summary charts, discussions and conclusions, together with material needed in reading the report. Part Two also contains the summary charts, in addition to the moment data and static properties charts.

It should be noted that the preliminary test data charts which were issued in Reference 7 have, in some instances, been revised and are presented here in final form.

SCOPE

Some knowledge of the relative influence of a reasonably large number of variables must be acquired before laying out a Standard Series which will establish a broad structure of quantitative information. In this preparatory work, the number of models can be effectively restricted by treating each variable individually in a radiating pattern.

Preliminary studies of this sort were made using the XPB2M-1 hull as the parent and investigating resistance, porpoising, main spray, bow spray, and yawing characteristics (References 1, 2, 8, 9, and 10). Since these tests and full-size experience seemed to indicate that resistance, porpoising, and main spray were the principal characteristics upon which systematic information was most needed, the present Standard Series work was limited to a consideration of those three characteristics and, in addition, static properties.

The research on the radiating pattern of models also indicated that the following hull-shape variables seemed to have the largest effects on resistance, porpoising, and main spray characteristics:

1) hull length-beam ratio,
2) sternpost or afterbody angle,
3) hull deadrise (in terms of deadrise at the main step),
4) forebody warping (after portion of the bottom).

In order to limit the number of variables included in the Standard Series, only the first three were considered, with the understanding that the program be expanded only when completed work showed this need. Many other important variables (such as step depth, afterbody warping and chine flare, forebody-afterbody proportion, step ventilation and step planform, to mention a few) had to be omitted to avoid an overwhelming multiplicity of models.

There was no guarantee that the preliminary experiments with radiating patterns of models did not overlook a very influential

GRID OF THE MODELS TESTED

Deadrise Angle, deg.	L/b	Afterbody Angle, deg. 3	5	7	9	11
0	5.07 6.19 7.32 8.45	556		532		557
10	5.07 6.19 7.32 8.45		610 604 624 695	533	611 605 625 696	
20	5.07 6.19 7.32 8.45	573 536 626 693	537	339-22 $\boxed{591}$ * 339-23 651	538	574 539 627 694
30	5.07 6.19 7.32 8.45		612 606 628 697	534	613 607 629 698	
40	5.07 6.19 7.32 8.45	558		535		559

* $\boxed{591}$ is a model of the XPB2M-1 and is the parent of the Series.

Note: The hulls in the Series are designated on the grid by their Stevens model numbers.

combination of variables. Therefore, the final program of models for the Series was arranged so that changes of more than one hull-shape variable were combined in the form of a multi-dimensional grid pattern. The grid pattern included five combinations of dead-rise angle, five combinations of afterbody angle, and four combinations of length-beam ratio — making a total of 4 x 5 x 5, or 100, models. As the tests progressed, it was found that adequate results could be obtained if over half this number of models was omitted. The chart on the facing page is a grid of the models tested.

Since it was found that the models in the extreme corners of the grid had serious deficiencies in one or more of the characteristics investigated, not too much emphasis was placed on these regions of the grid. Instead, the program was adjusted to place more emphasis on the region in the vicinity of the parent, Model No. 591.

Throughout the report, the models are designated by their combination of hull variables, so that the XPB2M-1 parent (Stevens Model No. 591) is designated "6.19-7-20", where the length-beam ratio is 6.19, the afterbody angle is 7°, and the deadrise at the main step is 20°.

The models of different length-beam ratio are considered to be hulls of constant length^2-beam products under one airplane superstructure. If the length-beam ratio is changed simply by increasing the length of the hull, it is apparent that the higher length-beam ratio hulls will be able to carry more load. In order to set up a suitable size relationship between the varying length-beam ratio hulls, it is assumed that the load carrying ability of all the models is the same if their length^2-beam products are constant (Reference 11).

The 1/30 scale model of the XPB2M-1 parent has a gross weight of 6.07 pounds, a beam of 5.40 inches, and a length-beam ratio of 6.19. The lengths and beams of the four different length-beam ratio hulls considered, together with other pertinent model design information, are tabulated at the top of page 33 on a constant length^2-

beam basis. This table would represent the test conditions and model particulars if all the hulls had been built to the same scale ratio. All the hulls on this basis have the same aerodynamic tail damping rate, M_q/V, as is shown. The longitudinal radii of gyration, K, of the hulls will only change as a result of changes in overall lengths. In computing the overall length, L_{OA}, it should be noted that only the hull length forward of the center of gravity is effective in increasing the L_{OA} and, consequently, the radius of gyration, K. The drawing on page 34 shows the dimensions, in terms of beam, of the various length-beam ratio hulls as determined on a constant L^2b basis.

The set of figures at the bottom of page 33 are the actual dimensions and particulars of the models at constant beam as used in the tests.

The equations and assumptions governing the choice of values in the table are noted.

The ranges of loading coefficient and getaway speed coefficient for the various length-beam ratio hull models were selected from an analysis of past practice (Reference 12). This analysis includes many varied types of flying-boat hulls and seaplane floats, which gives some assurance that a thoroughly practical range of coefficients is covered in the present Standard Series tests. The ranges used in the tests are listed below:

L/b		5.07	6.19	7.32	8.45
Ranges of C_{Δ_o}	High	1.00	1.40	2.00	2.77
	Mean	0.70	1.00	1.50	2.00
	Low	0.40	0.60	1.00	1.23
Ranges of C_{V_g}	High	10.2	11.0	11.6	12.3
	Mean	6.5	7.0	7.4	7.8
	Low	4.7	5.0	5.3	5.6

The pertinent charts for finding the test ranges of loading coefficient and getaway speed coefficient are reproduced on pages 35 and 36.

APPARATUS AND PROCEDURE

The apparatus and procedures used in conducting "general" porpoising, resistance and main spray tests at the Experimental Towing Tank have been described previously in References 1, 8, 9, 13, and 14.

At the inception of the investigation, all flying-boat hull tests were made in the 100-foot towing basin designated Tank No. 1. The equipment ordinarily used in this tank could not be utilized for the models having the two higher length-beam ratios because these models required loadings beyond a reasonable limit for the apparatus. In addition, it was impossible to obtain the required high speeds. Therefore, until extended test facilities became available, work was concentrated on the models having the two lower values of length-beam ratio.

When the new 300-foot tank, designated Tank No. 3, was completed, it was employed immediately for the tests which required either high speeds or heavy loadings. The equipment used in each of the tanks is essentially the same, except that the Tank No. 3 apparatus can be adapted for a greater variety of tests without making complicated conversions.

The static properties tests were made using either the Tank No. 1 or Tank No. 3 apparatus. The model was pivoted at its center of gravity, and the waterborne load was gradually increased until the model shipped water. The trims and drafts corresponding to each waterborne load were determined.

The center of gravity was located the same distance forward of the main step and the same distance above the forebody keel for all the models. The values used for the center of gravity position were:

35 percent of the beam forward of the main step and
90 percent of the beam above the forebody keel.

This location was chosen because it assured reasonable moment-trim relationships in the planing range (Reference 13).

The mass in vertical oscillation for each length-beam ratio was based upon the information used to determine its test range of loading. In each case, the mass in vertical oscillation used was the nominal gross weight of the flying-boat, this corresponded to the mean values of load coefficients given on page 8.

Appreciable scatter was noticed in the results of the early resistance tests. It was inferred that these discrepancies were due to irregularities in the boundary layer between the water and the boat, and that better results could be obtained with induced turbulence. Accordingly, an attachment was rigged to the towing carriage so that a strut, 0.040 inches in diameter, could be towed in the water immediately in front of the model to insure turbulent flow. The use of the strut produced more consistent resistance measurements which were slightly higher than those obtained without the strut. All of the tests reported here were made with the strut.

MODELS

The familiar hull of the XPB2M-1 flying boat was selected as the parent of the series. A parent hull form whose hydrodynamic characteristics were known was chosen so that the results for the numerous other hull forms could be viewed in proper perspective. The body plans of the 1/30 scale XPB2M-1 hull model are given on page 31.

All the models were built to the same beam, 5.40 inches, the length-beam ratio being altered by multiplying the station spacing of the parent model by a constant. The forebody stations were moved along lines parallel to the forebody keel at the main step; the afterbody stations were shifted along lines parallel to the after-body keel of the parent form. The step depth was the same, 0.27 inches, for all models.

Afterbody angles were changed by rotating the afterbody with respect to the forebody about the intersection of the afterbody keel and the main step, the tail cone being rotated with the after-body. Since the forebody-afterbody proportions and step-depth are the same for all the models, the sternpost angle varies with the length-beam ratio even if the afterbody angle is constant.

The hull deadrise was varied by adding a constant angle to the deadrise at each station of the parent. This procedure was adopted in order to avoid the large changes in deadrise near the bow which would occur if a constant multiplyer had been applied to the deadrise at each station.

Except at the bow, the keel profile and chine plan of all the models were the same as the parent's. The bow was sharper for the hulls with deadrise angles at the main step greater than 20° and blunter for the hulls with deadrise angles at the main step less than 20°. The chine heights above the keel were established for each model by multiplying the height of chine above the keel at each station of the parent model by the ratio of the deadrise angles. The points of tangency of the chine flare curves were

unaltered with varying deadrise angle. Hence, the chine flare curves were drawn with smaller radii of curvature for the models with high deadrise angles than for the models with the low deadrise angles. The zero degree deadrise hulls did not have any chine flare on either the forebody or afterbody.

When the length-beam ratio was altered, changes in variables resulting from expanding or contracting the forebody and afterbody were not eliminated. With regard to this, it should be noted that the parent form has a fully warped forebody bottom extending back to the main step.

The amount of warping for the other models was varied directly with changes in length, so that forebody warping, which was not taken into account but which is known to have independent effects on the hydrodynamic properties, may have produced small variations of its own.

The body plans and profile drawings for each model tested are shown, at reduced scale, at the top of the appropriate static properties chart, pages 133 through 170 of Part II.

NOTATION

The following notation and nondimensional coefficients are used:

Load coefficient,	$C_\Delta = \Delta / wb^3$
Speed coefficient,	$C_V = V/\sqrt{gb}$
Resistance coefficient,	$C_R = R/wb^3$
Trimming-moment coefficient,	$C_M = M/wb^4$
Longitudinal spray coefficient,	$C_X = X/b$
Lateral spray coefficient,	$C_Y = Y/b$
Vertical spray coefficient,	$C_Z = Z/b$
Draft coefficient,	$C_d = d/b$
Length-beam ratio,	L/b

where,

Δ = load on water, pounds

w = specific weight of water, pounds per cubic foot (62.3 for these tests)

b = beam at main step, feet

V = velocity, feet per second

g = acceleration of gravity, 32.2 feet per second per second

R = resistance, pounds

M = trimming moment, pound-feet

X = longitudinal position of main spray point of tangency to the spray blister envelope with reference to the main step, feet

Y = lateral position of main spray point of tangency to the spray blister envelope, measured from the hull center-line, feet

Z = vertical position of main spray point of tangency to the spray blister envelope, measured from the tangent to the forebody keel at the main step, feet

d = draft of keel at main step, feet

L = length of hull from forepoint to sternpost, feet

Trim (τ) is the angle between the tangent to the forebody keel at the main step and the horizontal.

Moment data are referred to the center of gravity, and water trimming moments which tend to raise the bow are considered positive.

PRESENTATION OF RESULTS

The spray, resistance and longitudinal stability characteristics of each model are presented in the form of one-sheet "Summary Charts" on pages 57 through 94. (These same Summary Charts are also included in Part II, pages 57 through 94.) Each summary chart is divided into three sections. In the uppermost section, the model body plans and main spray data are given. In the center section, the free-to-trim trim and resistance data are given for the displacement speed range, and in the bottom section, the resistance data for the planing range and the longitudinal stability limits are shown.

The spray data are plotted in terms of the three coordinates of the envelope, C_X, C_Y, and C_Z. In order to collapse the data, C_X and C_Y are divided by $C_\Delta^{1/3}$ and C_Z is divided by C_Δ (Reference 14). These ordinates ($C_X/C_\Delta^{1/3}$, $C_Y/C_\Delta^{1/3}$ and C_Z/C_Δ) are plotted against $C_V^2/C_\Delta^{1/3}$, a form of the Froude number.

The displacement speed resistance and trim data are plotted in the form C_R/C_Δ and τ against $C_V^2/C_\Delta^{1/3}$, with C_Δ as a parameter. Since the displacement speed resistance, trim and spray data are all plotted with the same abscissa scale, the data can be compared directly.

The resistance data for planing speeds are presented in the form of constant $\sqrt{C_R}/C_V$ contours plotted on a grid of trim angle versus $\sqrt{C_\Delta}/C_V$. The contours show the variation with trim angle when $\sqrt{C_\Delta}/C_V$ is fixed, as well as the values of trim angle and $\sqrt{C_R}/C_V$ for minimum resistance at a particular value of $\sqrt{C_\Delta}/C_V$.

The upper and lower longitudinal stability limits are superimposed on the resistance contours, and are plotted in the form of τ versus $\sqrt{C_\Delta}/C_V$ (Reference 15). When testing in the planing range, the stability limits were determined first, in order that the high speed resistance tests could be confined, for the most part, to the stable range of trim angles.

Moment data are presented in Part II, pages 95 through 132. The moment coefficient (C_M) is plotted on a τ versus $\sqrt{C_\Delta}/C_V$ grid. Because the scatter of data indicates that for a constant value of trimming moment, the trim angle is not a function of $\sqrt{C_\Delta}/C_V$, curves are not drawn through the moment data. They could, however, be sketched in to give an approximate indication of the moment spread. The load and speed coefficients are noted wherever data were obtained.

The static properties charts in Part II, pages 133 through 170, show how the draft coefficient (C_d) and trim (τ) vary with load coefficient (C_Δ), with zero moment. These charts also include the body plans and profile drawings for each model tested.

DISCUSSION

As is pointed out in the Scope on page 7 , the concept behind the treatment of the hulls in this series is that each of the models is considered as a variation of hull form to be used under one airplane structure. For convenience in testing, all the models are constructed with the same beam at the main step, 5.40 inches. This does not, however, alter the original assumption: that the load carrying ability of all the hulls be considered the same when their length^2-beam products are constant. (This is summarized numerically in the table on page 33.)

For this series of hulls, the constant length^2-beam basis is used in practically all comparisons. Actually, this will only affect the comparison of hulls with differing length-beam ratio, and means that the effects of the other shape variables will be shown on a specific, dimensional basis. For the specific comparisons, all the models were assumed to have a gross weight of 6.07 lb. and a getaway speed of 26.62 ft./sec. The parabolic unloading curve used is shown on page 37. By making the comparisons on a specific basis, the effects of each of the variables are made as distinct as possible. This is especially true for the resistance comparisons where no suitable method has yet been devised to present the data on one collapsed nondimensional plot throughout the complete speed range.

An exception to the specific basis of comparison are the charts showing the effect of afterbody angle and hull deadrise on the longitudinal stability limits. The stability limits are compared on a nondimensional basis because it is felt that the effects of these particular shape variables on the porpoising characteristics will not be clarified materially by making the comparison on a specific basis. In addition to this, the lower limit porpoising results in the transition region just below planing speeds are valid only for the loads and speeds at which they were tested. The lift supplied by the water in this vicinity is partly buoyancy and the data obtained do not collapse. The load and speed at which each

stability limit point was found may be obtained from the moment data charts in Part II, pages 95 through 132.

Effect of Varying Length-Beam Ratio

Since the forebody-afterbody proportions and step depth are the same for all the models, the sternpost angle varies with length-beam ratio even if the afterbody angle is constant. Therefore, the length-beam ratio comparisons will be affected, to some extent, by an additional variable, sternpost angle. The models chosen for the comparison are:

Model No.	Designation	Actual Sternpost Angle
339-22	5.07-7-20	8.25
591	6.19-7-20	8.00
339-23	7.32-7-20	7.90
651	8.45-7-20	7.80

The chart comparing the resistance, trimming and porpoising characteristics of these hulls with equivalent loading conditions on the constant L^2b basis is shown on page 38. The main spray comparison is shown on page 39, together with two other length-beam ratio, main spray comparisons. The two additional length-beam ratio, spray comparisons utilize models with 3° and 11° afterbody angles; they are made because the first comparison leaves some doubt as to the actual effect of hull fineness on main spray characteristics.

If the hulls are compared with equivalent loading conditions on the basis of constant length^2-beam products, variation of length-beam ratio produces the following effects:

1) There is a tendency for the high speed resistances to decrease with increasing length-beam ratio. This inclination, however, is not marked.

2) The magnitude of the hump resistance is not altered appreciably with increase in length-beam ratio, but the hump is shifted to higher speeds.

3) The resistance and trim at speeds below the hump is decreased with increase in length-beam ratio.

4) The stable range of trim angles is reduced with increasing length-beam ratio. This reduction is due mostly to increase in the lower stability limit trims.

5) The changes in main spray height caused by varying hull fineness are inconsistent but, in general, are not large. The indication is that length-beam ratio differences do not materially alter the main spray configuration.

6) Comments: The major detrimental effect of high length-beam ratio hulls is the reduction of the stable trim range. It has been indicated in a previous investigation (Reference 16) that a greater moment spread between porpoising limits could be obtained with high length-beam ratio hulls, especially at speeds near take-off. This series, however, does not indicate any material increase in stable moments with increase in length-beam ratio.

Effect of Varying Afterbody Angle

Because the step depth and forebody-afterbody proportions are constant for all the hulls of the series, variation of afterbody angle can, in general terms, be called direct variation of sternpost angle. The sternpost angles for all the models used in the comparisons are tabulated on page 32.

To determine the effects of afterbody angle on the hydrodynamic characteristics, one group of models with varying afterbody angle are chosen for comparison from each of the four length-beam ratio groups. The models chosen all have a deadrise angle of 20°.

1)	Model No. 573	5.07-3-20
	Model No. 339-22	5.07-7-20
	Model No. 574	5.07-11-20

2)	Model No. 536	6.19-3-20
	Model No. 537	6.19-5-20
	Model No. 591	6.19-7-20
	Model No. 538	6.19-9-20
	Model No. 539	6.19-11-20
3)	Model No. 626	7.32-3-20
	Model No. 339-23	7.32-7-20
	Model No. 627	7.32-11-20
4)	Model No. 693	8.45-3-20
	Model No. 651	8.45-7-20
	Model No. 694	8.45-11-20

The comparison charts are shown on pages 40 through 45. The effect of varying afterbody angles on the static properties is illustrated by the comparisons on pages 46 through 49.

If the deadrise angle, step depth and loading conditions are held constant, variation of afterbody angle within any one length-beam ratio group produces the following effects:

1) The resistance and trim at displacement speeds increases with increasing afterbody angle.

2) The hump trim and hump resistance increases with increasing afterbody angle. The increase in hump trim is approximately equal to the amount that the afterbody angle is increased.

3) The resistance at planing speeds (when the afterbody is clear) is not affected by changes in afterbody angle.

4) The peaks of the main spray blisters are, in general, raised with increasing afterbody angle. This is true primarily at moderate displacement and hump speeds where the spray pattern is extremely sensitive to trim. At low displacement speeds, there is a tendency for the main spray heights to be first lowered then raised with increasing afterbody angle. In other words, there is

an optimum afterbody angle (or trim) for minimum spray heights at low displacement speeds. This U-shaped effect can be shown by the curves on page 45 where the spray height at 5.40 inches forward of the main step is plotted against afterbody angle (which reflects trim). (It is assumed that the model propellers are located 5.40 inches forward of the step.) The tendency of the length-beam ratio 5.07 hulls toward the U-shaped effect is more clearly demonstrated at positions further forward (lower speeds) than 5.40 inches forward of the main step. This is shown by the curves on the lower portion of page 45, where spray height versus afterbody angle is plotted for positions 8.0 inches and 12.0 inches forward of the main step.

5) The longitudinal stability limits are, in general, widened with increasing afterbody angle. Increasing afterbody angle raises the upper stability limits and causes the lower stability limits to occur at higher trims and at lower speeds.

6) The static trims and drafts are raised with increase in afterbody angle. The increase in static trims is approximately equal to one-half the afterbody angle increase, in degrees, and the increase in the static draft coefficient is about equal to the afterbody angle increase, in radians. In other words,

if $\Delta\tau$ = increase in static trim with afterbody angle increase,

$\Delta\theta$ = increase in afterbody angle,

ΔC_d = increase in static draft coefficient,

then

$$\Delta\tau = \frac{\Delta\theta}{2}$$

and

$$\Delta C_d = \frac{\Delta\theta}{57.3}.$$

The effect of afterbody angle on the static properties

are shown by the comparison charts on pages 46 through 49, where the static draft coefficient and static trim are plotted against load coefficient for four groups of hulls on a 5.40 inch beam basis.

7) Comments: The afterbody angle for best main spray, resistance, and longitudinal stability characteristics must be, essentially, a compromise between the angles best for these hydrodynamic characteristics when each is considered individually. The spray and resistance are, for the most part, worsened by increasing afterbody angle. The longitudinal stability limits are improved by increasing afterbody angle.

Effect of Varying Deadrise Angle

The effects of varying deadrise angle on the hydrodynamic characteristics were determined by comparing the results for three different groups of models. All have the same length-beam ratio, 6.19, but three groups of afterbody angle, 5°, 7°, and 9°, are considered. The complete range of deadrise angle, 0°, 10°, 20°, 30°, and 40°, are covered only in the comparison of models with 7° afterbody angle. It was felt that more weight should be placed on the less extreme values of deadrise angle, since, as can be seen from the results, the 0° and 40° deadrise models are obviously inferior to the models with intermediate deadrise angles with regard to at least one hydrodynamic characteristic investigated (i.e., porpoising, high-speed resistance).

The hydrodynamic characteristics of the following three groups of models are compared:

1)	Model No. 604	6.19-5-10
	Model No. 537	6.19-5-20
	Model No. 606	6.19-5-30

2) Model No. 532 6.19-7-0
Model No. 533 6.19-7-10
Model No. 591 6.19-7-20
Model No. 534 6.19-7-30
Model No. 535 6.19-7-40

3) Model No. 605 6.19-9-10
Model No. 538 6.19-9-20
Model No. 607 6.19-9-30

The comparison charts are shown on pages 50 through 53. The effect of varying deadrise angle on the static properties is shown by the comparisons on pages 54 through 56.

Comparison of the results for the three groups of models at equivalent loading conditions indicate the following effects due to variation of deadrise angle:

1) The free-to-trim track is affected by changes in hull deadrise in three recognizable patterns, depending upon the speed range considered. At very low displacement speeds, the free-to-trim track is lowered as the deadrise angle is increased, though the effect of deadrise variation is small. From the moderate displacement speed region to speeds slightly beyond the hump, increase in deadrise angle causes a considerable decrease in the free-to-trim trims. At high (planing) speeds, a sudden reversal of trend in the zero moment trim track occurs. Here, increase in deadrise angle causes an increase in the zero moment trims. The velocity at which this sudden reversal in trend occurs is very nearly constant (regardless of afterbody angle); for the loading conditions used in these comparisons it is about 15.5 ft./sec.

2) At the very low displacement speeds where deadrise variation results in relatively small trim changes, the peaks of the main spray blisters are not influenced greatly by

increase in hull deadrise. At moderate displacement speeds, increase in deadrise angle lowers the main spray height. The 0° deadrise hulls, however, do not fit into the pattern. This is not surprising since the 0° deadrise hulls differ from the other hulls; they have no chine flare, the forebody being, for all practical purposes, all forebody flat. The 40° deadrise hulls also seem to behave erratically, as far as spray is concerned, indicating higher spray peaks than the other hulls at low speeds.

If the 10°, 20°, and 30° deadrise hulls only are considered, three general conclusions can be reached with regard to the effect of deadrise on the main spray blister:

a) Increasing the deadrise angle does not affect the peaks of the main spray blisters appreciably at very low speeds.

b) At moderate displacement and hump speeds, increasing deadrise angle lowers the peaks of the main spray blisters.

c) The speed at which increase in deadrise angle results in a noticeable decrease in spray height seems to vary with afterbody angle — the higher the afterbody angle, the more quickly (the lower the speed) the effect of increased deadrise angle becomes appreciable. This is because spray height is affected by trim, which is in turn a function of afterbody angle.

3) The effect of deadrise angle on hump resistance seems to be dependent upon afterbody angle. With low afterbody angles, i.e. 5°, the hump resistance increases with increase in deadrise angle; with high afterbody angles, i.e. 9°, the hump resistance decreases with

increase in hull deadrise.

4) The resistance at planing speeds (where the effect of deadrise angle is not dependent upon afterbody angle) increases abruptly and appreciably with increase in deadrise angle. The velocity at which this sudden increase in resistance occurs is about the same as the speed at which the sudden reversal of trend in the free-to-trim track occurs, about 15.5 ft./sec. for the loading conditions used.

5) Both the upper and lower longitudinal stability limits tend to be raised by increasing the deadrise angle from 10° to 30°. The models with very low deadrise angles, i.e., 0° and 10°, have the property of developing a completely unstable trim region near the low speed end of the stability limits. This is especially true when the low deadrise angles are combined with low afterbody angles. The models with very high deadrise angles, i.e. 40°, have the characteristic of developing completely unstable trim regions at the high speed end near take-off — again, especially when coupled with low afterbody angles.

6) Increasing the deadrise angle increases the static drafts and tends to decrease the static trims.

If $\Delta\beta$ is the increase in deadrise angle, and ΔC_d is the increase in static draft coefficient,

then

$$\Delta C_d = \frac{\Delta\beta}{200} \,.$$

The effects of deadrise angle on the static properties are shown by the comparison charts on pages 54 through 56, where the static draft coefficient and static trim are plotted against load coefficient for three groups of hulls on a 5.40 inch beam basis.

7) Comments: There is a close connection between afterbody angle and deadrise angle variation because both of these shape variables have a very appreciable effect on trim. In most instances, increasing afterbody angle and deadrise angle independently of each other produces opposite effects. At displacement speeds, increasing afterbody angle raises trim, while increasing deadrise angle lowers trim; increasing afterbody angle, for the most part, increases spray height, whereas increasing deadrise angle reduces spray height.

It would be advantageous if higher values of deadrise angle could be used in conventional flying-boat hull design, because with high deadrise angles very considerable reductions can be obtained in landing impact loads and main spray heights. The maximum limit of deadrise angle cannot, however, be increased very greatly over the present design values without seriously jeopardizing longitudinal stability and high speed resistance characteristics. The deadrise angles for satisfactory longitudinal stability characteristics alone are severely limited to a range from 20° to 30°.

CONCLUSIONS

The results of tank tests to determine the effects of varying three design parameters of conventional flying-boat hulls — length-beam ratio, afterbody angle, and hull deadrise — lead to the following conclusions:

1) When hulls of varying length-beam ratio are compared on the basis of equivalent loading for constant length^2-beam products, increasing hull fineness does not introduce any large detrimental effects on the hydrodynamic properties studied. This investigation does indicate, however, that increasing length-beam ratio reduces the stable range of trims.

2) Increasing afterbody angle increases the free-to-trim resistance and trim from displacement speeds up to speeds where the afterbody is clear. The increase in trim at hump speed is approximately equal to the amount that the afterbody angle is increased. The peaks of the main spray blisters are raised at moderate displacement speeds and hump speeds with increase in afterbody angle. At low displacement speeds and at one location on the hull, there is an optimum afterbody angle (or trim) for minimum spray heights. Increasing afterbody angle widens the stable range of trims by raising the upper limit and causing the lower limit to occur at higher trims and at lower speeds. The static trims and drafts are raised with afterbody angle, the increase in static trims being equal to about one-half the afterbody angle increase in degrees, and the increase in static draft coefficient being equal to about the afterbody angle increase in radians.

3) Increasing deadrise angle lowers the free-to-trim track from displacement speeds to speeds just beyond the hump,

and appreciably raises it at planing speeds. The resistance at planing speeds is increased considerably with increase in deadrise angle. Both the upper and lower longitudinal stability limits are raised by increasing deadrise angle from 10° to 30°. The extreme values of deadrise angle (0°, 10°, and 40°) have the property of developing completely unstable trim regions, the low deadrise angles near the low speed end of the stability limits and the high deadrise angles at the high speed end near take-off. Increasing deadrise angle from 10° to 30° does not affect the peaks of the main spray blisters at very low displacement speeds, but lowers the main spray peaks at moderate displacement and hump speeds. Increasing deadrise angle increases the static drafts and tends to decrease the static trims. The increase in static draft coefficient is approximately equal to the deadrise angle increase divided by 200.

4) Several combined effects of afterbody angle and deadrise angle were noted. The speed at which increase in deadrise angle causes any pronounced decrease in spray height is a function of afterbody angle: the higher the afterbody angle, the lower the speed at which the effect of deadrise angle becomes apparent. The effect of deadrise angle on hump resistance is also dependent upon afterbody angle: low afterbody angles cause an increase in hump resistance with increase in deadrise angle, while high afterbody angles cause a decrease in hump resistance with increase in hull deadrise. Low afterbody angles combined with either low or high deadrise angles intensify the tendency of these deadrise angles to develop completely unstable trim regions.

REFERENCES

1. Locke, F.W.S., Jr., and Bott, H.L.: "A Method for Making Quantitative Studies of the Main Spray Characteristics of Flying-Boat Hull Models", N.A.C.A. ARR No. 3K11, November 1943.

2. Locke, F.W.S., Jr.: "Some Systematic Model Experiments of the Bow-Spray Characteristics of Flying-Boat Hulls Operating at Low Speeds in Waves", N.A.C.A. ARR No. 3L04, 1943.

3. Davidson, Kenneth S.M., and Locke, F.W.S., Jr.: "General Tests on the Hydrodynamic Characteristics of Four Flying Boat Models of Differing Length-Beam Ratios", N.A.C.A. ARR 4F15, June 1944.

4. Shoemaker, James M., and Parkinson, John B.: "Tank Tests of a Family of Flying-Boat Hulls", N.A.C.A. TM No. 491, 1934.

5. Bell, J.W., Garrison, C.C., and Zeck, Howard: "Effect of Length-Beam Ratio on Resistance and Spray of Three Models of Flying-Boat Hulls", N.A.C.A. ARR No. 3J23, 1943.

6. Sottorf, W.: "The Design of Floats", N.A.C.A. TM No. 860, 1938.

7. Hugli, W.C., and Wright, C.A.: "Progress Report of Model Tests on Standard Series of Hull Models", E.T.T. Report No. 268, October 1, 1944.

8. Locke, F.W.S., Jr.: "General Resistance Tests on Flying-Boat Hull Models", N.A.C.A. ARR No. 4B19, February 1944.

9. Davidson, K.S.M., and Locke, F.W.S., Jr.: "Some Systematic Model Experiments on the Porpoising Characteristics of Flying-Boat Hulls", N.A.C.A. ARR No. 3F12, June 1943.

10. Locke, F.W.S., Jr.: "Some Yawing Tests of a 1/30 Scale Model of the Hull of the XPB2M-1 Flying Boat", N.A.C.A. ARR No. 3G06, July 1943.

11. Davidson, Kenneth S.M.: "Notes on Flying Boat Loadings", E.T.T. Note No. 5, April 1944.

12. Locke, F.W.S., Jr.: "A Correlation of the Dimensions, Proportions, and Loadings of Existing Seaplane Floats and Flying-Boat Hulls", E.T.T. TM No. 62, July 1942.

13. Locke, F.W.S., Jr.: "General Porpoising Tests of Flying-Boat Hull Models", N.A.C.A. ARR No. 3I17, September 1943.

14. Locke, F.W.S., Jr.: "'General' Main Spray Tests of Flying-Boat Models in the Displacement Range", N.A.C.A. ARR No. 5A02, April 1945.

15. Davidson, Kenneth S.M., and Locke, F.W.S., Jr.: "Some Analyses of Systematic Experiments on the Resistance and Porpoising Characteristics of Flying-Boat Hulls", N.A.C.A. ARR No. 3I06, September 1943.

16. Hugli, W.C., Jr., Strumpf, Albert, and Axt, W.C.: "An Investigation of the Effects of Hull Proportion and Step Depth on the Hydrodynamic Characteristics of Flying-Boat Hull Models with Varying Length-Beam Ratios", E.T.T. Report No. 312, February 1947.

BODY PLAN OF PARENT
XPB2M-1
STEVENS MODEL NO. 591
L/b = 6.19

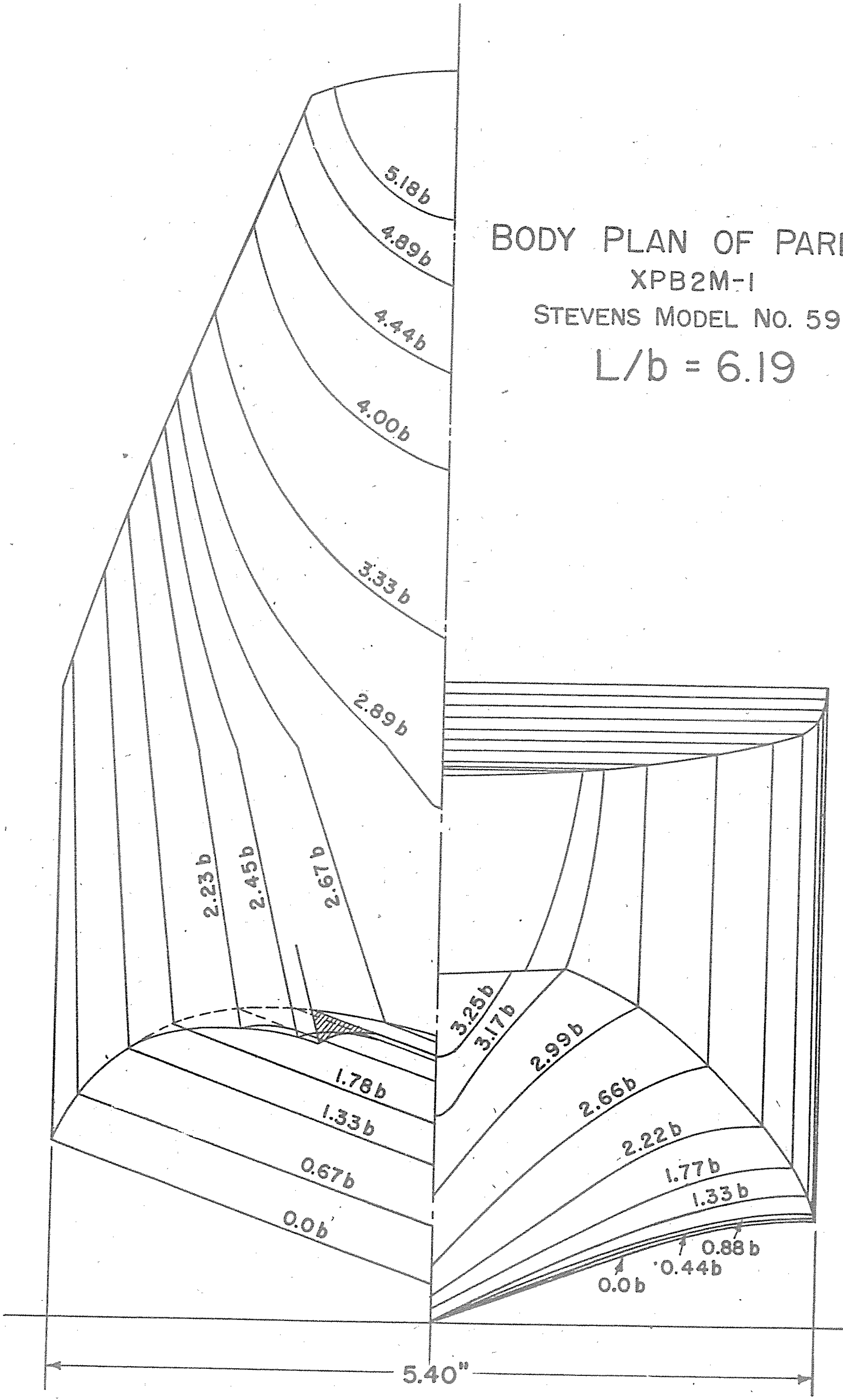

SCALE: FULL SIZE FOR MODEL

TABULATION OF STERNPOST ANGLE VALUES
FOR THE MODELS USED IN THE COMPARISONS

Model No.	Designation	Sternpost Height in.	Afterbody Length Along Afterbody Keel in.	Afterbody Length Along Baseline in.	Sternpost Angle deg.
573	5.07-3-20	0.91	12.24	12.20	4.25
339-22	5.07-7-20	1.76	12.24	12.15	8.25
574	5.07-11-20	2.61	12.24	12.00	12.3
532	6.19-7-0	2.09	14.96	14.85	8.0
533	6.19-7-10	2.09	14.96	14.85	8.0
591	6.19-7-20	2.09	14.96	14.85	8.0
534	6.19-7-30	2.09	14.96	14.85	8.0
535	6.19-7-40	2.09	14.96	14.85	8.0
536	6.19-3-20	1.05	14.96	14.94	4.0
537	6.19-5-20	1.57	14.96	14.90	6.0
538	6.19-9-20	2.61	14.96	14.88	10.1
539	6.19-11-20	3.13	14.96	14.70	12.0
605	6.19-9-10	2.61	14.96	14.88	10.1
606	6.19-5-30	1.57	14.96	14.90	6.0
607	6.19-9-30	2.61	14.96	14.88	10.1
626	7.32-3-20	1.19	17.67	17.65	3.9
339-23	7.32-7-20	2.43	17.67	17.55	7.9
627	7.32-11-20	3.64	17.67	17.35	11.65
693	8.45-3-20	1.34	20.40	20.35	3.75
651	8.45-7-20	2.76	20.40	20.25	7.8
694	8.45-11-20	4.15	20.40	20.05	11.7

DIMENSIONS AND PARTICULARS OF MODELS ON A L^2b (or K_2) CONSTANT BASIS

L/b	5.07	6.19	7.32	8.45	
L^2b	6040	6040	6040	6040	
K_2	0.0279	0.0279	0.0279	0.0279	
Δ_o	6.07	6.07	6.07	6.07	$\Delta_o = wL^2b\,K_2$
L	31.29	33.44	35.36	37.09	$L = \sqrt[3]{L^2b(L/b)}$
b	6.17	5.40	4.83	4.39	$b = \sqrt[3]{\frac{L^2b}{(L/b)^2}}$
C_{Δ_o}	0.72	1.07	1.49	1.99	$C_{\Delta_o} = K_2(L/b)^2$ or Δ_o/wb^3
L_B	15.23	16.70	17.97	19.09	$L_B = \left[\left(\frac{L_{f_o}}{L_o}\right)\frac{L}{b} - 0.35\right]b = \left[0.556\,\frac{L}{b} - 0.35\right]b$
L_{OA}	45.42	46.89	48.16	49.28	$L_{OA} = L_B + 30.19$
K	7.28	7.52	7.72	7.90	$K = K_o\,\frac{L_{OA}}{L_{OA_o}} = 7.52\,\frac{L_{OA}}{46.90} = \frac{L_{OA}}{6.24}$
K/L	0.233	0.225	0.218	0.213	
M_q/v	9.94	9.94	9.94	9.94	
$M_q/v\frac{\rho}{2}b^4$	0.147	0.250	0.391	0.572	$M_q/v\frac{\rho}{2}b^4 = (M_q/v\frac{\rho}{2}b^4)_o\left(\frac{b_o}{b}\right)^4 = 0.250\left(\frac{b_o}{b}\right)^4$

FOR MODELS OF CONSTANT 5.40" BEAM THESE VALUES BECOME FOR TEST MODELS

L/b	5.07	6.19	7.32	8.45	
Δ_{o_m}	4.07	6.07	8.50	11.29	$\Delta_{o_m} = 6.07\left(\frac{5.40}{b}\right)^3$
L_m	27.38	33.44	39.53	45.62	$L_m = L\left(\frac{5.40}{b}\right)$
K_m	6.37	7.52	8.63	9.72	$K_m = \left(\frac{K}{L}\right)L_m$ or $K\left(\frac{5.40}{b}\right)$
I_m	166	343	633	1067	$I_m = \Delta_{o_m}\,K_m^2$
$(M_q/v)_m$	5.83	9.94	15.54	22.75	$(M_q/v)_m = (M_q/v)\left(\frac{5.40}{b}\right)^4$

DIMENSIONS OF THE VARIOUS LENGTH-BEAM RATIO HULLS IN TERMS OF THEIR BEAMS DETERMINED ON A K_2 CONSTANT BASIS

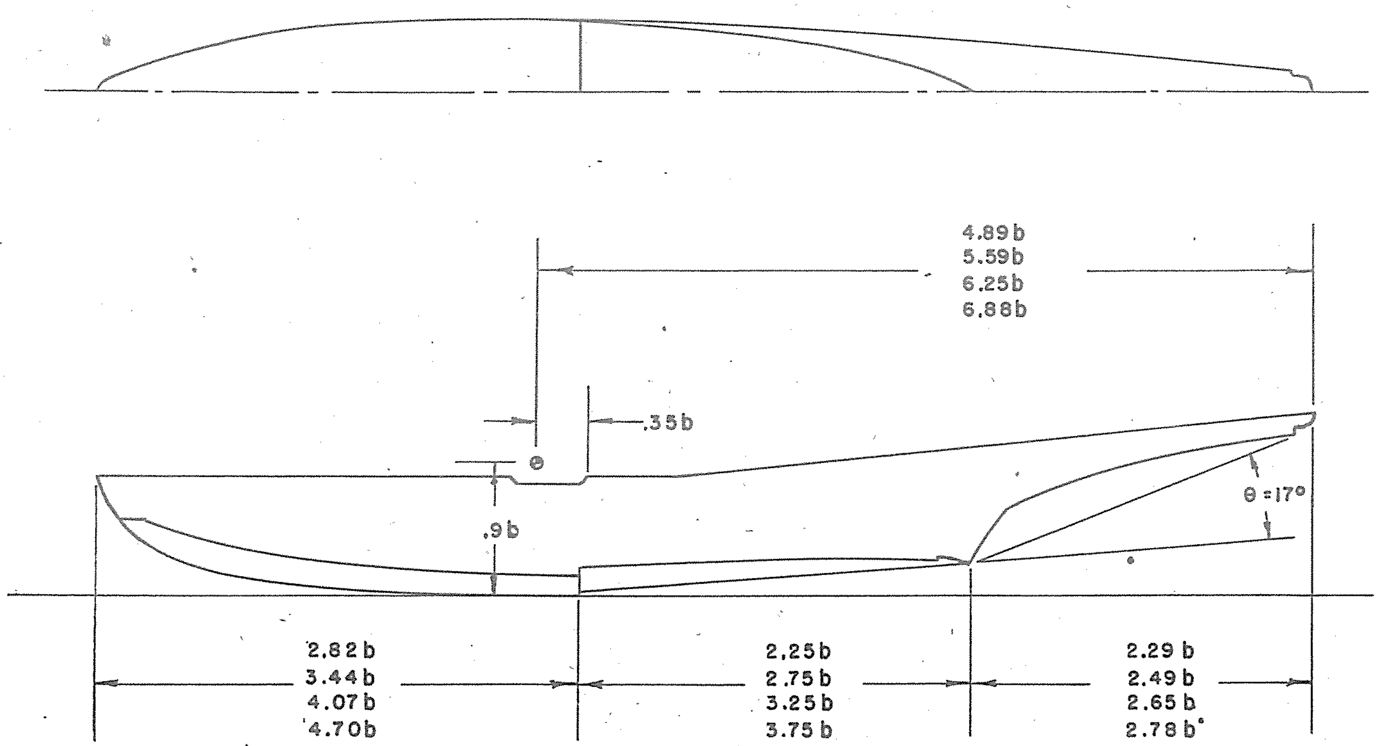

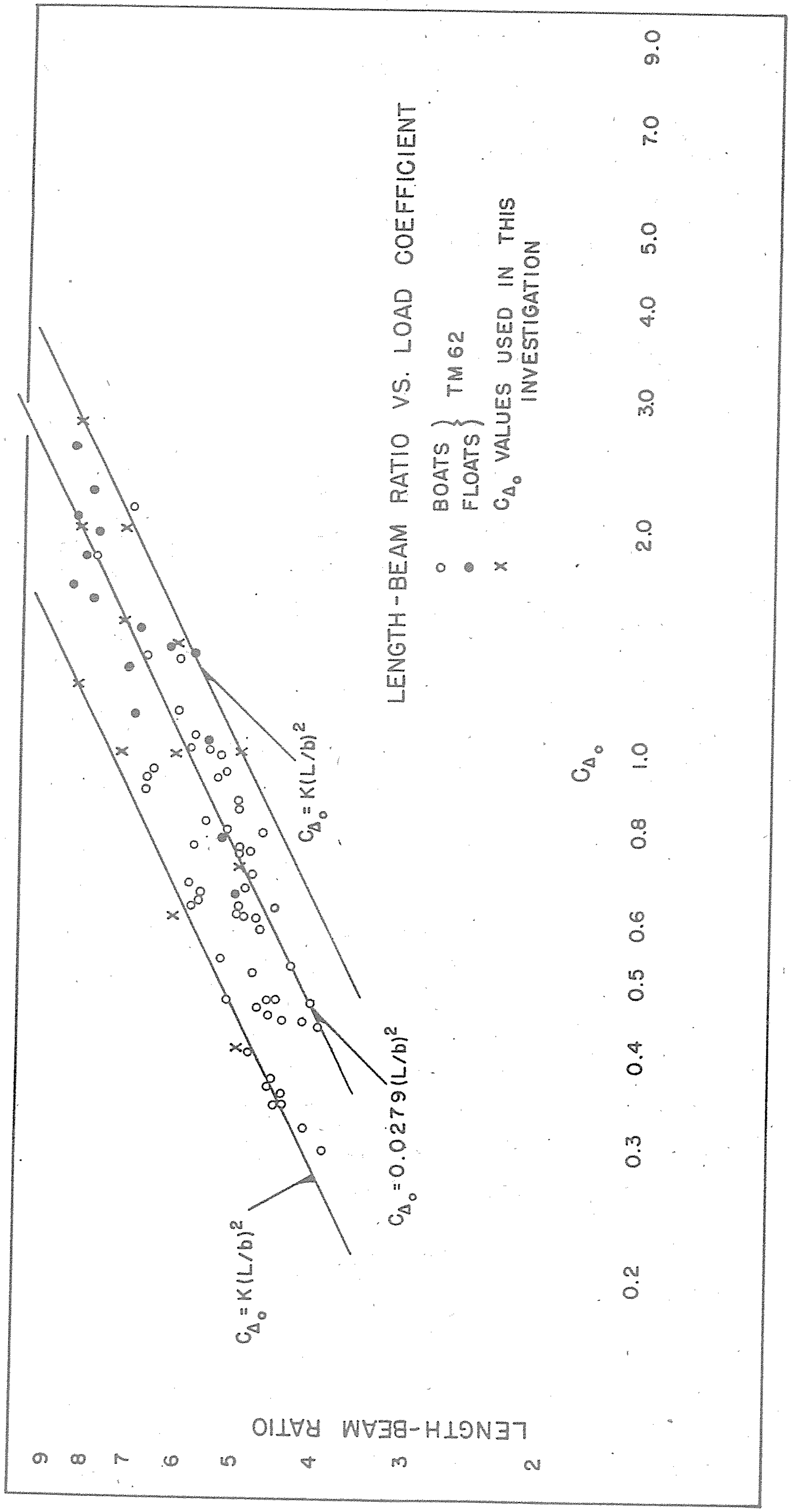
LENGTH-BEAM RATIO VS. LOAD COEFFICIENT
○ BOATS } TM 62
● FLOATS }
× C_{Δ_o} VALUES USED IN THIS INVESTIGATION
$C_{\Delta_o} = K(L/b)^2$
$C_{\Delta_o} = 0.0279(L/b)^2$
$C_{\Delta_o} = K(L/b)^2$
C_{Δ_o}
0.2
0.3
0.4
0.5
0.6
0.8
1.0
2.0
3.0
4.0
5.0
7.0
9.0
LENGTH-BEAM RATIO
2
3
4
5
6
7
8
9

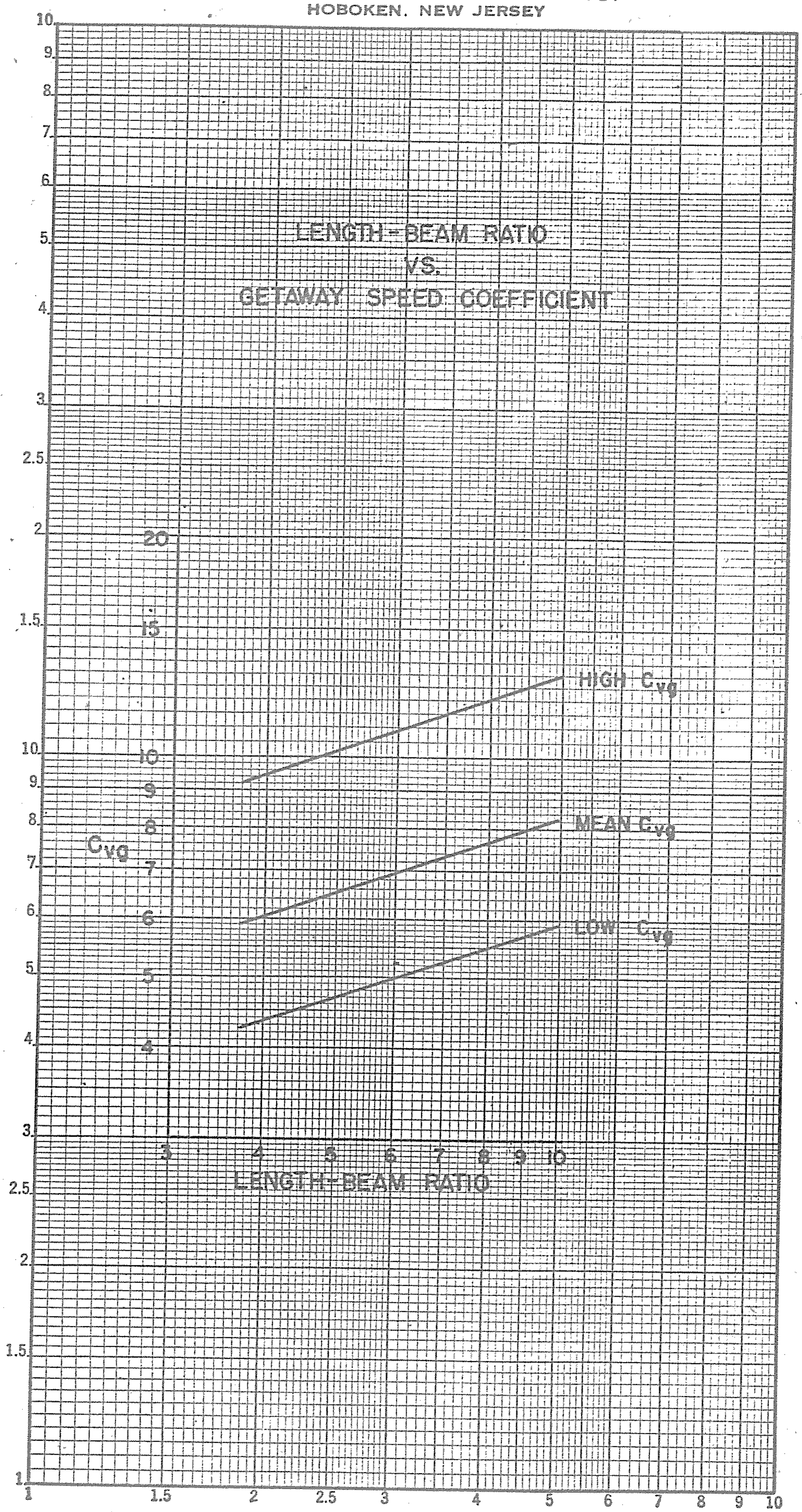
LENGTH-BEAM RATIO
VS.
GETAWAY SPEED COEFFICIENT
HIGH C_{vg}
MEAN C_{vg}
LOW C_{vg}
C_{vg}
20
15
10
9
8
7
6
5
4
3
4
5
6
7
8
9
10
LENGTH-BEAM RATIO

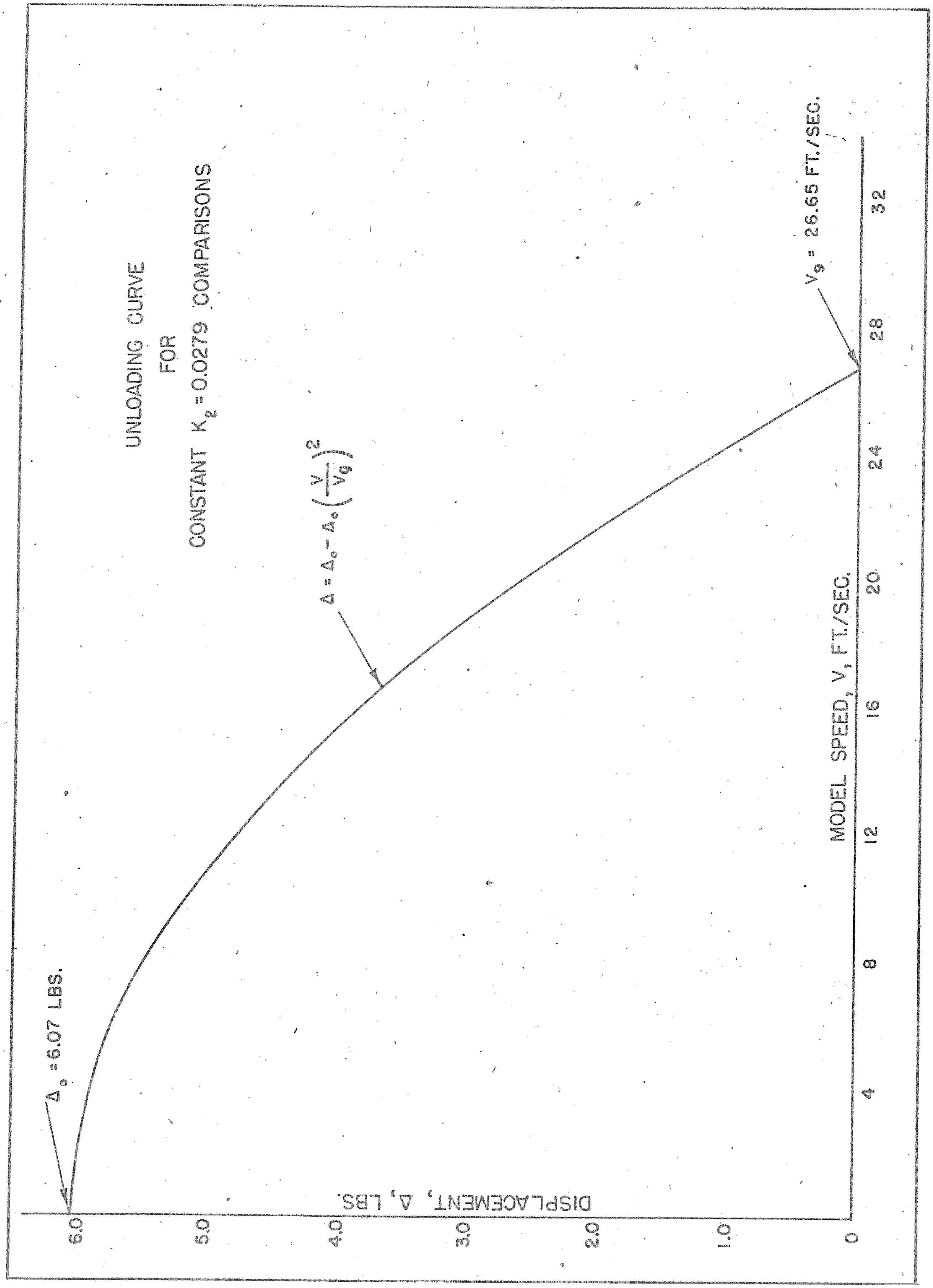
UNLOADING CURVE
FOR
CONSTANT $K_2 = 0.0279$ COMPARISONS
$\Delta = \Delta_o - \Delta_o \left(\frac{V}{V_g}\right)^2$
$\Delta_o = 6.07$ LBS.
$V_g = 26.65$ FT./SEC.
DISPLACEMENT, Δ, LBS.
MODEL SPEED, V, FT./SEC.
0
1.0
2.0
3.0
4.0
5.0
6.0
4
8
12
16
20
24
28
32

EFFECT OF LENGTH-BEAM RATIO ON HYDRODYNAMIC CHARACTERISTICS OF FOUR MODELS WITH $K_2 = 0.0279$ CONSTANT

MODEL NUMBER	DESIGNATION	LINE SYMBOL
339-22	5.07-7-20	- - - - -
591	6.19-7-20	———
339-23	7.32-7-20	— —
651	8.45-7-20	—-—

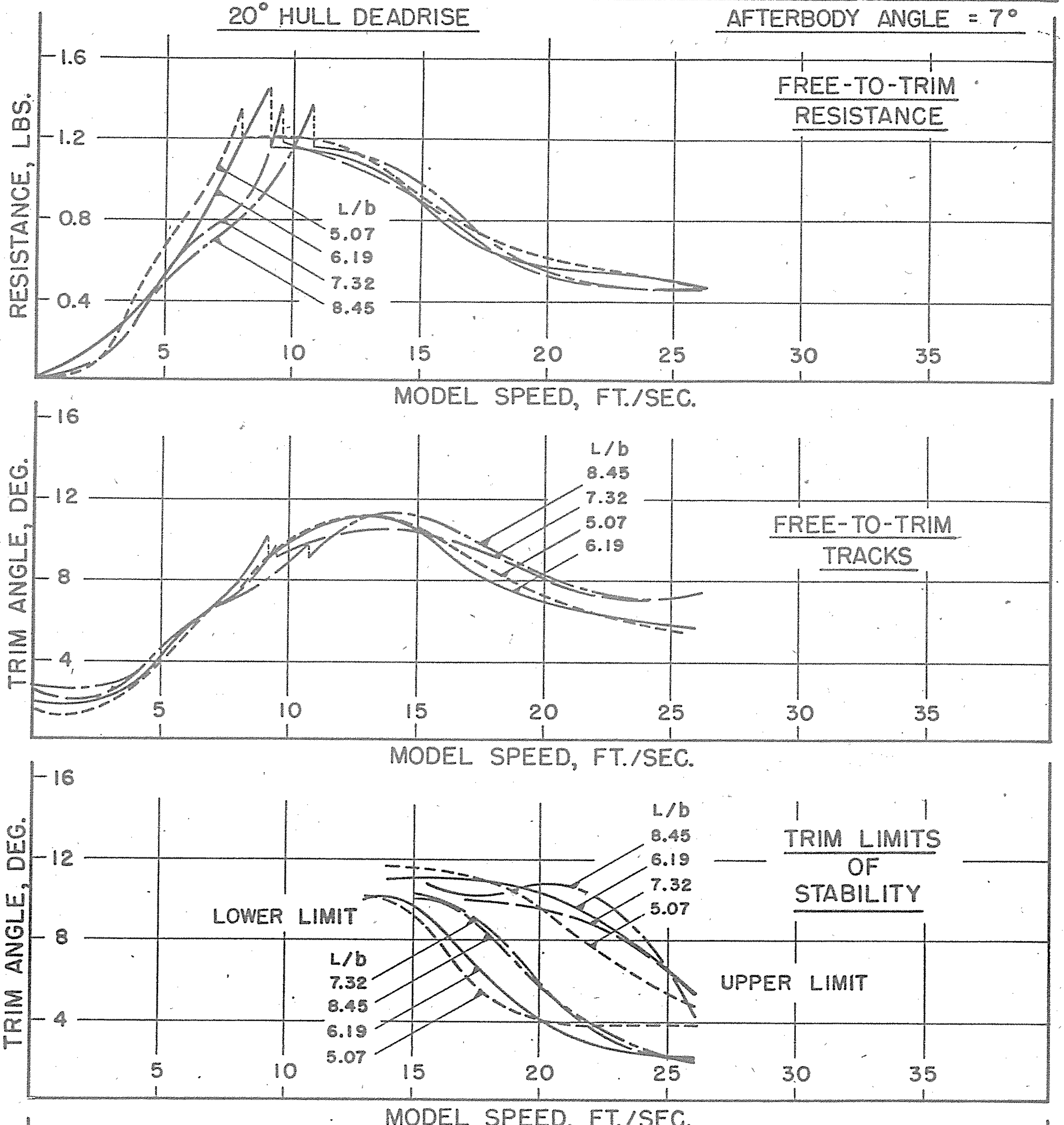

MODEL PARTICULARS

LENGTH-BEAM RATIO	5.07	6.19	7.32	8.45
DEADRISE ANGLE	20°	20°	20°	20°
AFTERBODY ANGLE	7°	7°	7°	7°
STERNPOST ANGLE	8.25°	8.0°	7.9°	7.8°
$C_{\Delta o}$	0.72	1.07	1.49	1.99
BEAM	6.17"	5.40"	4.83"	4.39"

EFFECT OF LENGTH-BEAM RATIO ON SPRAY CHARACTERISTICS FOR MODELS OF 20° HULL DEADRISE AND DIFFERING AFTERBODY ANGLES WITH $K_2 = 0.0279$ CONSTANT

L/b	$C_{\Delta o}$	BEAM	LINE SYMBOL
5.07	0.72	6.17"	– – – – –
6.19	1.07	5.40"	————
7.32	1.49	4.83"	—— ——
8.45	1.99	4.39"	—— – ——

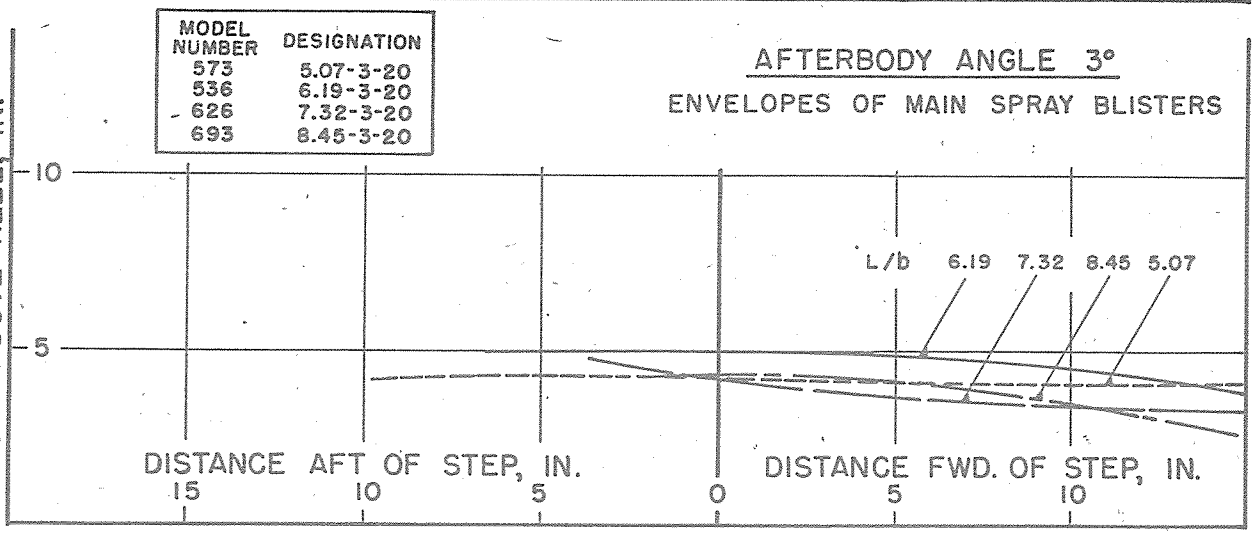

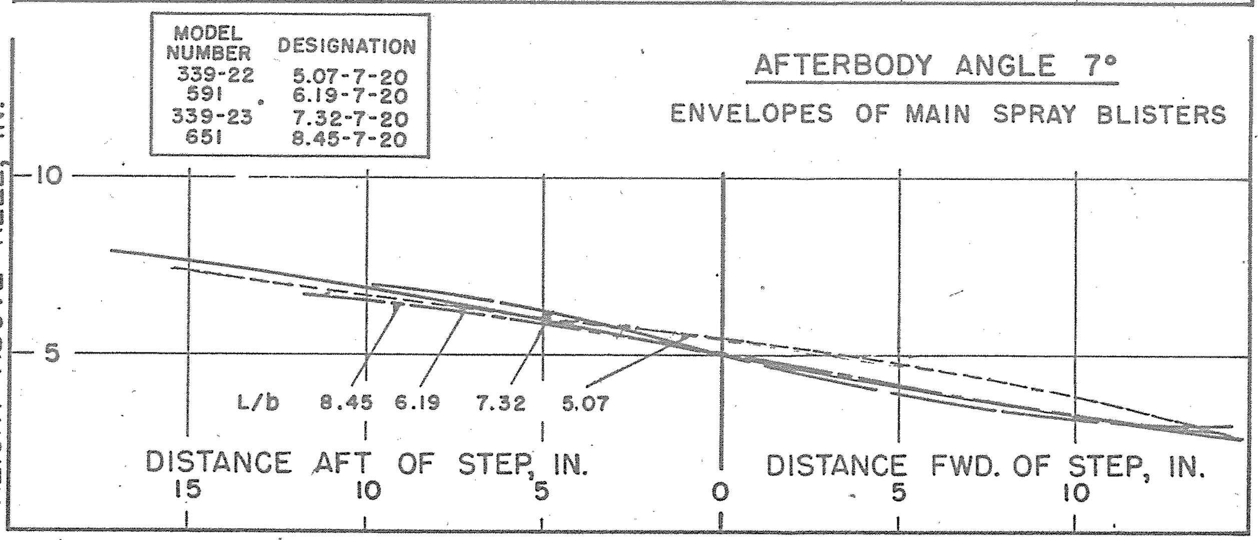

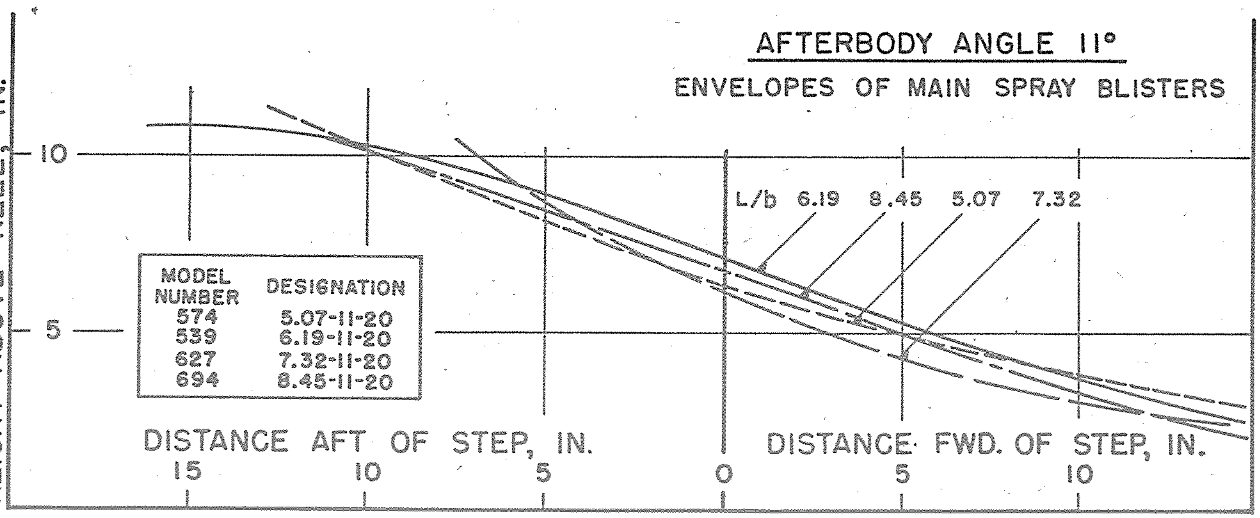

EXPERIMENTAL TOWING TANK
STEVENS INSTITUTE OF TECHNOLOGY
HOBOKEN, NEW JERSEY

EFFECT OF AFTERBODY ANGLE ON HYDRODYNAMIC CHARACTERISTICS OF THREE MODELS WITH $K_2 = 0.0279$ CONSTANT	MODEL NUMBER	DESIGNATION	LINE SYMBOL
	573	5.07-3-20	— — — —
	339-22	5.07-7-20	—— - ——
	574	5.07-11-20	————

20° HULL DEADRISE L/b = 5.07

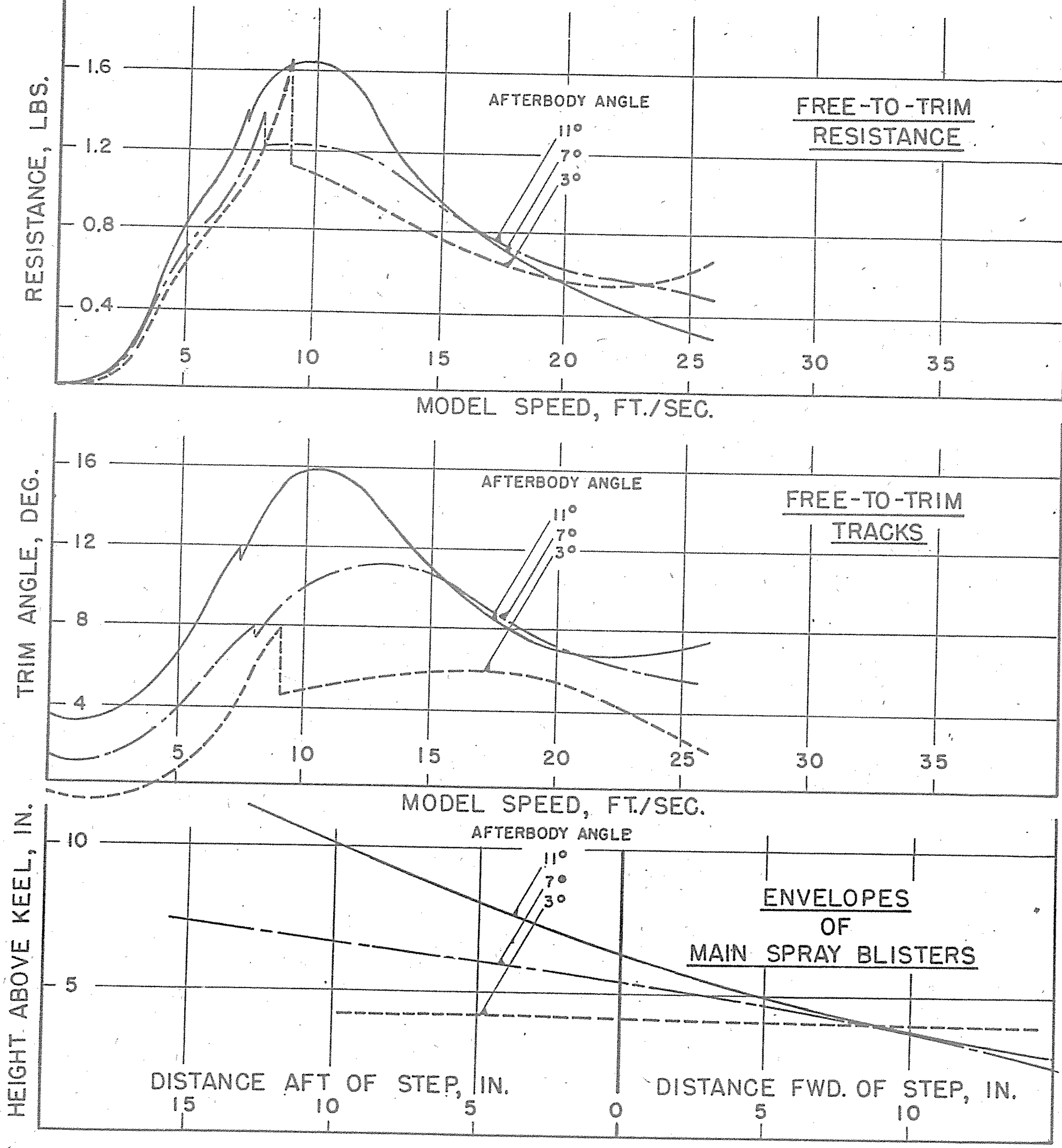

MODEL PARTICULARS

AFTERBODY ANGLE	3°	7°	11°
DEADRISE ANGLE	20°	20°	20°
L/b	5.07	5.07	5.07
$C_{\Delta o}$	0.72	0.72	0.72
BEAM	6.17	6.17	6.17

EFFECT OF AFTERBODY ANGLE ON HYDRODYNAMIC CHARACTERISTICS OF FIVE MODELS WITH $K_2 = 0.0279$ CONSTANT

MODEL NUMBER	DESISNATION	LINE SYMBOL
536	6.19-3-20	
537	6.19-5-20	
591	6.19-7-20	
538	6.19-9-20	
539	6.19-11-20	

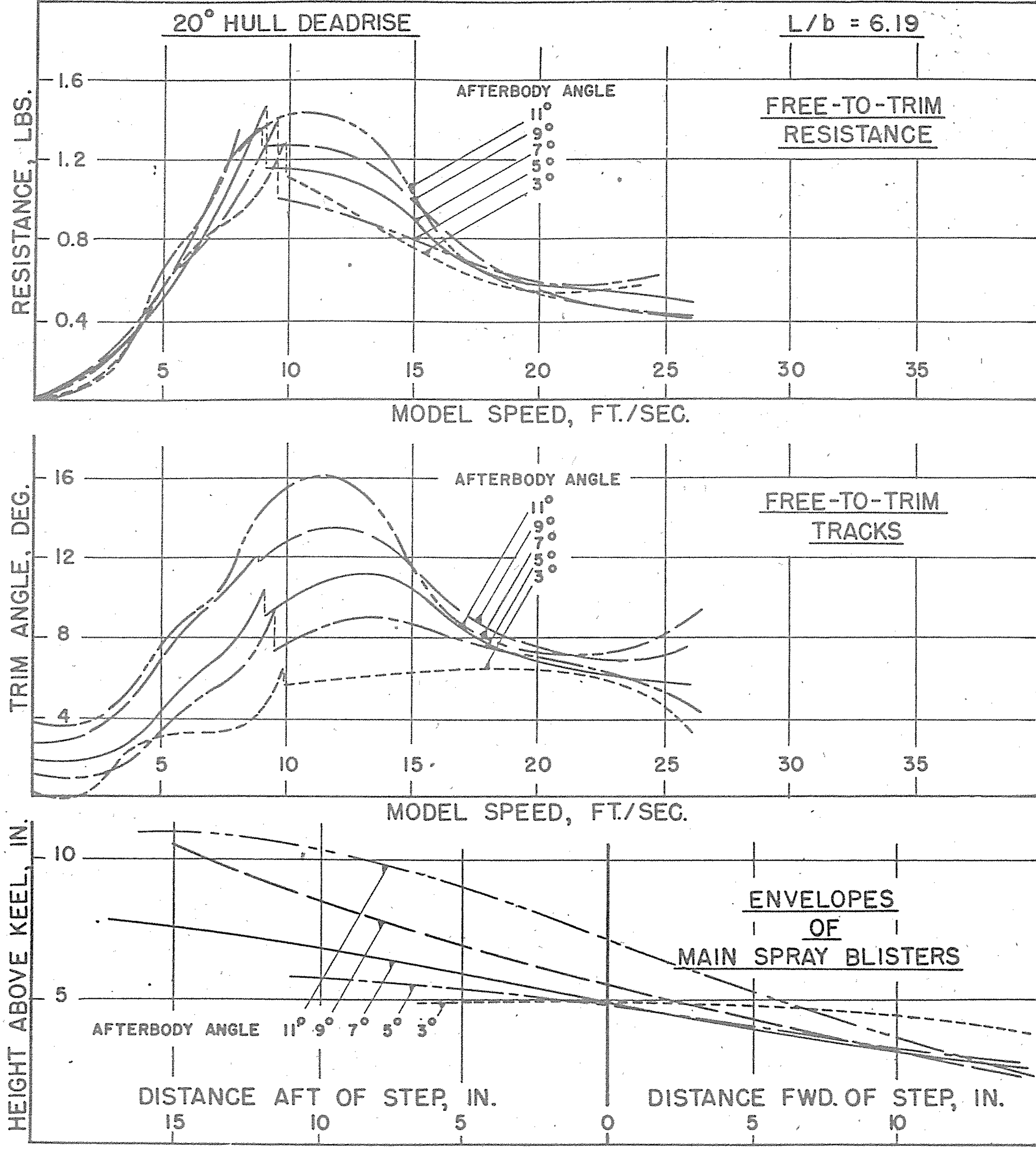

MODEL PARTICULARS

AFTERBODY ANGLE	3°	5°	7°	9°	11°
DEADRISE ANGLE	7°	7°	7°	7°	7°
L/b	6.19	6.19	6.19	6.19	6.19
C_{Δ_o}	1.07	1.07	1.07	1.07	1.07
BEAM	5.4	5.4	5.4	5.4	5.4

EFFECT OF AFTERBODY ANGLE ON HYDRODYNAMIC CHARACTERISTICS OF THREE MODELS WITH $K_2 = 0.0279$ CONSTANT	MODEL NUMBER	DESIGNATION	LINE SYMBOL
	626	7.32-3-20	------
	339-23	7.32-7-20	— - —
	627	7.32-11-20	———

20° HULL DEADRISE   L/b = 7.32

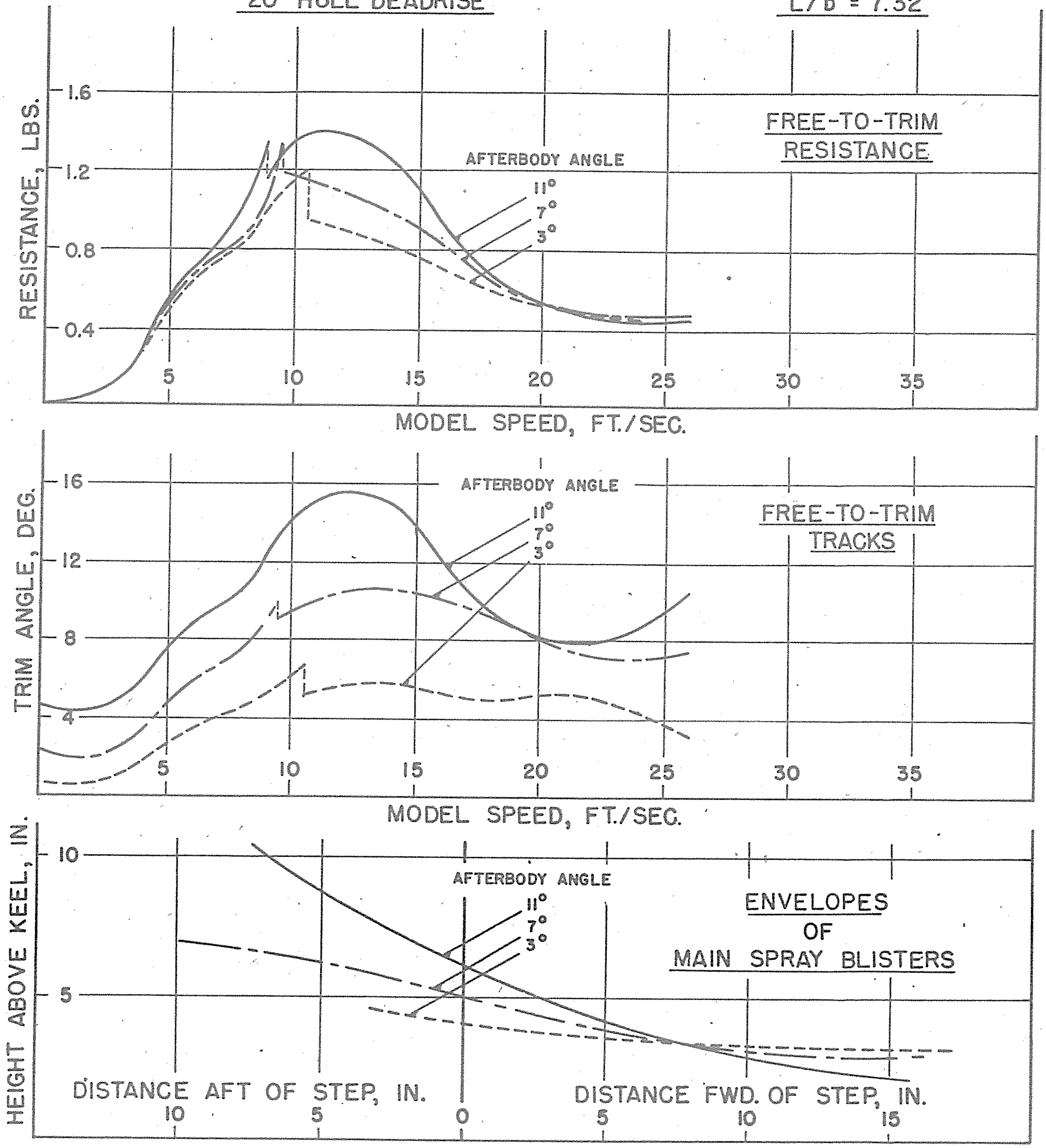

MODEL PARTICULARS

AFTERBODY ANGLE	3°	7°	11°
DEADRISE ANGLE	20°	20°	20°
L/b	7.32	7.32	7.32
$C_{\Delta o}$	1.49	1.49	1.49
BEAM	4.83"	4.83"	4.83"

EFFECT OF AFTERBODY ANGLE ON HYDRODYNAMIC CHARACTERISTICS OF THREE MODELS WITH $K_2 = 0.0279$ CONSTANT

MODEL NUMBER	DESIGNATION	LINE SYMBOL
693	8.45-3-20	------
651	8.45-7-20	—·—·—
694	8.45-11-20	———

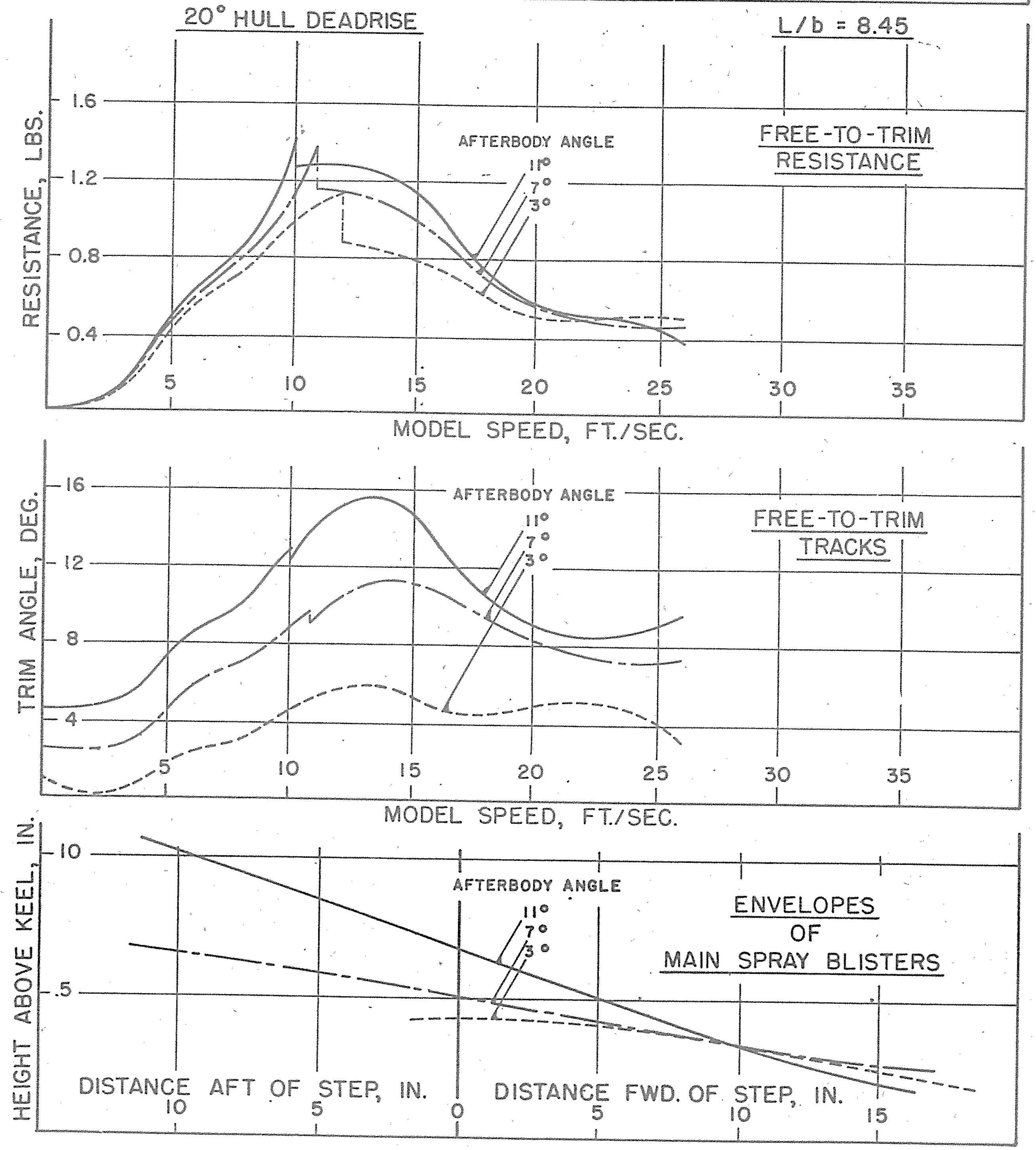

MODEL PARTICULARS

AFTERBODY ANGLE	3°	7°	11°
DEADRISE ANGLE	20°	20°	20°
L/b	8.45	8.45	8.45
$C_{\Delta o}$	1.99	1.99	1.99
BEAM	4.39"	4.39"	4.39"

EFFECT OF AFTERBODY ANGLE ON TRIM LIMITS OF STABILITY
FOR MODELS OF DIFFERING LENGTH-BEAM RATIO
HULL DEADRISE OF 20° CONSTANT

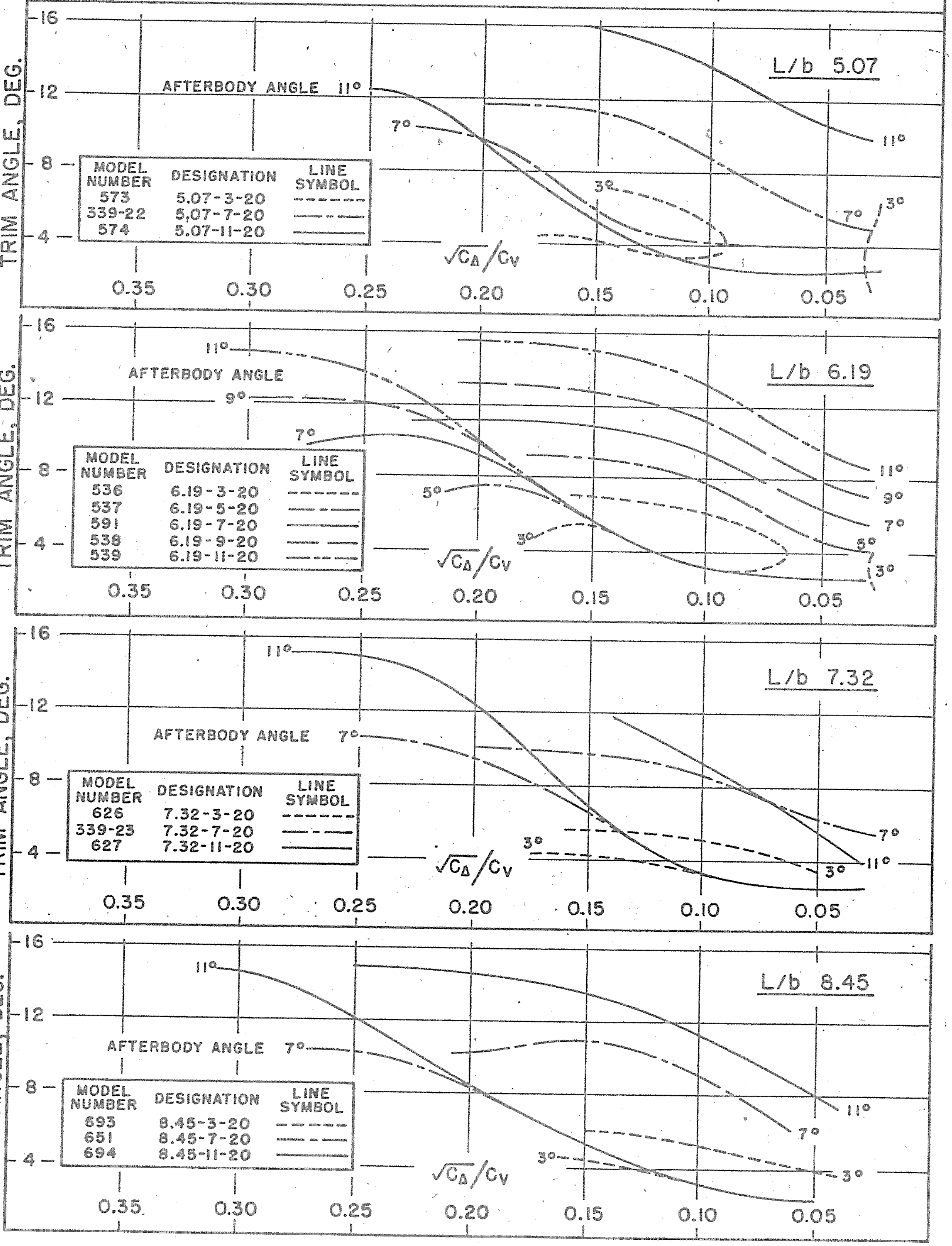

EFFECT OF AFTERBODY ANGLE ON SPRAY HEIGHT
IN THE VICINITY OF THE PROPELLERS
WITH K = 0.0279 CONSTANT
FOR HULLS WITH 20° DEADRISE AT MAIN STEP

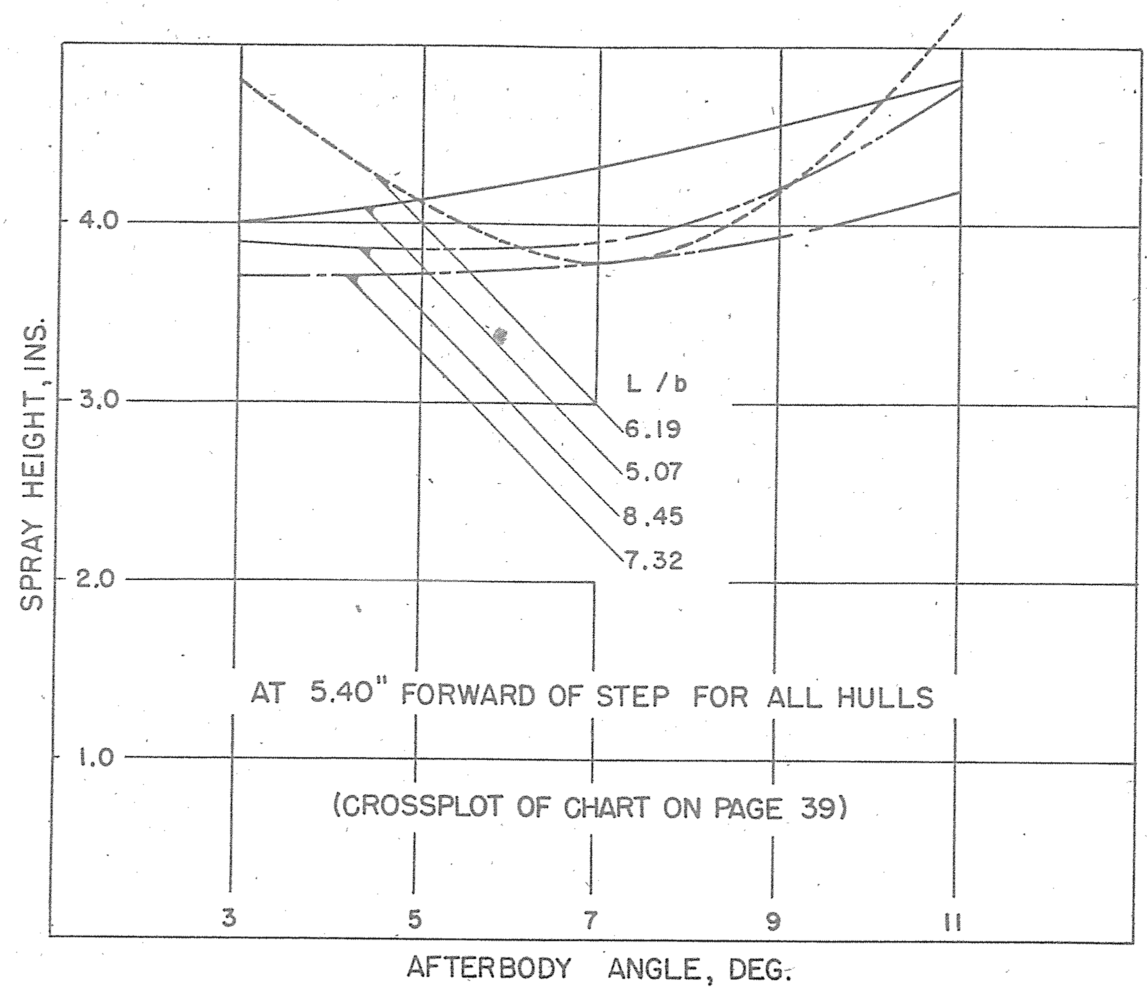

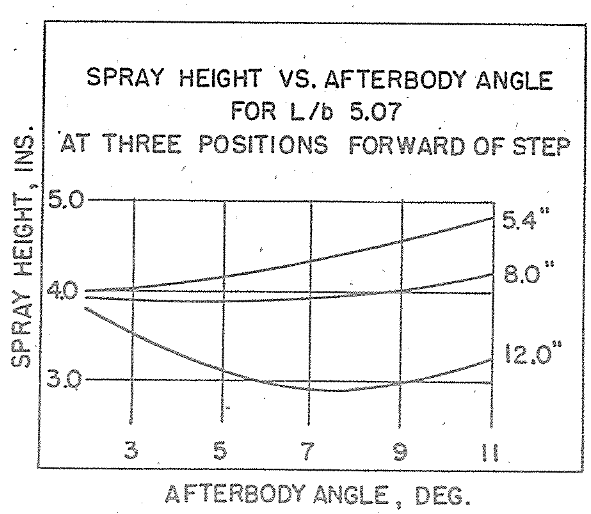

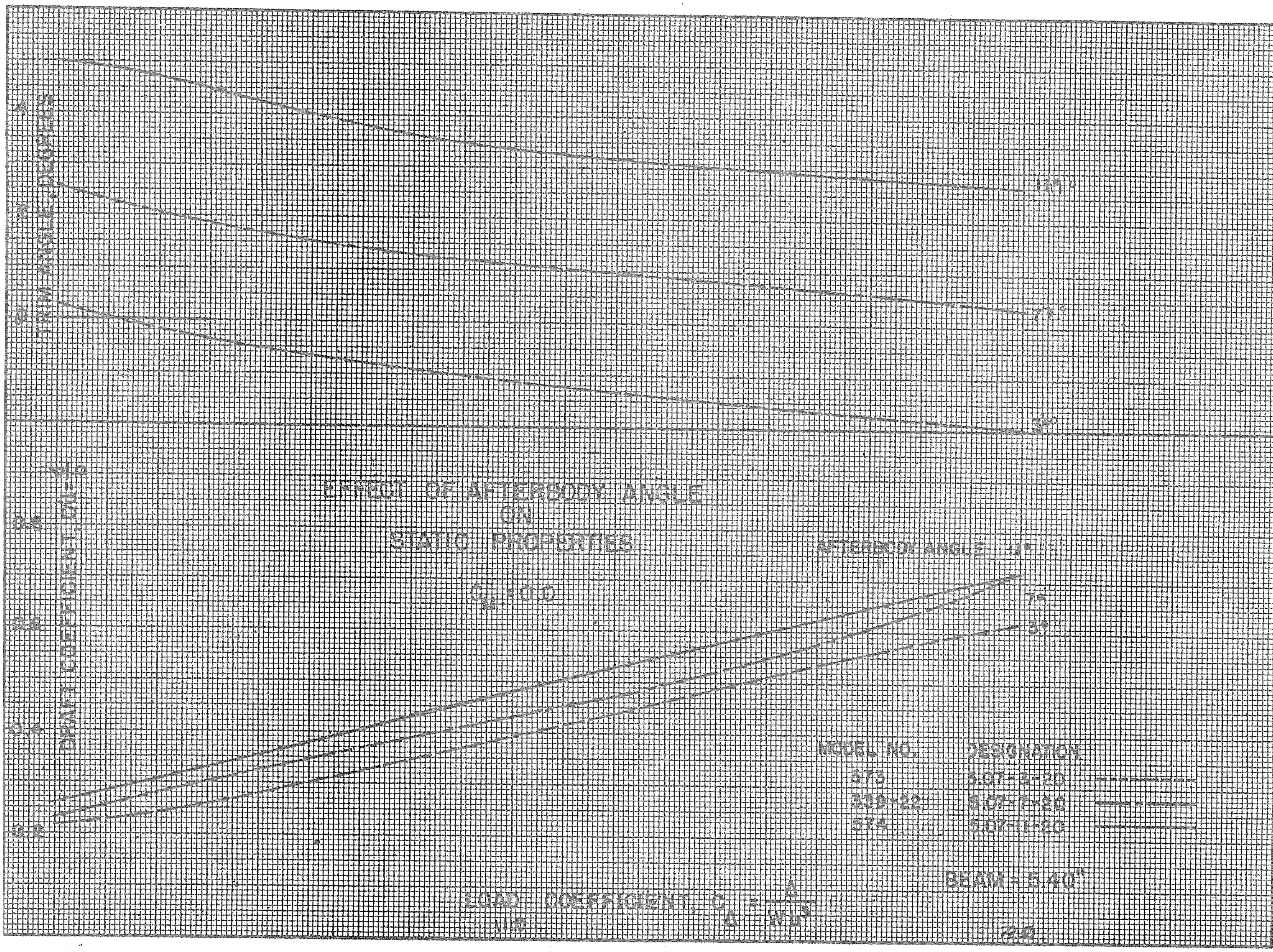
EFFECT OF AFTERBODY ANGLE
ON
STATIC PROPERTIES
$C_v = 0.0$
TRIM ANGLE, DEGREES
DRAFT COEFFICIENT, $C_d = \frac{d}{b}$
LOAD COEFFICIENT, $C_\Delta = \frac{\Delta}{wb^3}$
AFTERBODY ANGLE 11°
7°
3°
MODEL NO. DESIGNATION
573 5.07-3-20
339-22 5.07-7-20
574 5.07-11-20
BEAM = 5.40"
4
2
0
0.8
0.6
0.4
0.2
1.0
2.0

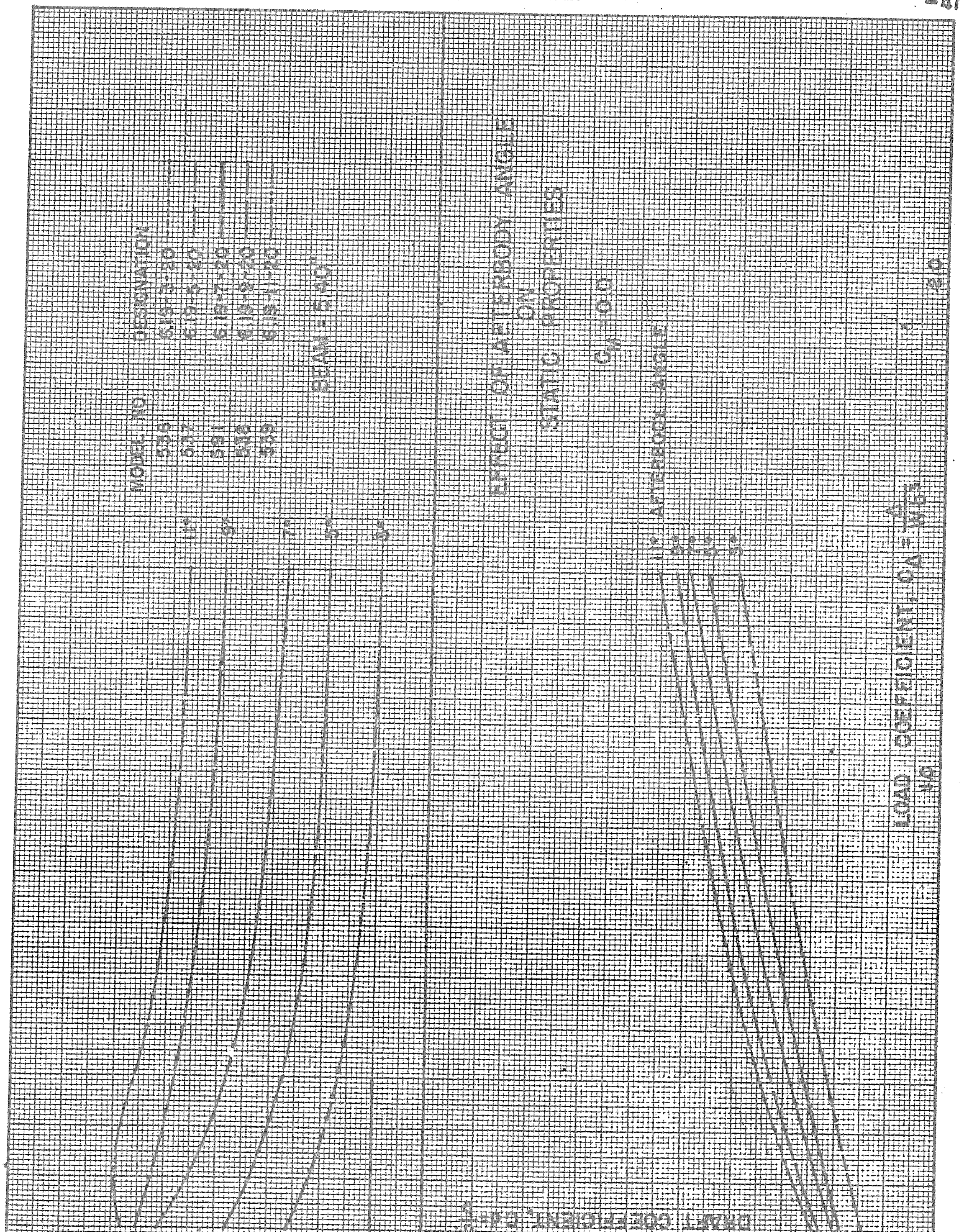
MODEL NO. DESIGNATION
536 6.19-3-20
537 6.19-5-20
591 6.19-7-20
538 6.19-9-20
539 6.19-11-20
BEAM = 5.40"
EFFECT OF AFTERBODY ANGLE
ON
STATIC PROPERTIES
$C_M = 0.0$
TRIM ANGLE, DEGREES
DRAFT COEFFICIENT
11° AFTERBODY ANGLE
11°
9°
7°
5°
3°
LOAD COEFFICIENT, $C_\Delta = \frac{\Delta}{wb^3}$
1.0
2.0

EXPERIMENTAL TOWING TANK
STEVENS INSTITUTE OF TECHNOLOGY
HOBOKEN, NEW JERSEY

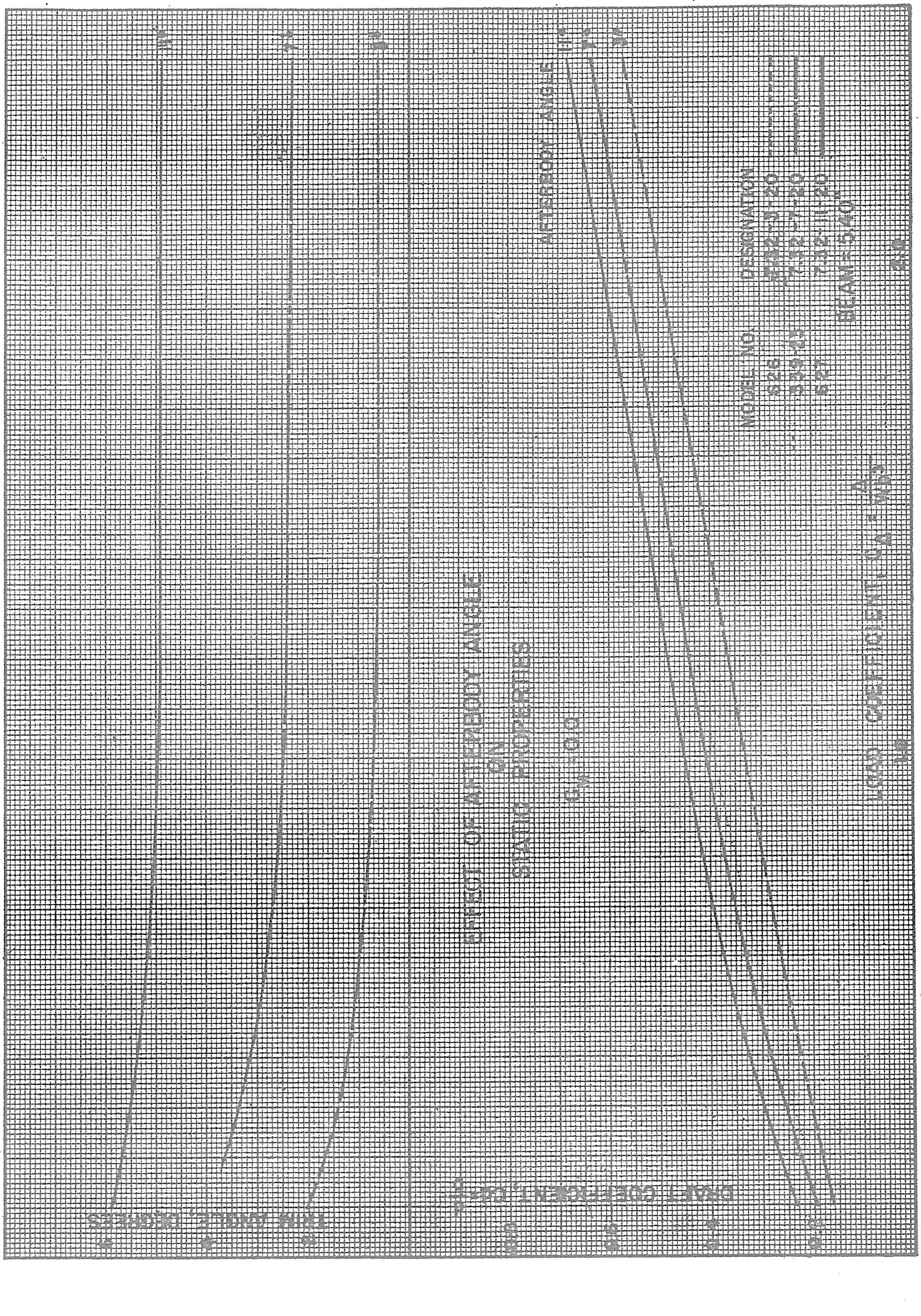

EXPERIMENTAL TOWING TANK
STEVENS INSTITUTE OF TECHNOLOGY
HOBOKEN, NEW JERSEY

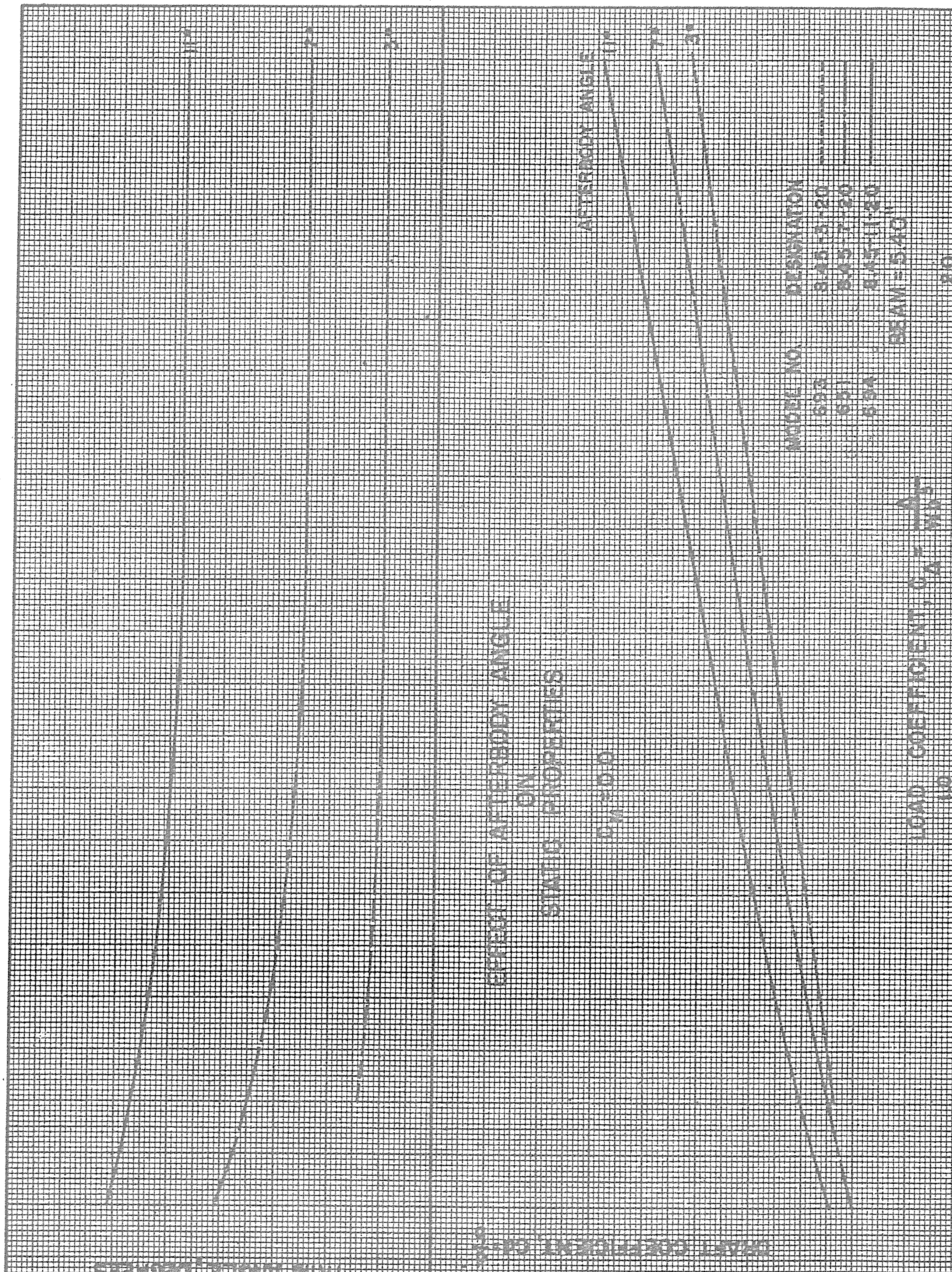

EFFECT OF HULL DEADRISE ON HYDRODYNAMIC CHARACTERISTICS OF THREE MODELS WITH $K_2 = 0.0279$ CONSTANT

MODEL NUMBER	DESIGNATION	LINE SYMBOL
604	6.19-5-10	- - - - - -
537	6.19-5-20	—— - ——
606	6.19-5-30	————

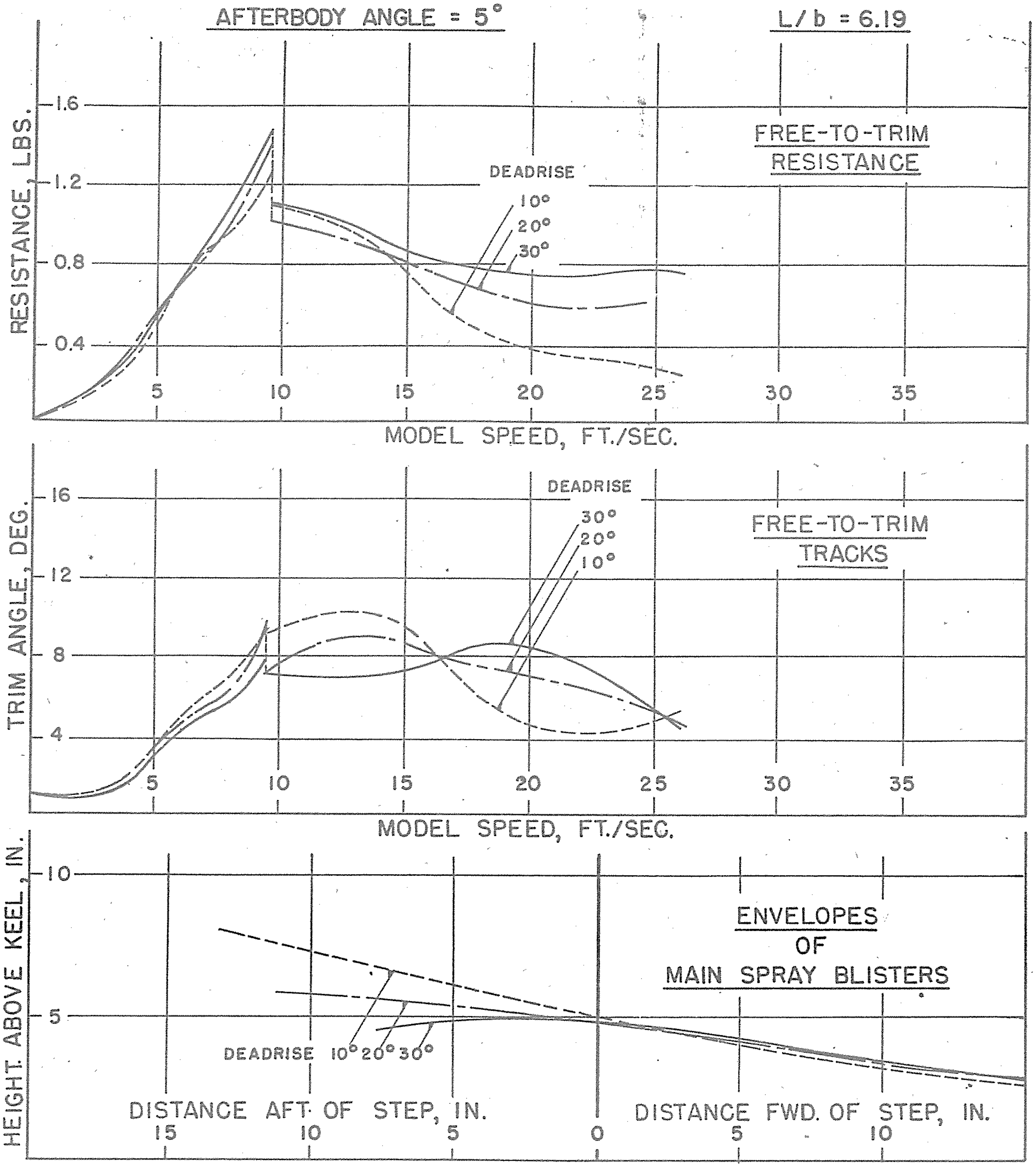

MODEL PARTICULARS

DEADRISE ANGLE	10°	20°	30°
AFTERBODY ANGLE	5°	5°	5°
L/b	6.19	6.19	6.19
$C_{\Delta o}$	1.07	1.07	1.07
BEAM	5.4"	5.4"	5.4"

EFFECT OF HULL DEADRISE ON HYDRODYNAMIC CHARACTERISTICS OF FIVE MODELS WITH $K_2 = 0.0279$ CONSTANT

MODEL NUMBER	DESIGNATION	LINE SYMBOL
532	6.19-7-0	
533	6.19-7-10	
591	6.19-7-20	
534	6.19-7-30	
535	6.19-7-40	

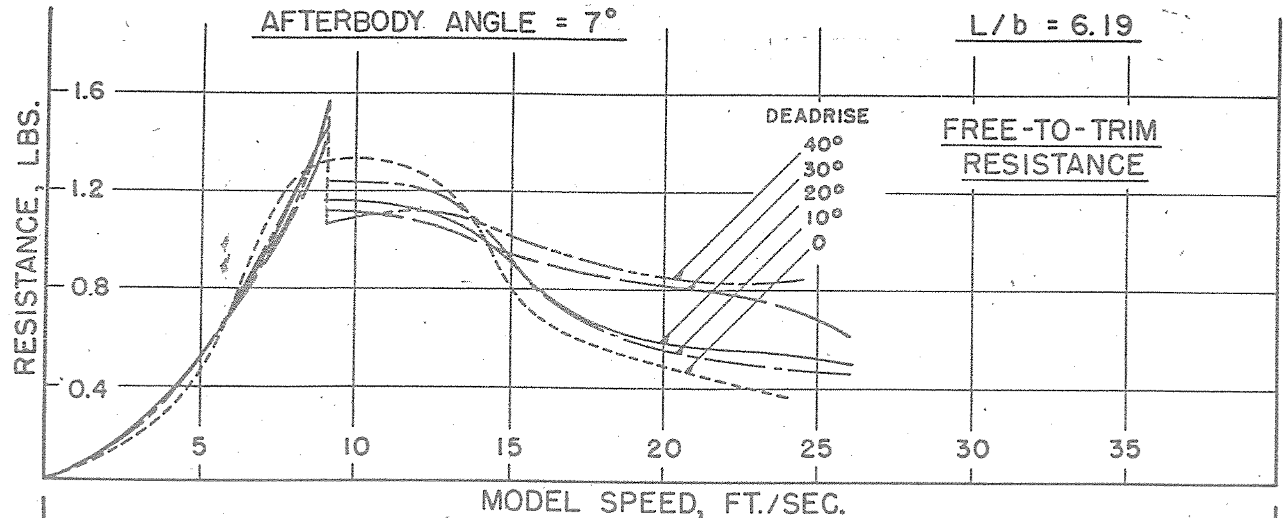

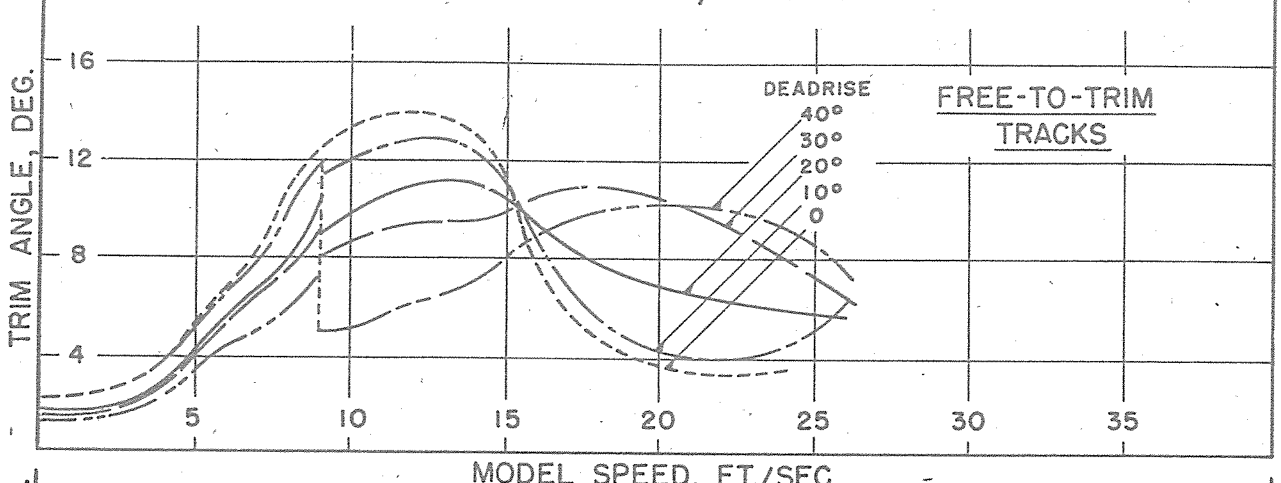

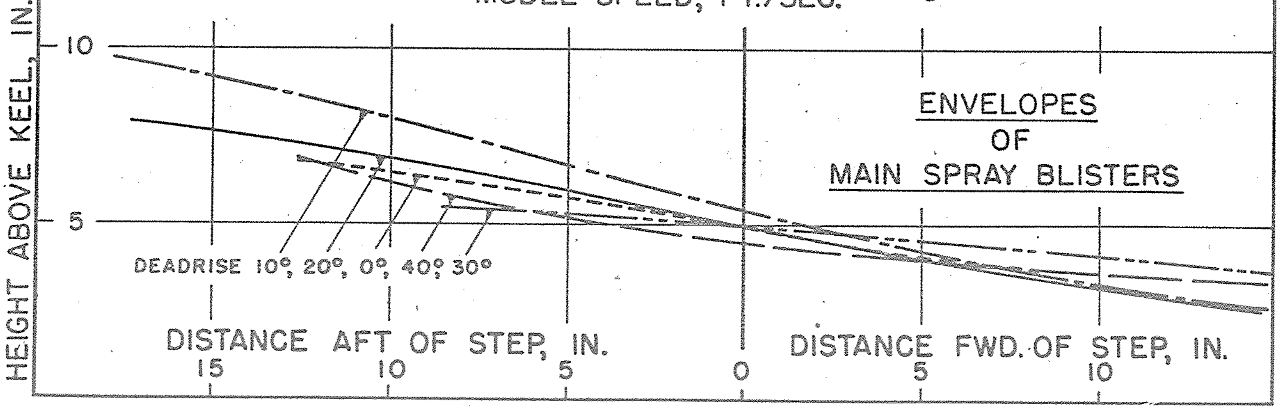

MODEL PARTICULARS

DEADRISE ANGLE	0°	10°	20°	30°	40°
AFTERBODY ANGLE	7°	7°	7°	7°	7°
L/b	6.19	6.19	6.19	6.19	6.19
$C_{\Delta o}$	1.07	1.07	1.07	1.07	1.07
BEAM	5.4"	5.4"	5.4"	5.4"	5.4"

EFFECT OF HULL DEADRISE ON HYDRODYNAMIC CHARACTERISTICS OF THREE MODELS WITH $K_2 = 0.0279$ CONSTANT	MODEL NUMBER	DESIGNATION	LINE SYMBOL
	605	6.19-9-10	———
	538	6.19-9-20	------
	607	6.19-9-30	—-·—

AFTERBODY ANGLE = 9° L/b = 6.19

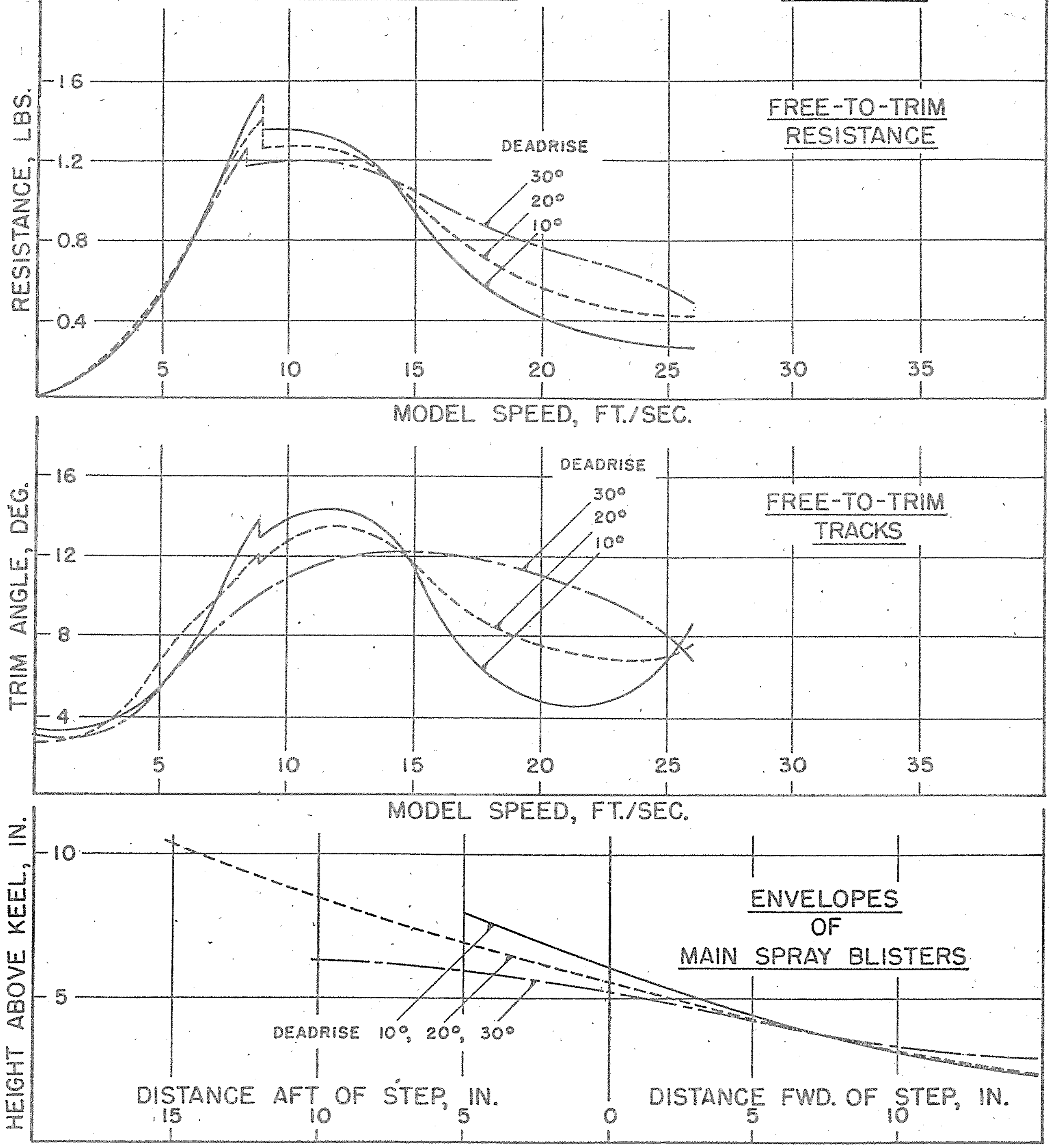

MODEL PARTICULARS

DEADRISE ANGLE	10°	20°	30°
AFTERBODY ANGLE	9°	9°	9°
L/b	6.19	6.19	6.19
C_{Δ_o}	1.07	1.07	1.07
BEAM	5.4"	5.4"	5.4"

EFFECT OF HULL DEADRISE ON TRIM LIMITS OF STABILITY FOR MODELS OF DIFFERING AFTERBODY ANGLES LENGTH-BEAM RATIO 6.19 CONSTANT

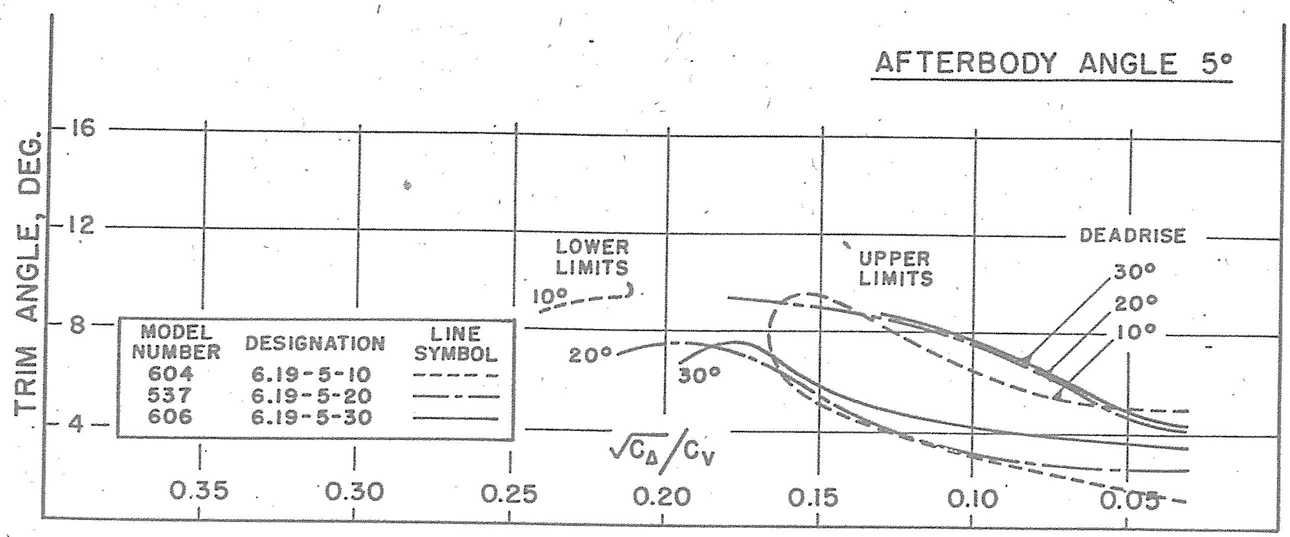

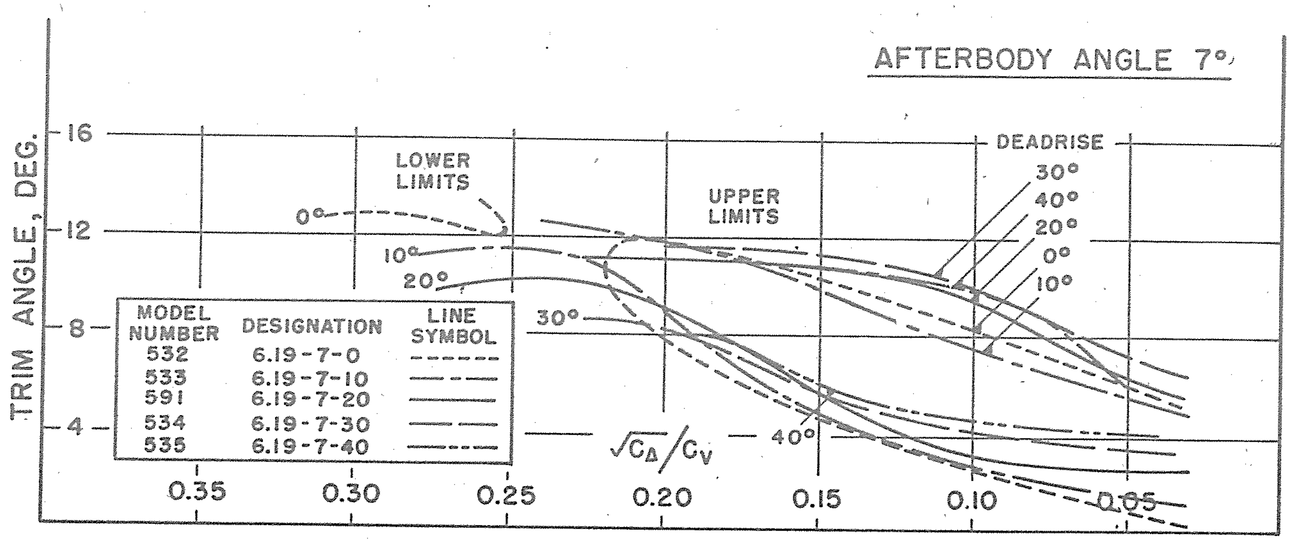

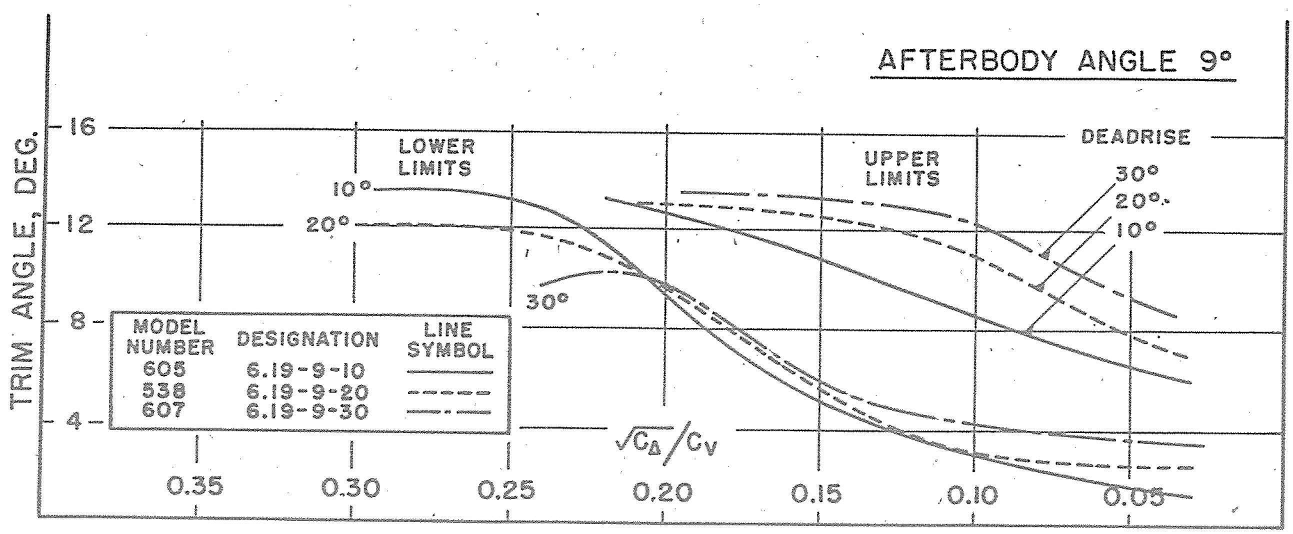

EXPERIMENTAL TOWING TANK
STEVENS INSTITUTE OF TECHNOLOGY
HOBOKEN, NEW JERSEY

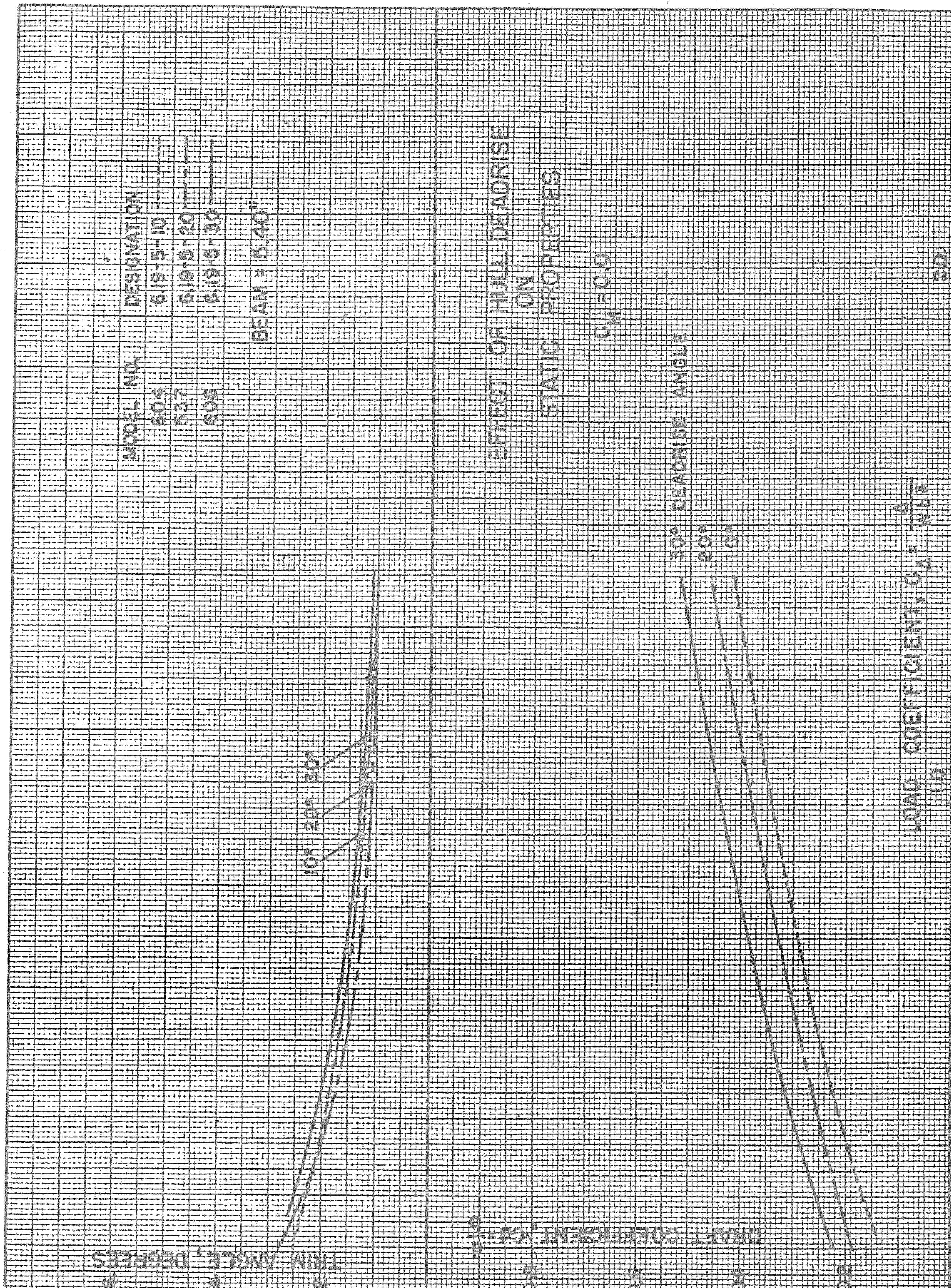

EXPERIMENTAL TOWING TANK
STEVENS INSTITUTE OF TECHNOLOGY
HOBOKEN, NEW JERSEY

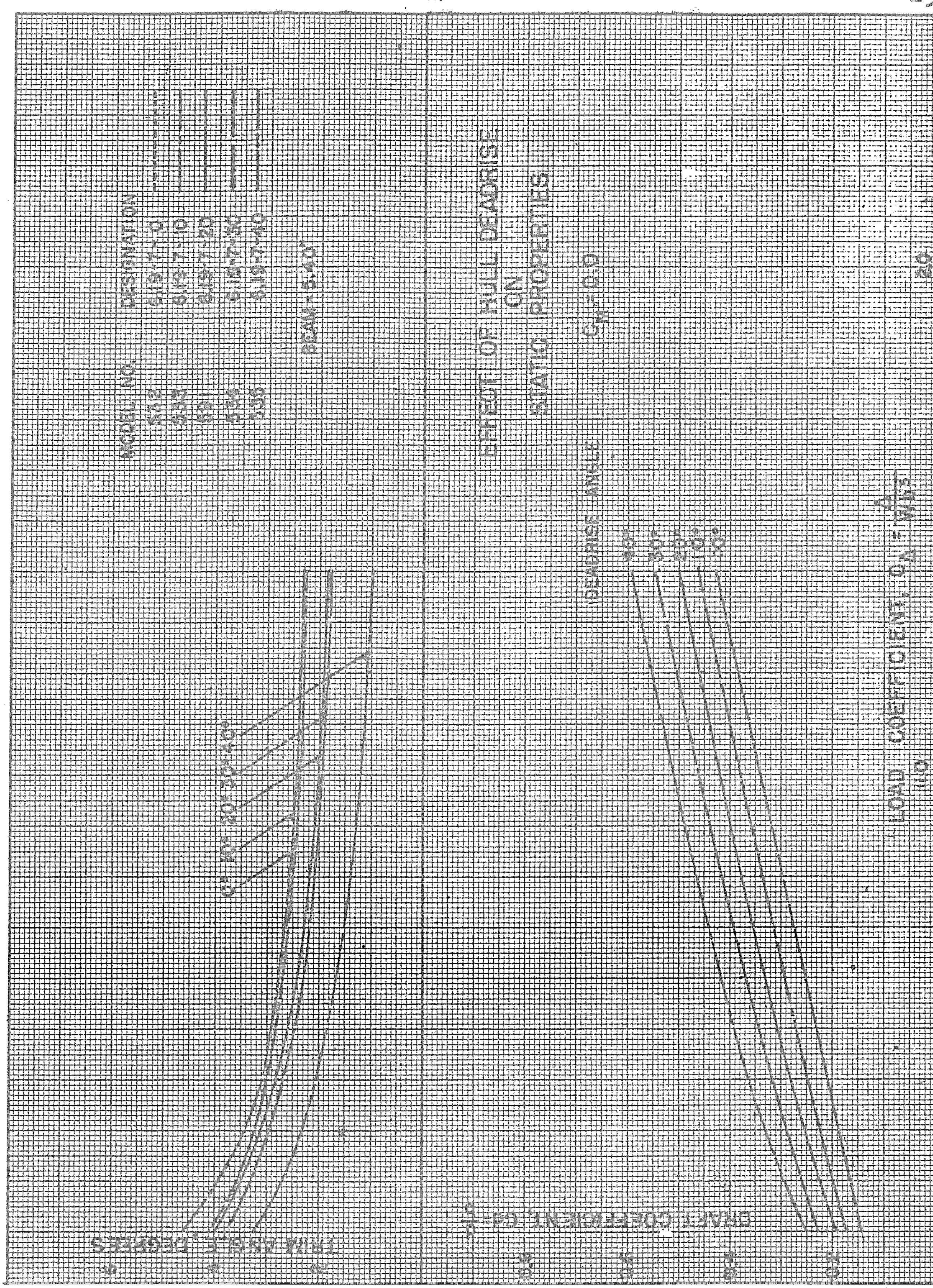

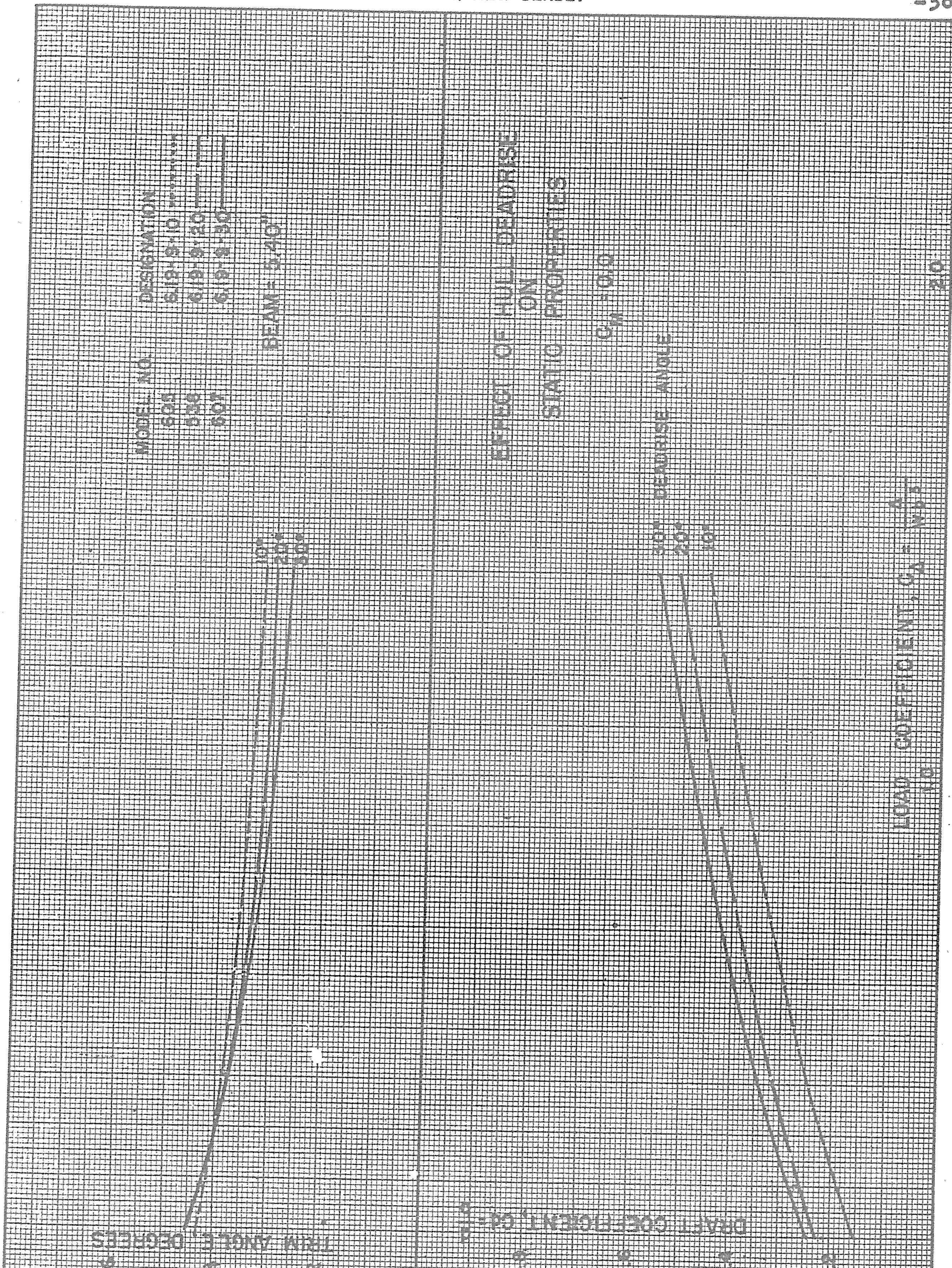
MODEL NO. DESIGNATION
605 6.19-9-10
536 6.19-9-20
607 6.19-9-30
BEAM = 5.40"
EFFECT OF HULL DEADRISE
ON
STATIC PROPERTIES
C_V = 0.0
10°
20°
30°
30° 20° 10° DEADRISE ANGLE
LOAD COEFFICIENT, $C_\Delta = \frac{\Delta}{wb^3}$
1.0
2.0
TRIM ANGLE, DEGREES
6
4
2
DRAFT COEFFICIENT, C_d
1.0
0.8
0.6
0.4
0.2

SUMMARY CHARTS

FOR LENGTH-BEAM RATIO 5.07 HULLS

Pages 57 through 63

EXPERIMENTAL TOWING TANK
STEVENS INSTITUTE OF TECHNOLOGY
HOBOKEN, NEW JERSEY

SUMMARY CHART OF PRINCIPAL HYDRODYNAMIC CHARACTERISTICS

DATE: 3-27-45
MODEL BEAM: 5.40"
C.G. = 0.35 b FWD. OF STEP, 0.90 b ABOVE KEEL
$C_{\Delta_0} = 0.72$ (NOMINAL)
$k/L = 0.234$
DESIGNATION: 5.07-5-10
MODEL NO. 610

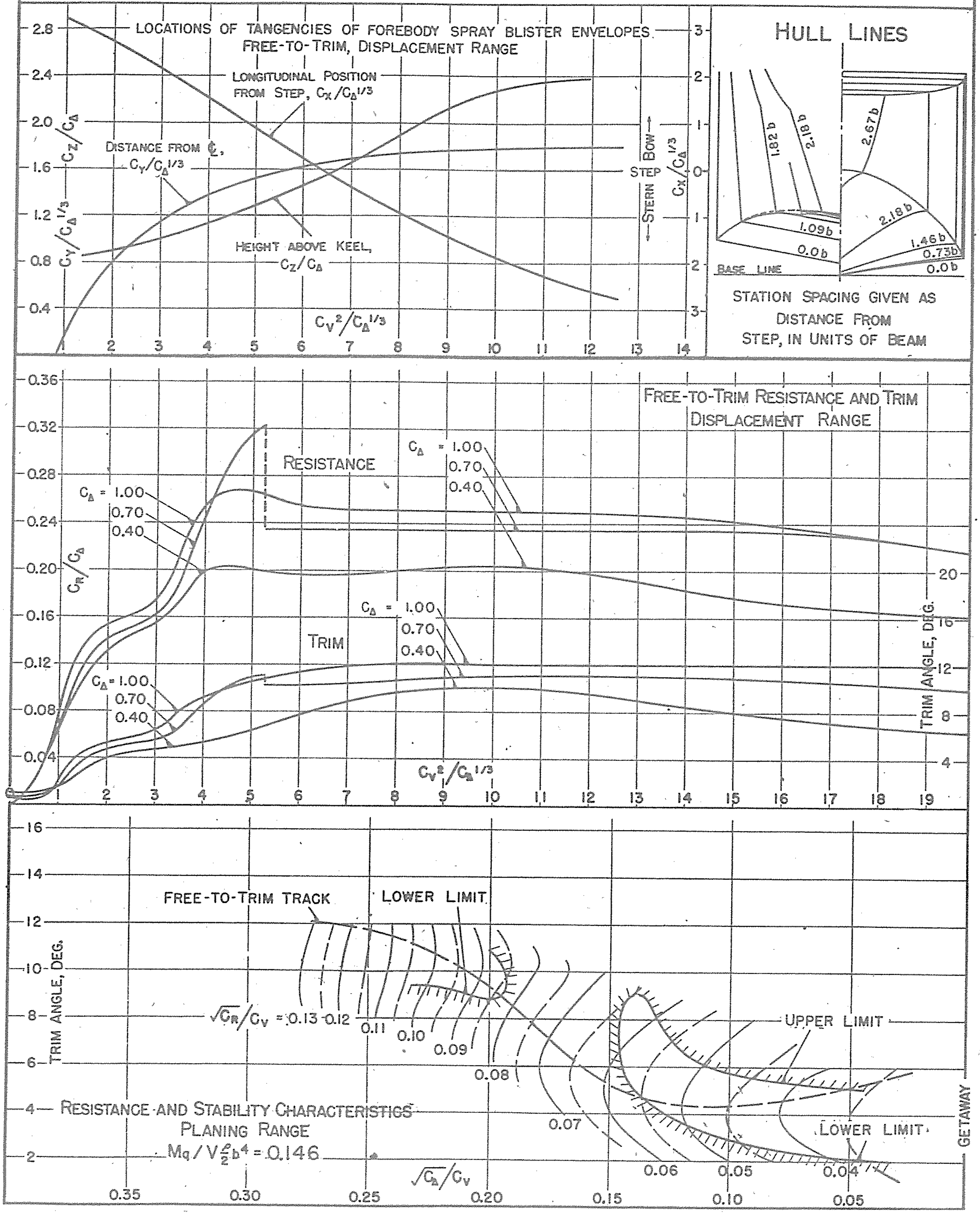

EXPERIMENTAL TOWING TANK
STEVENS INSTITUTE OF TECHNOLOGY
HOBOKEN, NEW JERSEY

SUMMARY CHART OF PRINCIPAL HYDRODYNAMIC CHARACTERISTICS

DATE: 3-27-45
MODEL BEAM: 5.40"
C.G.= 0.35 b FWD. OF STEP, 0.90 b ABOVE KEEL
C_{Δ_0} = 0.72 (NOMINAL)
k/L=0.234
DESIGNATION: 5.07-9-10
MODEL NO. 611

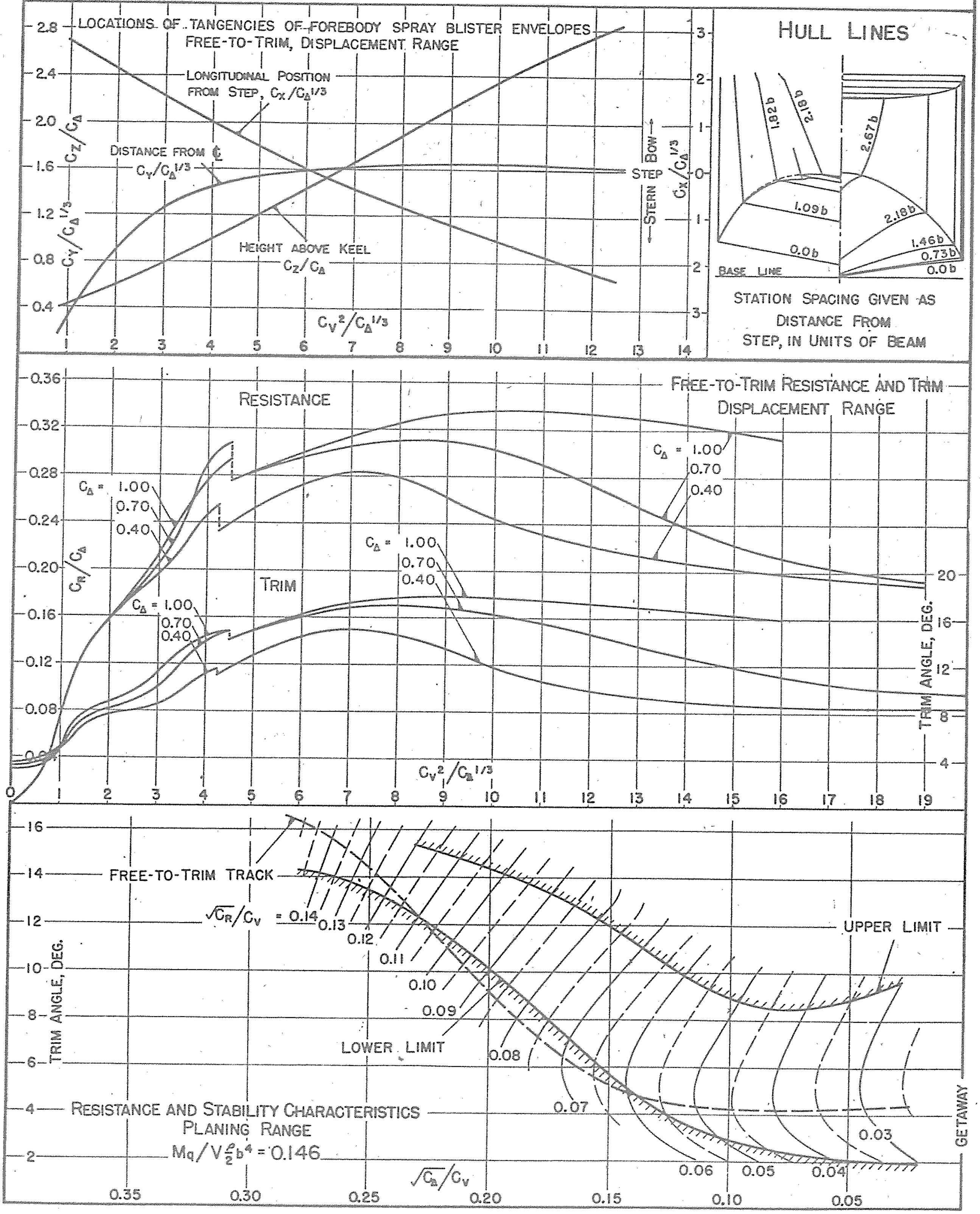

EXPERIMENTAL TOWING TANK
STEVENS INSTITUTE OF TECHNOLOGY
HOBOKEN, NEW JERSEY

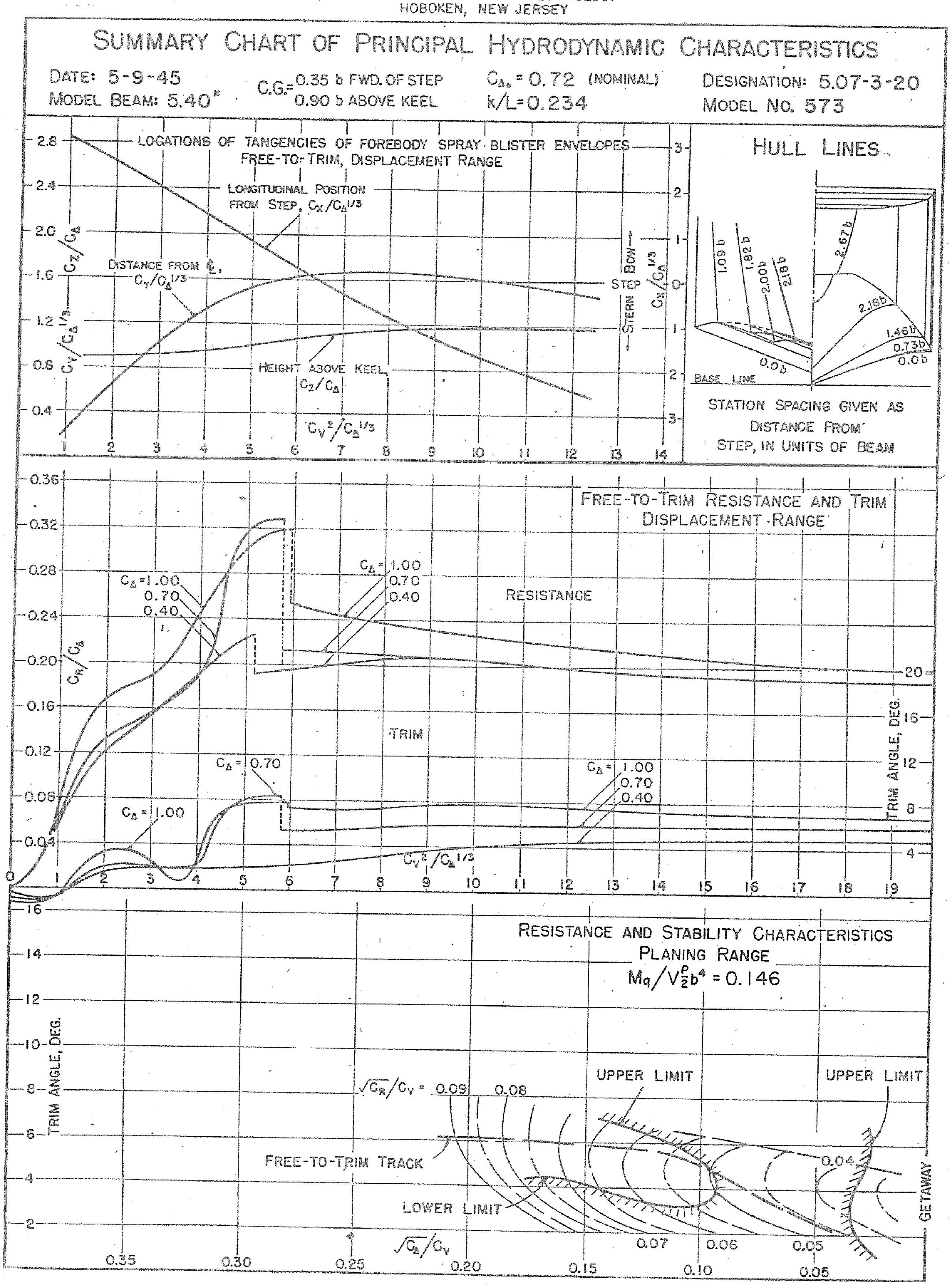

EXPERIMENTAL TOWING TANK
STEVENS INSTITUTE OF TECHNOLOGY
HOBOKEN, NEW JERSEY

SUMMARY CHART OF PRINCIPAL HYDRODYNAMIC CHARACTERISTICS

DATE: 5-9-45
MODEL BEAM: 5.40"
C.G.= 0.35 b FWD. OF STEP, 0.90 b ABOVE KEEL
C_{Δ_0} = 0.72 (NOMINAL)
k/L=0.234
DESIGNATION: 5.07-7-20
MODEL NO. 339-22

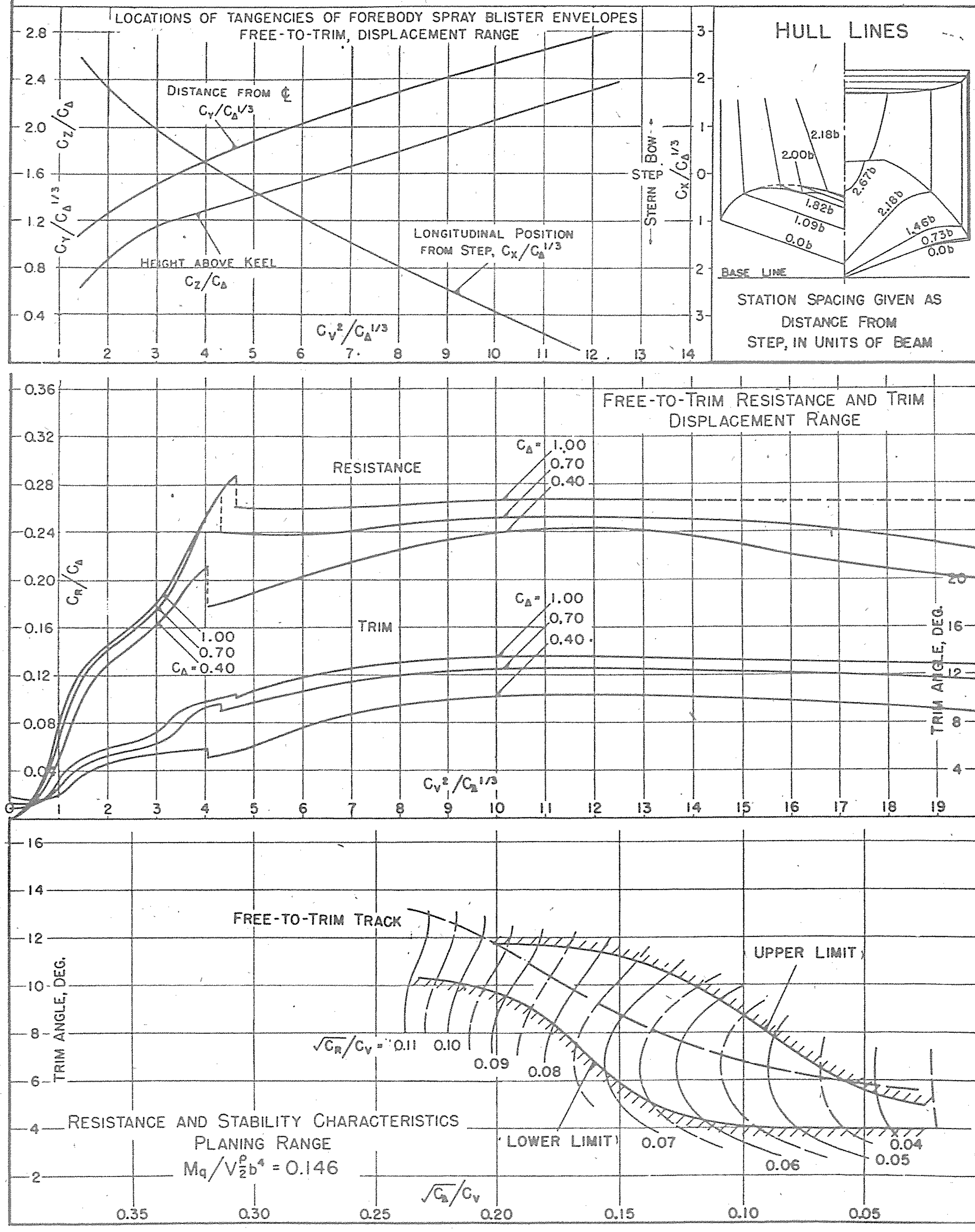

EXPERIMENTAL TOWING TANK
STEVENS INSTITUTE OF TECHNOLOGY
HOBOKEN, NEW JERSEY

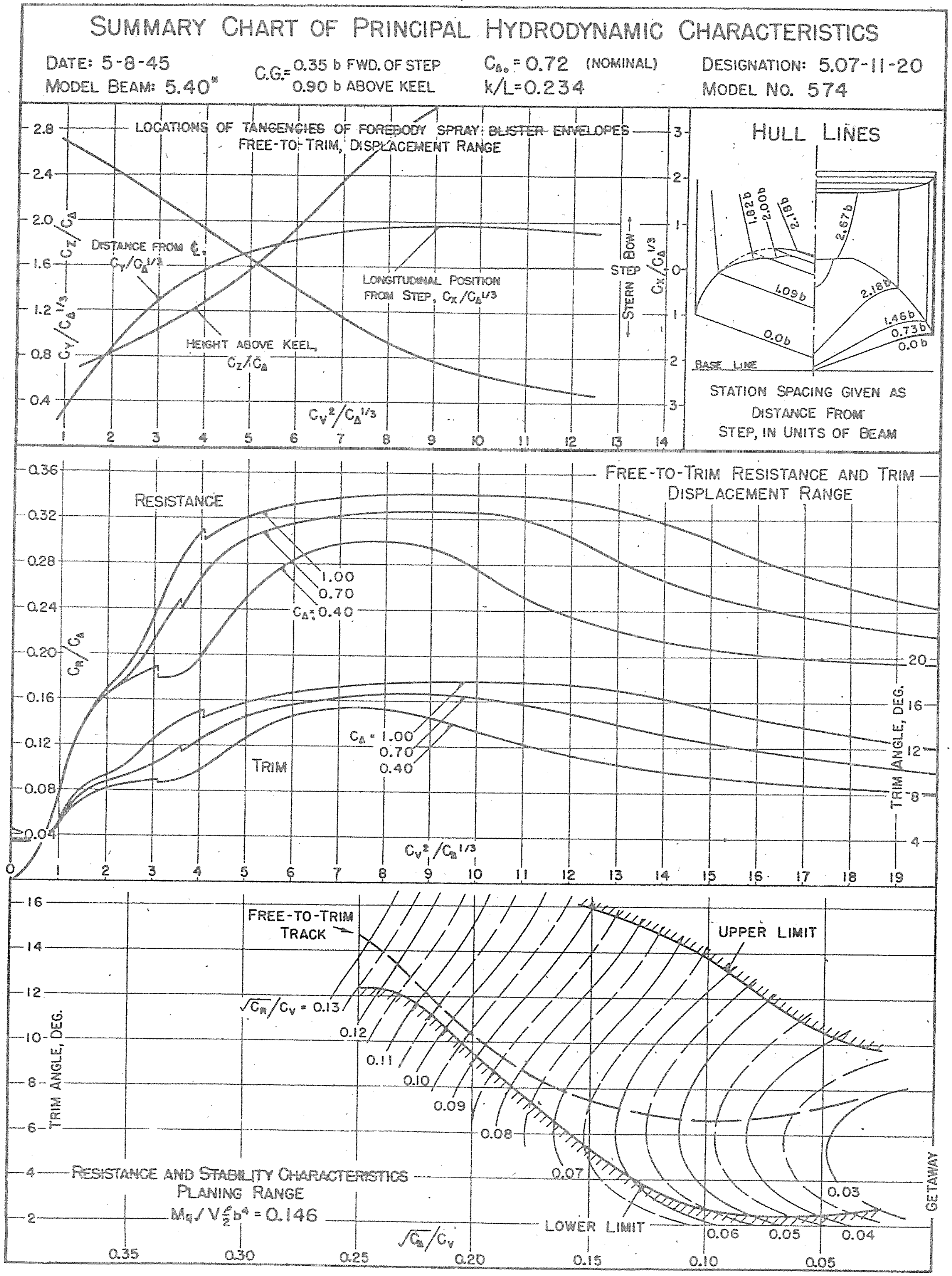

EXPERIMENTAL TOWING TANK
STEVENS INSTITUTE OF TECHNOLOGY
HOBOKEN, NEW JERSEY

SUMMARY CHART OF PRINCIPAL HYDRODYNAMIC CHARACTERISTICS

DATE: 3-27-45
MODEL BEAM: 5.40"
C.G.= 0.35 b FWD. OF STEP, 0.90 b ABOVE KEEL
C_{Δ_0} = 0.72 (NOMINAL)
k/L = 0.234
DESIGNATION: 5.07-5-30
MODEL NO. 612

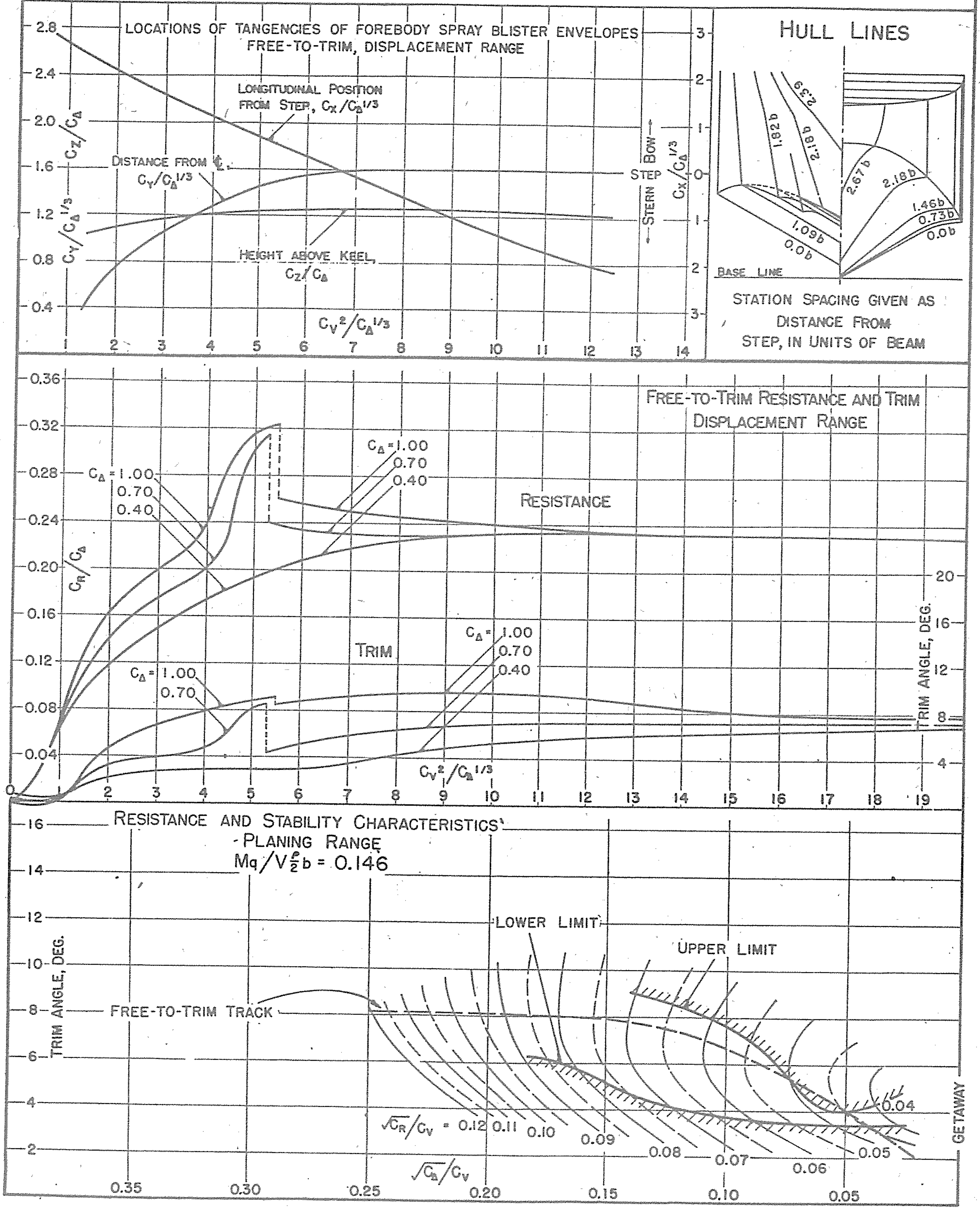

EXPERIMENTAL TOWING TANK
STEVENS INSTITUTE OF TECHNOLOGY
HOBOKEN, NEW JERSEY

SUMMARY CHART OF PRINCIPAL HYDRODYNAMIC CHARACTERISTICS

DATE: 3-27-45
MODEL BEAM: 5.40"
C.G.= 0.35 b FWD. OF STEP, 0.90 b ABOVE KEEL
C_{Δ_0} = 0.72 (NOMINAL)
k/L = 0.234
DESIGNATION: 5.07-9-30
MODEL NO. 613

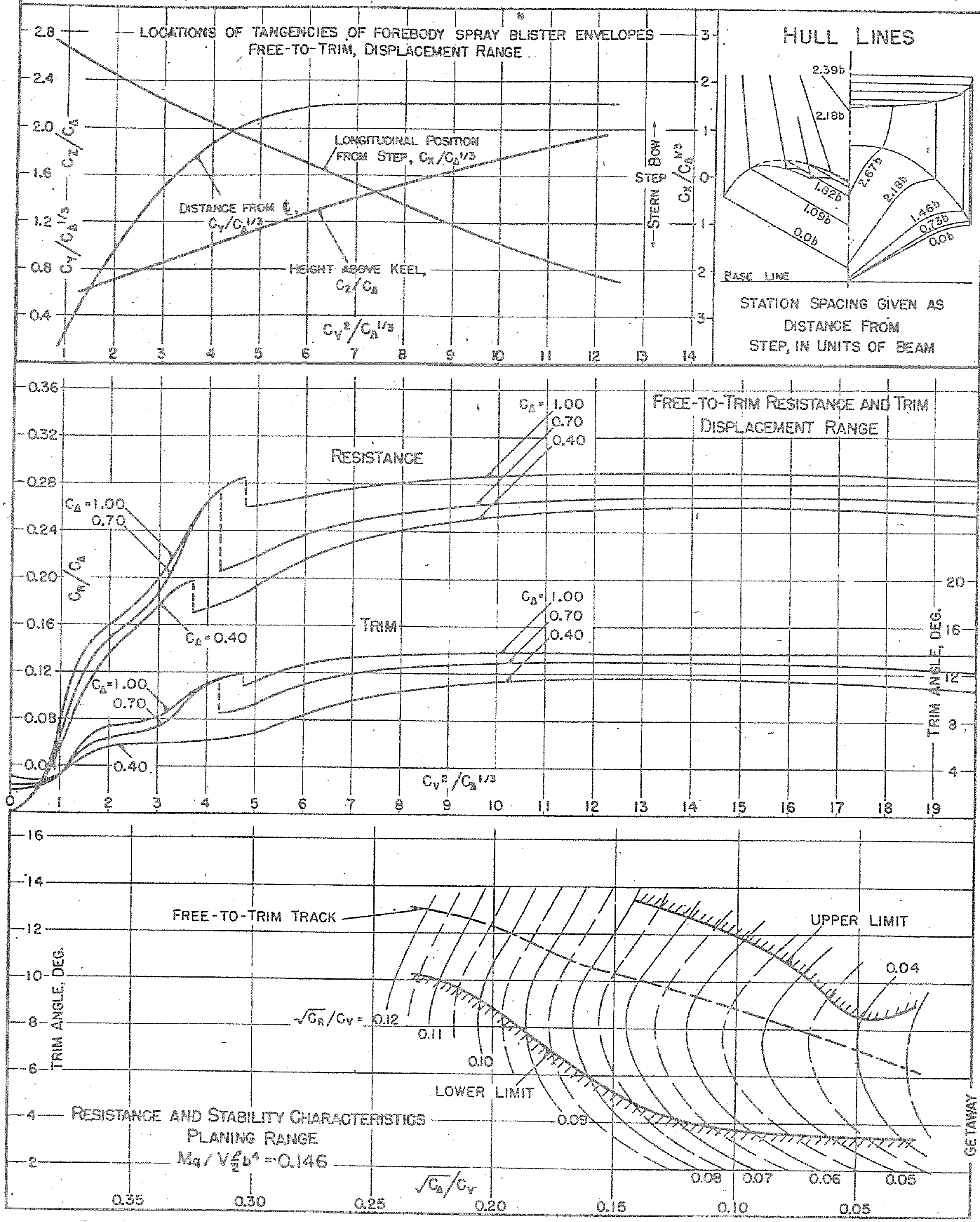

SUMMARY CHARTS

FOR LENGTH-BEAM RATIO 6.19 HULLS

Pages 64 through 80

EXPERIMENTAL TOWING TANK
STEVENS INSTITUTE OF TECHNOLOGY
HOBOKEN, NEW JERSEY

SUMMARY CHART OF PRINCIPAL HYDRODYNAMIC CHARACTERISTICS

DATE: 8-8-44, 12-26-45 (REVISED) C.G.= 0.35b FWD. OF STEP, 0.90b ABOVE KEEL C_{Δ_0} = 1.07 (NOMINAL) DESIGNATION: 6.19-3-0
MODEL BEAM: 5.40" k/L = 0.225 MODEL No. 556

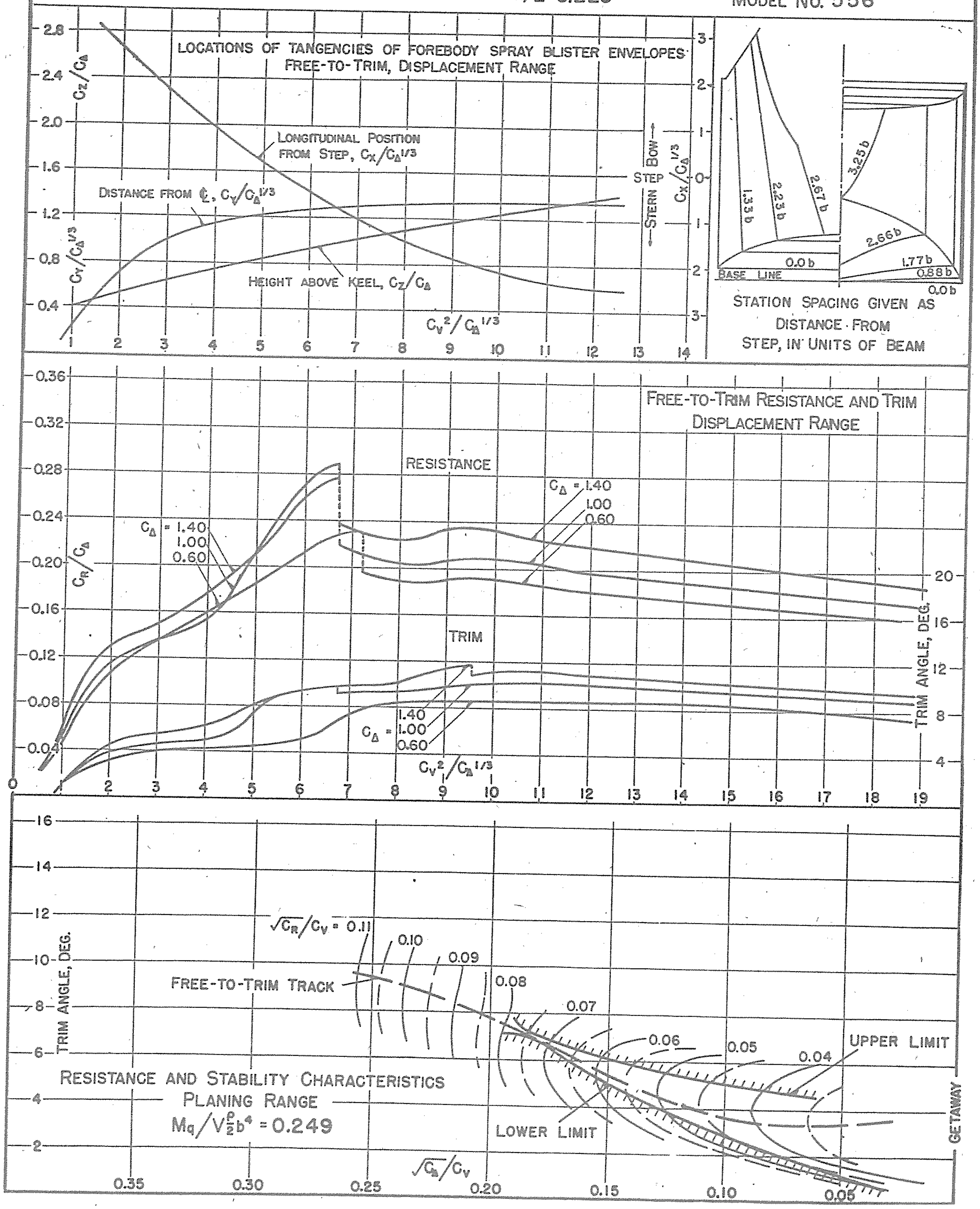

EXPERIMENTAL TOWING TANK
STEVENS INSTITUTE OF TECHNOLOGY
HOBOKEN, NEW JERSEY

SUMMARY CHART OF PRINCIPAL HYDRODYNAMIC CHARACTERISTICS

DATE: 8-8-44, 7-20-45 (REVISED)
C.G. = 0.35b FWD. OF STEP, 0.90b ABOVE KEEL
C_{Δ_0} = 1.07 (NOMINAL)
DESIGNATION: 6.19-7-0
MODEL BEAM: 5.40"
k/L = 0.225
MODEL NO. 532

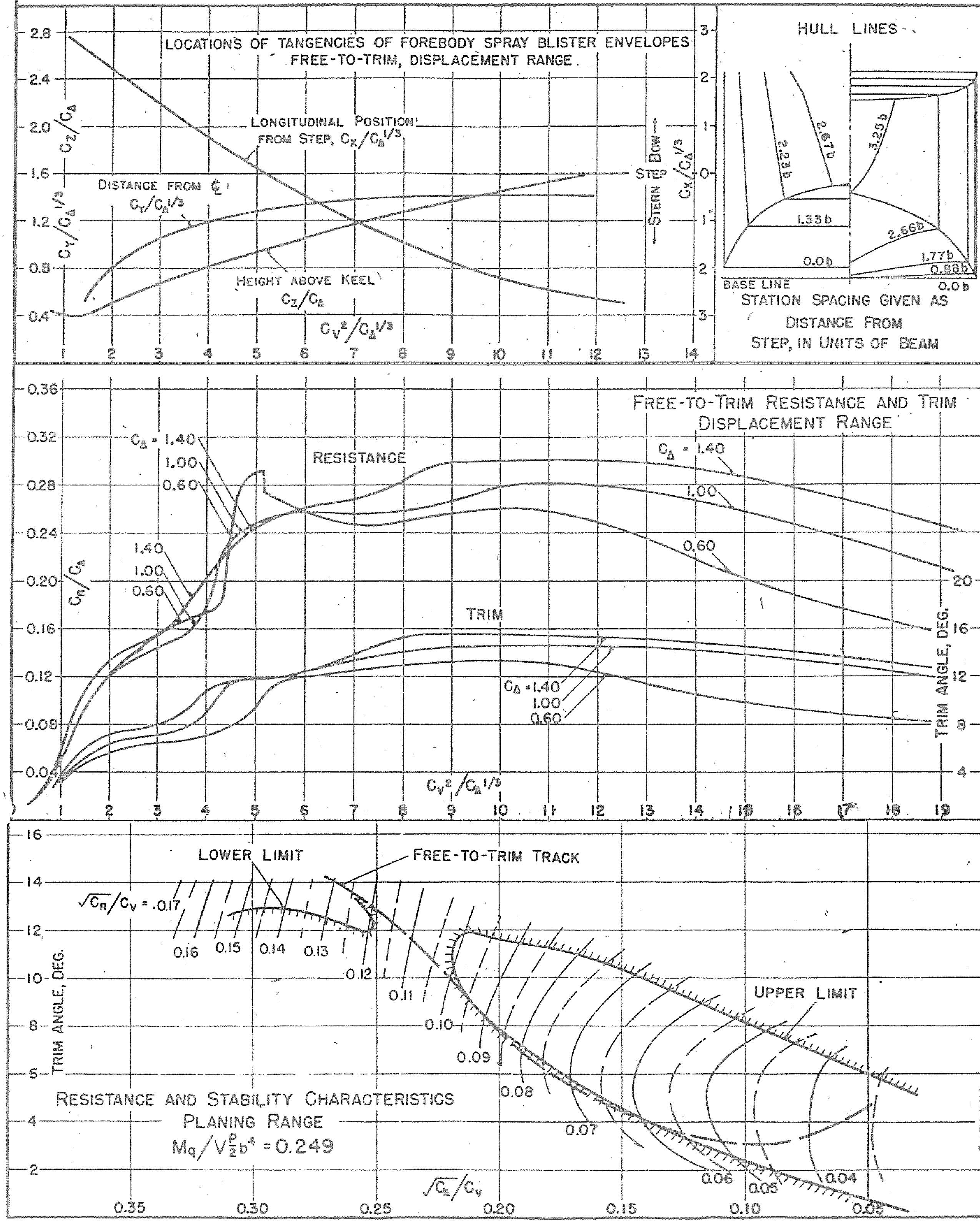

SUMMARY CHART OF PRINCIPAL HYDRODYNAMIC CHARACTERISTICS

DATE: 8-8-44, 12-4-45 (REVISED)
C.G. = 0.35b FWD. OF STEP, 0.90b ABOVE KEEL
C_{Δ_0} = 1.07 (NOMINAL)
DESIGNATION: 6.19-11-0
MODEL BEAM: 5.40"
k/L = 0.225
MODEL NO. 557

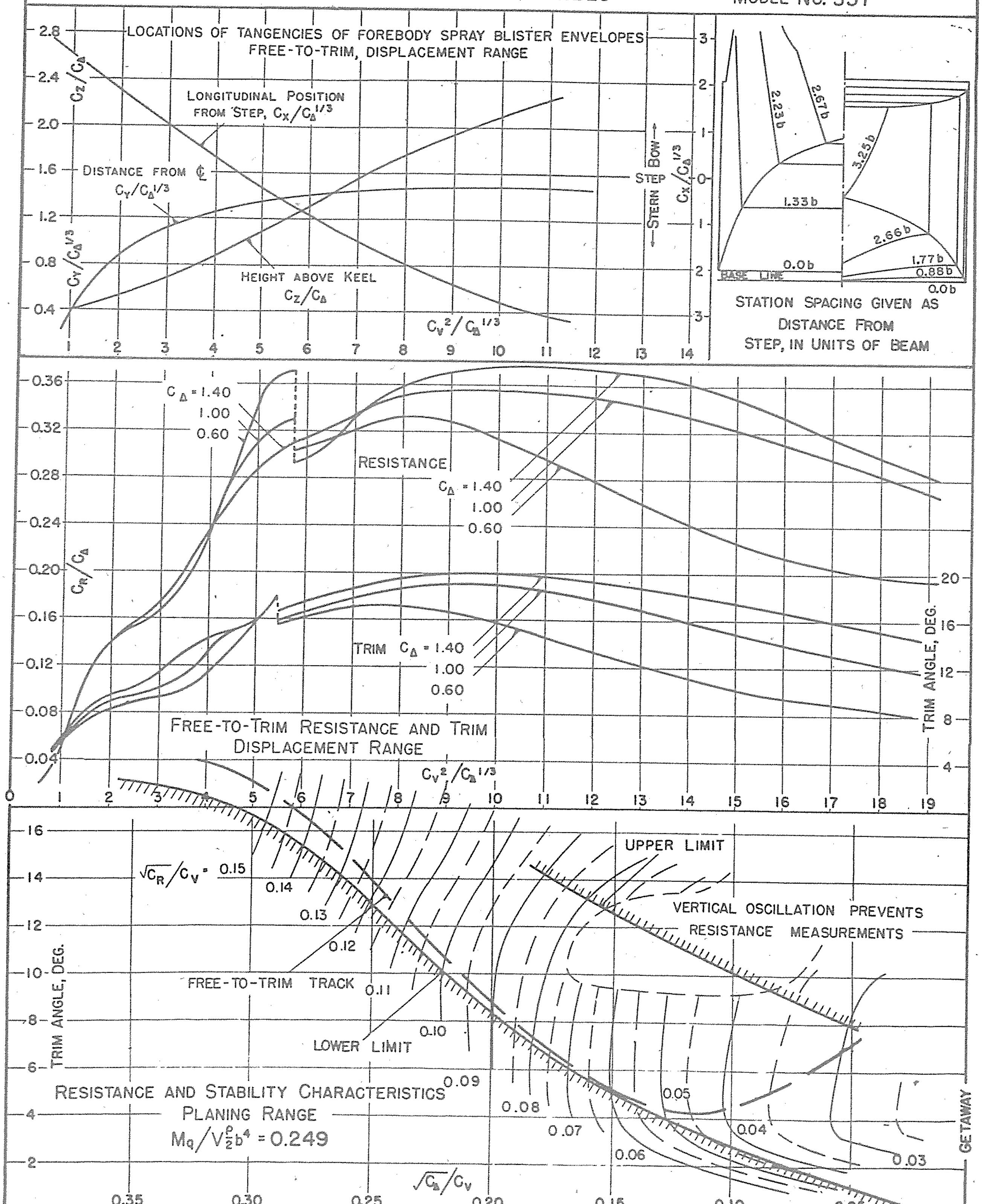

EXPERIMENTAL TOWING TANK
STEVENS INSTITUTE OF TECHNOLOGY
HOBOKEN, NEW JERSEY

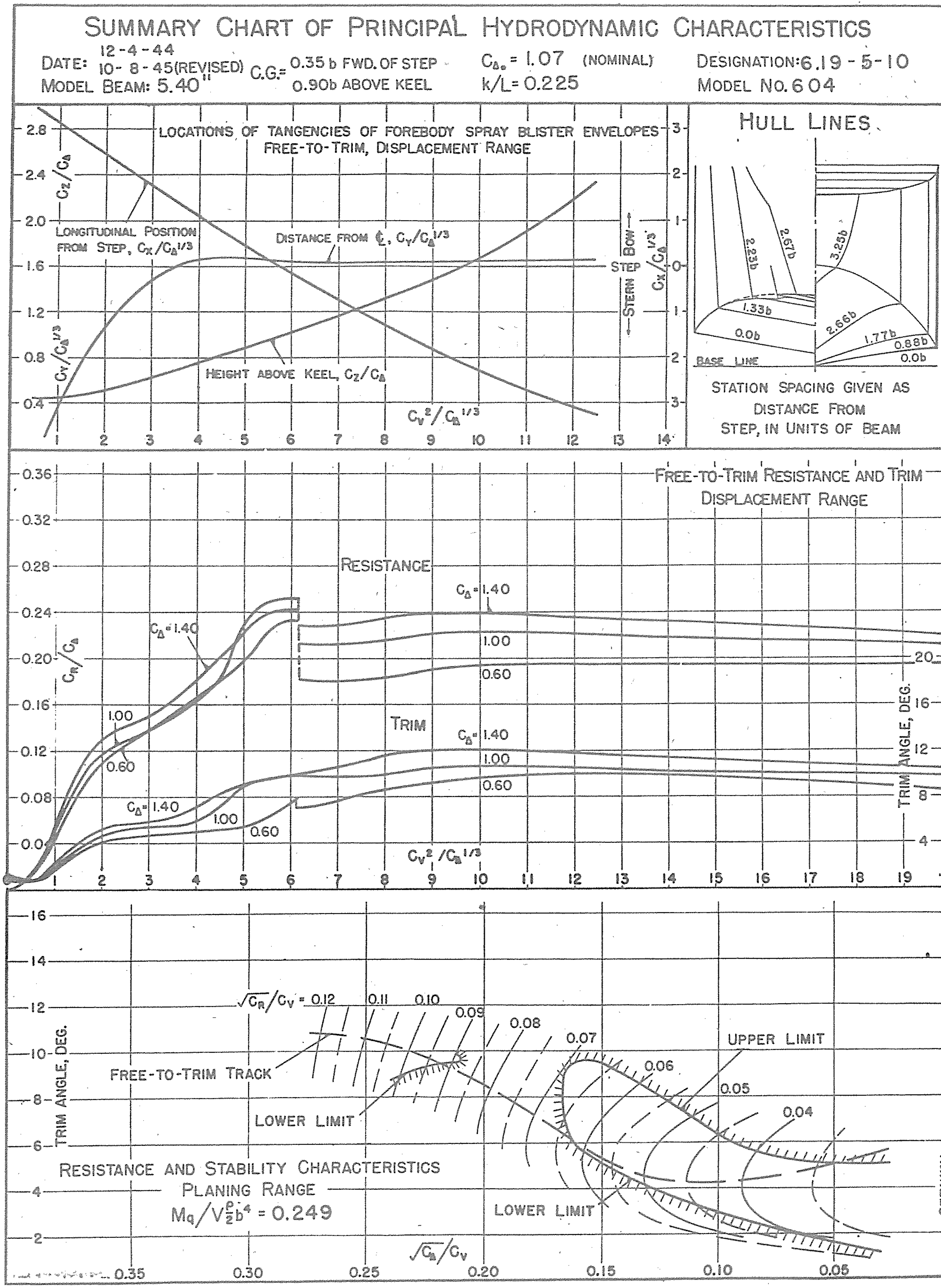

EXPERIMENTAL TOWING TANK
STEVENS INSTITUTE OF TECHNOLOGY
HOBOKEN, NEW JERSEY

SUMMARY CHART OF PRINCIPAL HYDRODYNAMIC CHARACTERISTICS

DATE: 8-8-44 / 7-13-45(REVISED) C.G.= 0.35b FWD. OF STEP / 0.90b ABOVE KEEL C_{Δ_0} = 1.07 (NOMINAL) DESIGNATION: 6.19-7-10
MODEL BEAM: 5.40" k/L = 0.225 MODEL No. 533

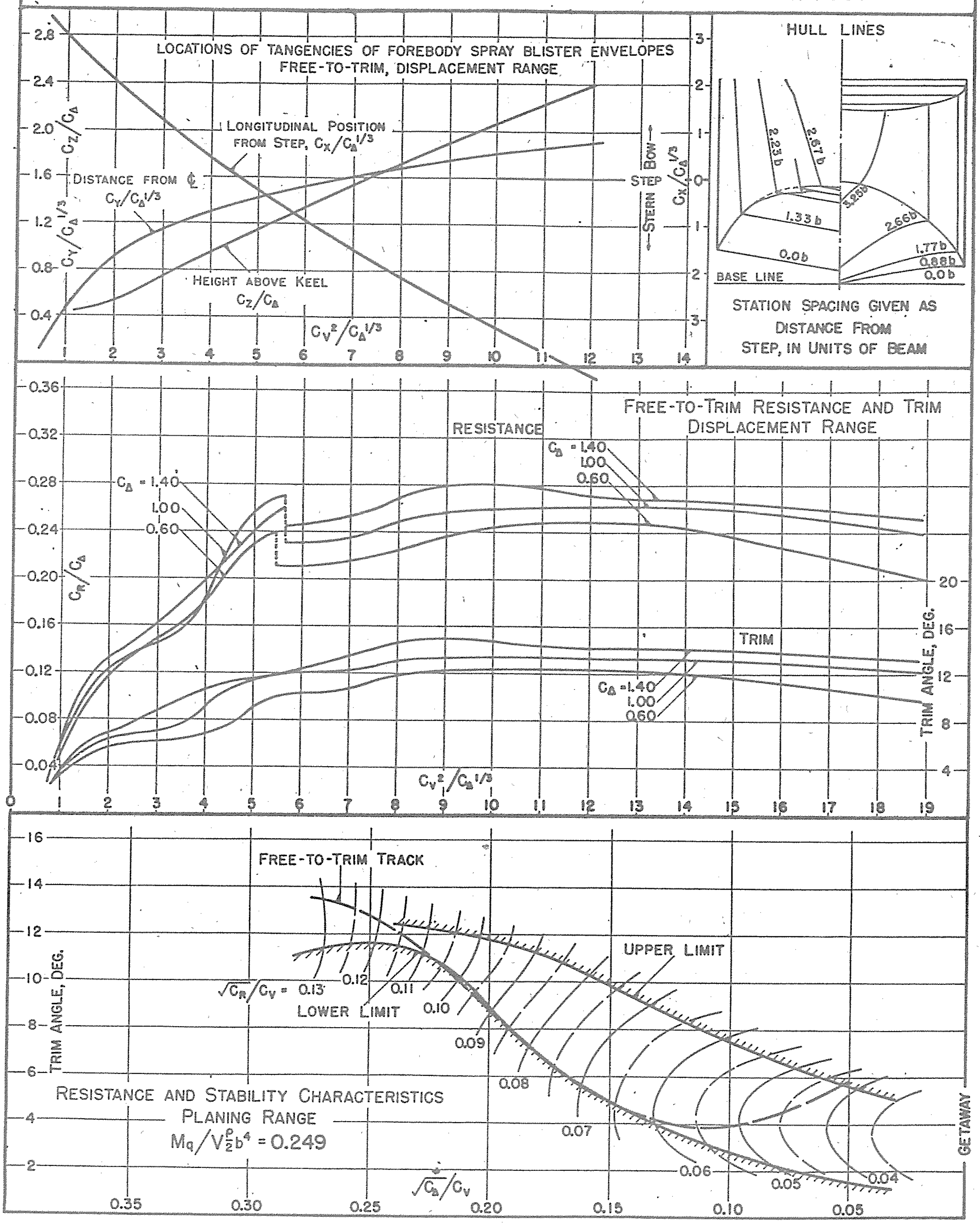

EXPERIMENTAL TOWING TANK
STEVENS INSTITUTE OF TECHNOLOGY
HOBOKEN, NEW JERSEY

SUMMARY CHART OF PRINCIPAL HYDRODYNAMIC CHARACTERISTICS

DATE: 12-23-44, 10-23-45 (REVISED)
MODEL BEAM: 5.40"
C.G. = 0.35b FWD. OF STEP; 0.90b ABOVE KEEL
$C_{\Delta_0} = 1.07$ (NOMINAL)
$k/L = 0.225$
DESIGNATION: 6.19-9-10
MODEL NO. 605

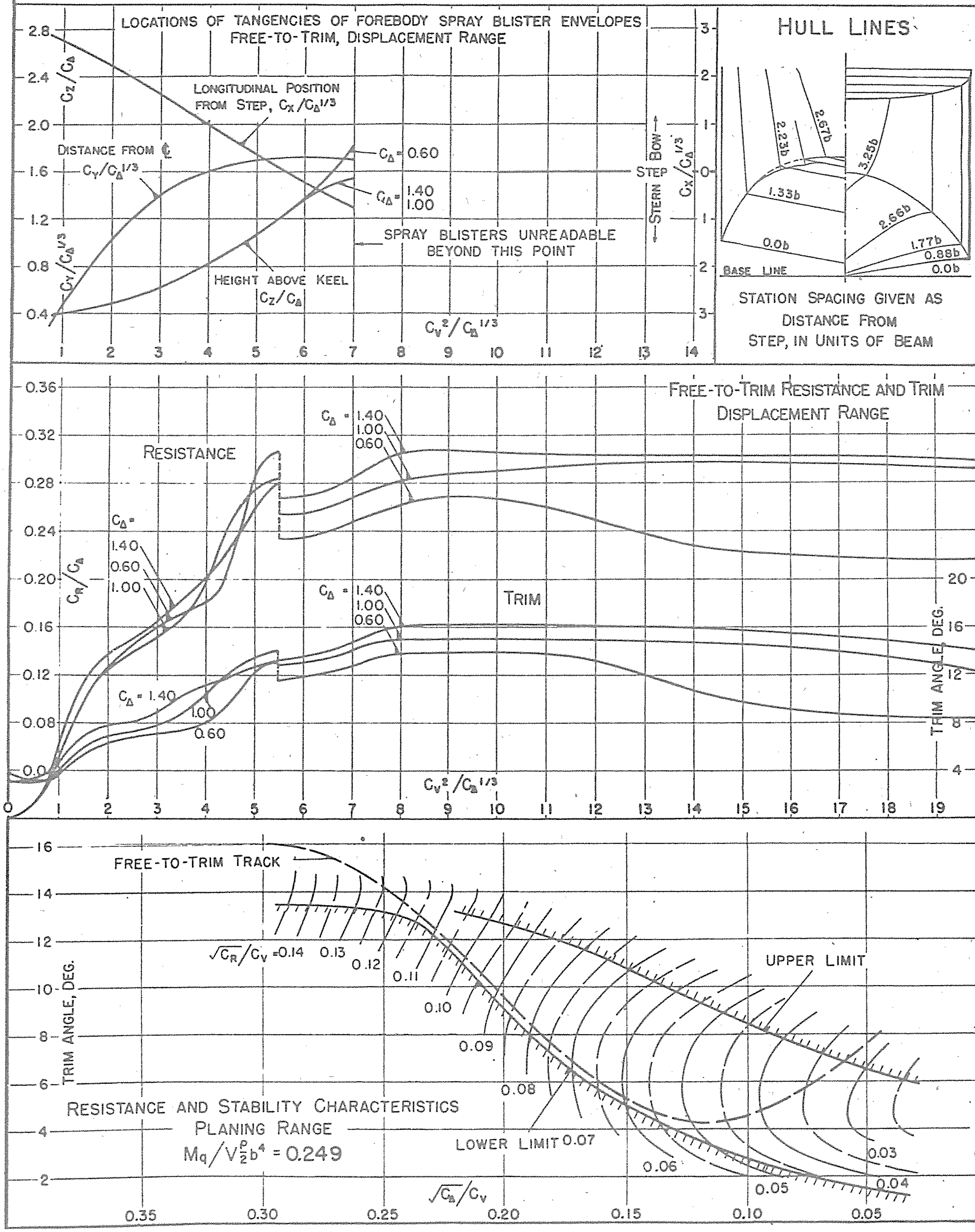

EXPERIMENTAL TOWING TANK
STEVENS INSTITUTE OF TECHNOLOGY
HOBOKEN, NEW JERSEY

SUMMARY CHART OF PRINCIPAL HYDRODYNAMIC CHARACTERISTICS

DATE: 8-8-44, 10-23-45 (REVISED)
MODEL BEAM: 5.40"
C.G. = 0.35b FWD. OF STEP, 0.90b ABOVE KEEL
C_{Δ_0} = 1.07 (NOMINAL)
k/L = 0.225
DESIGNATION: 6.19-3-20
MODEL NO. 536

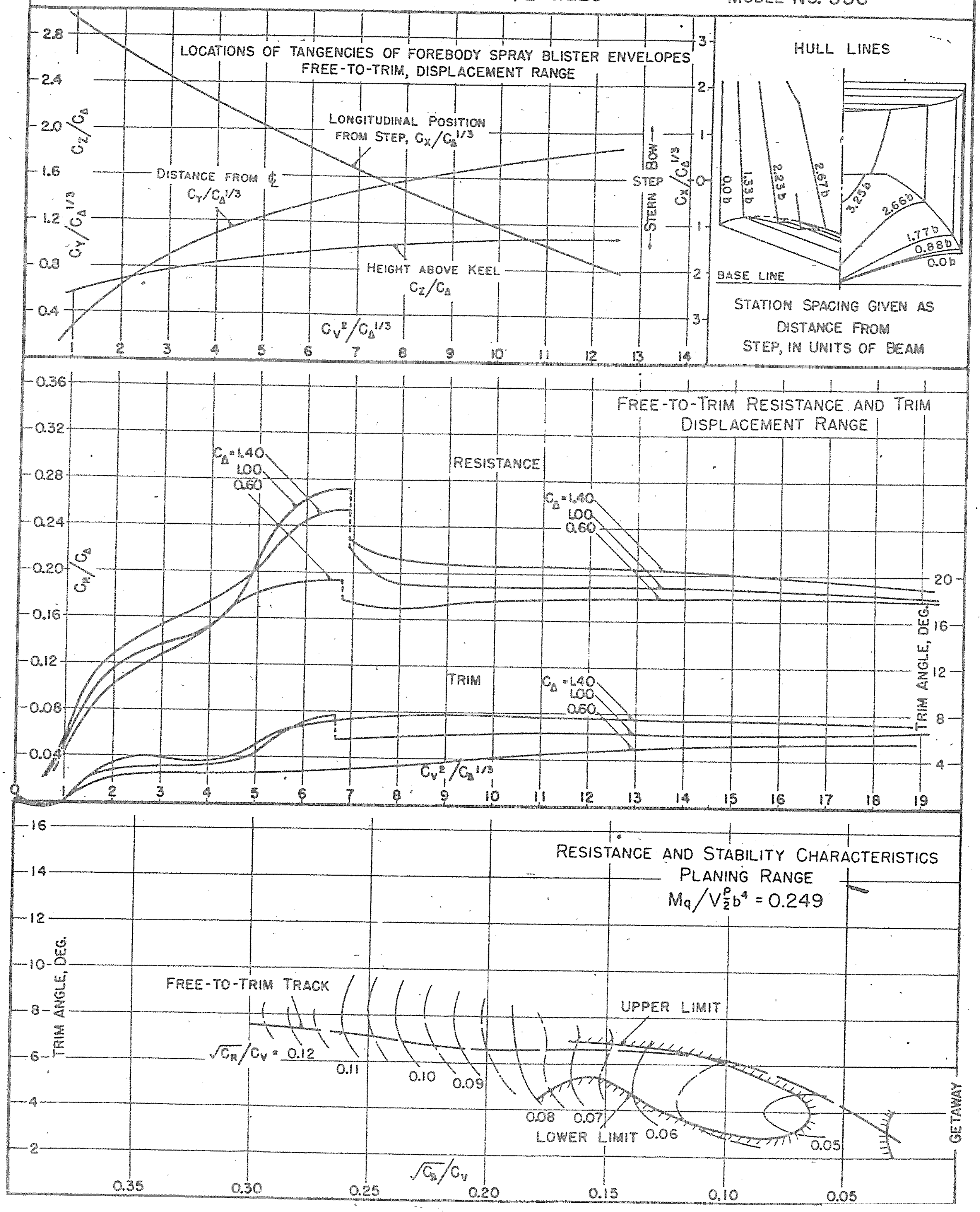

EXPERIMENTAL TOWING TANK
STEVENS INSTITUTE OF TECHNOLOGY
HOBOKEN, NEW JERSEY

SUMMARY CHART OF PRINCIPAL HYDRODYNAMIC CHARACTERISTICS

DATE: 8-8-44 9-18-45 (REVISED)	C.G.= 0.35b FWD. OF STEP	C_{Δ_0} = 1.07 (NOMINAL)	DESIGNATION: 6.19-5-20
MODEL BEAM: 5.40"	0.90b ABOVE KEEL	k/L = 0.225	MODEL NO. 537

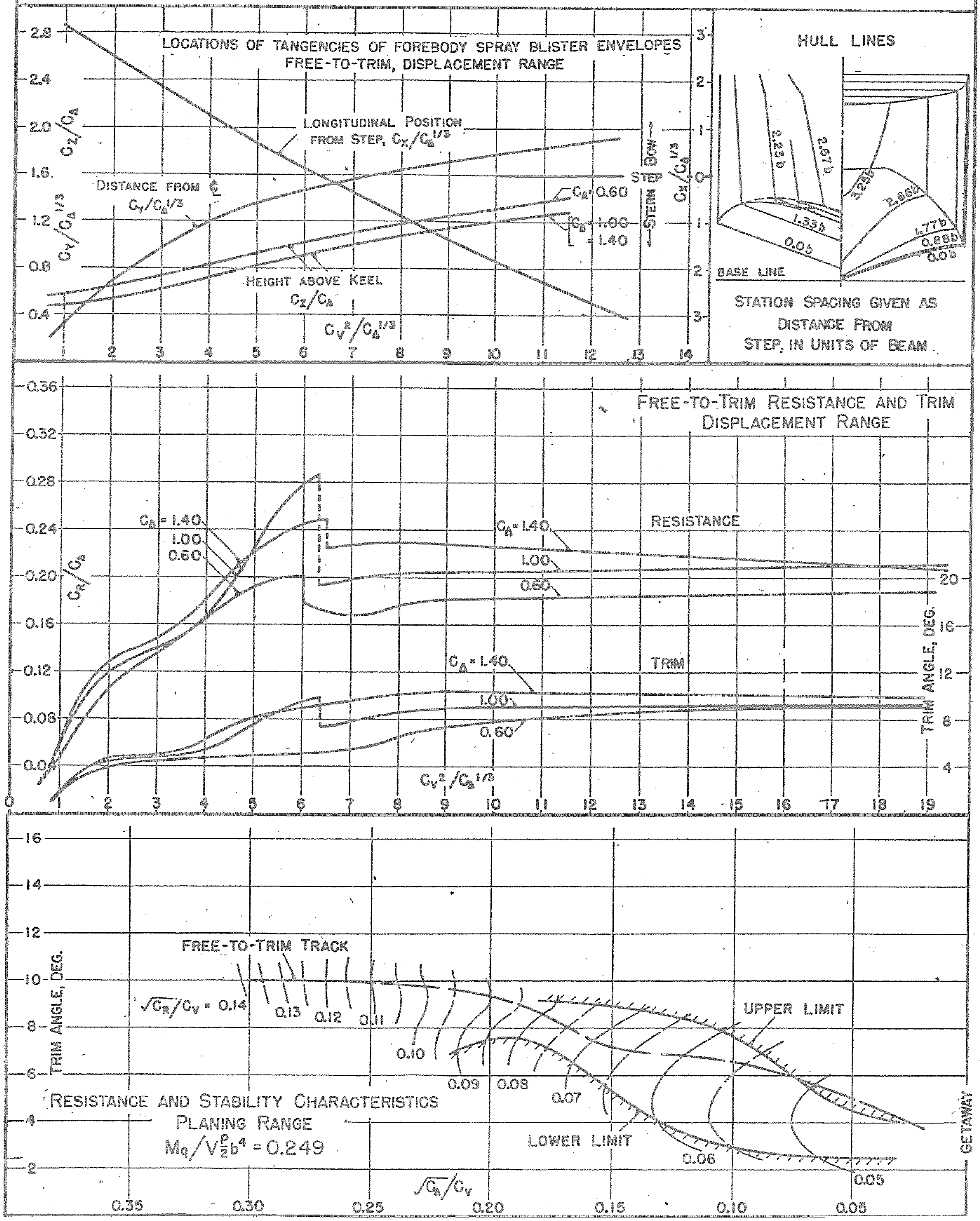

EXPERIMENTAL TOWING TANK
STEVENS INSTITUTE OF TECHNOLOGY
HOBOKEN, NEW JERSEY

SUMMARY CHART OF PRINCIPAL HYDRODYNAMIC CHARACTERISTICS

DATE: 11-4-43, 8-15-45 (REVISED)
MODEL BEAM: 5.40"
C.G.= 0.35b FWD. OF STEP, 0.90b ABOVE KEEL
C_{Δ_0} = 1.07 (NOMINAL)
k/L = 0.225
DESIGNATION: 6.19-7-20
MODEL No. 591

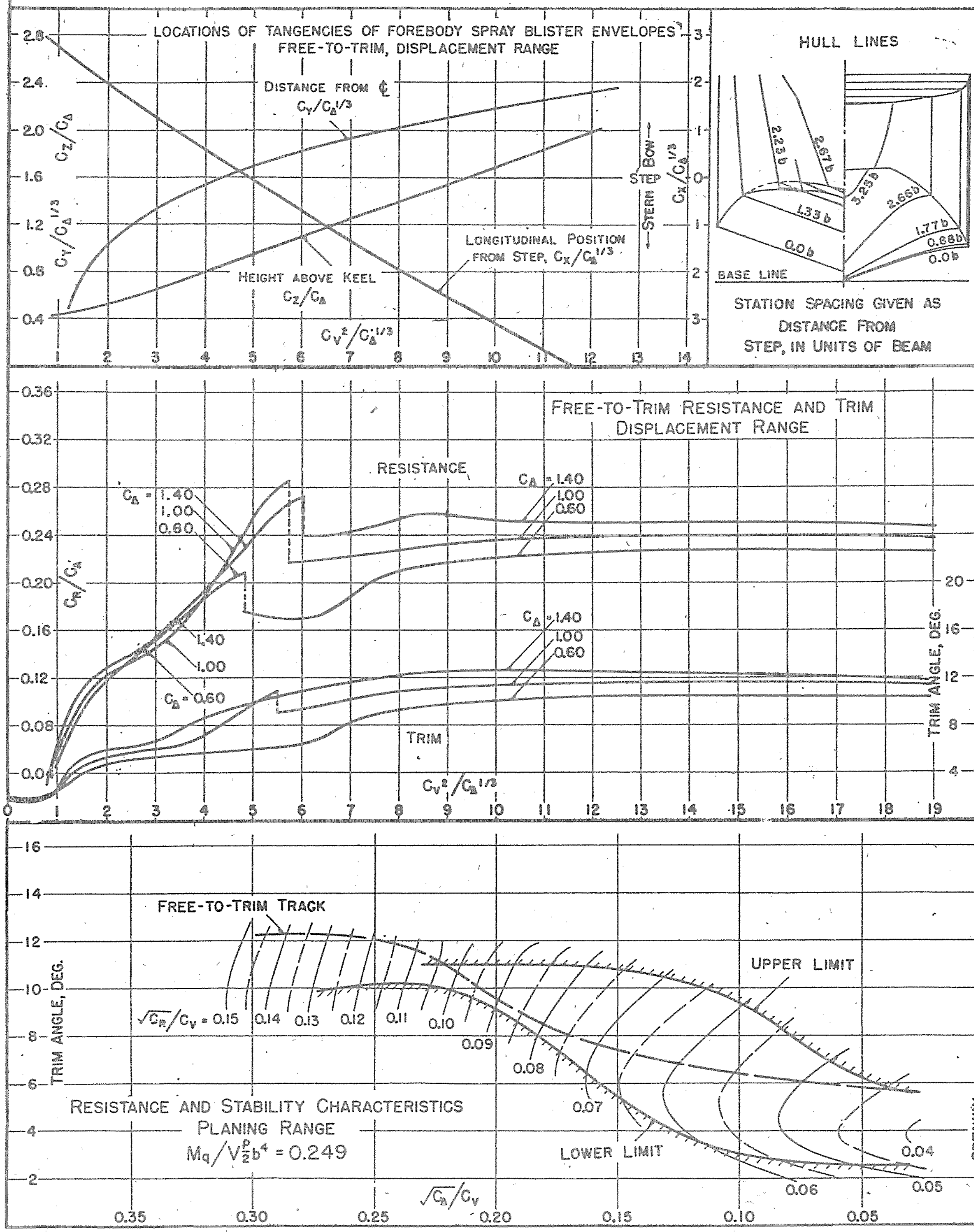

EXPERIMENTAL TOWING TANK
STEVENS INSTITUTE OF TECHNOLOGY
HOBOKEN, NEW JERSEY

SUMMARY CHART OF PRINCIPAL HYDRODYNAMIC CHARACTERISTICS

DATE: 8-8-44, 10-25-45 (REVISED)	C.G. = 0.35b FWD. OF STEP	C_{Δ_0} = 1.07 (NOMINAL)	DESIGNATION: 6.19-9-20
MODEL BEAM: 5.40"	0.90b ABOVE KEEL	k/L = 0.225	MODEL No. 538

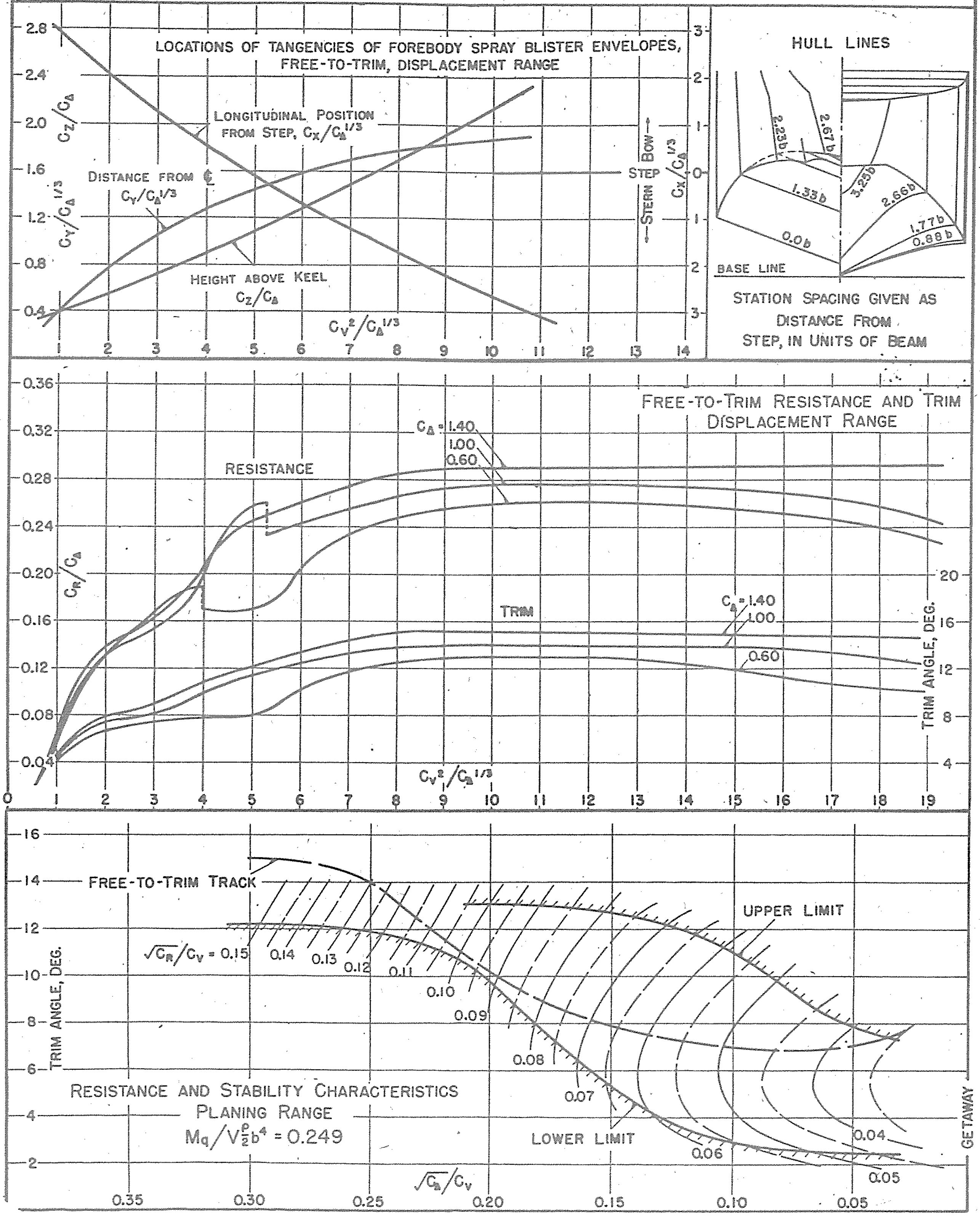

EXPERIMENTAL TOWING TANK
STEVENS INSTITUTE OF TECHNOLOGY
HOBOKEN, NEW JERSEY

SUMMARY CHART OF PRINCIPAL HYDRODYNAMIC CHARACTERISTICS

DATE: 8-8-44, 10-12-45 (REVISED)
C.G. = 0.35b FWD. OF STEP, 0.90b ABOVE KEEL
C_{Δ_0} = 1.07 (NOMINAL)
k/L = 0.225
DESIGNATION: 6.19-11-20
MODEL BEAM: 5.40"
MODEL No. 539

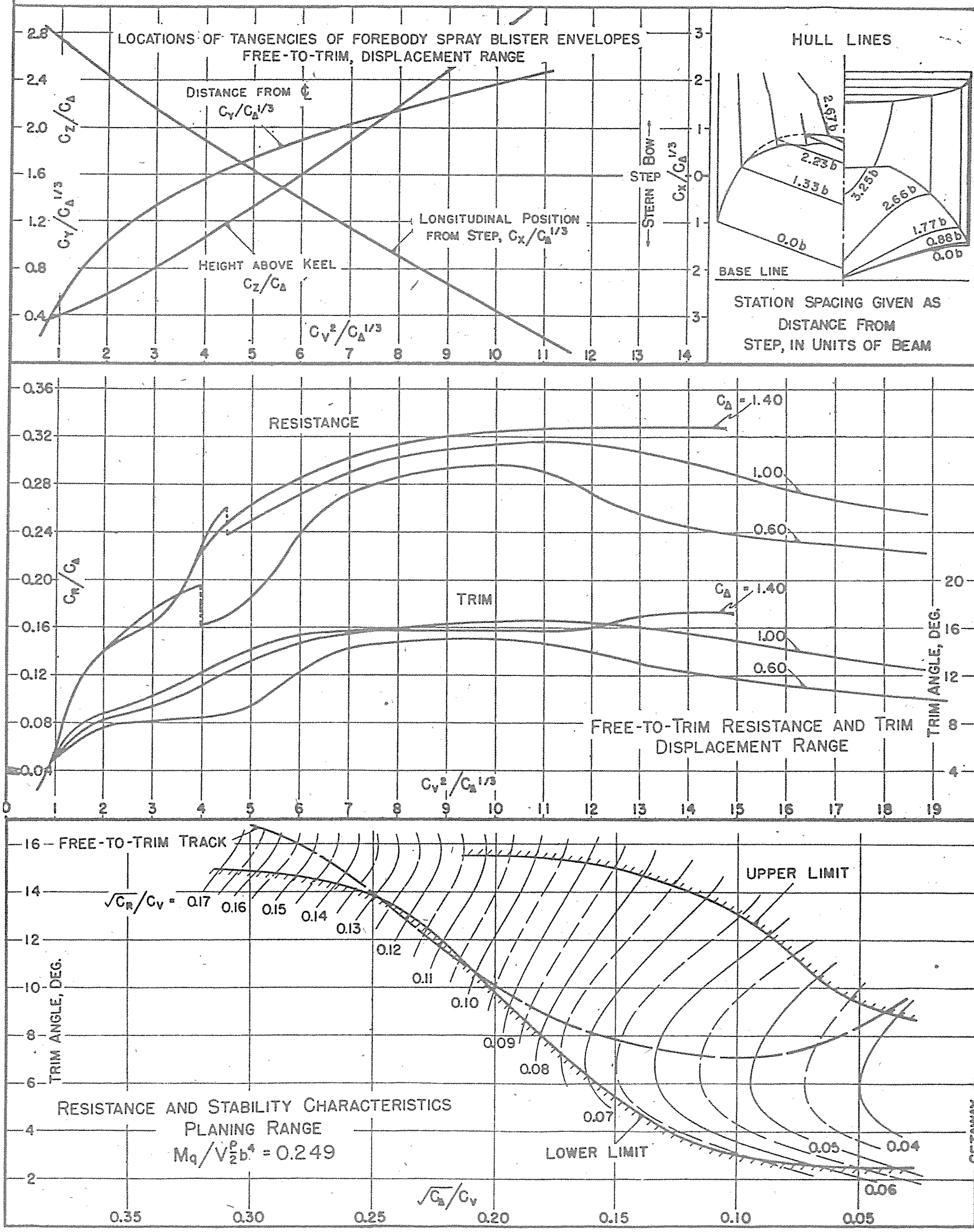

EXPERIMENTAL TOWING TANK
STEVENS INSTITUTE OF TECHNOLOGY
HOBOKEN, NEW JERSEY

SUMMARY CHART OF PRINCIPAL HYDRODYNAMIC CHARACTERISTICS

DATE: 12-6-44, 9-17-45 (REVISED)
C.G. = 0.35b FWD. OF STEP, 0.90b ABOVE KEEL
C_{Δ_0} = 1.07 (NOMINAL)
k/L = 0.225
DESIGNATION: 6.19-5-30
MODEL BEAM: 5.40"
MODEL NO. 606

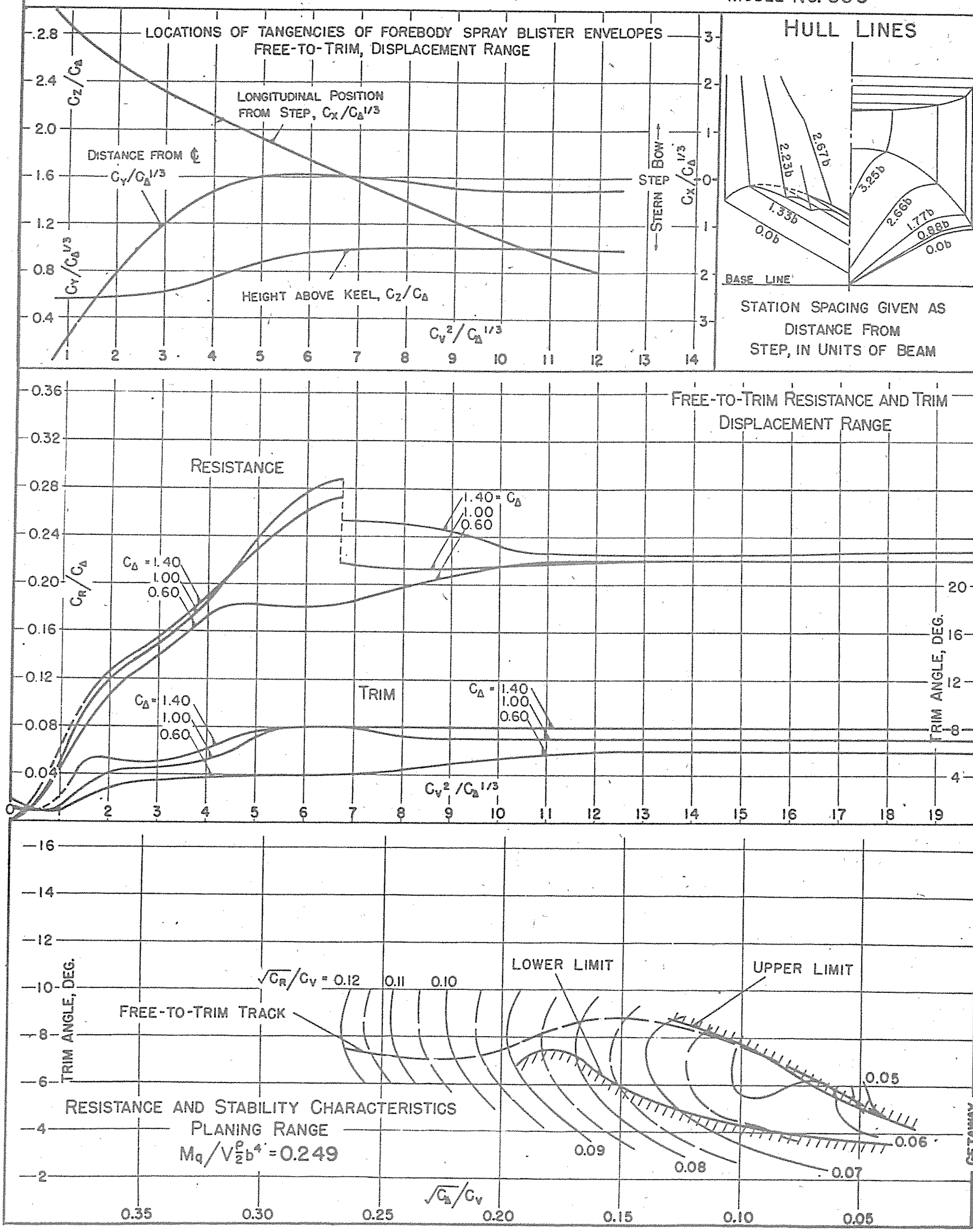

EXPERIMENTAL TOWING TANK
STEVENS INSTITUTE OF TECHNOLOGY
HOBOKEN, NEW JERSEY

SUMMARY CHART OF PRINCIPAL HYDRODYNAMIC CHARACTERISTICS

DATE: 8-8-44, 7-25-45 (REVISED) C.G.= 0.35b FWD. OF STEP, 0.90b ABOVE KEEL C_{Δ_0} = 1.07 (NOMINAL) DESIGNATION: 6.19-7-30
MODEL BEAM: 5.40" k/L = 0.225 MODEL No. 534

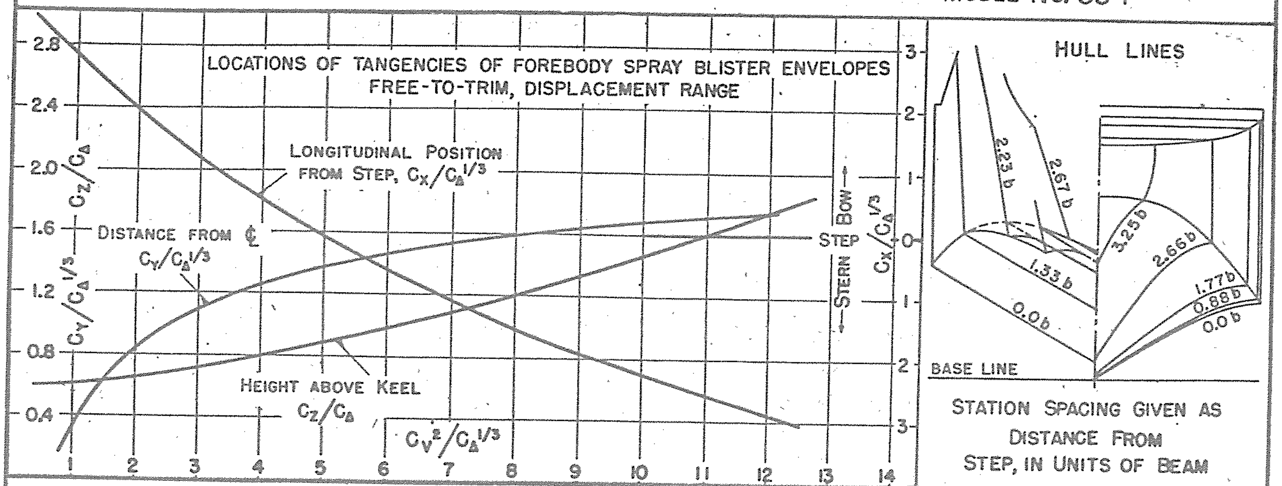

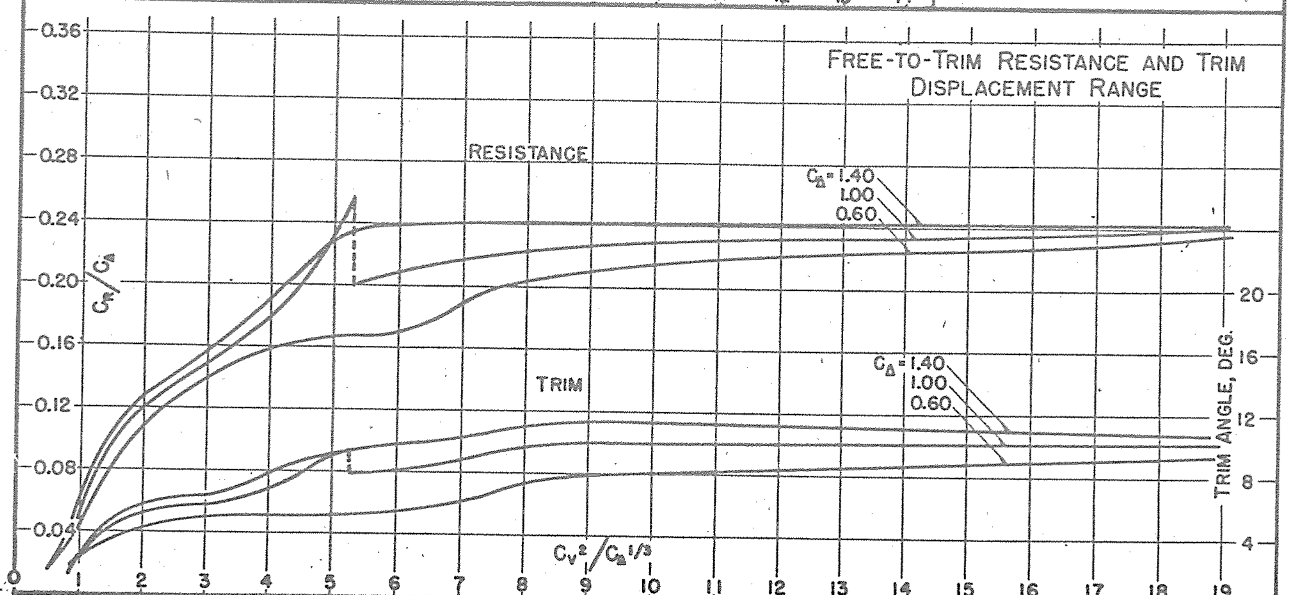

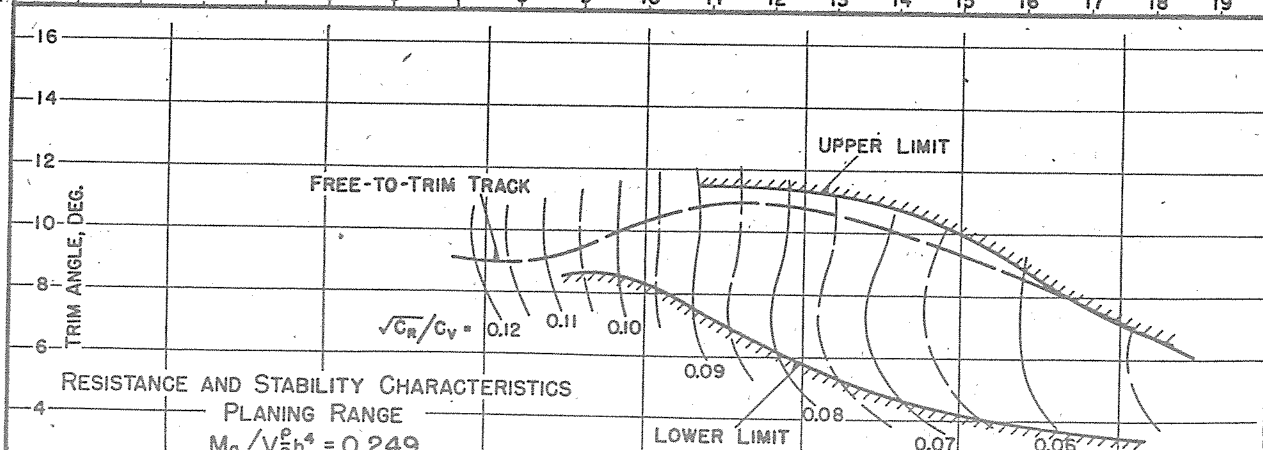

EXPERIMENTAL TOWING TANK
STEVENS INSTITUTE OF TECHNOLOGY
HOBOKEN, NEW JERSEY

SUMMARY CHART OF PRINCIPAL HYDRODYNAMIC CHARACTERISTICS

DATE: 12-23-44, 9-14-45 (REVISED) C.G. = 0.35 b FWD. OF STEP, 0.90 b ABOVE KEEL C_{Δ_0} = 1.07 (NOMINAL) DESIGNATION: 6.19-9-30
MODEL BEAM: 5.40" k/L = 0.225 MODEL NO. 607

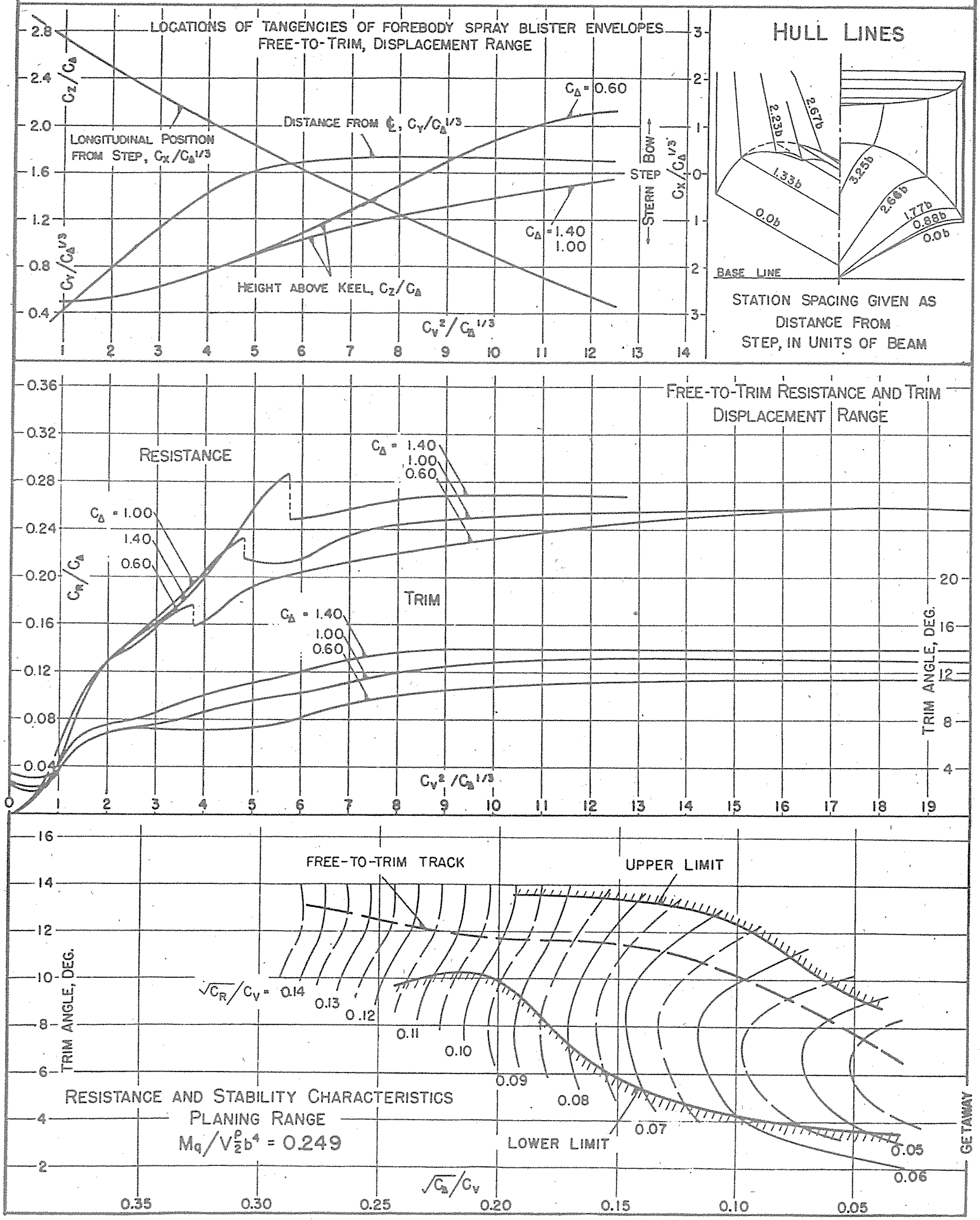

EXPERIMENTAL TOWING TANK
STEVENS INSTITUTE OF TECHNOLOGY
HOBOKEN, NEW JERSEY

SUMMARY CHART OF PRINCIPAL HYDRODYNAMIC CHARACTERISTICS

DATE: 8-8-44
12-28-45 (REVISED)
MODEL BEAM: 5.40"
C.G.= 0.35 b FWD. OF STEP
0.90b ABOVE KEEL
C_{Δ_0} = 1.07 (NOMINAL)
k/L = 0.225
DESIGNATION: 6.19-3-40
MODEL NO. 558

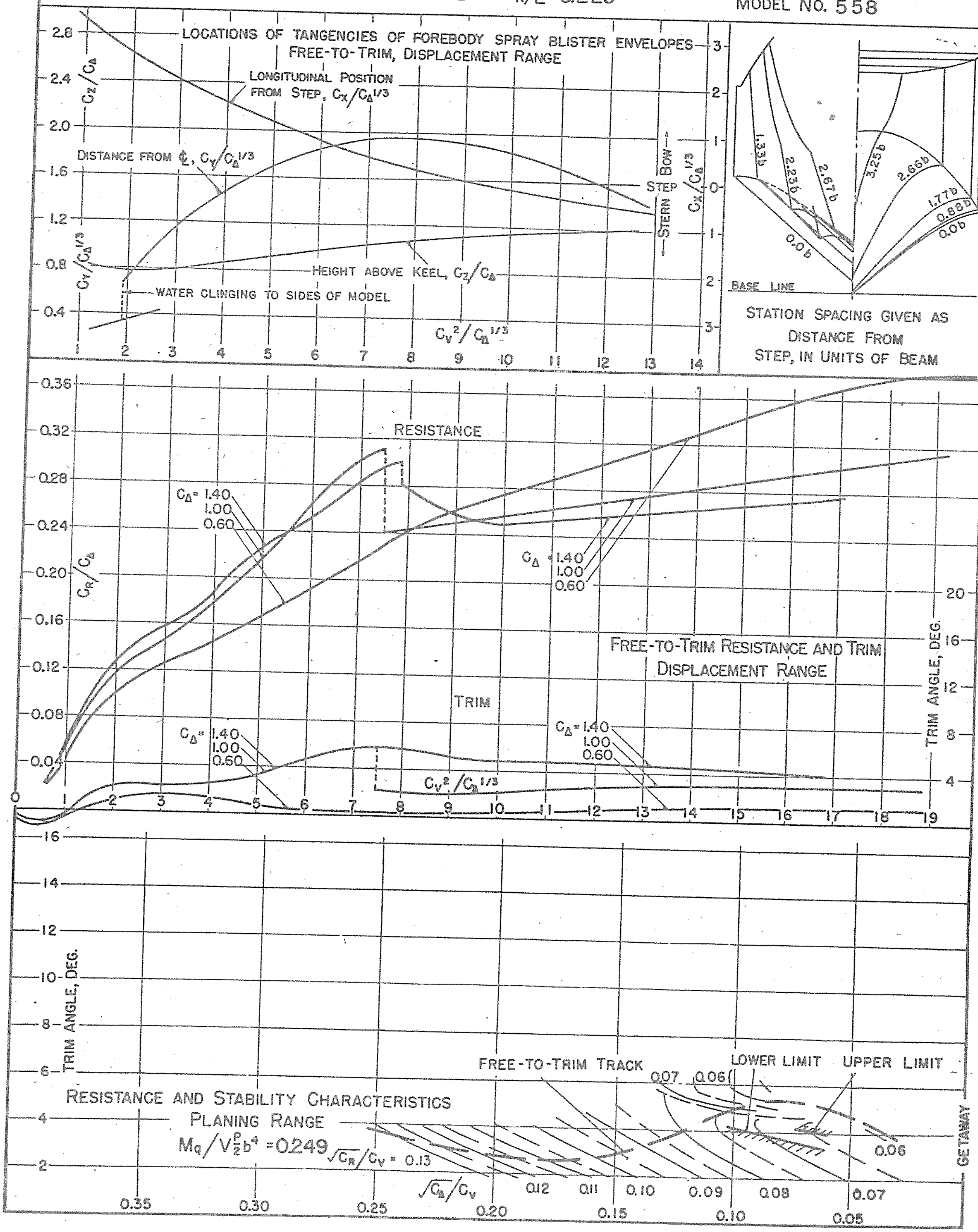

EXPERIMENTAL TOWING TANK
STEVENS INSTITUTE OF TECHNOLOGY
HOBOKEN, NEW JERSEY

SUMMARY CHART OF PRINCIPAL HYDRODYNAMIC CHARACTERISTICS

DATE: 8-8-44, 8-23-45 (REVISED) C.G. = 0.35b FWD. OF STEP, 0.90b ABOVE KEEL C_{Δ_0} = 1.07 (NOMINAL) DESIGNATION: 6.19-7-40

MODEL BEAM: 5.40" k/L = 0.225 MODEL NO. 535

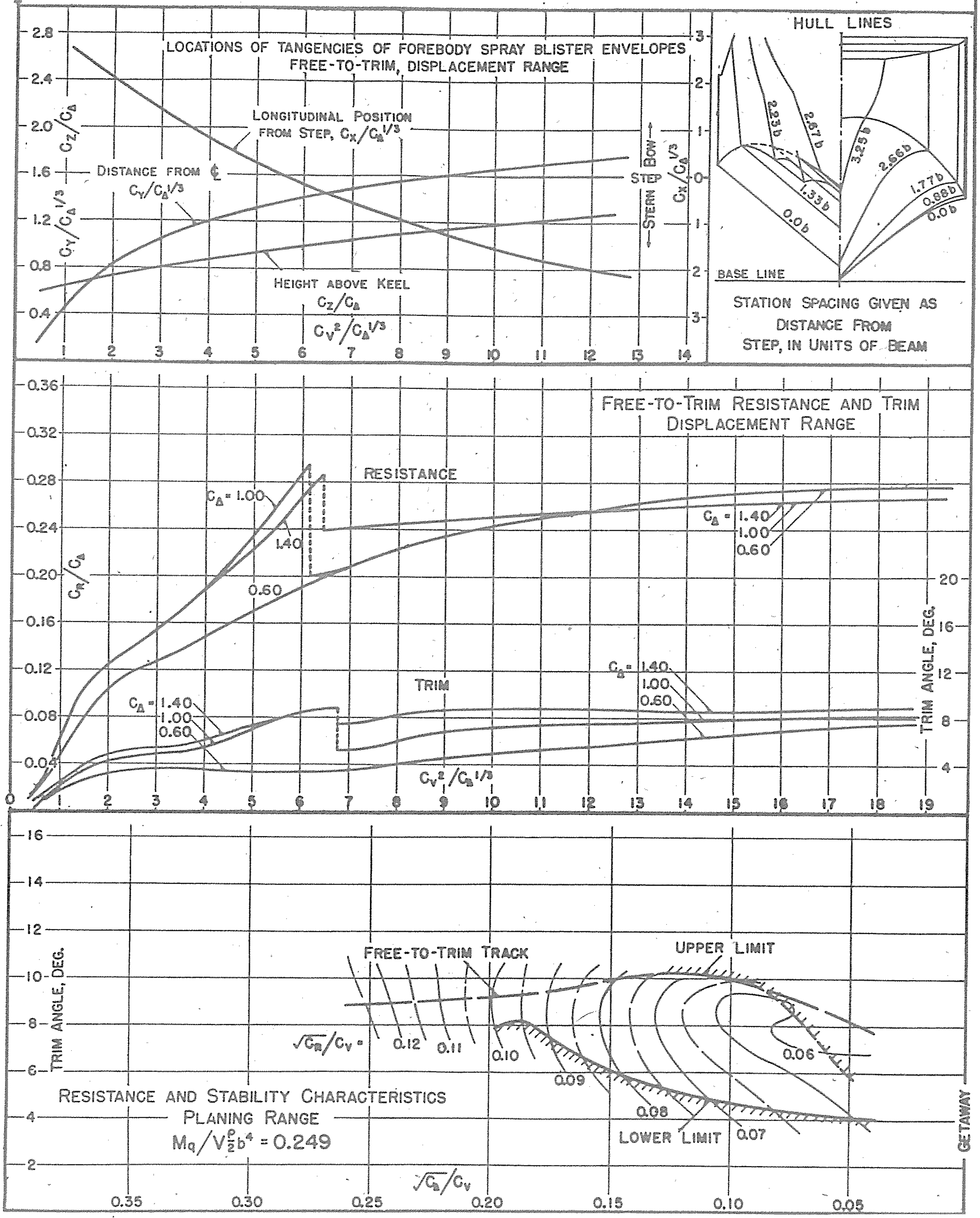

EXPERIMENTAL TOWING TANK
STEVENS INSTITUTE OF TECHNOLOGY
HOBOKEN, NEW JERSEY

SUMMARY CHART OF PRINCIPAL HYDRODYNAMIC CHARACTERISTICS

DATE: 8-8-44 / 1-15-46 (REVISED)
MODEL BEAM: 5.40"
C.G.= 0.35 b FWD. OF STEP, 0.90 b ABOVE KEEL
C_{Δ_0} = 1.07 (NOMINAL)
k/L = 0.225
DESIGNATION: 6.19-11-40
MODEL No. 559

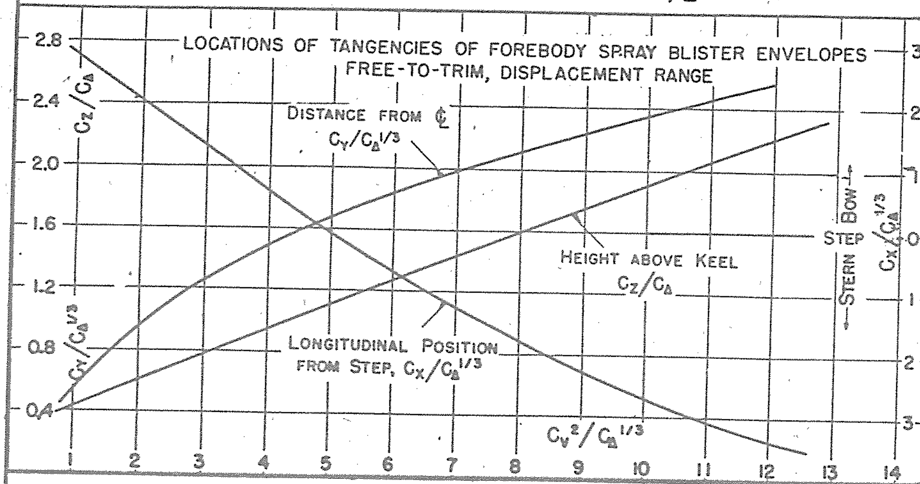

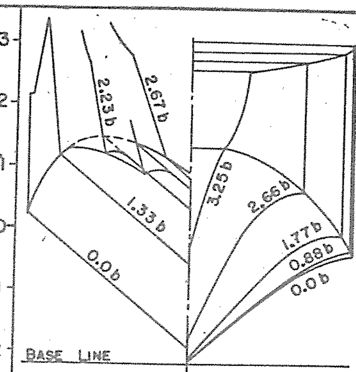

STATION SPACING GIVEN AS DISTANCE FROM STEP, IN UNITS OF BEAM

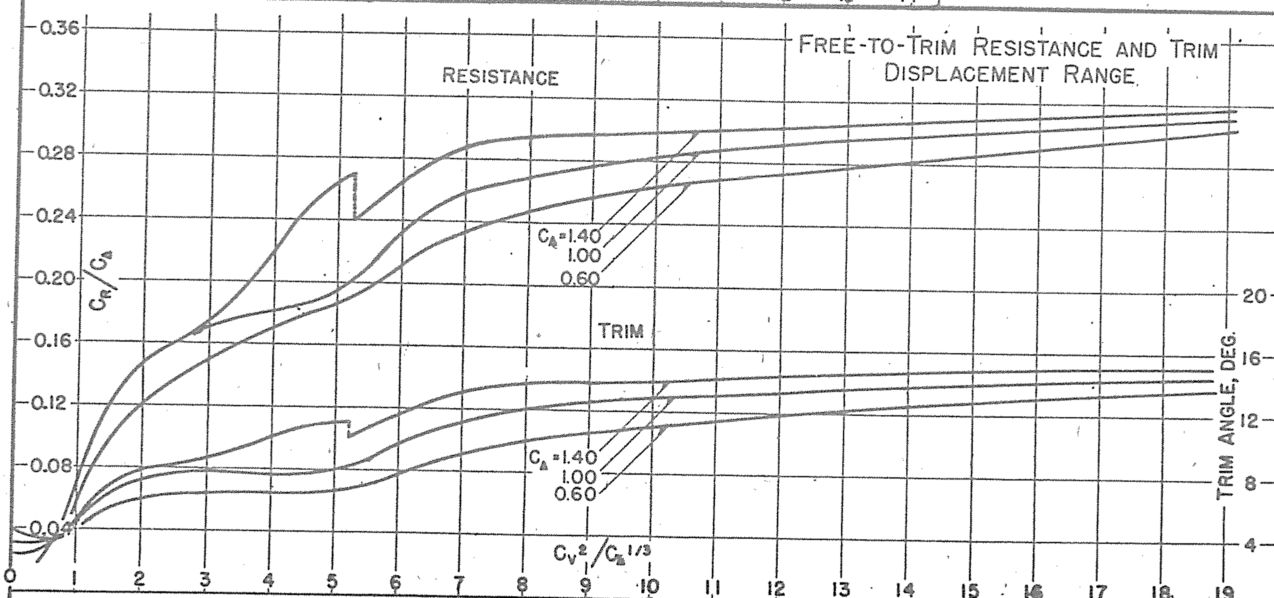

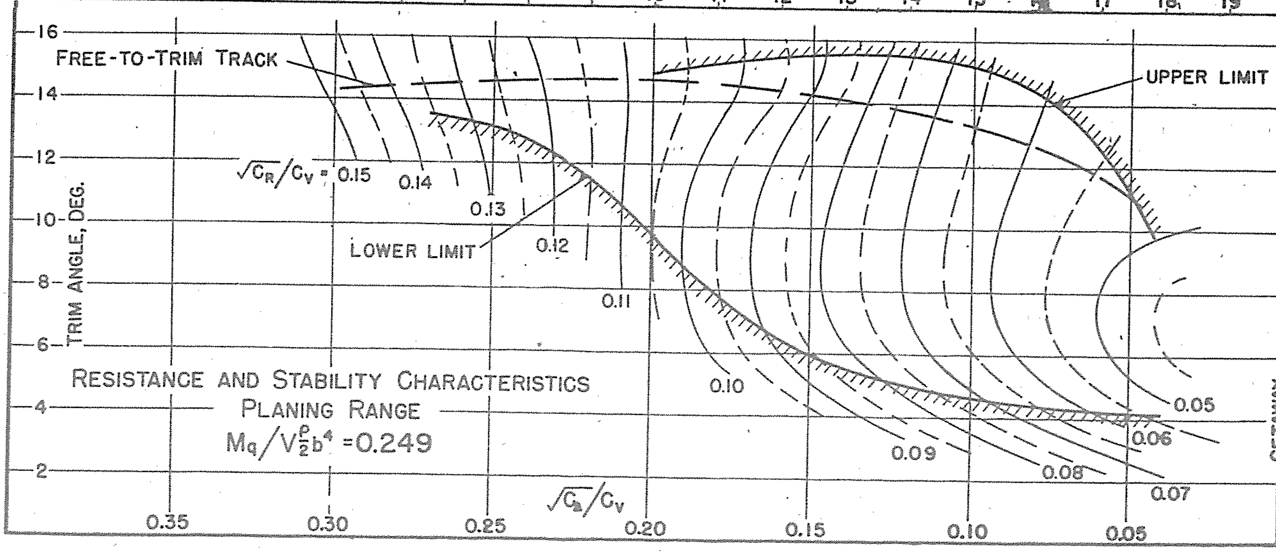

RESISTANCE AND STABILITY CHARACTERISTICS
PLANING RANGE
$M_q/V^2\frac{\rho}{2}b^4$ = 0.249

SUMMARY CHARTS

FOR LENGTH-BEAM RATIO 7.32 HULLS

Pages 81 through 87

EXPERIMENTAL TOWING TANK
STEVENS INSTITUTE OF TECHNOLOGY
HOBOKEN, NEW JERSEY

SUMMARY CHART OF PRINCIPAL HYDRODYNAMIC CHARACTERISTICS

DATE: 5-25-45 C.G.= 0.35 b FWD. OF STEP, 0.90 b ABOVE KEEL C_{Δ_0} = 1.49 (NOMINAL) DESIGNATION: 7.32-5-10
MODEL BEAM: 5.40" k/L = 0.217 MODEL NO. 624

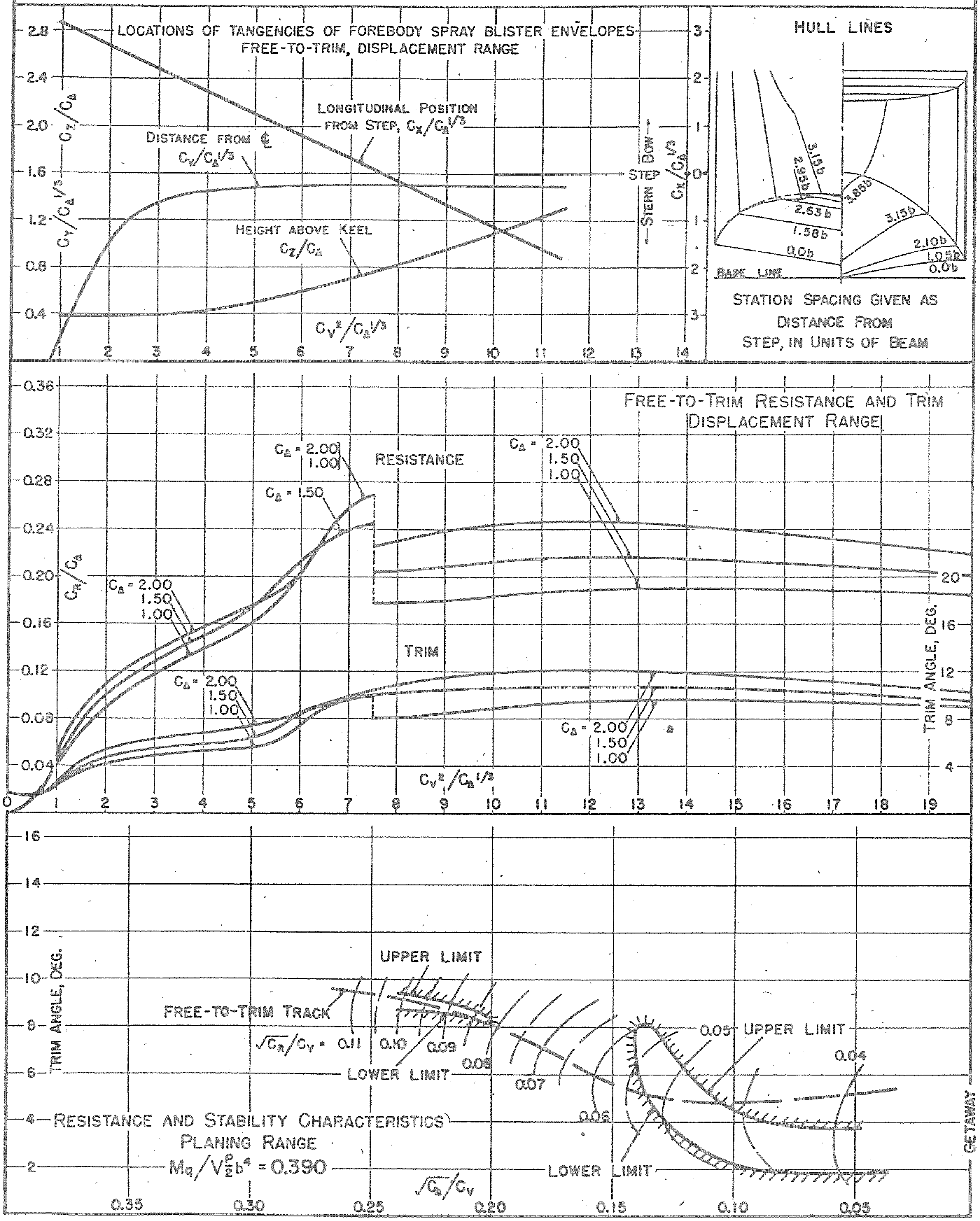

EXPERIMENTAL TOWING TANK
STEVENS INSTITUTE OF TECHNOLOGY
HOBOKEN, NEW JERSEY

SUMMARY CHART OF PRINCIPAL HYDRODYNAMIC CHARACTERISTICS

DATE: 7-5-45 | C.G.= 0.35 b FWD. OF STEP, 0.90 b ABOVE KEEL | C_{Δ_0} = 1.49 (NOMINAL) | DESIGNATION: 7.32-9-10

MODEL BEAM: 5.40" | k/L = 0.217 | MODEL NO. 625

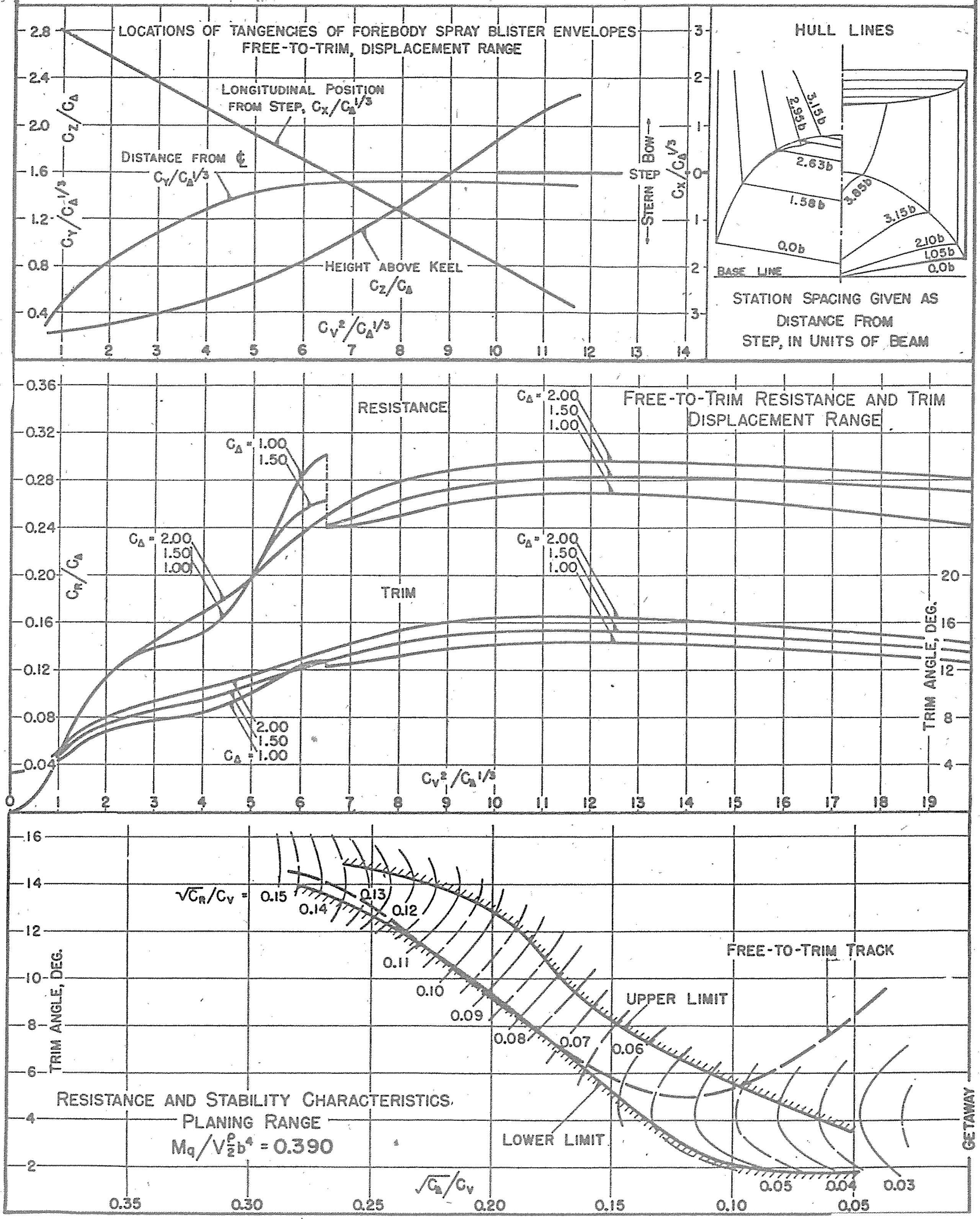

EXPERIMENTAL TOWING TANK
STEVENS INSTITUTE OF TECHNOLOGY
HOBOKEN, NEW JERSEY

SUMMARY CHART OF PRINCIPAL HYDRODYNAMIC CHARACTERISTICS

DATE: 6-20-45	C.G.= 0.35 b FWD. OF STEP	C_{Δ_0} = 1.49 (NOMINAL)	DESIGNATION: 7.32-3-20
MODEL BEAM: 5.40"	0.90 b ABOVE KEEL	k/L = 0.217	MODEL NO. 626

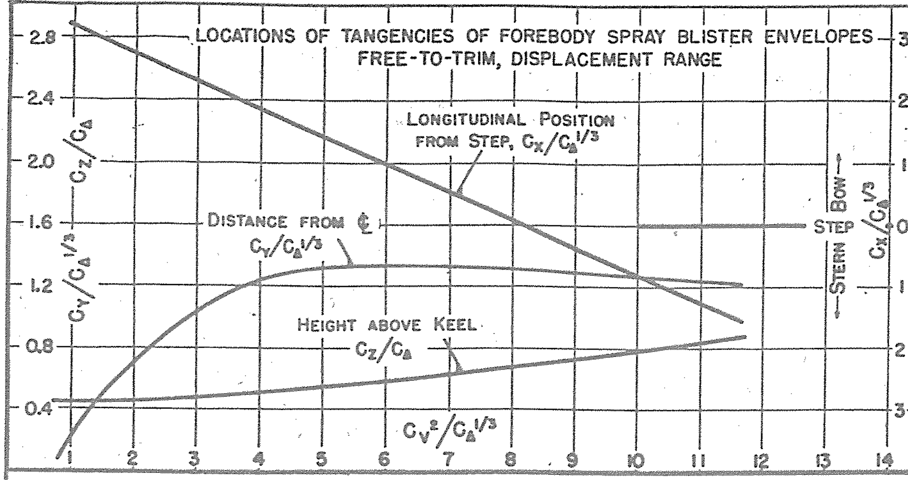

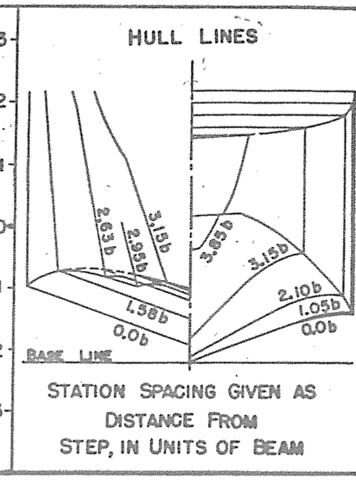

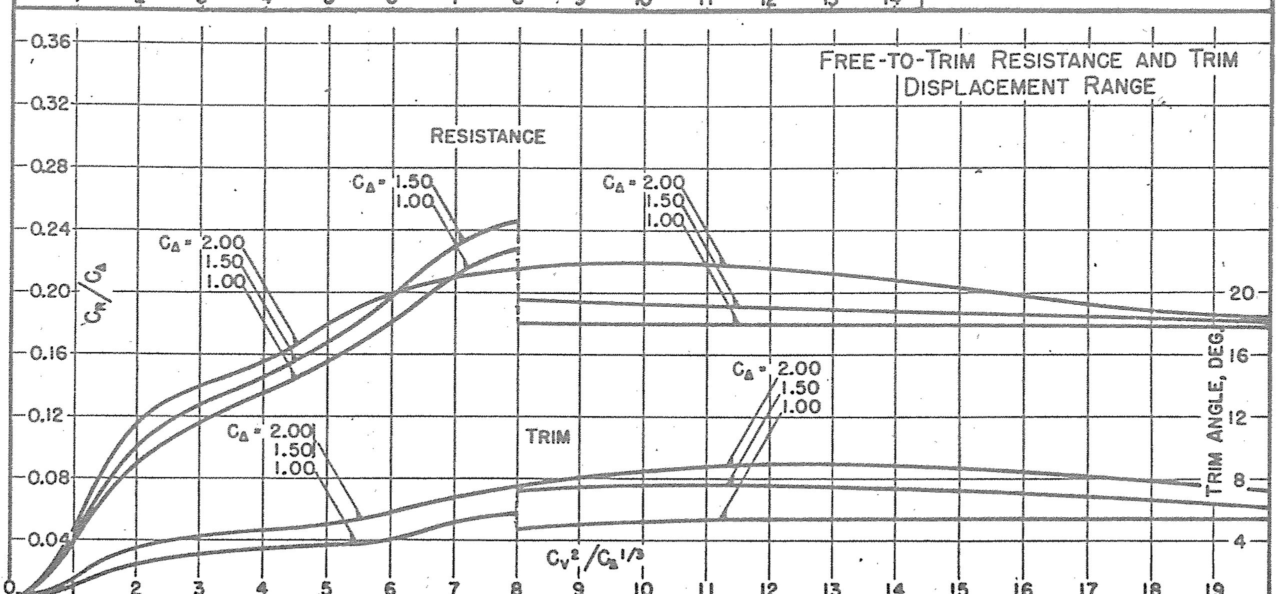

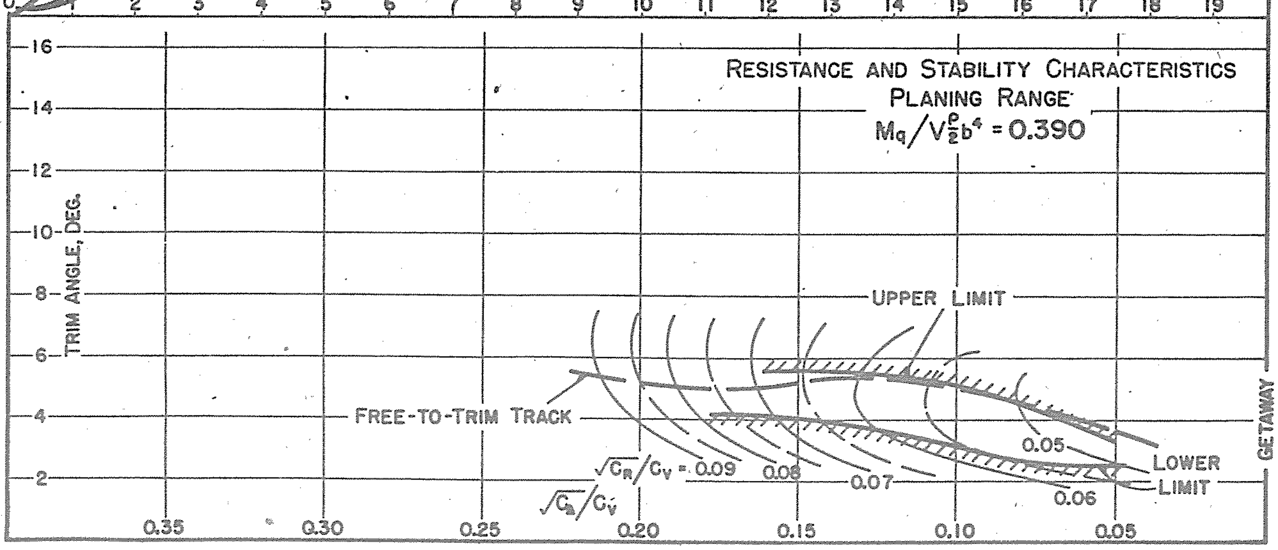

EXPERIMENTAL TOWING TANK
STEVENS INSTITUTE OF TECHNOLOGY
HOBOKEN, NEW JERSEY

SUMMARY CHART OF PRINCIPAL HYDRODYNAMIC CHARACTERISTICS

DATE: 7-31-45
MODEL BEAM: 5.40"
C.G. = 0.35 b FWD. OF STEP, 0.90 b ABOVE KEEL
C_{Δ_0} = 1.49 (NOMINAL)
k/L = 0.217
DESIGNATION: 7.32-7-20
MODEL NO. 339-23

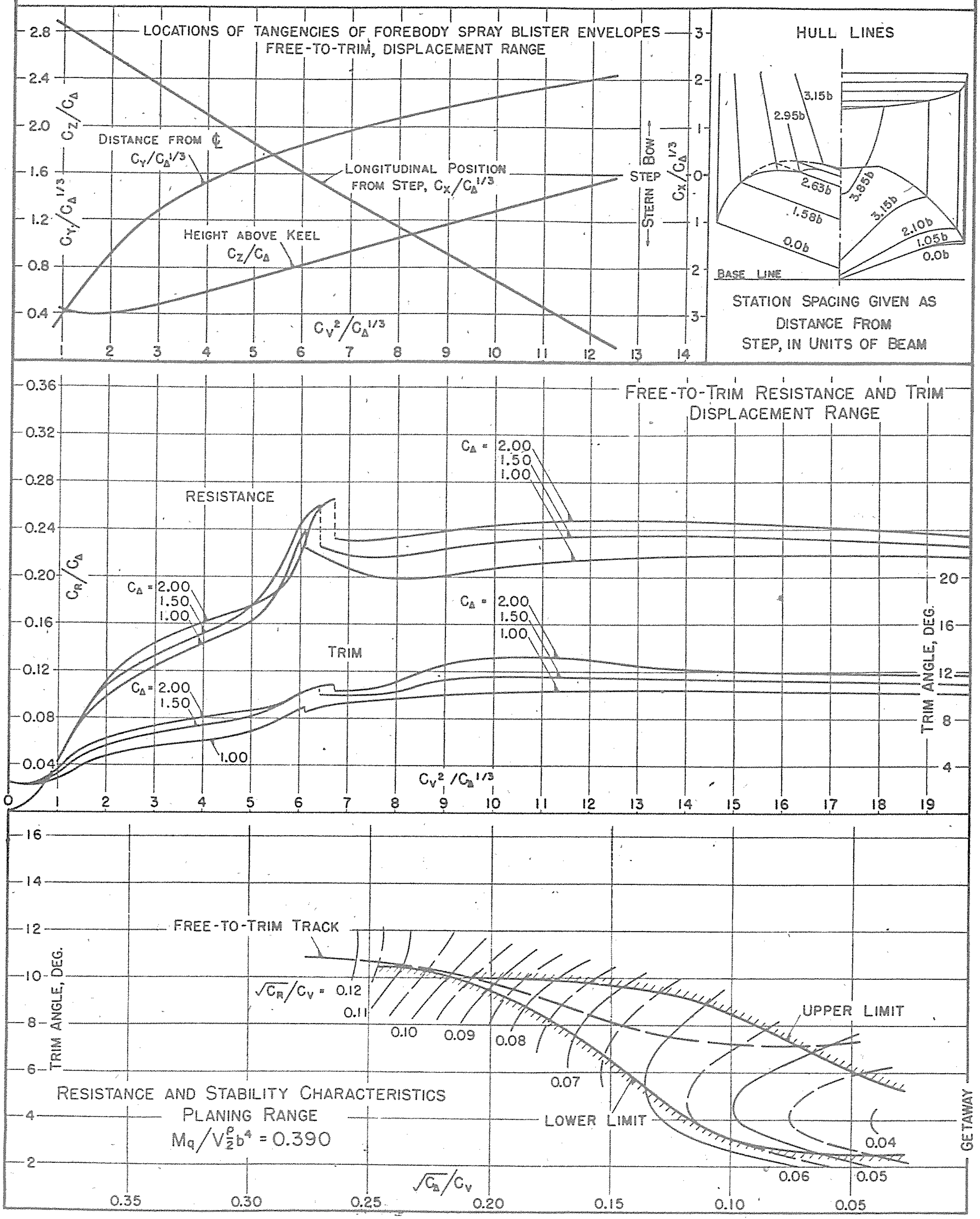

EXPERIMENTAL TOWING TANK
STEVENS INSTITUTE OF TECHNOLOGY
HOBOKEN, NEW JERSEY

SUMMARY CHART OF PRINCIPAL HYDRODYNAMIC CHARACTERISTICS

DATE: 4-25-45
MODEL BEAM: 5.40"
C.G. = 0.35 b FWD. OF STEP, 0.90 b ABOVE KEEL
C_{Δ_0} = 1.49 (NOMINAL)
k/L = 0.217
DESIGNATION: 7.32-11-20
MODEL NO. 627

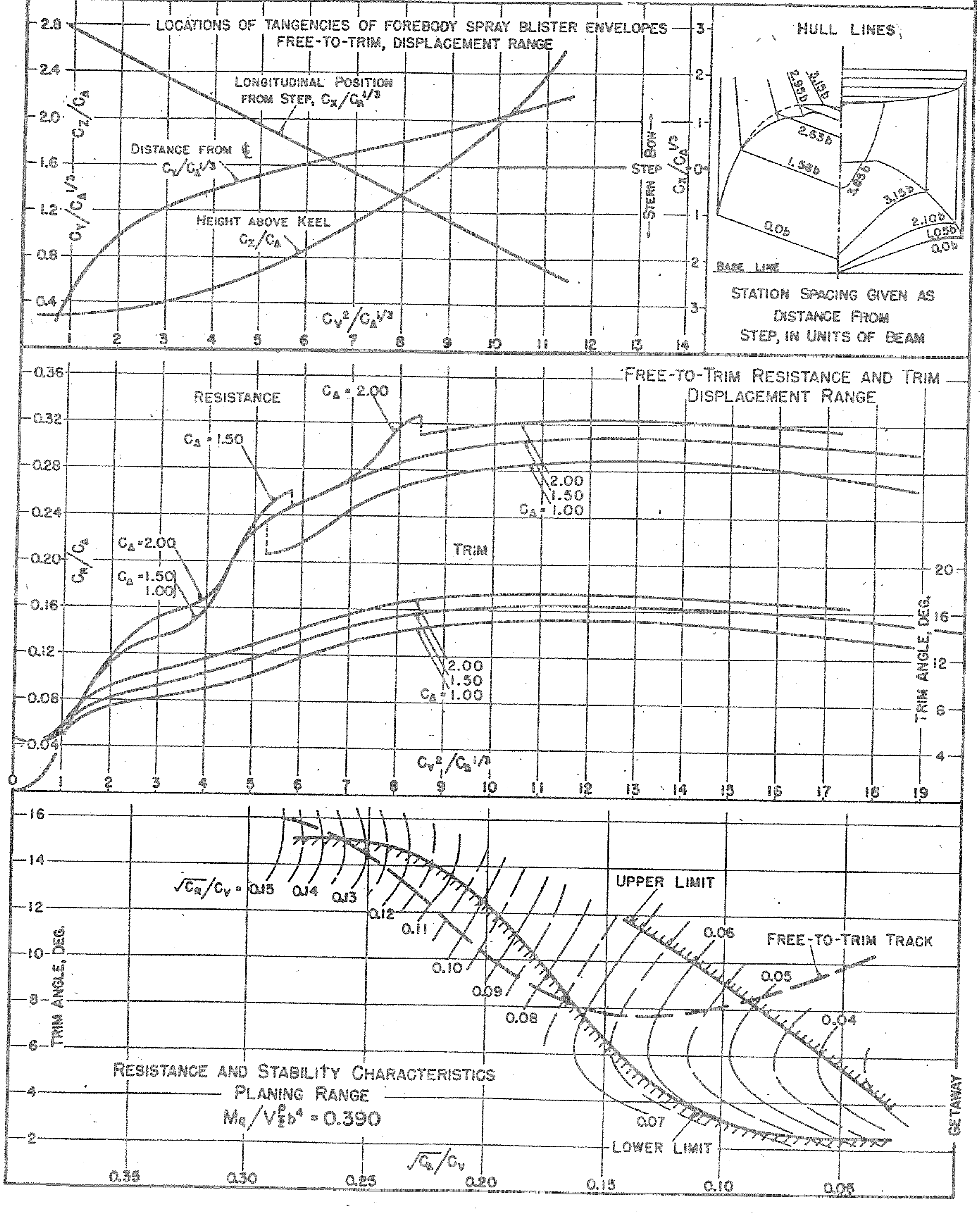

EXPERIMENTAL TOWING TANK
STEVENS INSTITUTE OF TECHNOLOGY
HOBOKEN, NEW JERSEY

SUMMARY CHART OF PRINCIPAL HYDRODYNAMIC CHARACTERISTICS

DATE: 7-18-45	C.G.= 0.35 b FWD. OF STEP	C_{Δ_0} = 1.49 (NOMINAL)	DESIGNATION: 7.32-5-30
MODEL BEAM: 5.40"	0.90 b ABOVE KEEL	k/L = 0.217	MODEL NO. 628

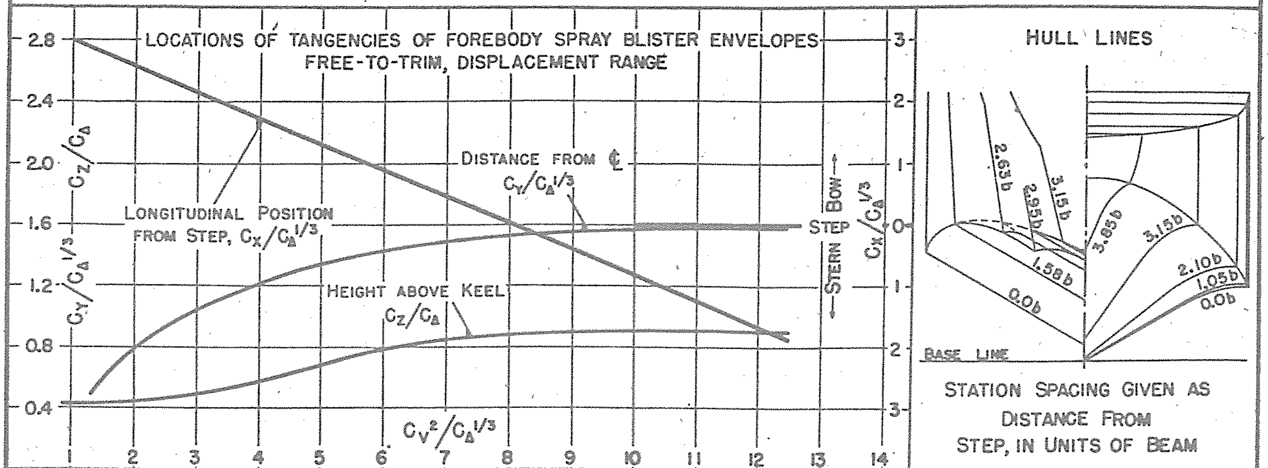

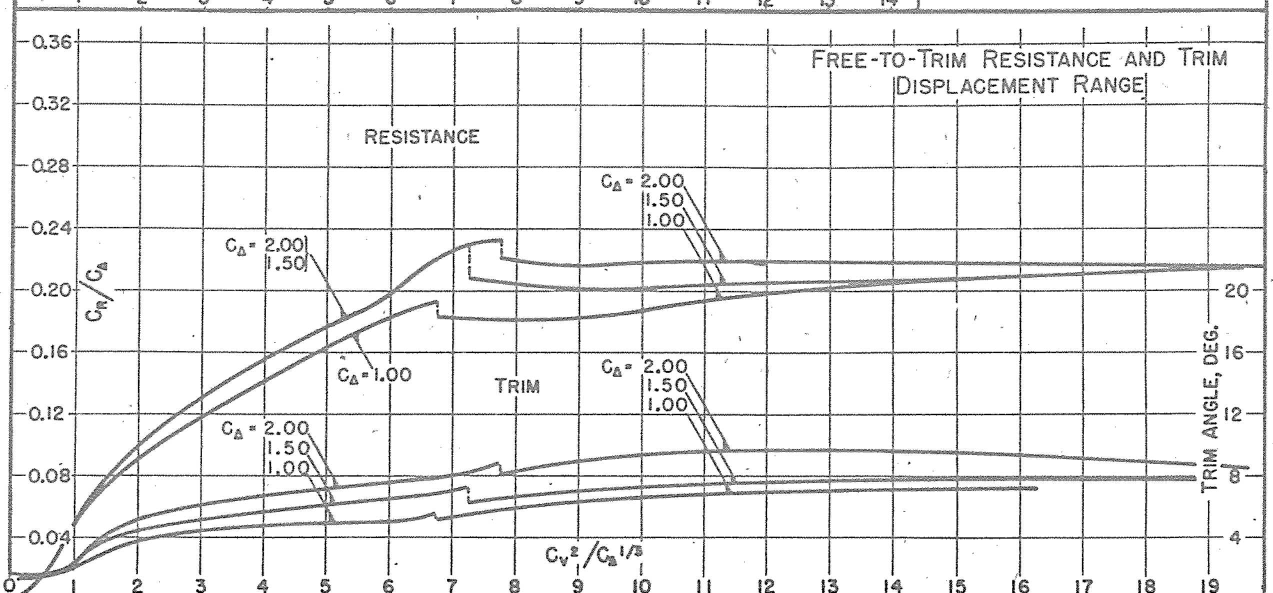

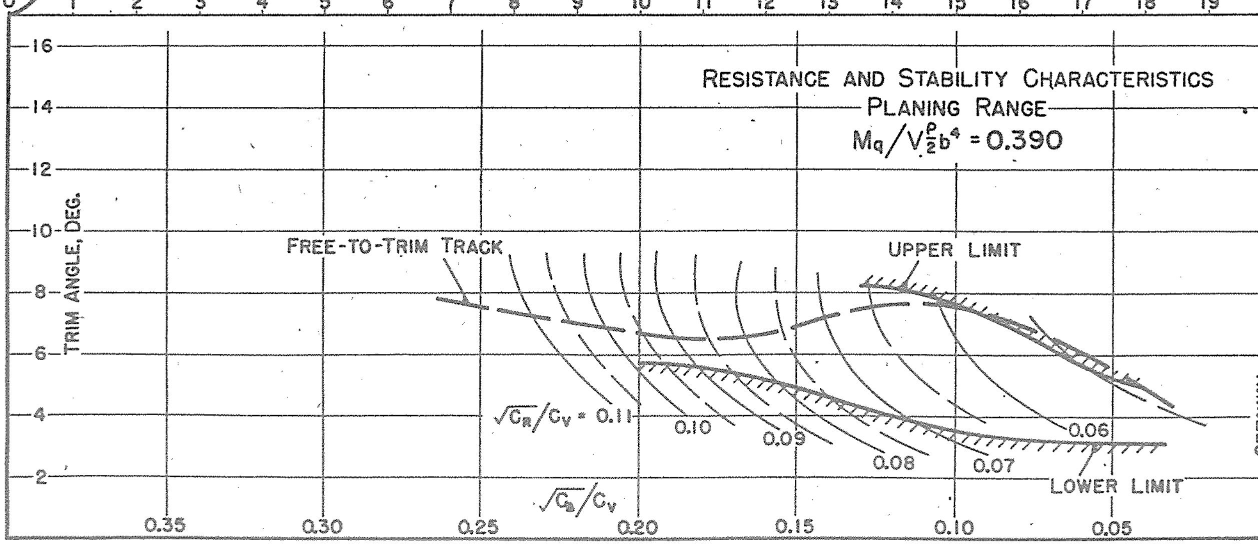

EXPERIMENTAL TOWING TANK
STEVENS INSTITUTE OF TECHNOLOGY
HOBOKEN, NEW JERSEY

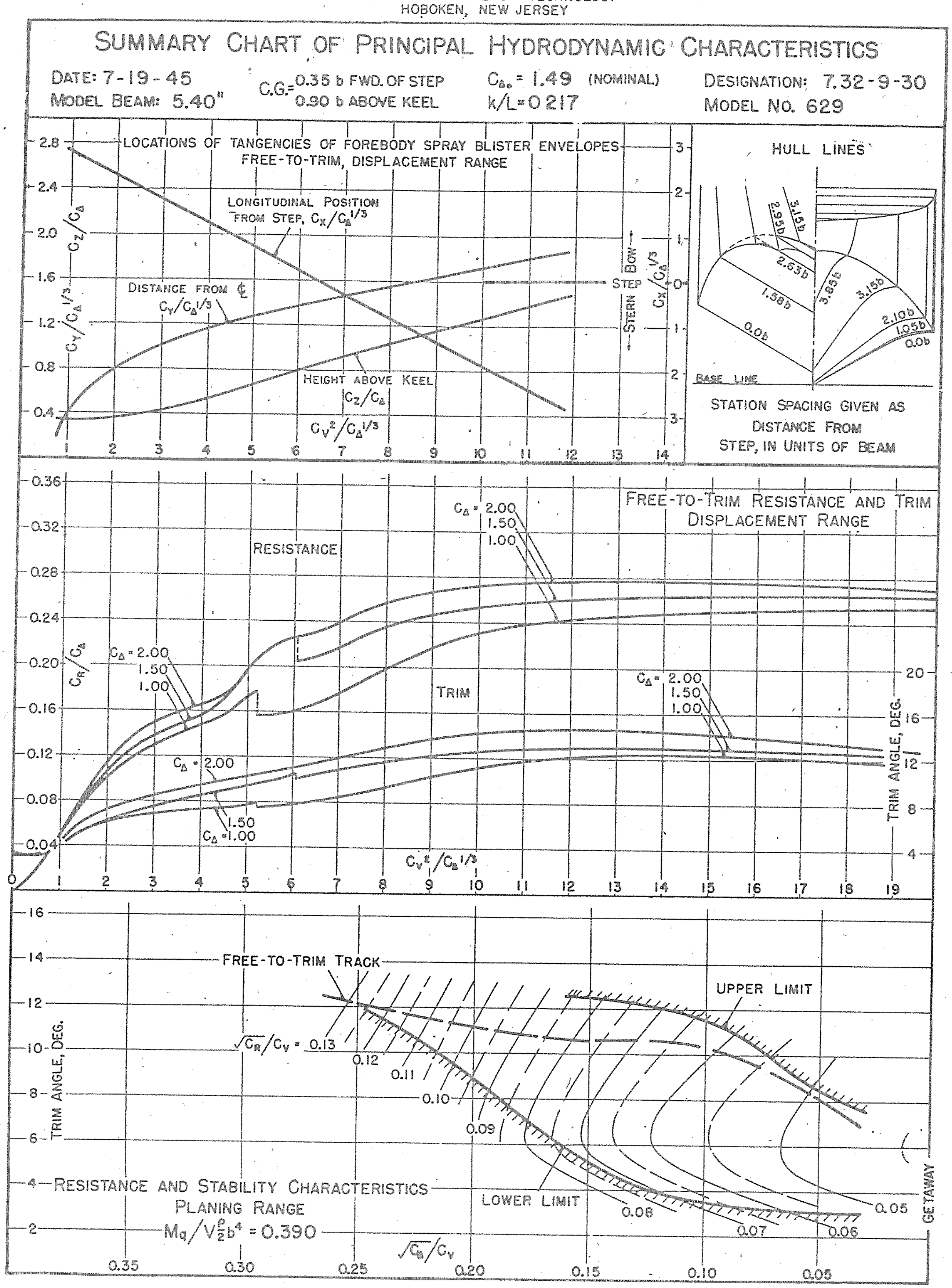

SUMMARY CHARTS

FOR LENGTH-BEAM RATIO 8.45 HULLS

Pages 88 through 94

EXPERIMENTAL TOWING TANK
STEVENS INSTITUTE OF TECHNOLOGY
HOBOKEN, NEW JERSEY

SUMMARY CHART OF PRINCIPAL HYDRODYNAMIC CHARACTERISTICS

DATE: 12-10-45
MODEL BEAM: 5.40
C.G.= 0.35 b FWD. OF STEP, 0.90 b ABOVE KEEL
C_{Δ_0} = 2.00 (NOMINAL)
k/L = 0.212
DESIGNATION: 8.45-5-10
MODEL No. 695

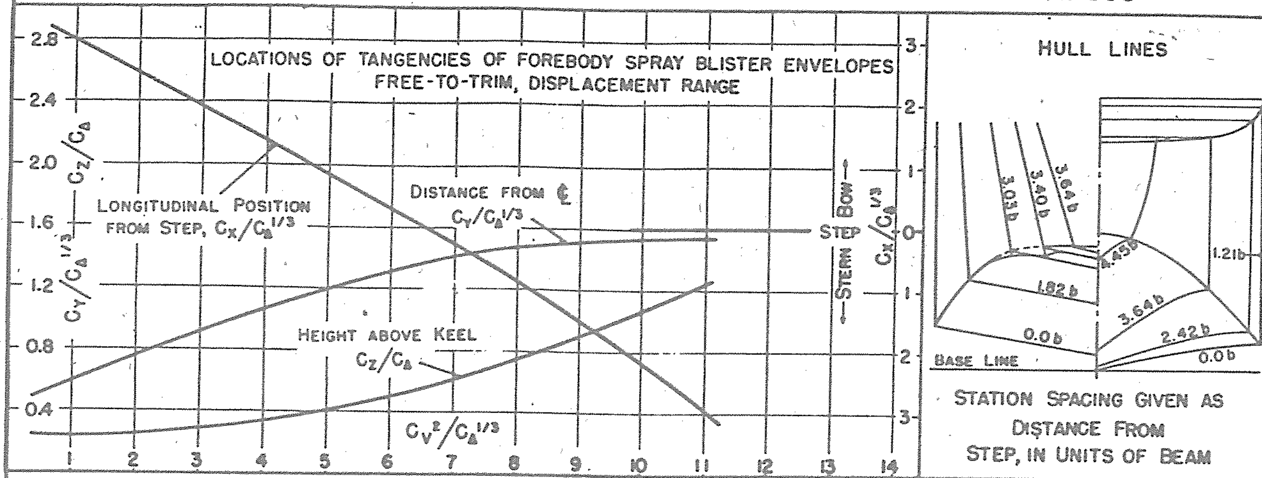

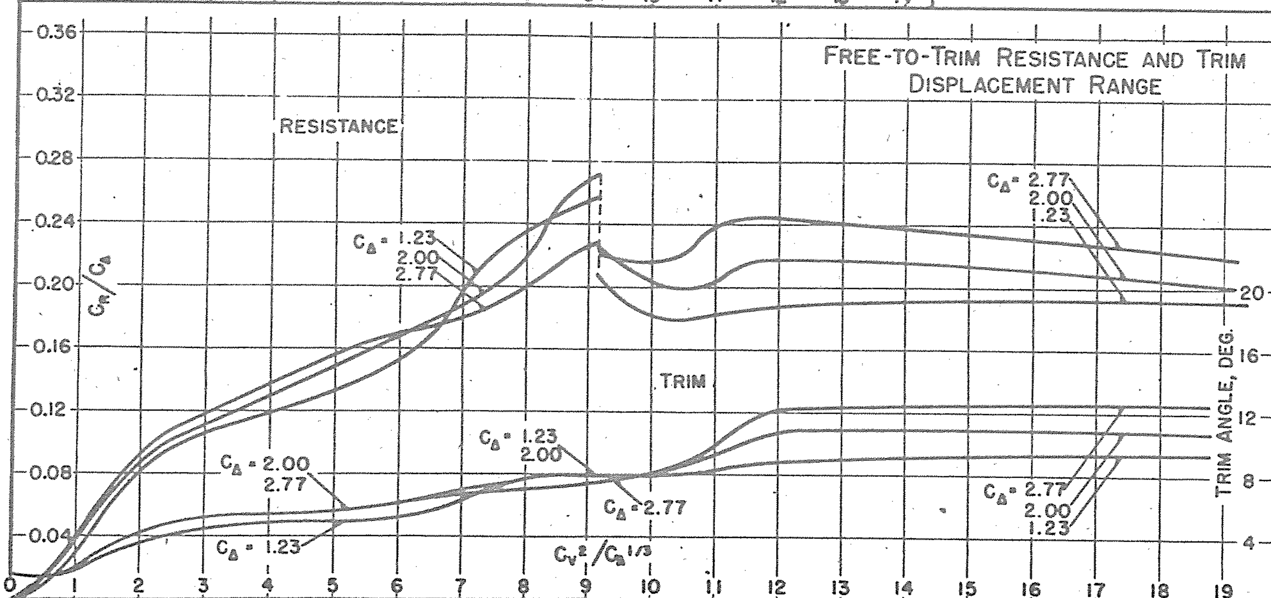

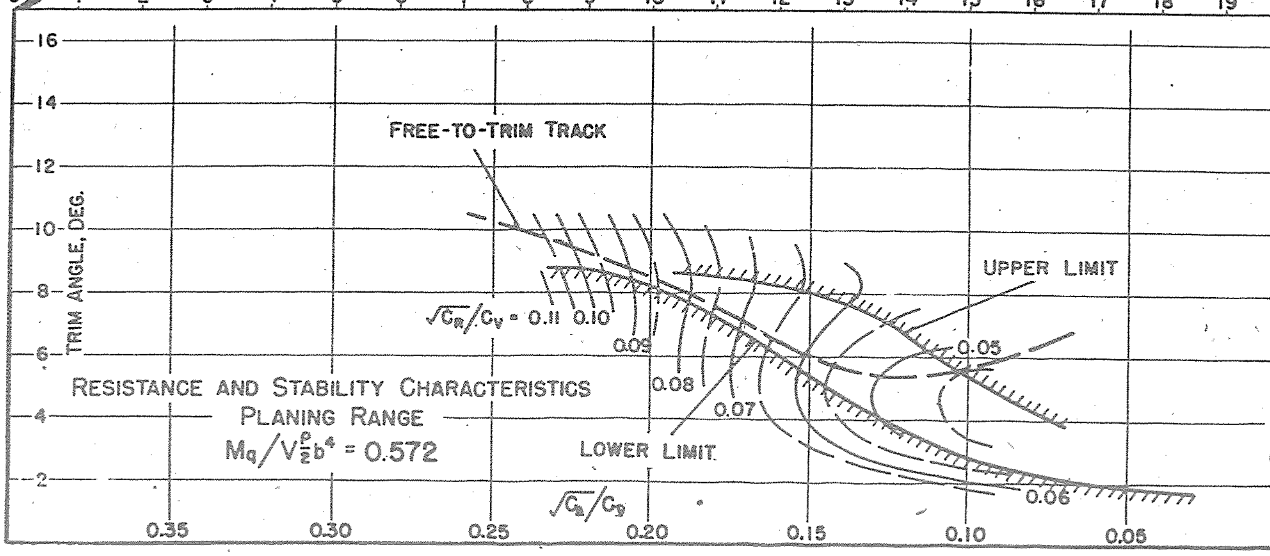

EXPERIMENTAL TOWING TANK
STEVENS INSTITUTE OF TECHNOLOGY
HOBOKEN, NEW JERSEY

SUMMARY CHART OF PRINCIPAL HYDRODYNAMIC CHARACTERISTICS

DATE: 12-13-45
MODEL BEAM: 5.40
C.G.= 0.35 b FWD. OF STEP, 0.90 b ABOVE KEEL
C_{Δ_0} = 2.00 (NOMINAL)
k/L = 0.212
DESIGNATION: 8.45-9-10
MODEL No. 696

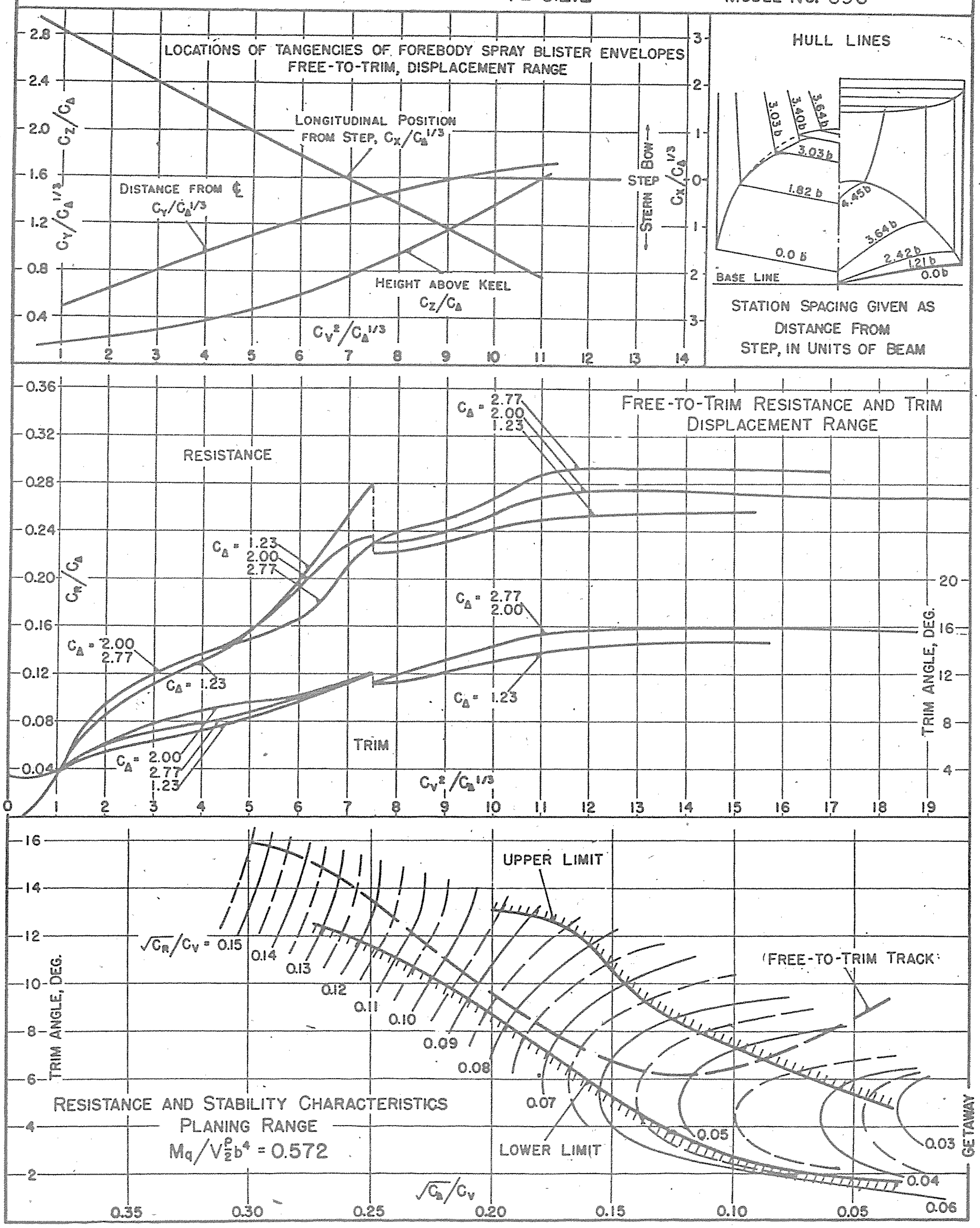

EXPERIMENTAL TOWING TANK
STEVENS INSTITUTE OF TECHNOLOGY
HOBOKEN, NEW JERSEY

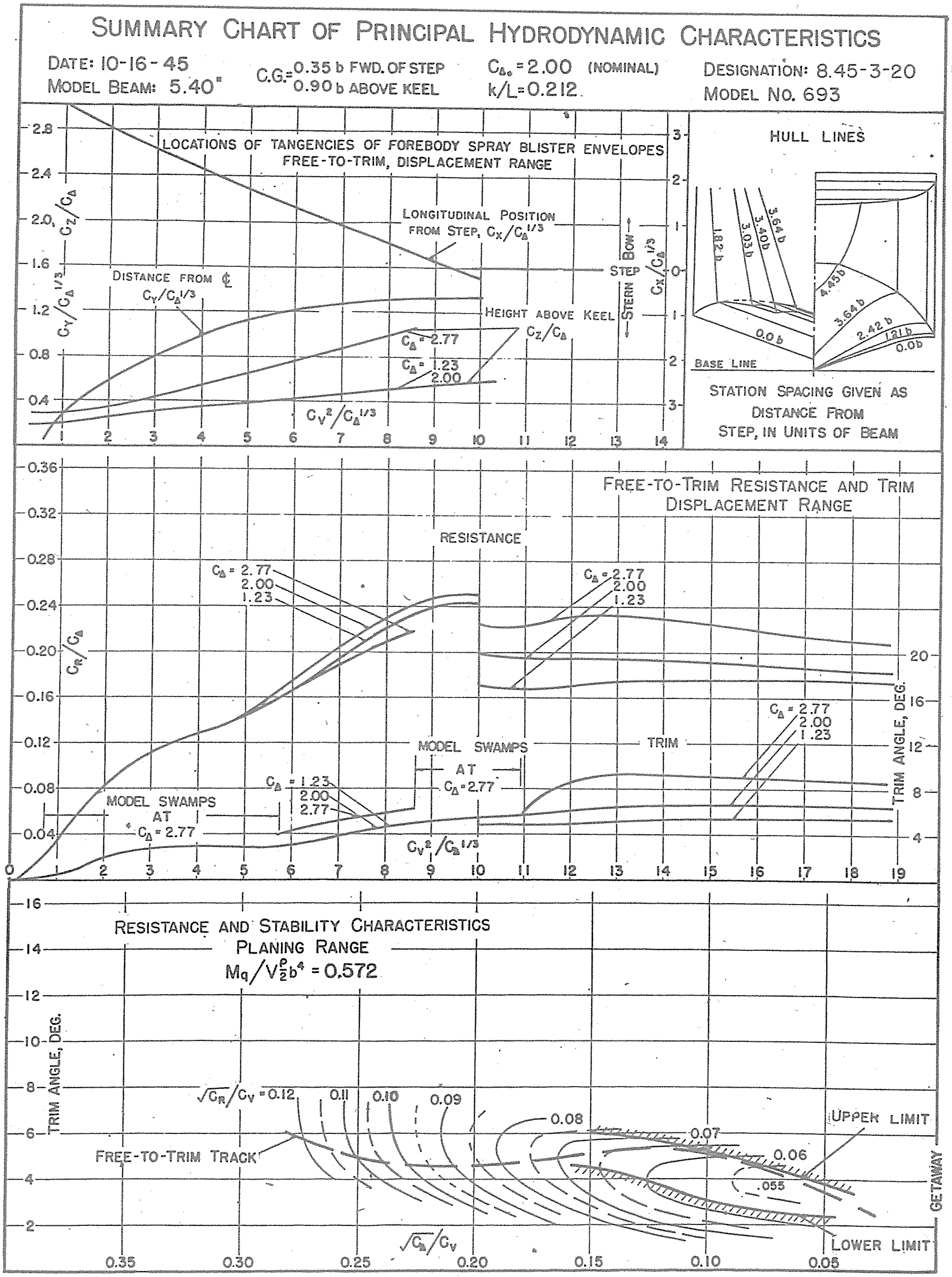

EXPERIMENTAL TOWING TANK
STEVENS INSTITUTE OF TECHNOLOGY
HOBOKEN, NEW JERSEY

SUMMARY CHART OF PRINCIPAL HYDRODYNAMIC CHARACTERISTICS

DATE: 7-31-45 | C.G.= 0.35 b FWD. OF STEP, 0.90 b ABOVE KEEL | C_{Δ_0} = 2.00 (NOMINAL) | DESIGNATION: 8.45-7-20

MODEL BEAM: 5.40" | k/L=0.212 | MODEL NO. 651

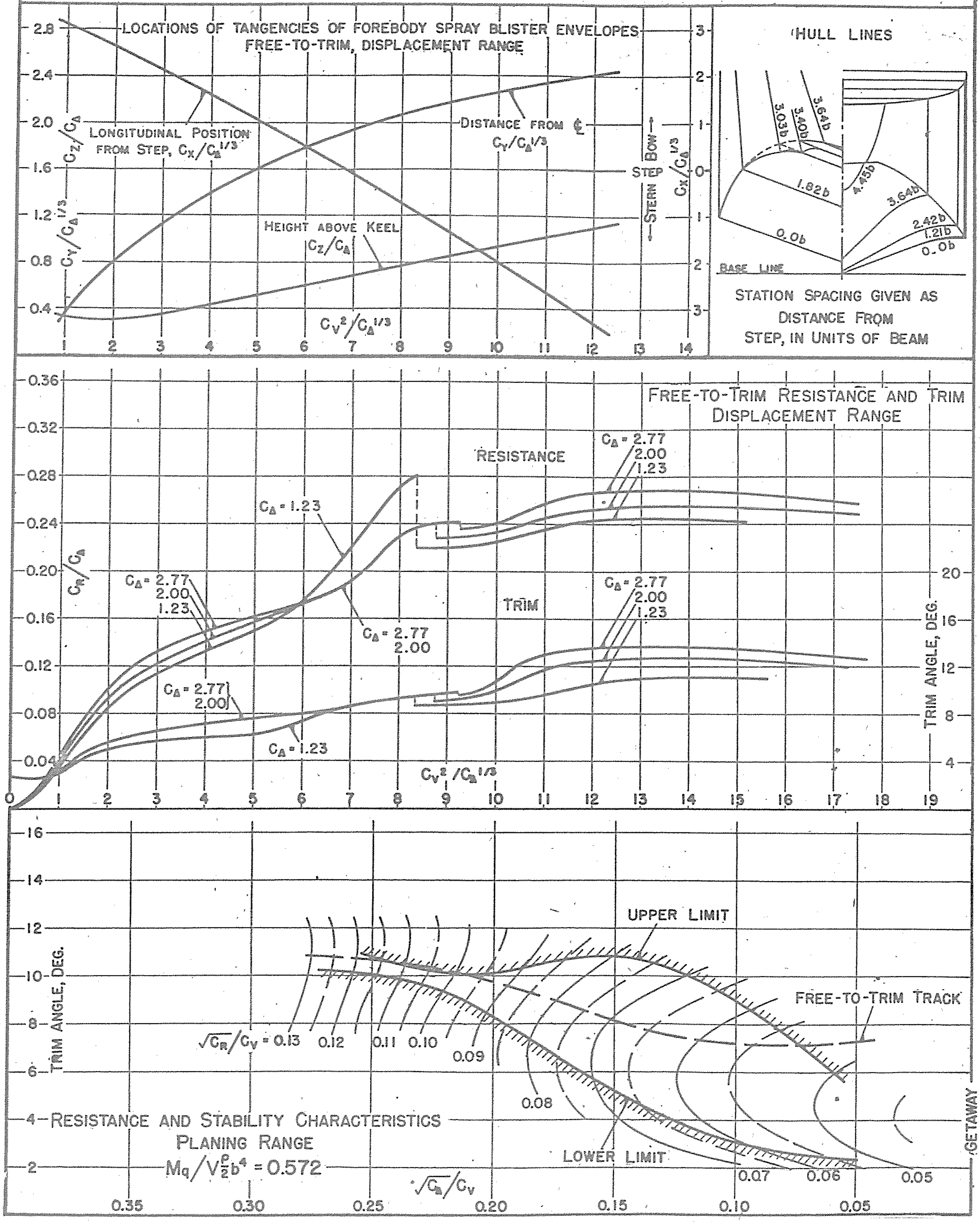

EXPERIMENTAL TOWING TANK
STEVENS INSTITUTE OF TECHNOLOGY
HOBOKEN, NEW JERSEY

SUMMARY CHART OF PRINCIPAL HYDRODYNAMIC CHARACTERISTICS

DATE: 10-16-45 | C.G.= 0.35 b FWD. OF STEP, 0.90 b ABOVE KEEL | C_{Δ_0} = 2.00 (NOMINAL) | DESIGNATION: 8.45-11-20
MODEL BEAM: 5.40 | k/L = 0.212 | MODEL No. 694

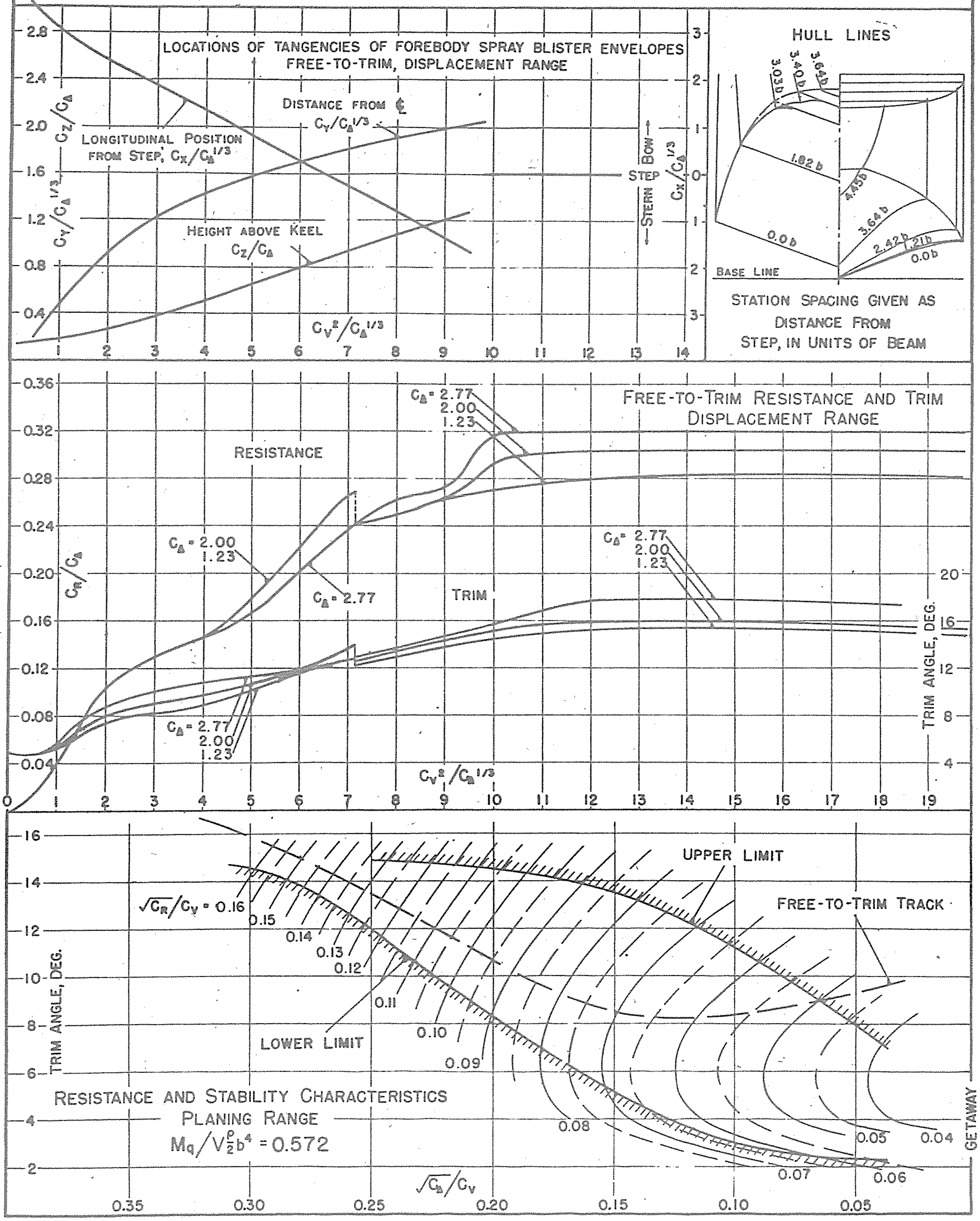

EXPERIMENTAL TOWING TANK
STEVENS INSTITUTE OF TECHNOLOGY
HOBOKEN, NEW JERSEY

SUMMARY CHART OF PRINCIPAL HYDRODYNAMIC CHARACTERISTICS

DATE: 11-8-45
MODEL BEAM: 5.40"
C.G.=0.35 b FWD. OF STEP
0.90 b ABOVE KEEL
C_{Δ_0}=2.00 (NOMINAL)
k/L=0.212
DESIGNATION: 8.45-5-30
MODEL NO. 697

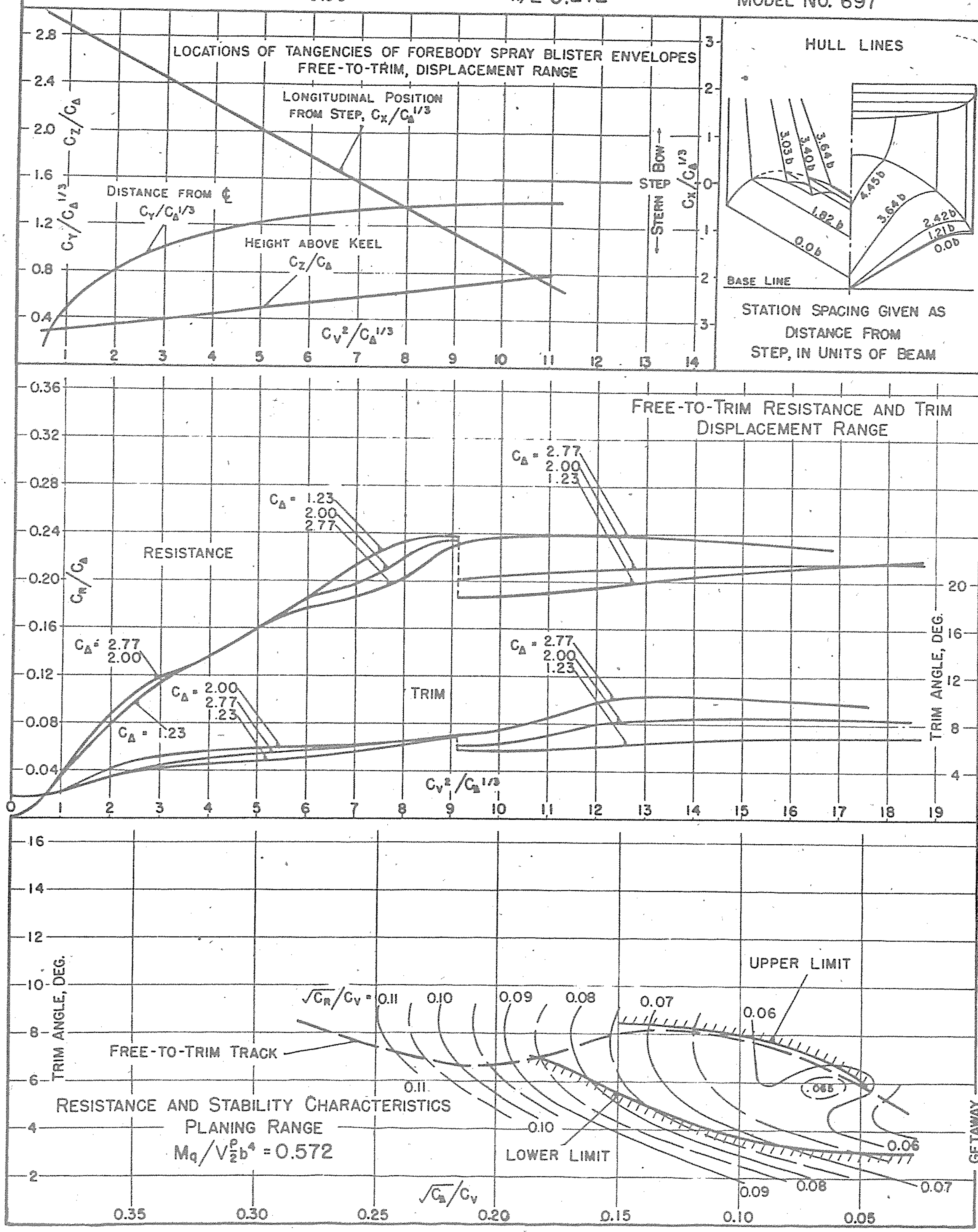

EXPERIMENTAL TOWING TANK
STEVENS INSTITUTE OF TECHNOLOGY
HOBOKEN, NEW JERSEY

SUMMARY CHART OF PRINCIPAL HYDRODYNAMIC CHARACTERISTICS

DATE: 11-5-45 | C.G. = 0.35 b FWD. OF STEP, 0.90 b ABOVE KEEL | C_{Δ_0} = 2.00 (NOMINAL) | DESIGNATION: 8.45-9-30
MODEL BEAM: 5.40 | k/L = 0.212 | MODEL NO. 698

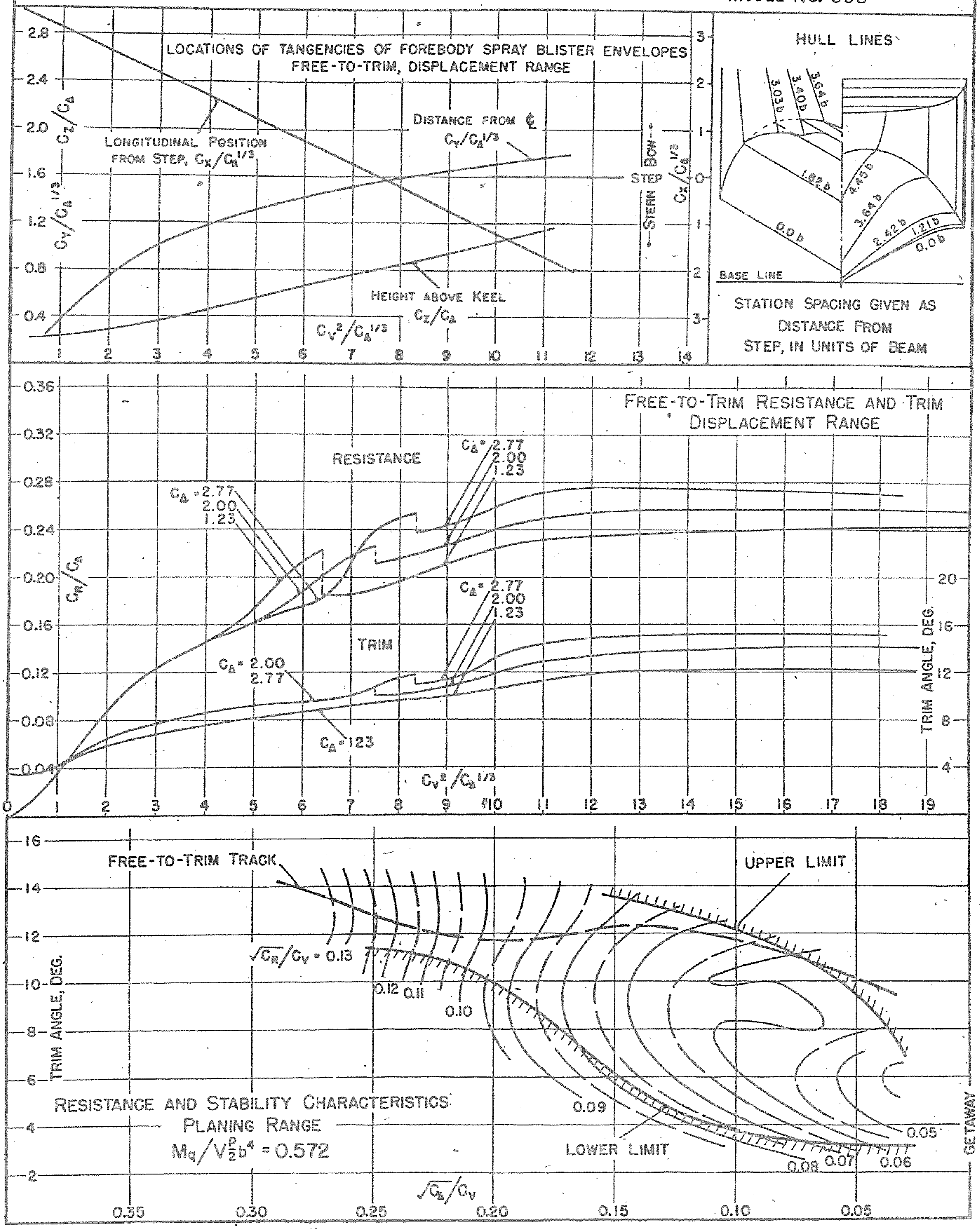

EXPERIMENTAL TOWING TANK
STEVENS INSTITUTE OF TECHNOLOGY

REPORT NO. 325

PART II

MODEL TESTS ON A STANDARD SERIES OF FLYING-BOAT HULLS

by

Albert Strumpf

HOBOKEN, NEW JERSEY
MAY, 1947

MOMENT DATA CHARTS

FOR LENGTH-BEAM RATIO 5.07 HULLS

Pages 95 through 101

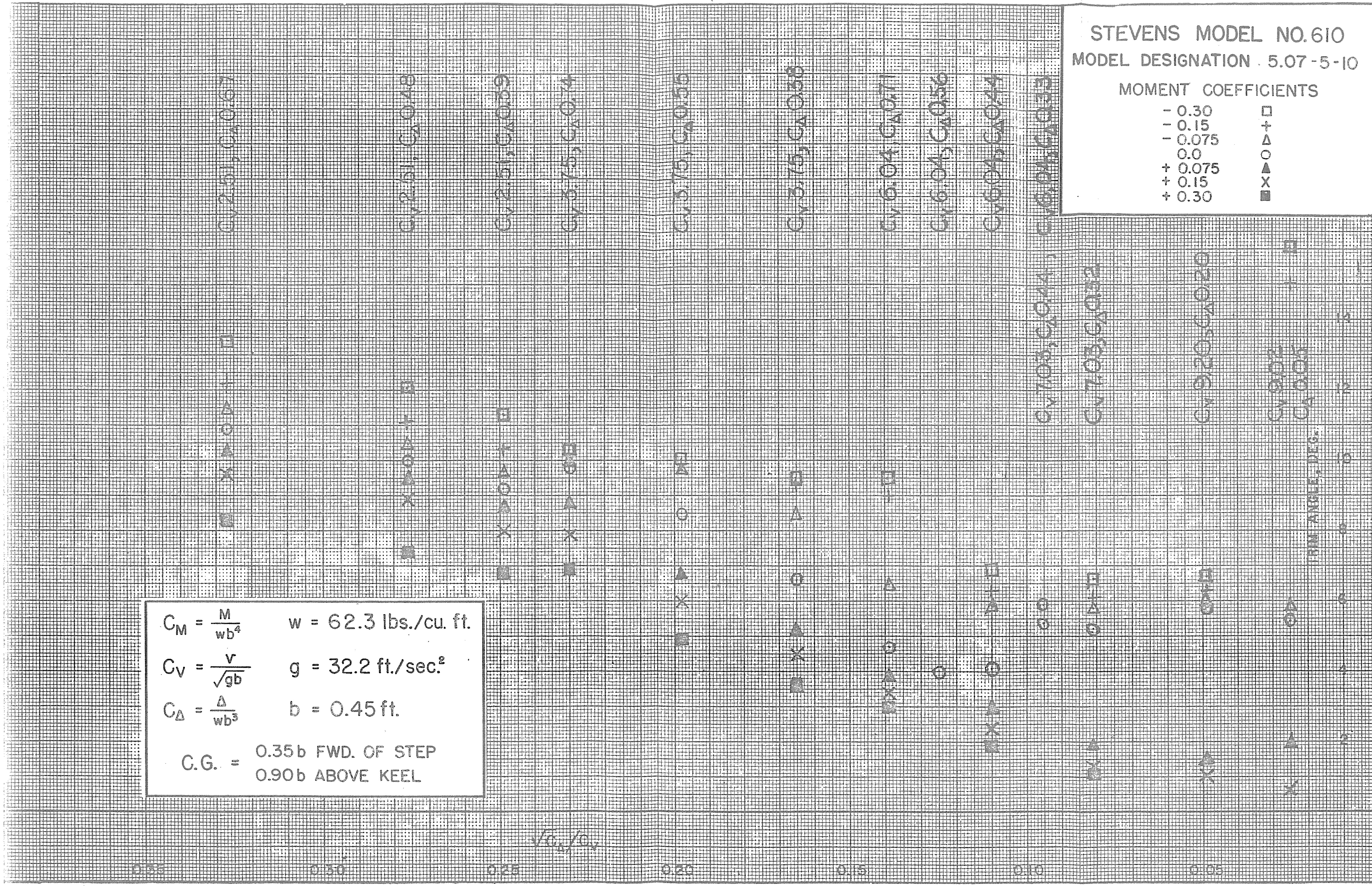
STEVENS MODEL NO. 610
MODEL DESIGNATION 5.07-5-10
MOMENT COEFFICIENTS
− 0.30 □
− 0.15 +
− 0.075 Δ
0.0 ○
+ 0.075 ▲
+ 0.15 X
+ 0.30 ■
C_V 2.51, C_Δ 0.67
C_V 2.51, C_Δ 0.48
C_V 2.51, C_Δ 0.39
C_V 3.75, C_Δ 0.74
C_V 3.75, C_Δ 0.55
C_V 3.75, C_Δ 0.38
C_V 6.04, C_Δ 0.71
C_V 6.04, C_Δ 0.56
C_V 6.04, C_Δ 0.44
C_V 6.04, C_Δ 0.33
C_V 7.03, C_Δ 0.44
C_V 7.03, C_Δ 0.32
C_V 9.20, C_Δ 0.20
C_V 9.02 C_Δ 0.06
TRIM ANGLE, DEG.
$C_M = \frac{M}{wb^4}$
$C_V = \frac{V}{\sqrt{gb}}$
$C_\Delta = \frac{\Delta}{wb^3}$
w = 62.3 lbs./cu. ft.
g = 32.2 ft./sec.^{2}
b = 0.45 ft.
C.G. = 0.35 b FWD. OF STEP
0.90 b ABOVE KEEL
$\sqrt{C_\Delta}/C_V$
0.35
0.30
0.25
0.20
0.15
0.10
0.05
0

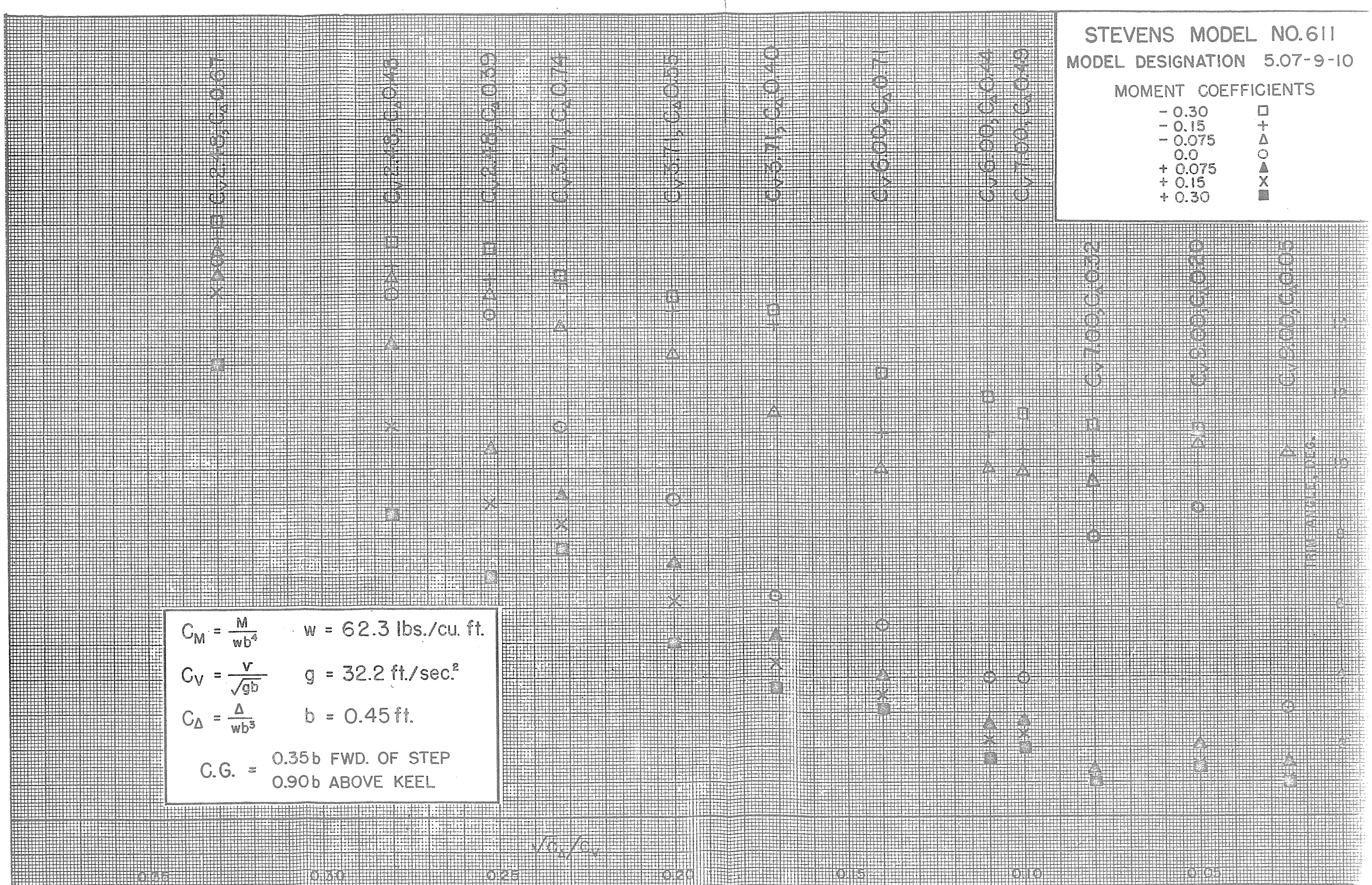
STEVENS MODEL NO.611
MODEL DESIGNATION 5.07-9-10
MOMENT COEFFICIENTS
− 0.30 □
− 0.15 +
− 0.075 Δ
0.0 ○
+ 0.075 ▲
+ 0.15 X
+ 0.30 ■
CM = M / wb⁴
w = 62.3 lbs./cu. ft.
CV = v / √gb
g = 32.2 ft./sec.²
CΔ = Δ / wb³
b = 0.45 ft.
C.G. = 0.35b FWD. OF STEP
0.90b ABOVE KEEL
Cv 2.48, CΔ 0.67
Cv 2.48, CΔ 0.48
Cv 2.48, CΔ 0.39
Cv 3.71, CΔ 0.74
Cv 3.71, CΔ 0.55
Cv 3.71, CΔ 0.40
Cv 6.00, CΔ 0.71
Cv 6.00, CΔ 0.44
Cv 7.00, CΔ 0.49
Cv 7.00, CΔ 0.32
Cv 9.00, CΔ 0.20
Cv 9.00, CΔ 0.05
TRIM ANGLE, DEG.
√CΔ/CV
0.35
0.30
0.25
0.20
0.15
0.10
0.05

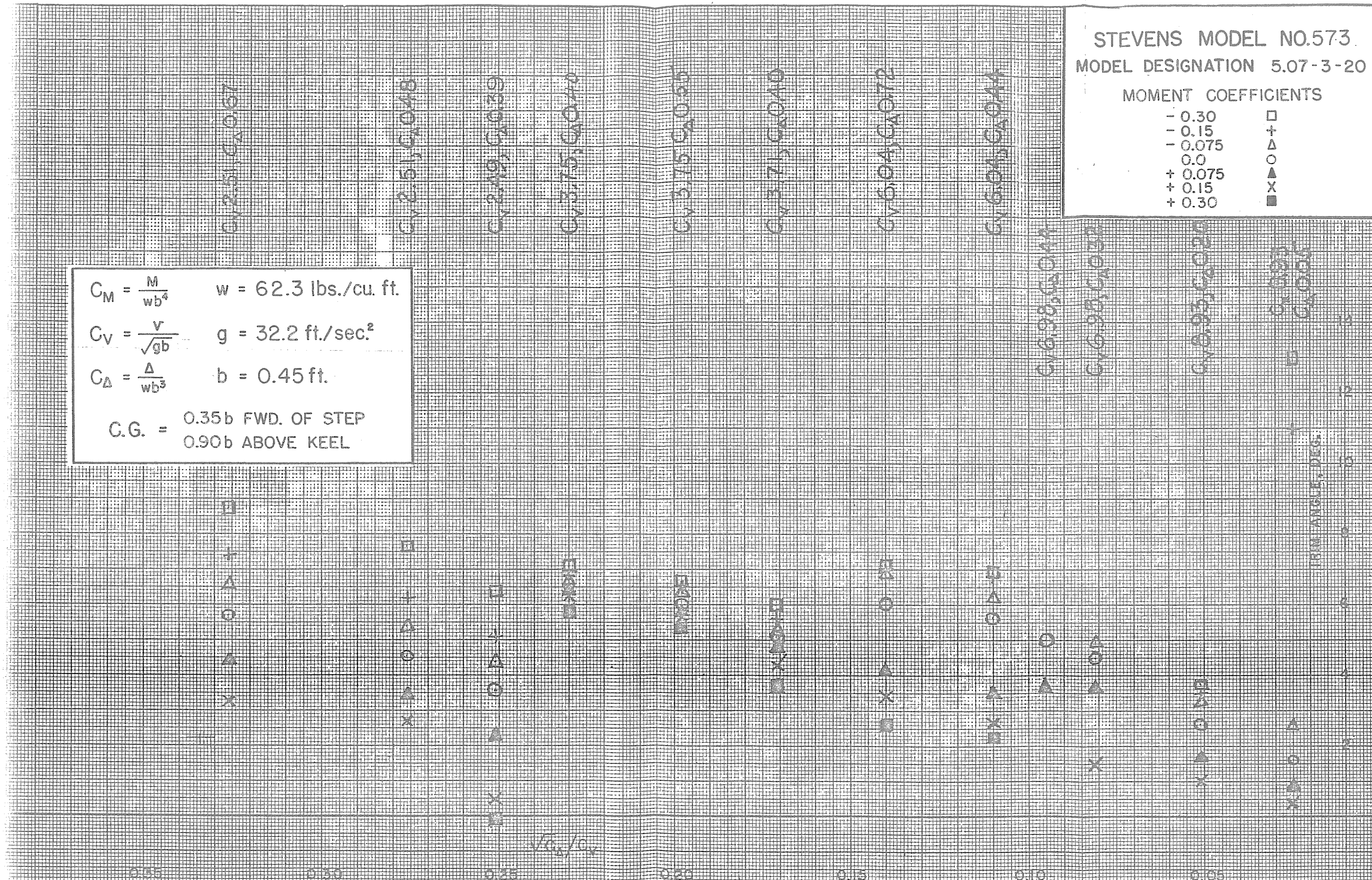
STEVENS MODEL NO.573
MODEL DESIGNATION 5.07-3-20
MOMENT COEFFICIENTS
- 0.30 □
- 0.15 +
- 0.075 Δ
0.0 ○
+ 0.075 ▲
+ 0.15 X
+ 0.30 ■
$C_M = \frac{M}{wb^4}$
$w = 62.3$ lbs./cu. ft.
$C_V = \frac{V}{\sqrt{gb}}$
$g = 32.2$ ft./sec.^{2}
$C_\Delta = \frac{\Delta}{wb^3}$
$b = 0.45$ ft.
C.G. = 0.35b FWD. OF STEP
0.90b ABOVE KEEL
C_V 2.51, C_Δ 0.67
C_V 2.51, C_Δ 0.48
C_V 2.49, C_Δ 0.39
C_V 3.75, C_Δ 0.40
C_V 3.75, C_Δ 0.55
C_V 3.71, C_Δ 0.40
C_V 6.04, C_Δ 0.72
C_V 6.04, C_Δ 0.44
C_V 6.98, C_Δ 0.44
C_V 6.98, C_Δ 0.30
C_V 8.93, C_Δ 0.20
TRIM ANGLE, DEG.
$\sqrt{C_\Delta}/C_V$
0.35
0.30
0.25
0.20
0.15
0.10
0.05
0

EXPERIMENTAL TOWING TANK
STEVENS INSTITUTE OF TECHNOLOGY
HOBOKEN, NEW JERSEY

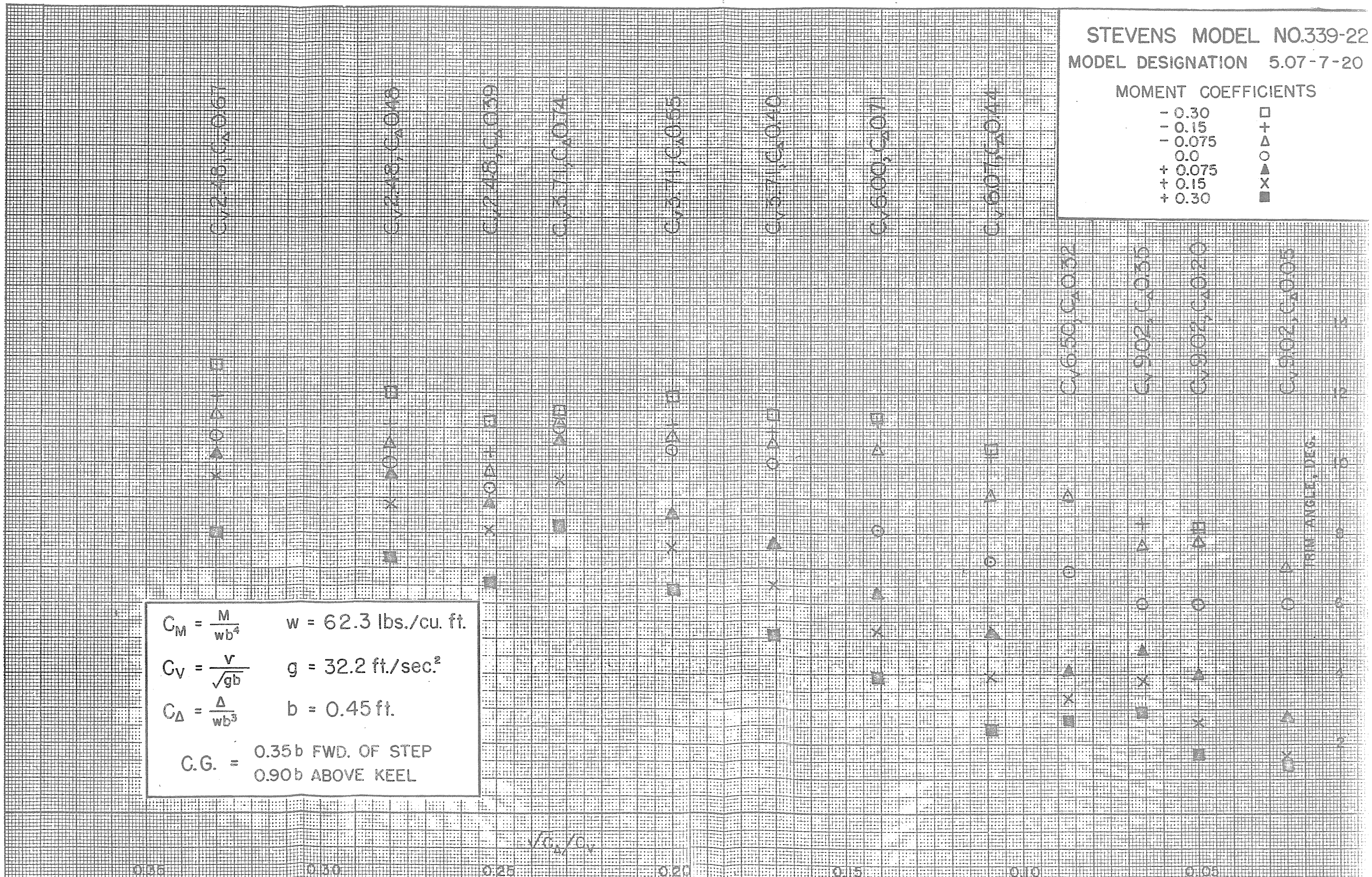

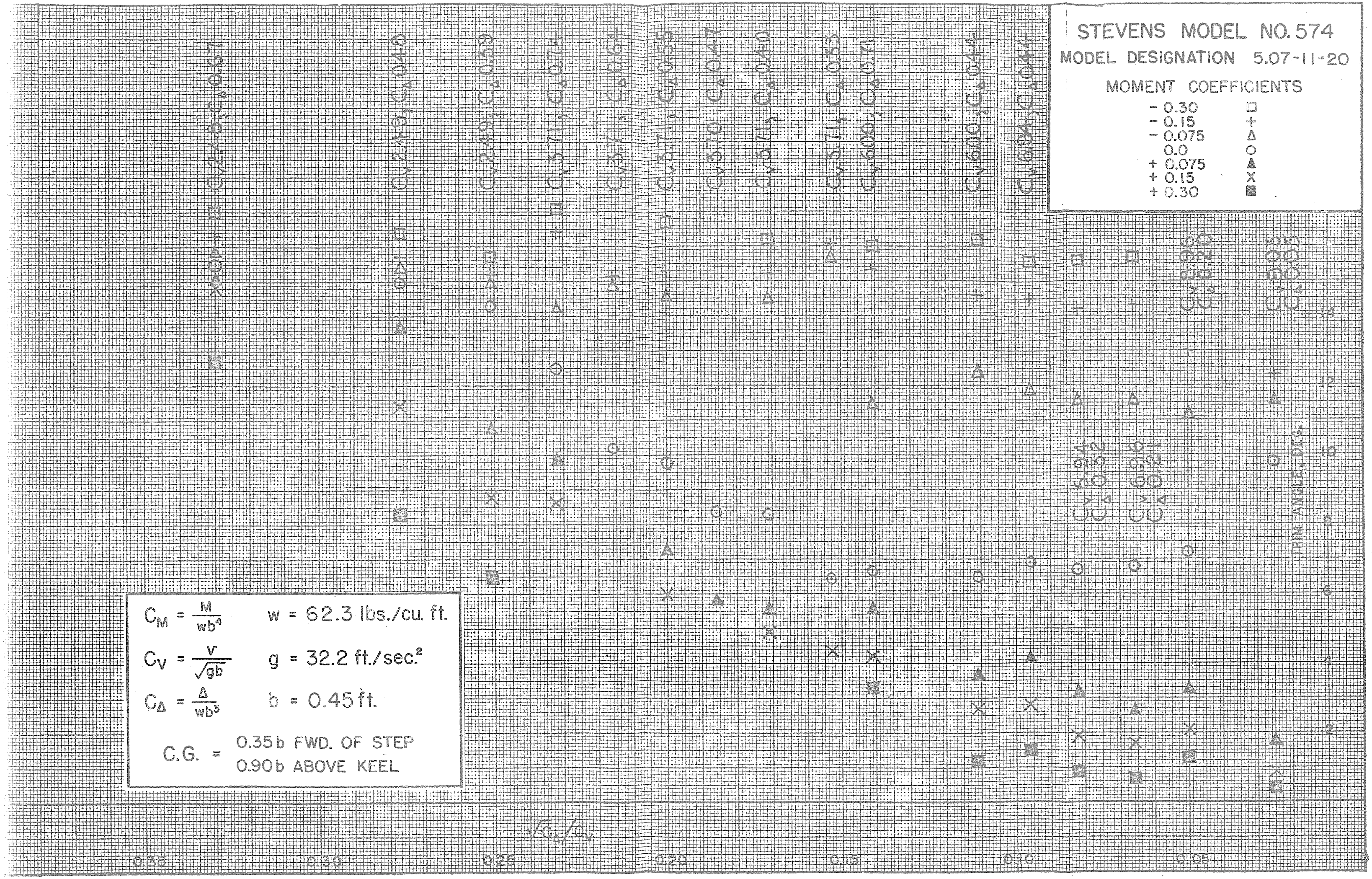
STEVENS MODEL NO. 574
MODEL DESIGNATION 5.07-11-20
MOMENT COEFFICIENTS
- 0.30 □
- 0.15 +
- 0.075 Δ
0.0 ○
+ 0.075 ▲
+ 0.15 X
+ 0.30 ■
$C_M = \frac{M}{wb^4}$ w = 62.3 lbs./cu. ft.
$C_V = \frac{V}{\sqrt{gb}}$ g = 32.2 ft./sec.²
$C_\Delta = \frac{\Delta}{wb^3}$ b = 0.45 ft.
C.G. = 0.35 b FWD. OF STEP
0.90 b ABOVE KEEL
$\sqrt{C_\Delta}/C_V$
TRIM ANGLE, DEG.
0.35
0.30
0.25
0.20
0.15
0.10
0.05
0


STEVENS MODEL NO. 612
MODEL DESIGNATION 5.07-5-30
MOMENT COEFFICIENTS
− 0.30 □
− 0.15 +
− 0.075 Δ
0.0 ○
+ 0.075 ▲
+ 0.15 X
+ 0.30 ■
$C_M = \frac{M}{wb^4}$ w = 62.3 lbs./cu. ft.
$C_V = \frac{v}{\sqrt{gb}}$ g = 32.2 ft./sec.²
$C_\Delta = \frac{\Delta}{wb^3}$ b = 0.45 ft.
C.G. = 0.35 b FWD. OF STEP
0.90 b ABOVE KEEL
C_V 2.48, C_Δ 0.67
C_V 2.48, C_Δ 0.46
C_V 2.48, C_Δ 0.39
C_V 3.71, C_Δ 0.14
C_V 3.71, C_Δ 0.55
C_V 3.71, C_Δ 0.38
C_V 6.00, C_Δ 0.71
C_V 6.00, C_Δ 0.44
C_V 7.04, C_Δ 0.44
C_V 7.04, C_Δ 0.32
C_V 9.03, C_Δ 0.34
C_V 9.01, C_Δ 0.20
C_V 9.03, C_Δ 0.051
TRIM ANGLE, DEG.
$\sqrt{C_\Delta}/C_V$
0.35
0.30
0.25
0.20
0.15
0.10
0.05
0

EXPERIMENTAL TOWING TANK
STEVENS INSTITUTE OF TECHNOLOGY
HOBOKEN, NEW JERSEY

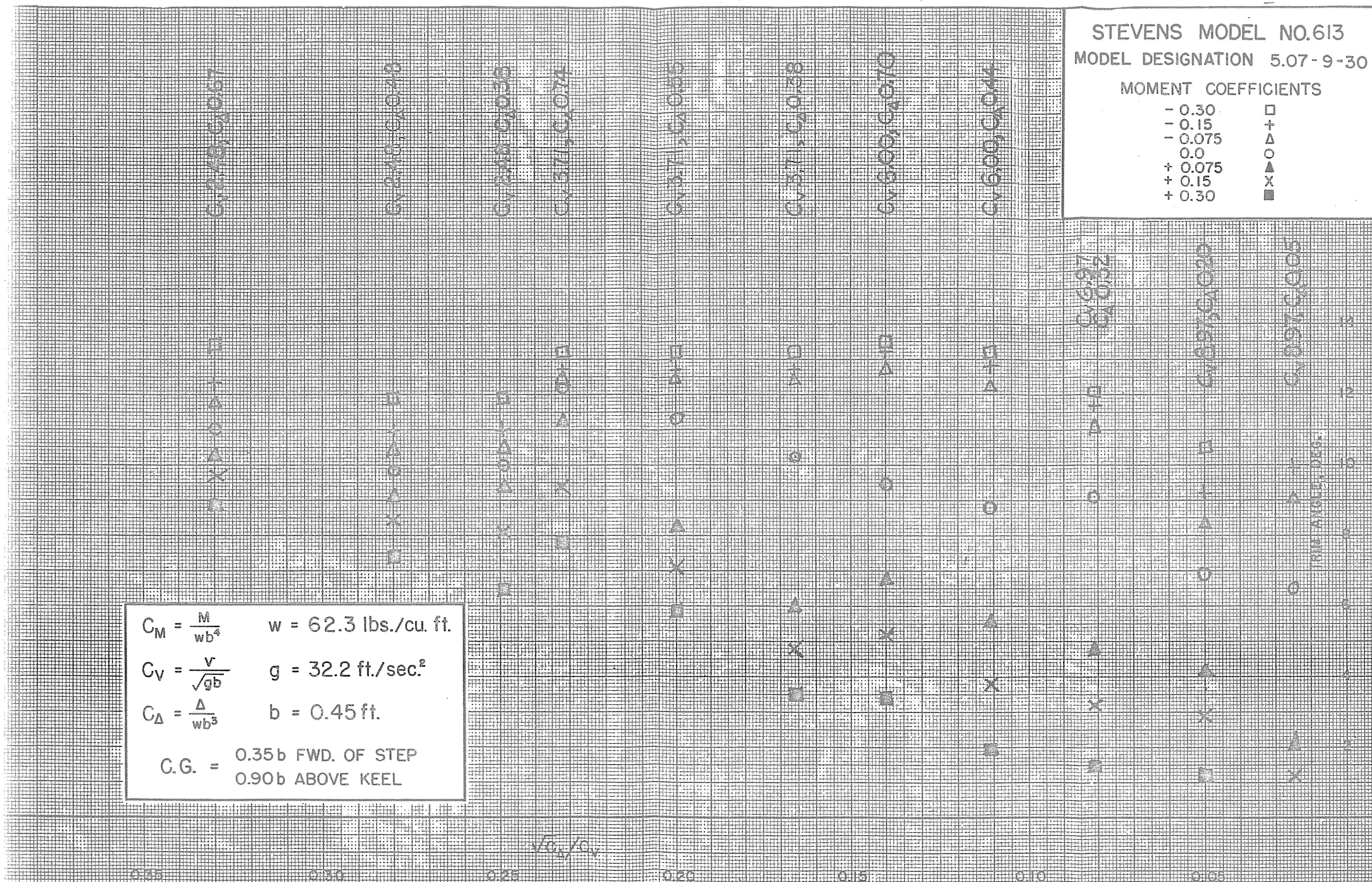

MOMENT DATA CHARTS

FOR LENGTH-BEAM RATIO 6.19 HULLS

Pages 102 through 118

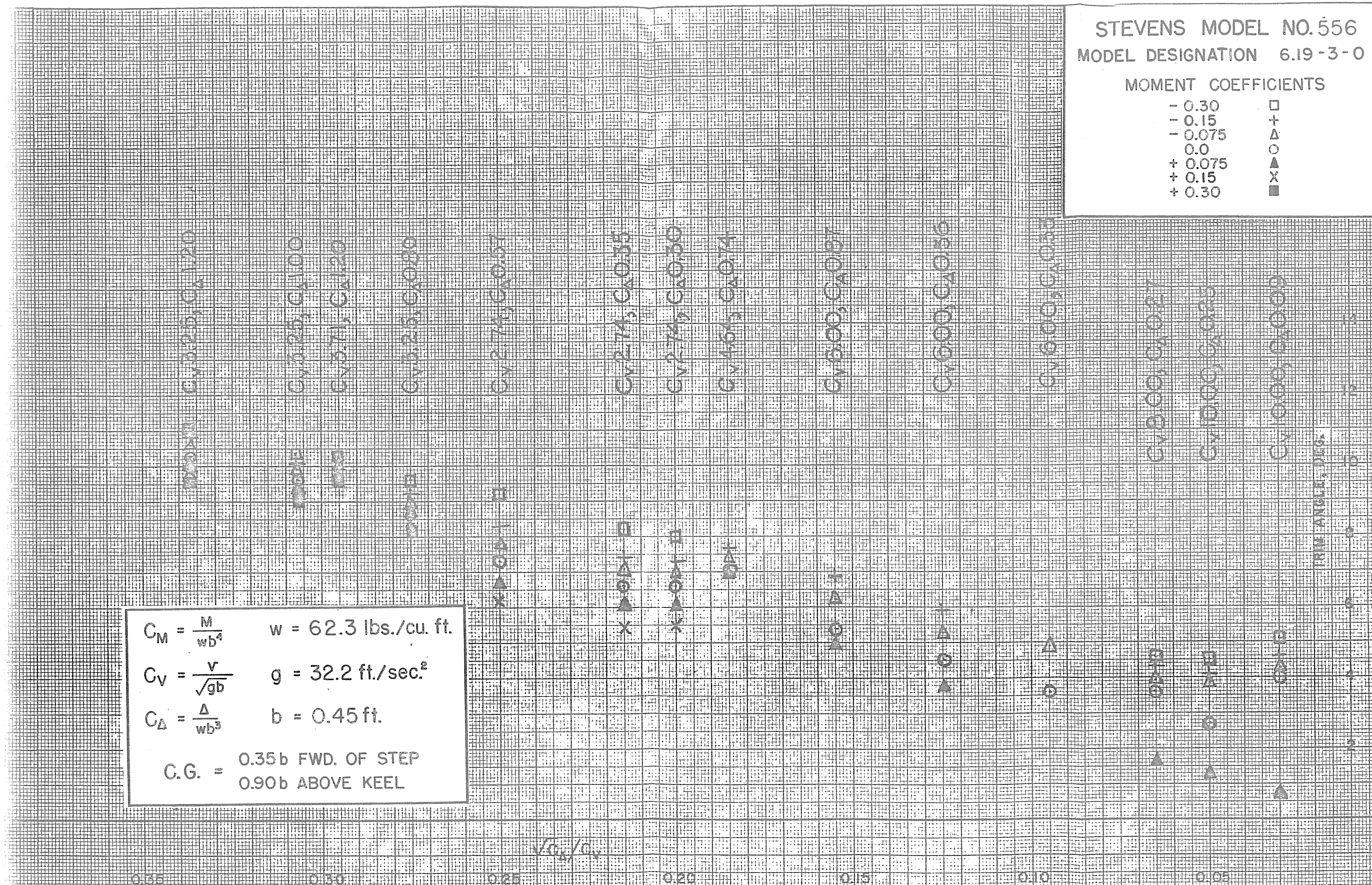
STEVENS MODEL NO. 556
MODEL DESIGNATION 6.19 - 3 - 0
MOMENT COEFFICIENTS
- 0.30 □
- 0.15 +
- 0.075 Δ
0.0 ○
+ 0.075 ▲
+ 0.15 X
+ 0.30 ■
$C_M = \frac{M}{wb^4}$ w = 62.3 lbs./cu. ft.
$C_V = \frac{V}{\sqrt{gb}}$ g = 32.2 ft./sec.^{2}
$C_\Delta = \frac{\Delta}{wb^3}$ b = 0.45 ft.
C.G. = 0.35 b FWD. OF STEP
0.90 b ABOVE KEEL
TRIM ANGLE, DEG.
$\sqrt{C_\Delta}/C_V$
0.35
0.30
0.25
0.20
0.15
0.10
0.05
0

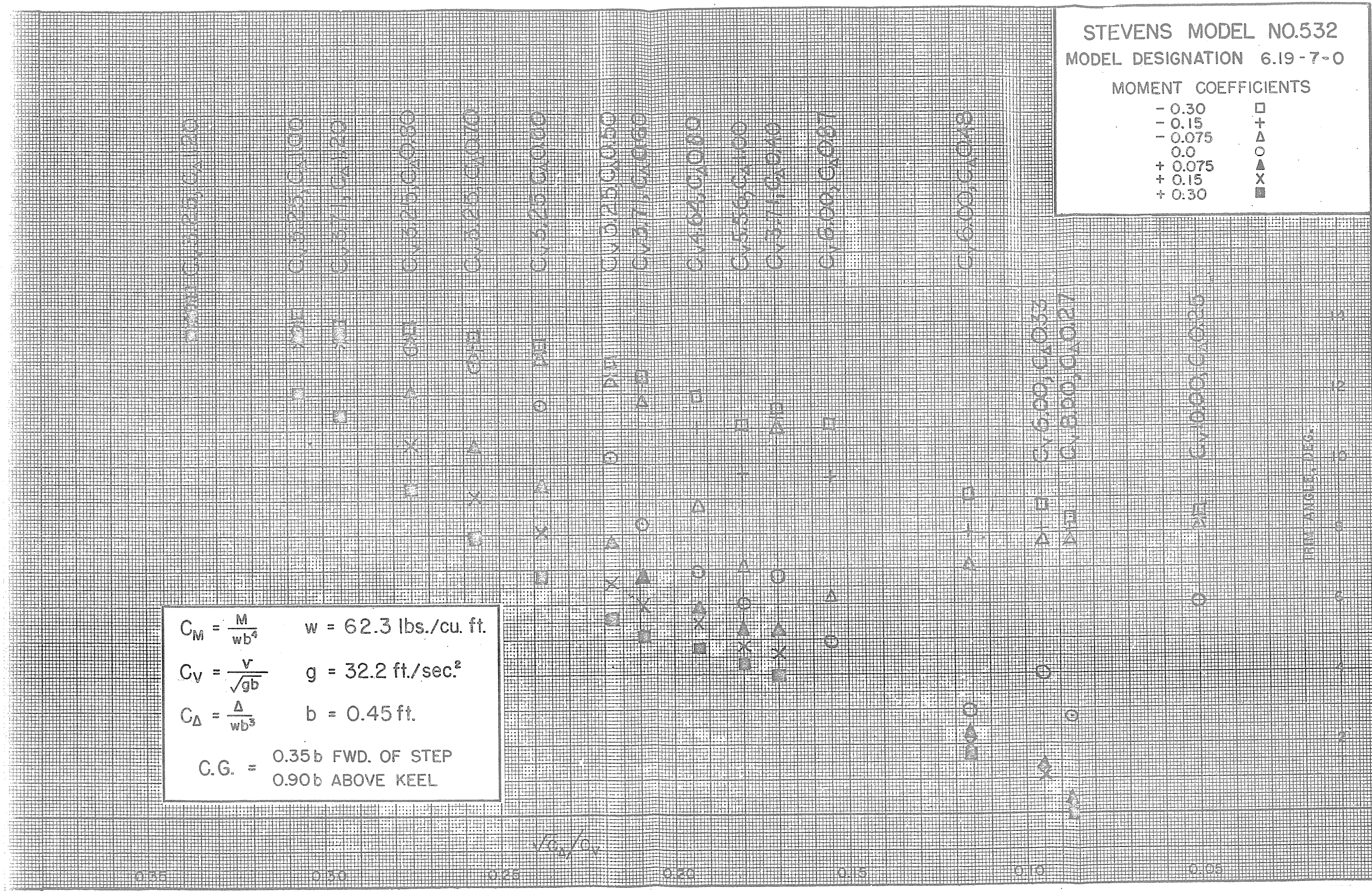
STEVENS MODEL NO.532
MODEL DESIGNATION 6.19-7-0
MOMENT COEFFICIENTS
- 0.30
- 0.15
- 0.075
0.0
+ 0.075
+ 0.15
+ 0.30
$C_M = \frac{M}{wb^4}$
w = 62.3 lbs./cu. ft.
$C_V = \frac{v}{\sqrt{gb}}$
g = 32.2 ft./sec.^{2}
$C_\Delta = \frac{\Delta}{wb^3}$
b = 0.45 ft.
C.G. = 0.35b FWD. OF STEP
0.90b ABOVE KEEL
$\sqrt{C_\Delta}/C_V$
TRIM ANGLE, DEG.
0.35
0.30
0.25
0.20
0.15
0.10
0.05

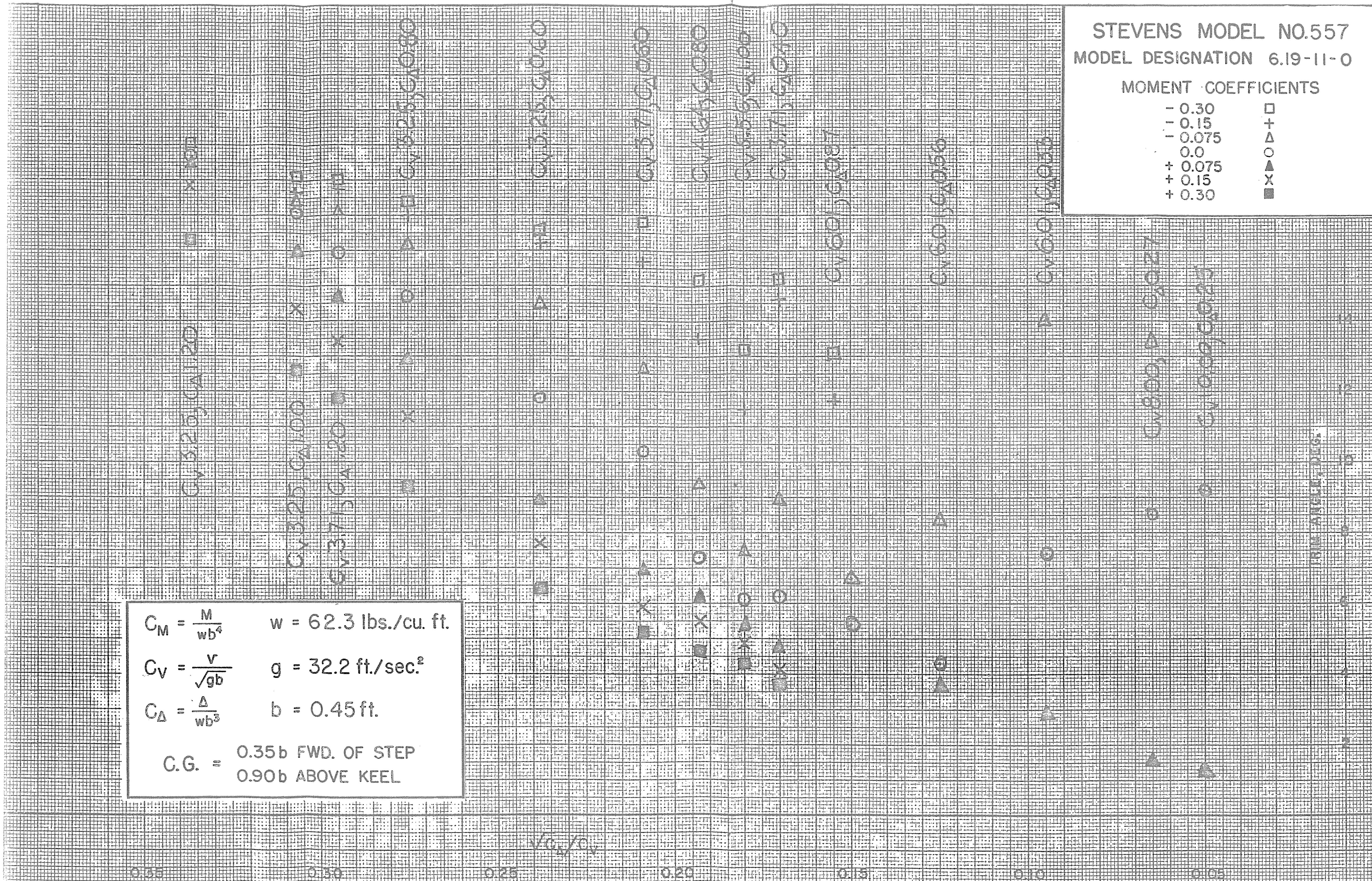
STEVENS MODEL NO.557
MODEL DESIGNATION 6.19-11-0
MOMENT COEFFICIENTS
- 0.30 □
- 0.15 +
- 0.075 △
0.0 ○
+ 0.075 ▲
+ 0.15 X
+ 0.30 ■
$C_M = \frac{M}{wb^4}$
w = 62.3 lbs./cu. ft.
$C_V = \frac{V}{\sqrt{gb}}$
g = 32.2 ft./sec.^{2}
$C_\Delta = \frac{\Delta}{wb^3}$
b = 0.45 ft.
C.G. = 0.35b FWD. OF STEP
0.90b ABOVE KEEL
TRIM ANGLE, DEG.
$\sqrt{C_\Delta}/C_V$
0.35
0.30
0.25
0.20
0.15
0.10
0.05
0

EXPERIMENTAL TOWING TANK
STEVENS INSTITUTE OF TECHNOLOGY
HOBOKEN, NEW JERSEY

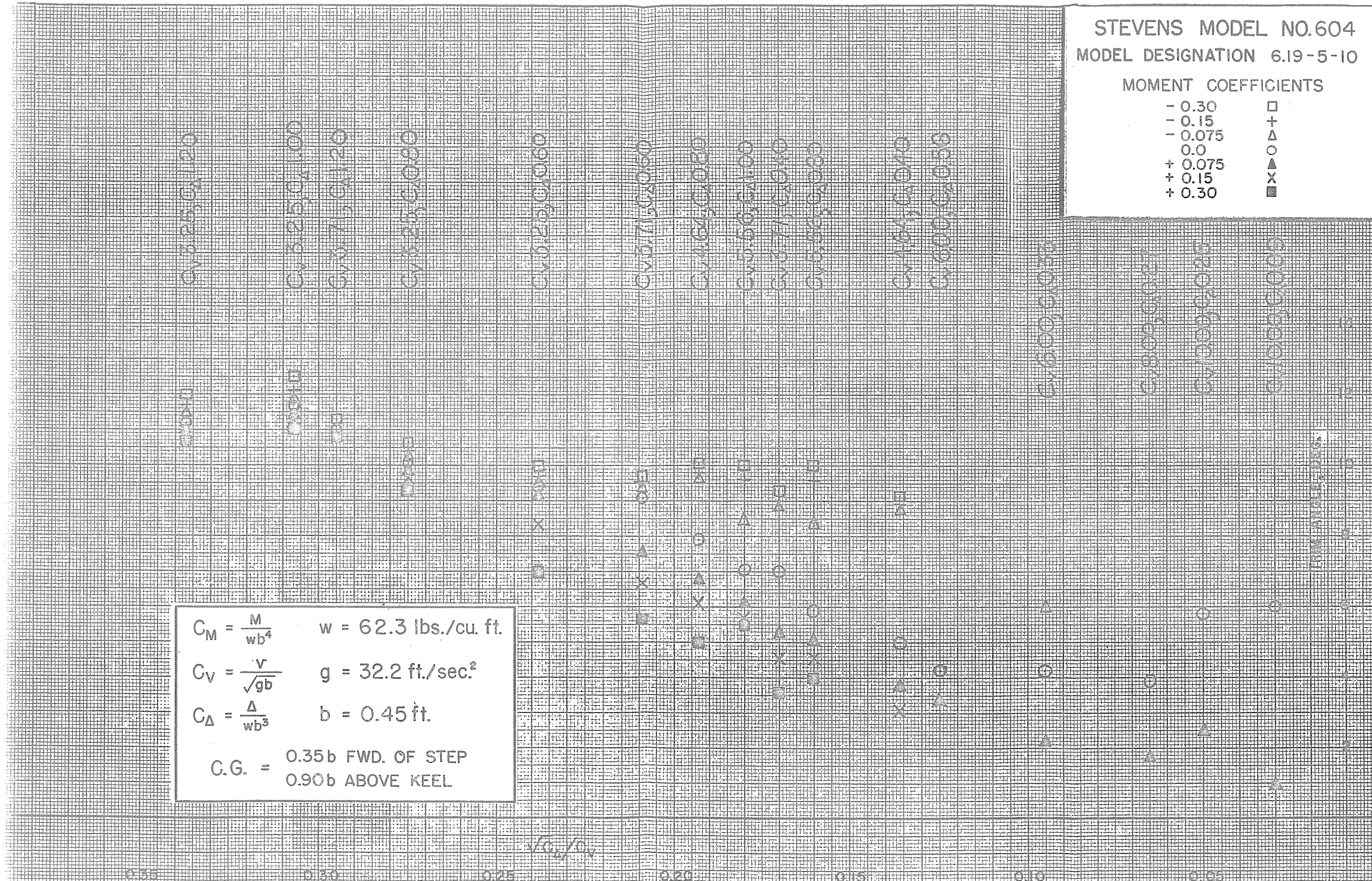

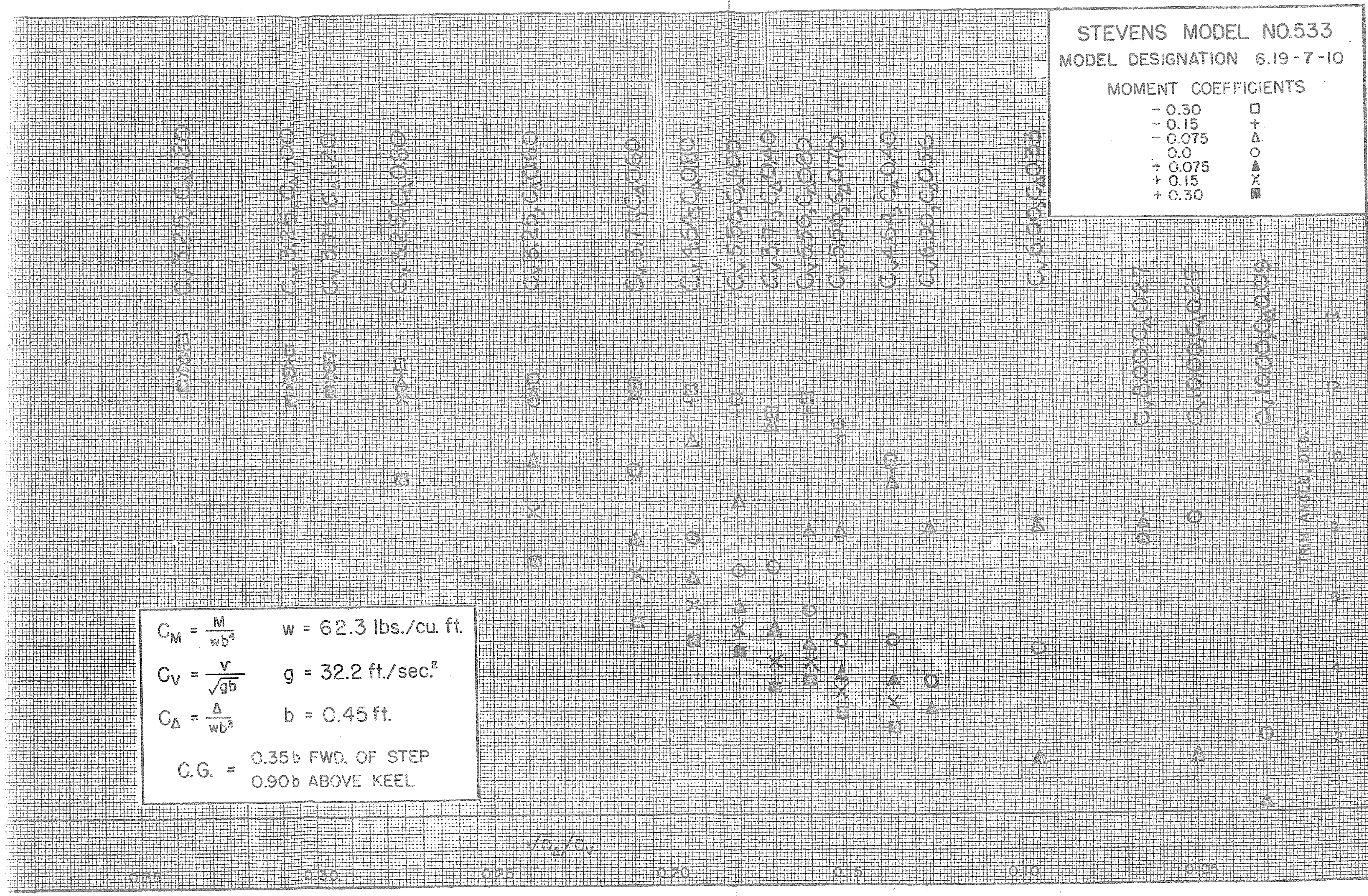
STEVENS MODEL NO.533
MODEL DESIGNATION 6.19-7-10
MOMENT COEFFICIENTS
- 0.30 □
- 0.15 +
- 0.075 Δ
0.0 ○
+ 0.075 ▲
+ 0.15 X
+ 0.30 ■
$C_M = \frac{M}{wb^4}$ w = 62.3 lbs./cu. ft.
$C_V = \frac{v}{\sqrt{gb}}$ g = 32.2 ft./sec.²
$C_\Delta = \frac{\Delta}{wb^3}$ b = 0.45 ft.
C.G. = 0.35b FWD. OF STEP
0.90b ABOVE KEEL
TRIM ANGLE, DEG.
$\sqrt{C_\Delta}/C_V$
0.35
0.30
0.25
0.20
0.15
0.10
0.05
0

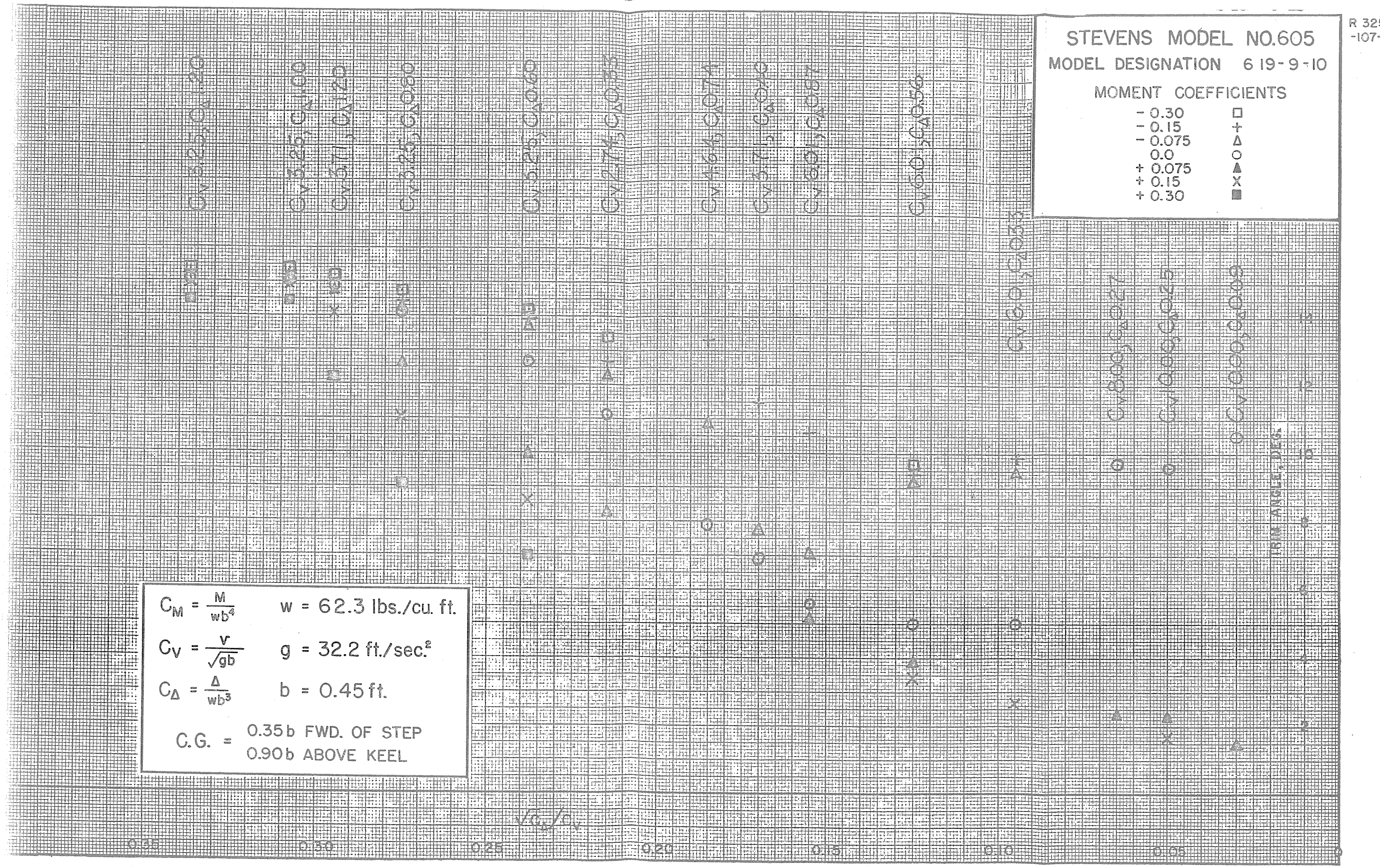
STEVENS MODEL NO.605
MODEL DESIGNATION 6 19-9-10
MOMENT COEFFICIENTS
- 0.30 □
- 0.15 +
- 0.075 Δ
0.0 ○
+ 0.075 ▲
+ 0.15 X
+ 0.30 ■
$C_M = \frac{M}{wb^4}$ w = 62.3 lbs./cu. ft.
$C_V = \frac{V}{\sqrt{gb}}$ g = 32.2 ft./sec.^{2}
$C_\Delta = \frac{\Delta}{wb^3}$ b = 0.45 ft.
C.G. = 0.35 b FWD. OF STEP
0.90 b ABOVE KEEL
C_V 3.25, C_Δ 1.20
C_V 3.25, C_Δ 1.00
C_V 3.71, C_Δ 1.20
C_V 3.25, C_Δ 0.80
C_V 3.25, C_Δ 0.60
C_V 2.74, C_Δ 0.33
C_V 4.64, C_Δ 0.74
C_V 3.71, C_Δ 0.40
C_V 6.01, C_Δ 0.87
C_V 6.01, C_Δ 0.56
C_V 6.01, C_Δ 0.33
C_V 8.00, C_Δ 0.27
C_V 10.00, C_Δ 0.25
C_V 10.00, C_Δ 0.09
TRIM ANGLE, DEG.
$\sqrt{C_\Delta}/C_V$
0.35
0.30
0.25
0.20
0.15
0.10
0.05
0

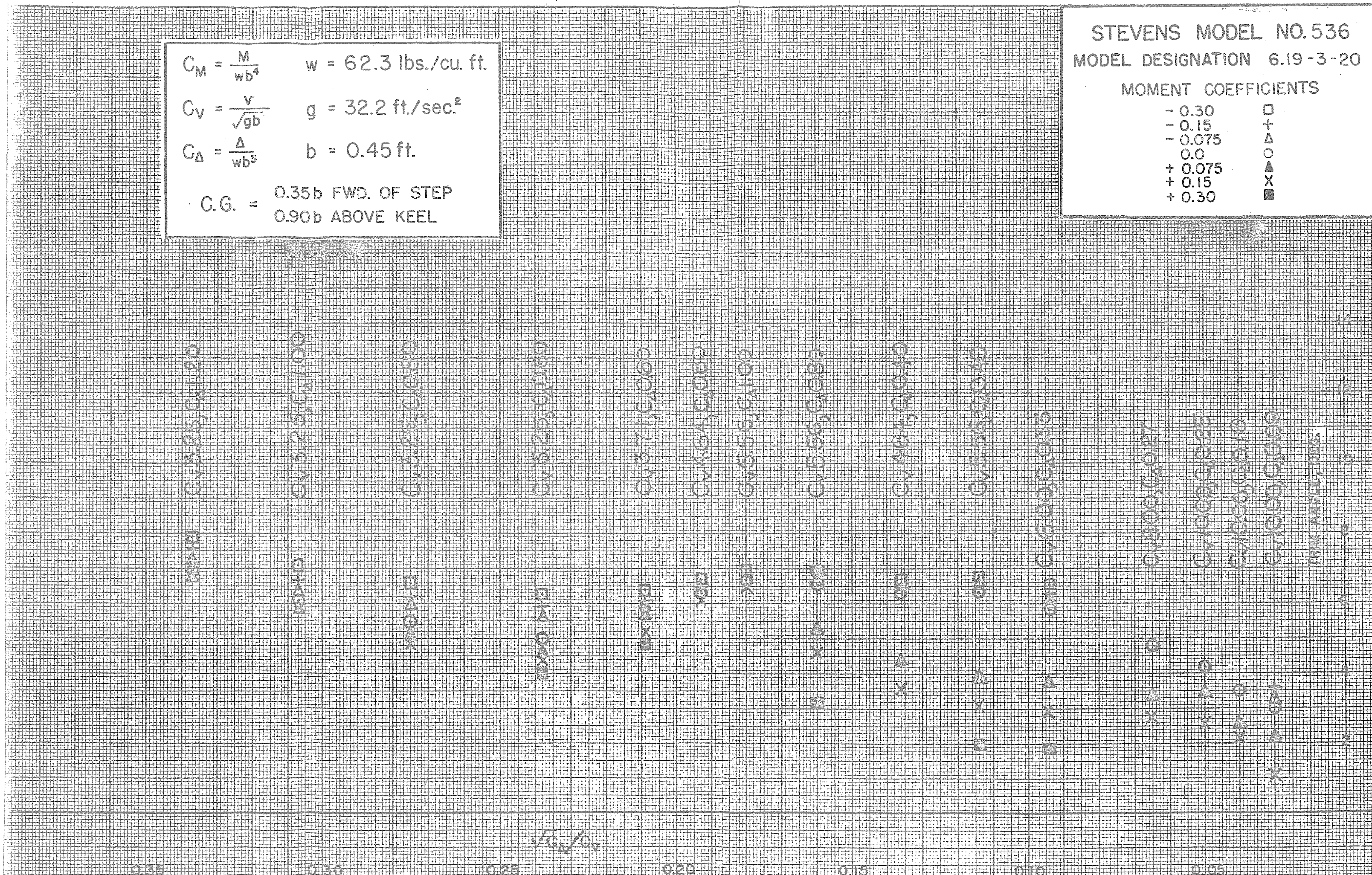
$C_M = \frac{M}{wb^4}$
w = 62.3 lbs./cu. ft.
$C_V = \frac{V}{\sqrt{gb}}$
g = 32.2 ft./sec.^{2}
$C_\Delta = \frac{\Delta}{wb^3}$
b = 0.45 ft.
C.G. = 0.35 b FWD. OF STEP
0.90 b ABOVE KEEL
STEVENS MODEL NO. 536
MODEL DESIGNATION 6.19-3-20
MOMENT COEFFICIENTS
− 0.30
− 0.15
− 0.075
0.0
+ 0.075
+ 0.15
+ 0.30
TRIM ANGLE, DEG.
$\sqrt{C_\Delta}/C_V$
0.35
0.30
0.25
0.20
0.15
0.10
0.05
0

EXPERIMENTAL TOWING TANK
STEVENS INSTITUTE OF TECHNOLOGY
HOBOKEN, NEW JERSEY

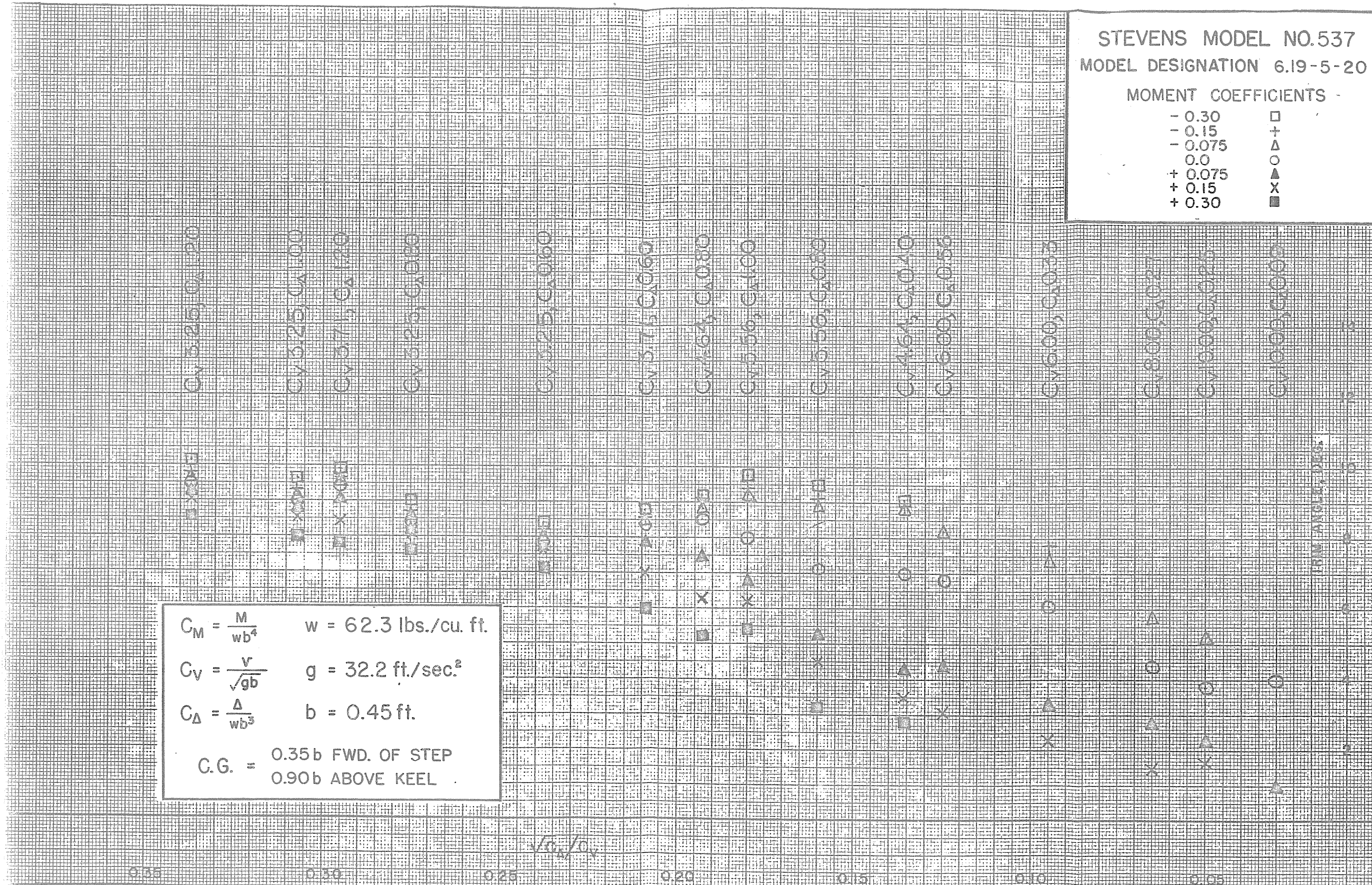

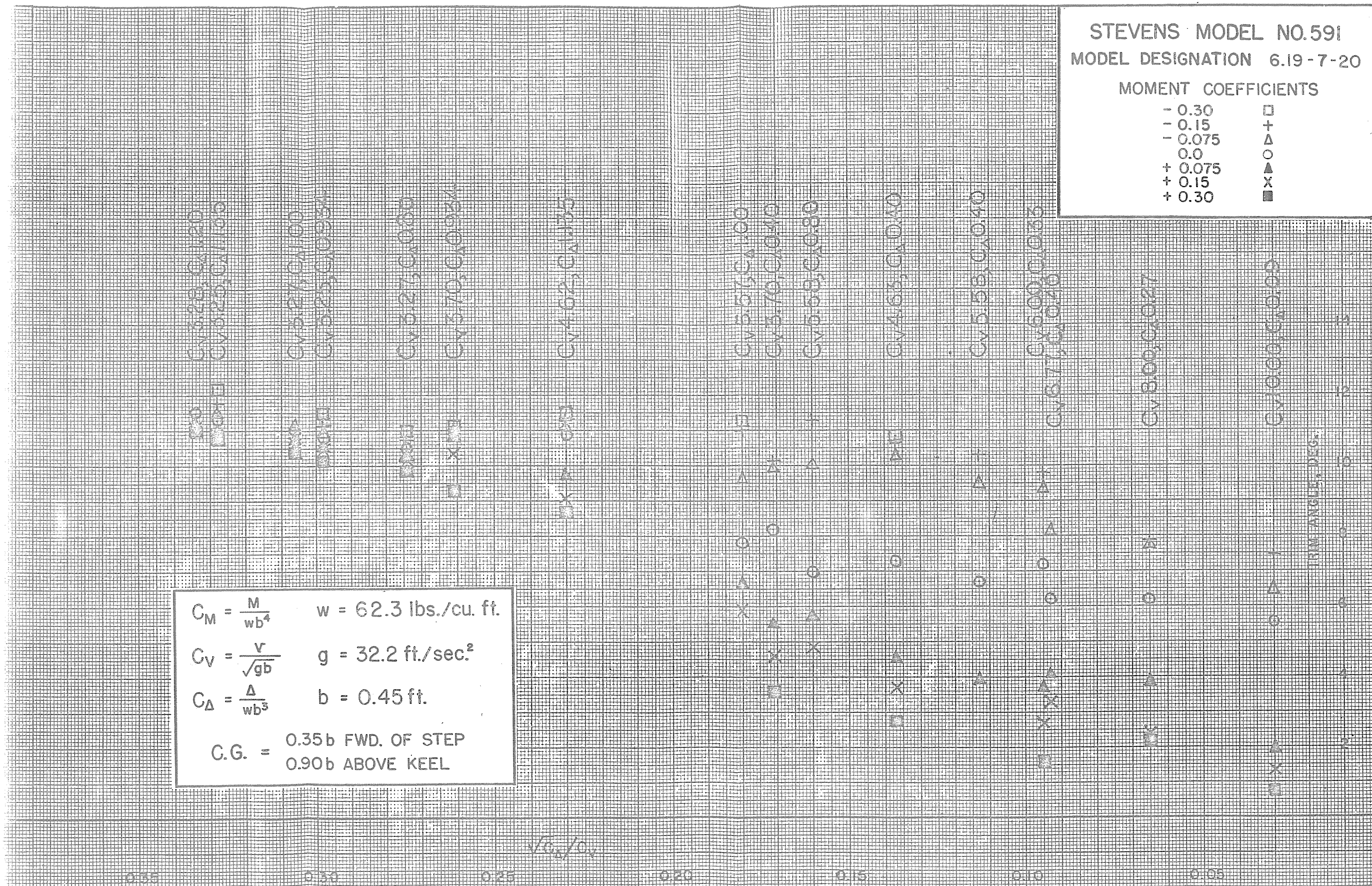
STEVENS MODEL NO. 591
MODEL DESIGNATION 6.19-7-20
MOMENT COEFFICIENTS
− 0.30 □
− 0.15 +
− 0.075 Δ
0.0 ○
+ 0.075 ▲
+ 0.15 X
+ 0.30 ■
$C_M = \frac{M}{wb^4}$ w = 62.3 lbs./cu. ft.
$C_V = \frac{V}{\sqrt{gb}}$ g = 32.2 ft./sec.^{2}
$C_\Delta = \frac{\Delta}{wb^3}$ b = 0.45 ft.
C.G. = 0.35 b FWD. OF STEP
0.90 b ABOVE KEEL
TRIM ANGLE, DEG.
$\sqrt{C_\Delta}/C_V$
0.35
0.30
0.25
0.20
0.15
0.10
0.05
0

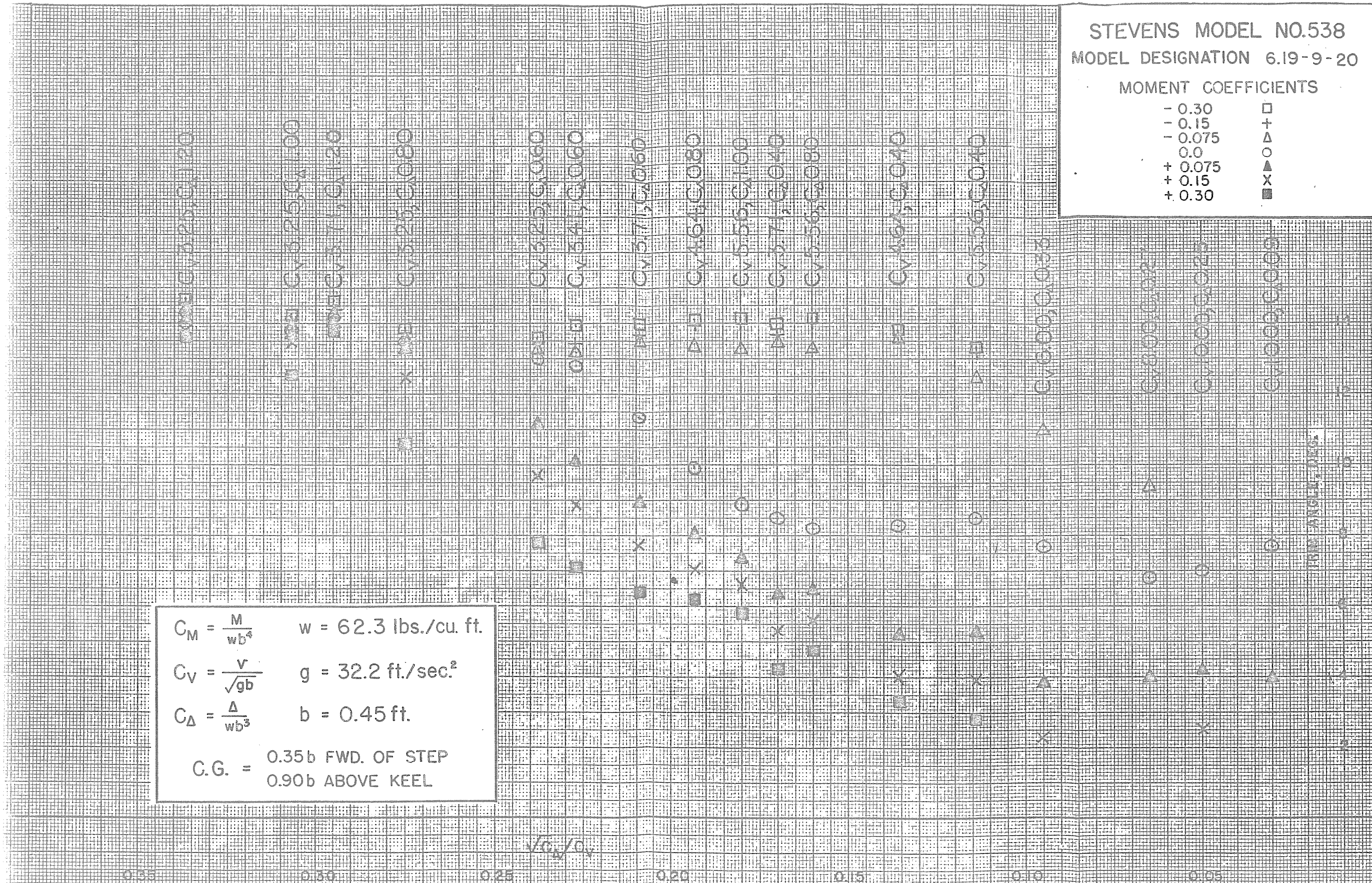
STEVENS MODEL NO.538
MODEL DESIGNATION 6.19-9-20
MOMENT COEFFICIENTS
- 0.30 □
- 0.15 +
- 0.075 △
0.0 ○
+ 0.075 ▲
+ 0.15 X
+ 0.30 ■
C_V 3.25, C_Δ 1.20
C_V 3.25, C_Δ 1.00
C_V 3.71, C_Δ 1.20
C_V 3.25, C_Δ 0.80
C_V 3.25, C_Δ 0.60
C_V 3.41, C_Δ 0.60
C_V 3.71, C_Δ 0.60
C_V 4.64, C_Δ 0.80
C_V 5.56, C_Δ 1.00
C_V 3.71, C_Δ 0.40
C_V 5.56, C_Δ 0.80
C_V 4.64, C_Δ 0.40
C_V 5.56, C_Δ 0.40
$C_M = \frac{M}{wb^4}$ w = 62.3 lbs./cu. ft.
$C_V = \frac{V}{\sqrt{gb}}$ g = 32.2 ft./sec.^{2}
$C_\Delta = \frac{\Delta}{wb^3}$ b = 0.45 ft.
C.G. = 0.35b FWD. OF STEP
0.90b ABOVE KEEL
TRIM ANGLE, DEG.
$\sqrt{C_\Delta}/C_V$
0.35
0.30
0.25
0.20
0.15
0.10
0.05
0

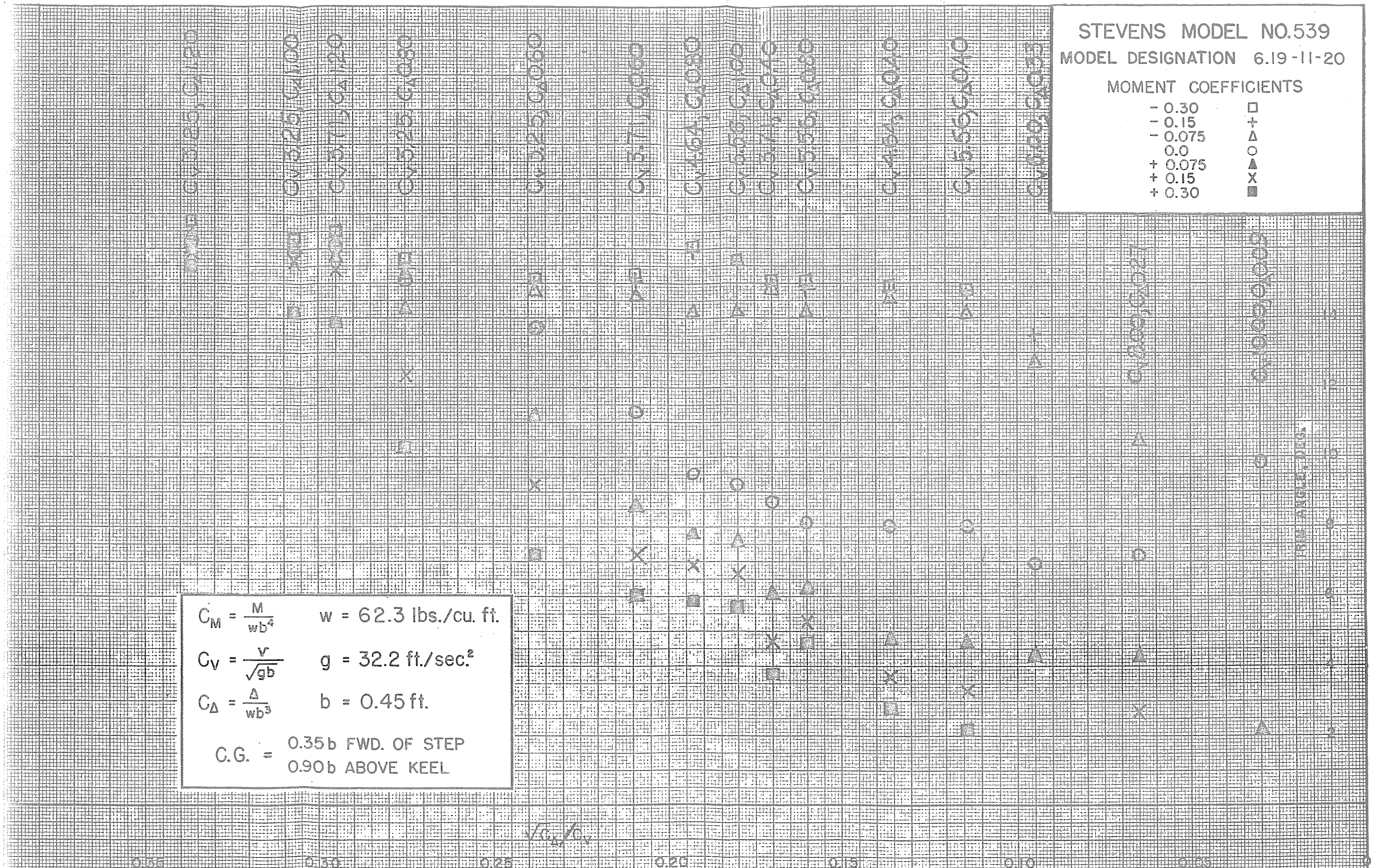
STEVENS MODEL NO.539
MODEL DESIGNATION 6.19-11-20
MOMENT COEFFICIENTS
− 0.30 □
− 0.15 +
− 0.075 △
0.0 ○
+ 0.075 ▲
+ 0.15 X
+ 0.30 ■
$C_M = \frac{M}{wb^4}$ w = 62.3 lbs./cu. ft.
$C_V = \frac{V}{\sqrt{gb}}$ g = 32.2 ft./sec.²
$C_\Delta = \frac{\Delta}{wb^3}$ b = 0.45 ft.
C.G. = 0.35 b FWD. OF STEP
0.90 b ABOVE KEEL
$\sqrt{C_\Delta}/C_V$
TRIM ANGLE, DEG.
0.35
0.30
0.25
0.20
0.15
0.10
0.05
0

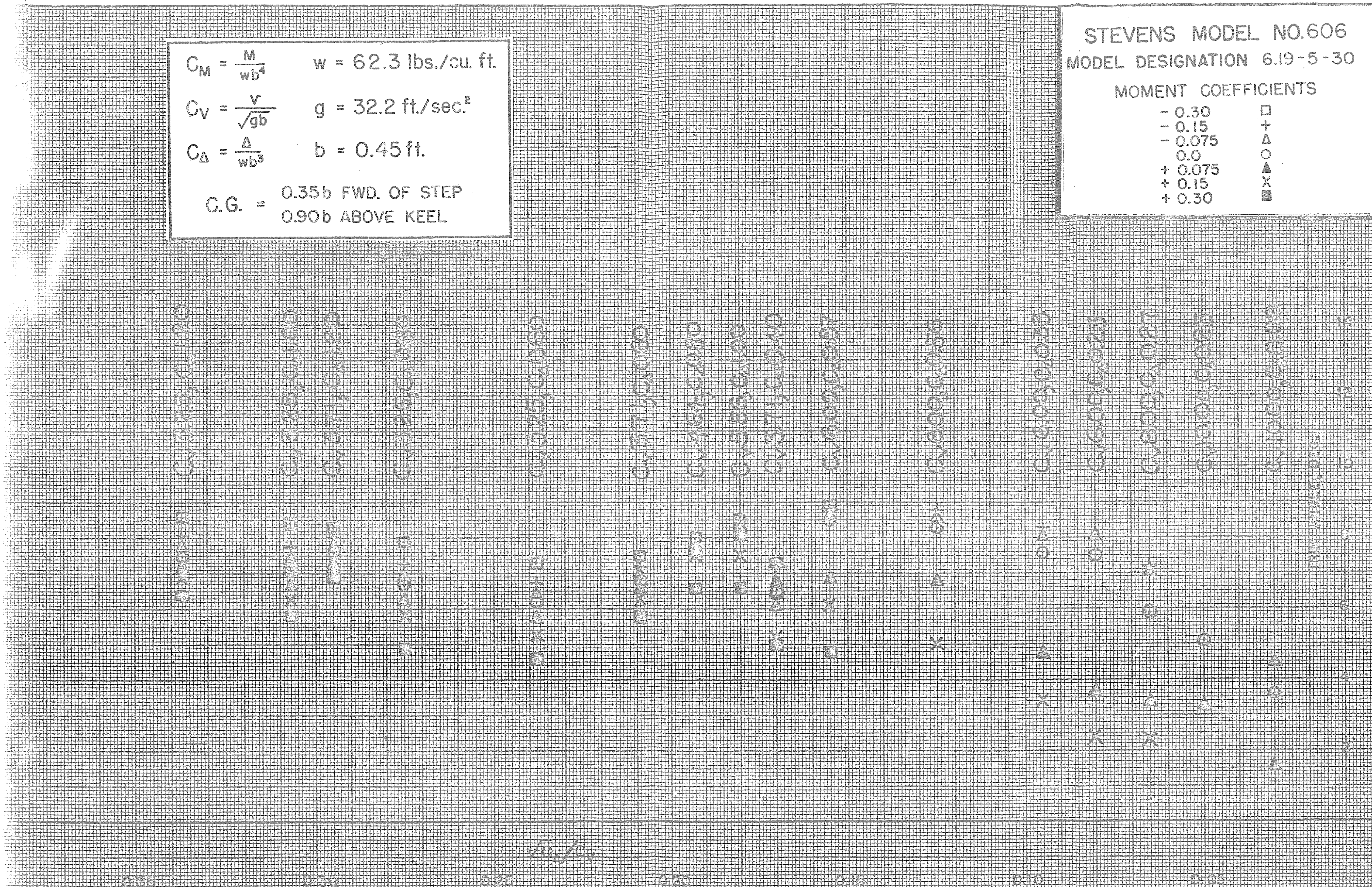
$C_M = \frac{M}{wb^4}$ w = 62.3 lbs./cu. ft.
$C_V = \frac{V}{\sqrt{gb}}$ g = 32.2 ft./sec.^{2}
$C_\Delta = \frac{\Delta}{wb^3}$ b = 0.45 ft.
C.G. = 0.35 b FWD. OF STEP
0.90 b ABOVE KEEL
STEVENS MODEL NO. 606
MODEL DESIGNATION 6.19-5-30
MOMENT COEFFICIENTS
- 0.30 □
- 0.15 +
- 0.075 △
0.0 ○
+ 0.075 ▲
+ 0.15 X
+ 0.30 ■

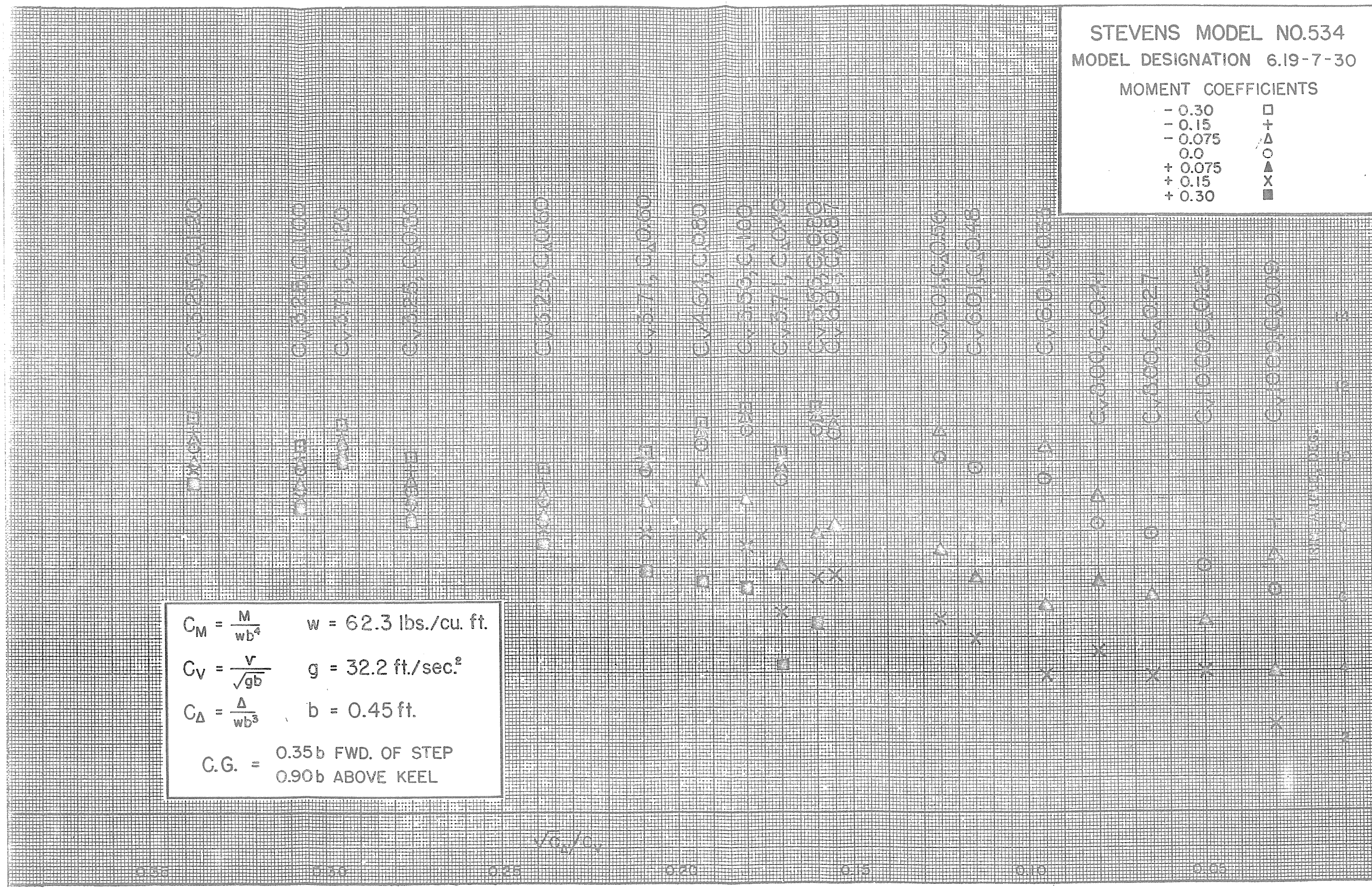
STEVENS MODEL NO.534
MODEL DESIGNATION 6.19-7-30
MOMENT COEFFICIENTS
- 0.30 □
- 0.15 +
- 0.075 △
0.0 ○
+ 0.075 ▲
+ 0.15 X
+ 0.30 ■
$C_M = \frac{M}{wb^4}$ w = 62.3 lbs./cu. ft.
$C_V = \frac{v}{\sqrt{gb}}$ g = 32.2 ft./sec.^{2}
$C_\Delta = \frac{\Delta}{wb^3}$ b = 0.45 ft.
C.G. = 0.35 b FWD. OF STEP
0.90 b ABOVE KEEL
$\sqrt{C_\Delta}/C_V$
TRIM ANGLE, DEG.
0.35
0.30
0.25
0.20
0.15
0.10
0.05

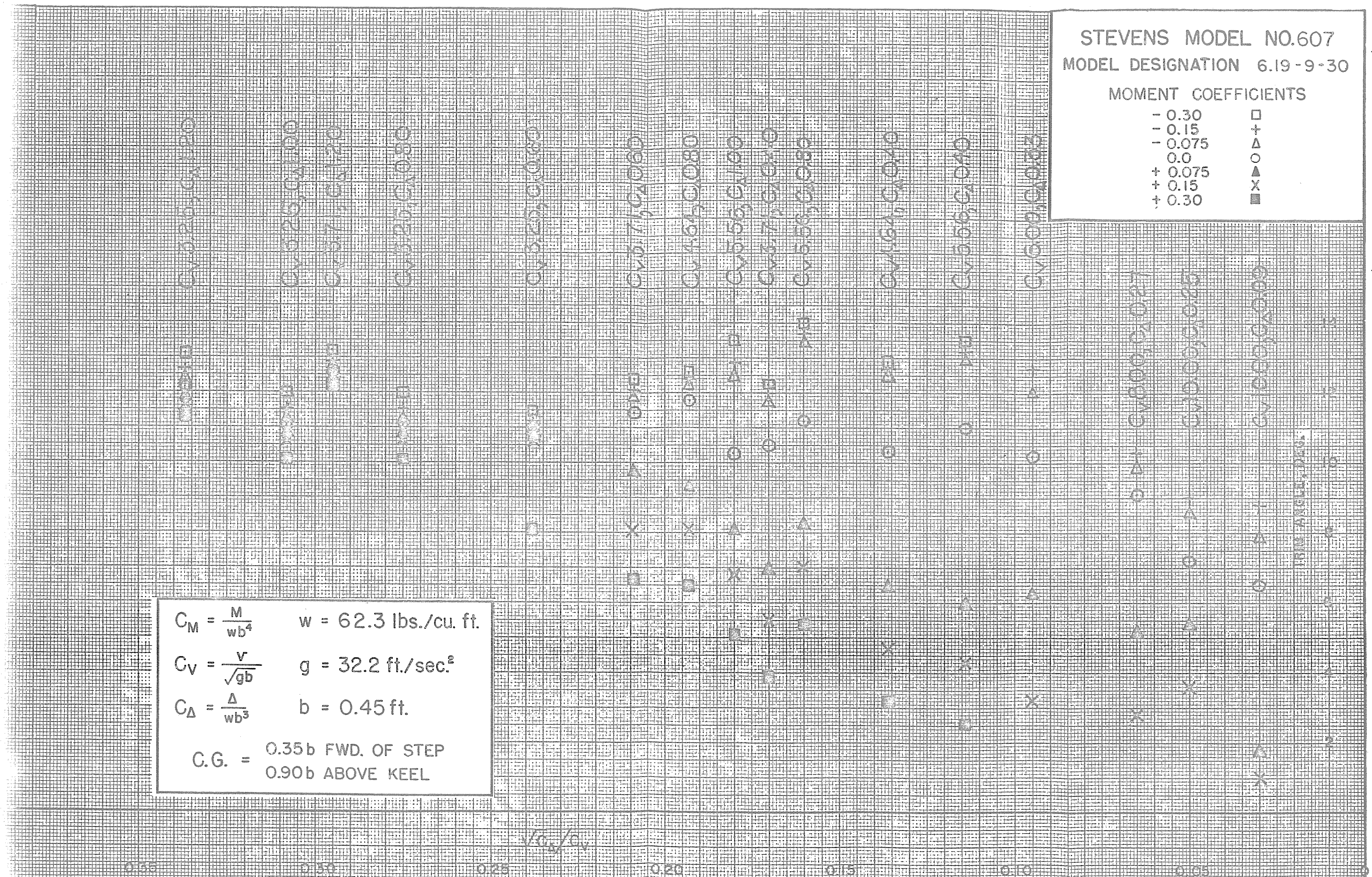
STEVENS MODEL NO.607
MODEL DESIGNATION 6.19-9-30
MOMENT COEFFICIENTS
- 0.30
- 0.15
- 0.075
0.0
+ 0.075
+ 0.15
+ 0.30
$C_M = \frac{M}{wb^4}$
w = 62.3 lbs./cu. ft.
$C_V = \frac{V}{\sqrt{gb}}$
g = 32.2 ft./sec.^{2}
$C_\Delta = \frac{\Delta}{wb^3}$
b = 0.45 ft.
C.G. = 0.35 b FWD. OF STEP
0.90 b ABOVE KEEL
$\sqrt{C_\Delta}/C_V$
0.35
0.30
0.25
0.20
0.15
0.10
0.05
0
TRIM ANGLE, DEG.

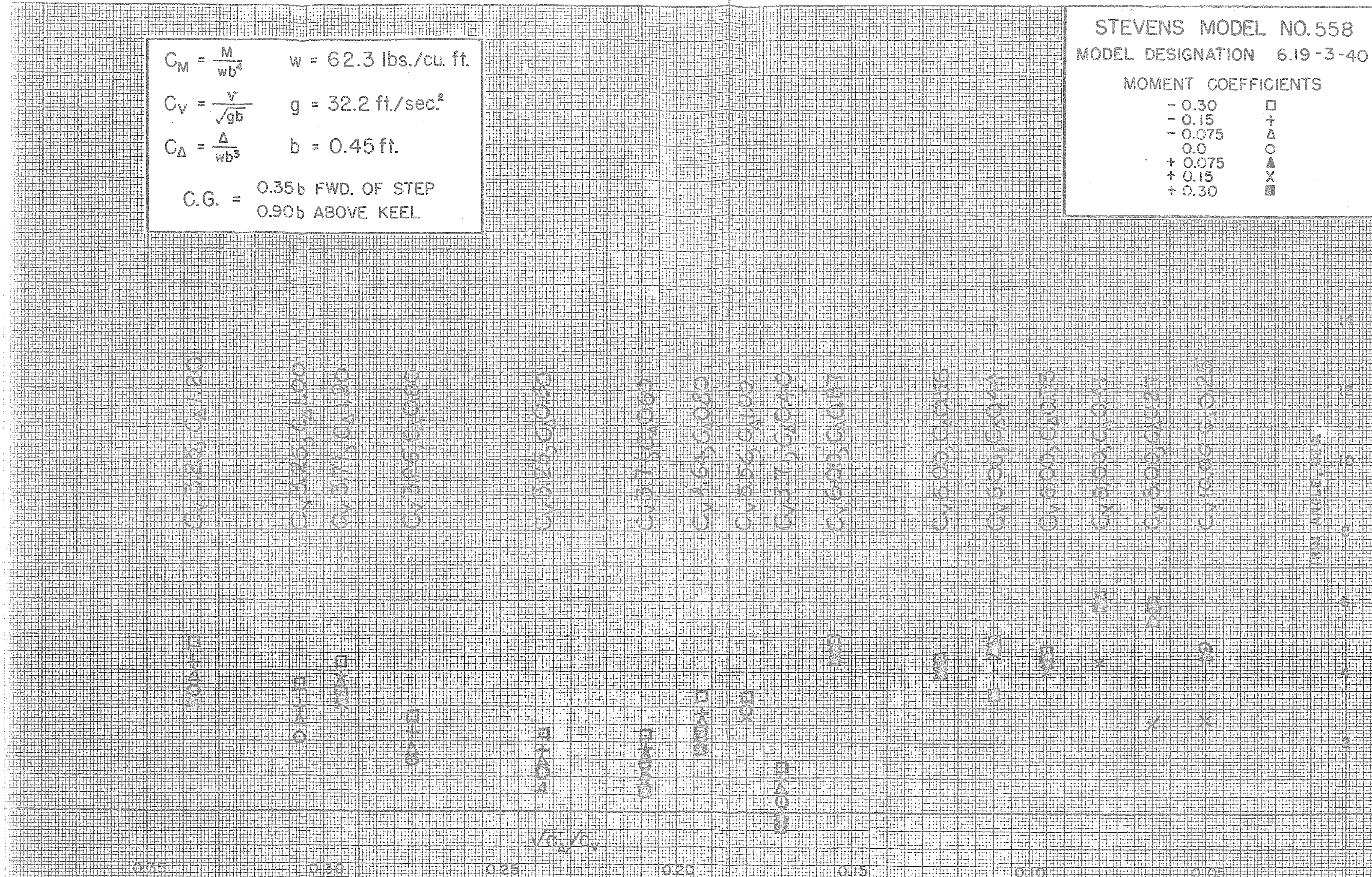
$C_M = \frac{M}{wb^4}$ w = 62.3 lbs./cu. ft.
$C_V = \frac{V}{\sqrt{gb}}$ g = 32.2 ft./sec.^{2}
$C_\Delta = \frac{\Delta}{wb^3}$ b = 0.45 ft.
C.G. = 0.35b FWD. OF STEP
0.90b ABOVE KEEL
STEVENS MODEL NO. 558
MODEL DESIGNATION 6.19-3-40
MOMENT COEFFICIENTS
− 0.30 □
− 0.15 +
− 0.075 △
0.0 ○
+ 0.075 ▲
+ 0.15 X
+ 0.30 ■
TRIM ANGLE, DEG.
$\sqrt{C_\Delta}/C_V$
0.35
0.30
0.25
0.20
0.15
0.10
0.05
0

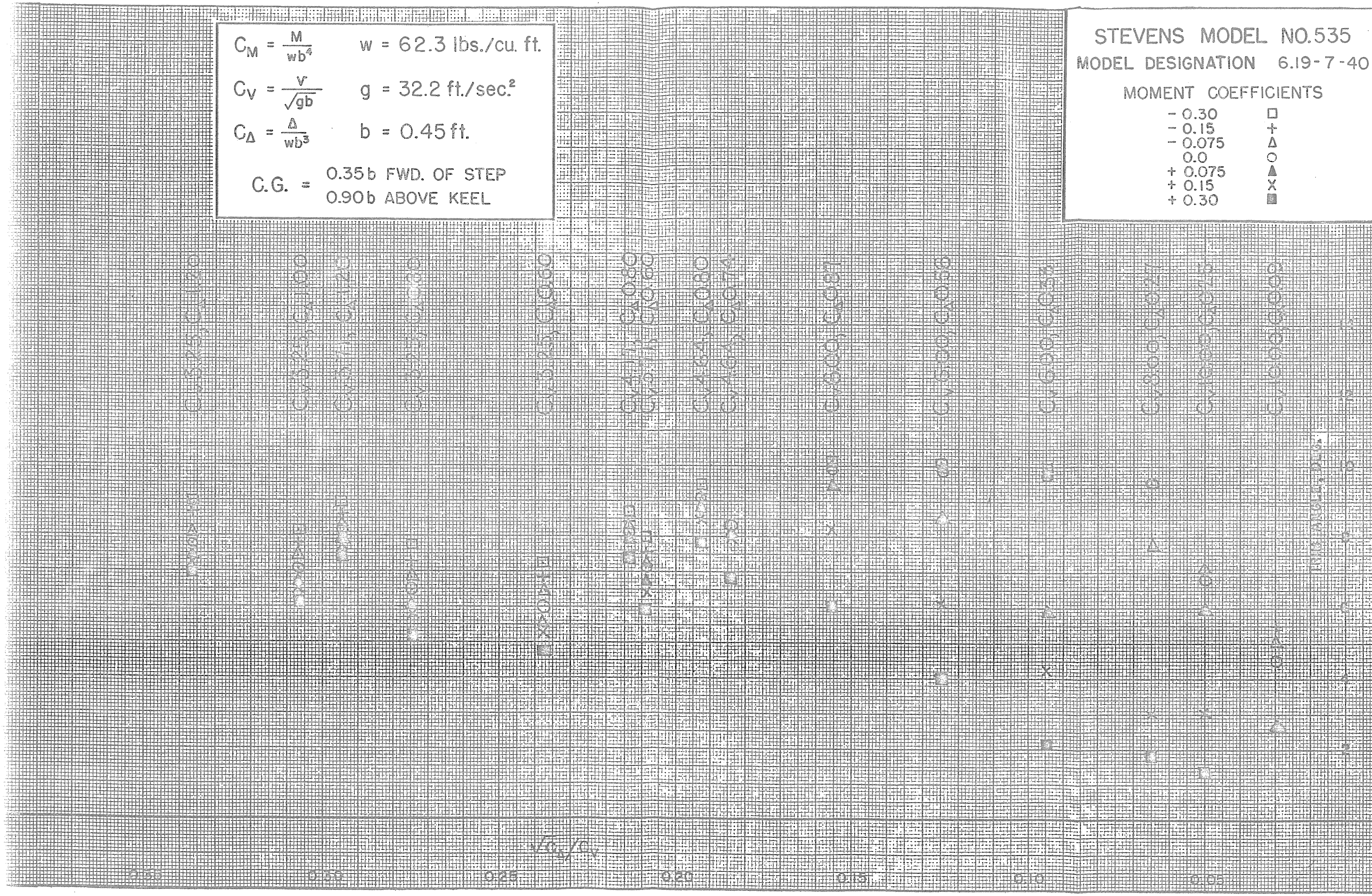
$C_M = \frac{M}{wb^4}$ w = 62.3 lbs./cu. ft.
$C_V = \frac{V}{\sqrt{gb}}$ g = 32.2 ft./sec.^{2}
$C_\Delta = \frac{\Delta}{wb^3}$ b = 0.45 ft.
C.G. = 0.35 b FWD. OF STEP
0.90 b ABOVE KEEL
STEVENS MODEL NO.535
MODEL DESIGNATION 6.19-7-40
MOMENT COEFFICIENTS
- 0.30 □
- 0.15 +
- 0.075 Δ
0.0 ○
+ 0.075 ▲
+ 0.15 X
+ 0.30 ■
TRIM ANGLE, DEG.
$\sqrt{C_\Delta}/C_V$
0.35
0.30
0.25
0.20
0.15
0.10
0.05
0

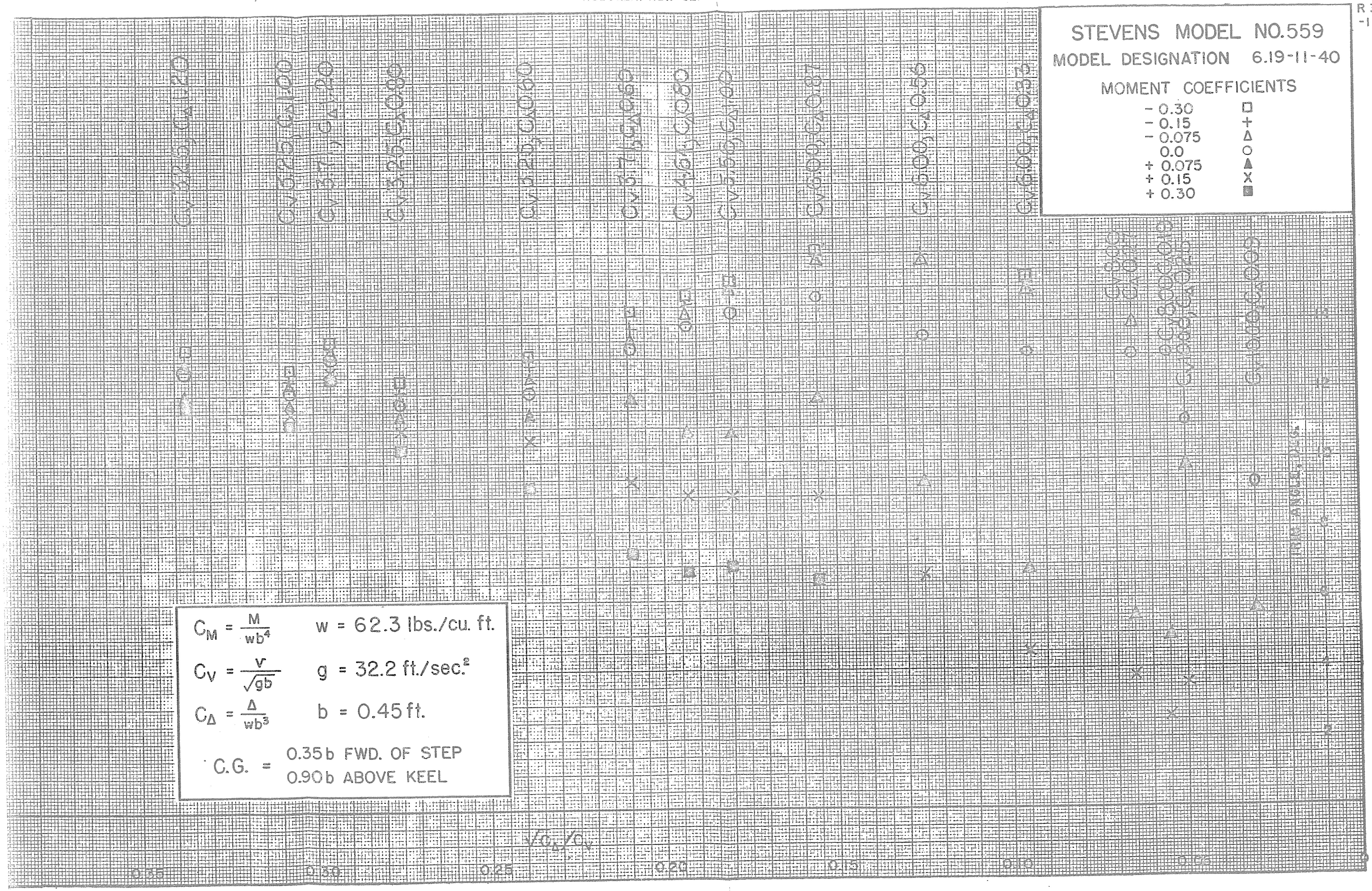
STEVENS MODEL NO.559
MODEL DESIGNATION 6.19-11-40
MOMENT COEFFICIENTS
- 0.30 □
- 0.15 +
- 0.075 △
0.0 ○
+ 0.075 ▲
+ 0.15 X
+ 0.30 ■
$C_M = \frac{M}{wb^4}$ w = 62.3 lbs./cu. ft.
$C_V = \frac{V}{\sqrt{gb}}$ g = 32.2 ft./sec.^{2}
$C_\Delta = \frac{\Delta}{wb^3}$ b = 0.45 ft.
C.G. = 0.35b FWD. OF STEP
0.90b ABOVE KEEL
$\sqrt{C_\Delta}/C_V$
0.35
0.30
0.25
0.20
0.15
0.10
0.05
0
TRIM ANGLE, DEG.

MOMENT DATA CHARTS

FOR LENGTH-BEAM RATIO 7.32 HULLS

Pages 119 through 125

EXPERIMENTAL TOWING TANK
STEVENS INSTITUTE OF TECHNOLOGY
HOBOKEN, NEW JERSEY

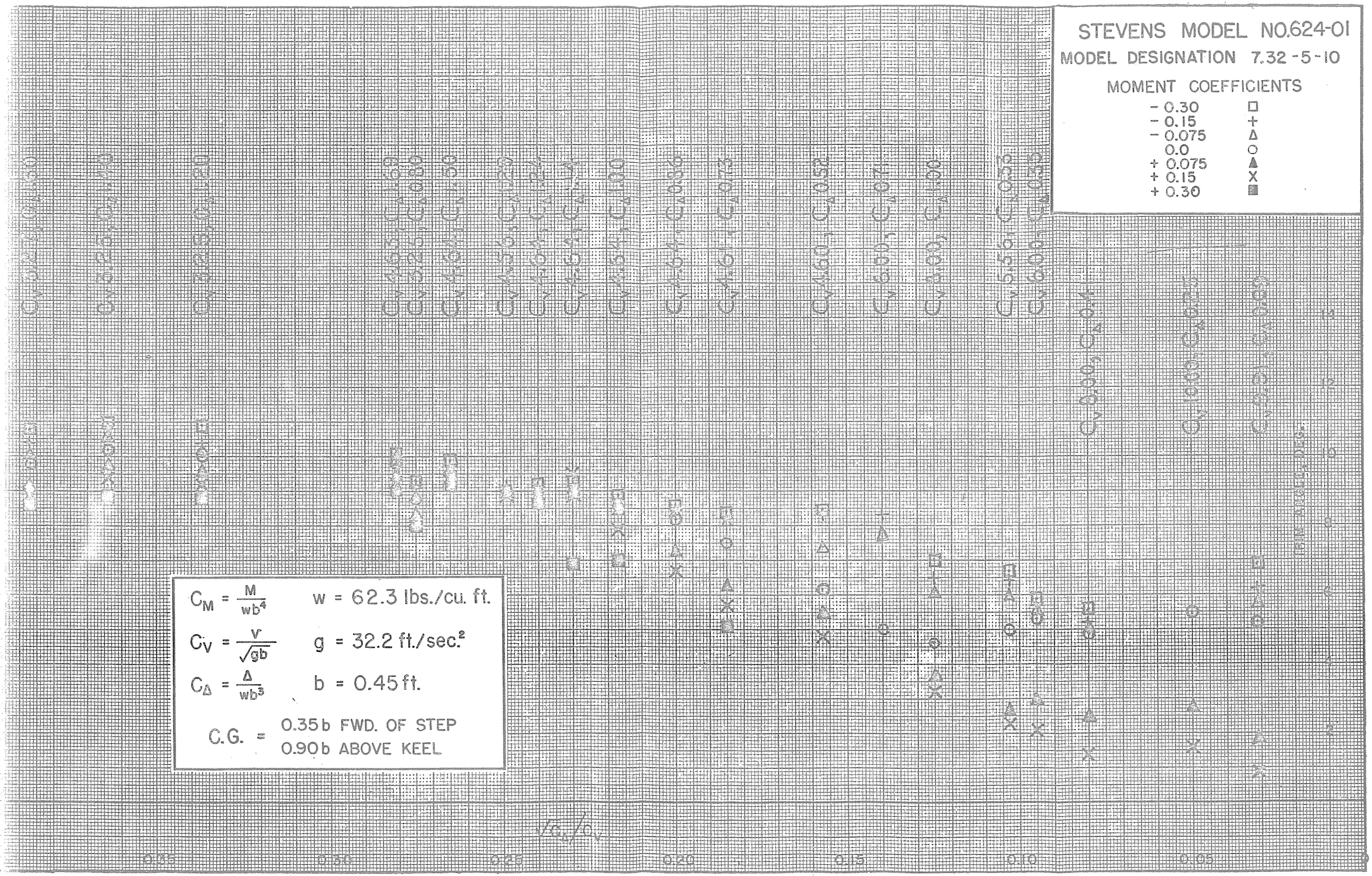

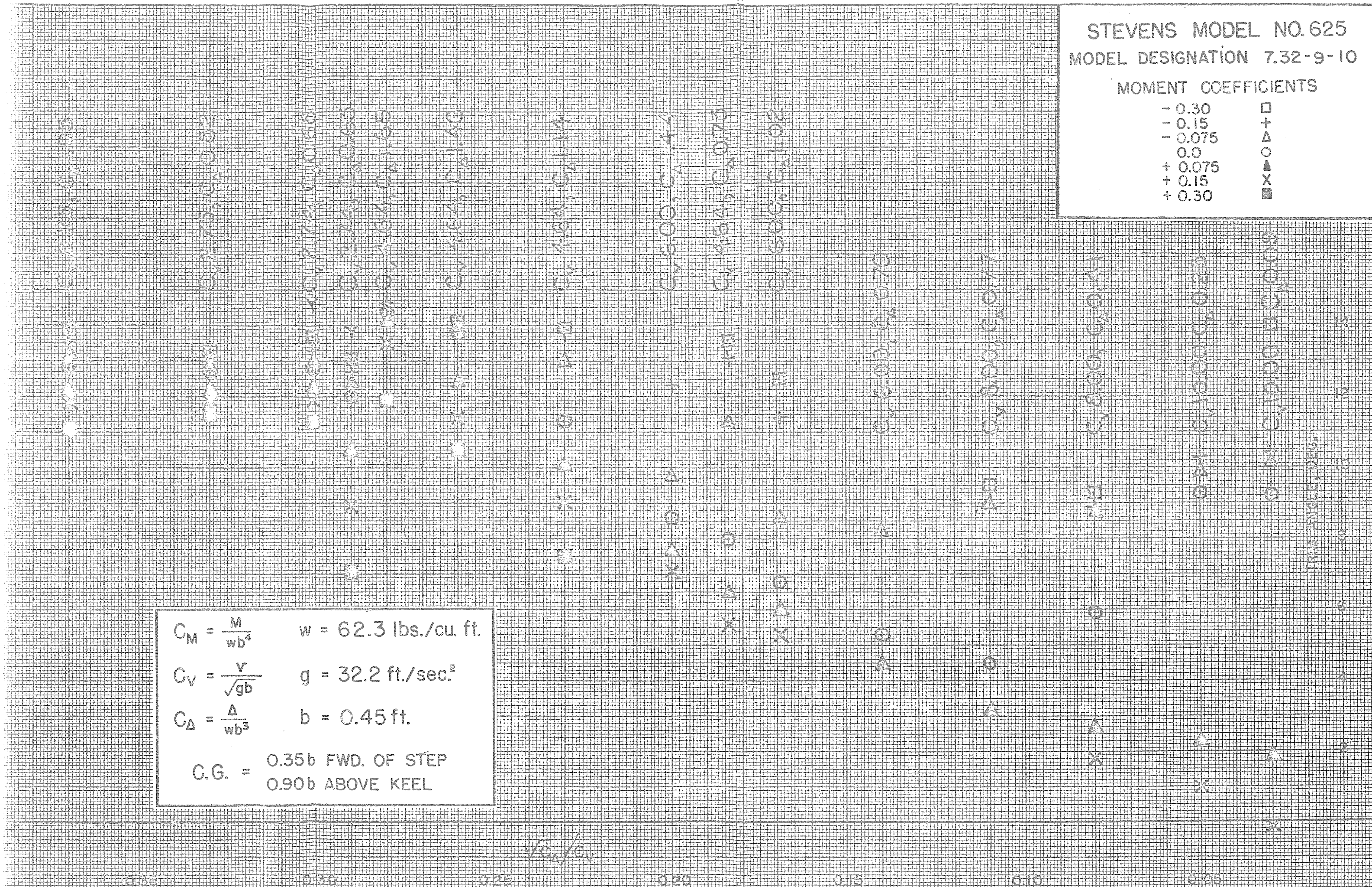
STEVENS MODEL NO. 625
MODEL DESIGNATION 7.32-9-10
MOMENT COEFFICIENTS
- 0.30 □
- 0.15 +
- 0.075 Δ
0.0 ○
+ 0.075 ▲
+ 0.15 X
+ 0.30 ■
$C_M = \frac{M}{wb^4}$
w = 62.3 lbs./cu. ft.
$C_V = \frac{V}{\sqrt{gb}}$
g = 32.2 ft./sec.^{2}
$C_\Delta = \frac{\Delta}{wb^3}$
b = 0.45 ft.
C.G. = 0.35b FWD. OF STEP
0.90b ABOVE KEEL
$\sqrt{C_\Delta}/C_V$
TRIM ANGLE, DEG.

EXPERIMENTAL TOWING TANK
STEVENS INSTITUTE OF TECHNOLOGY
HOBOKEN, NEW JERSEY

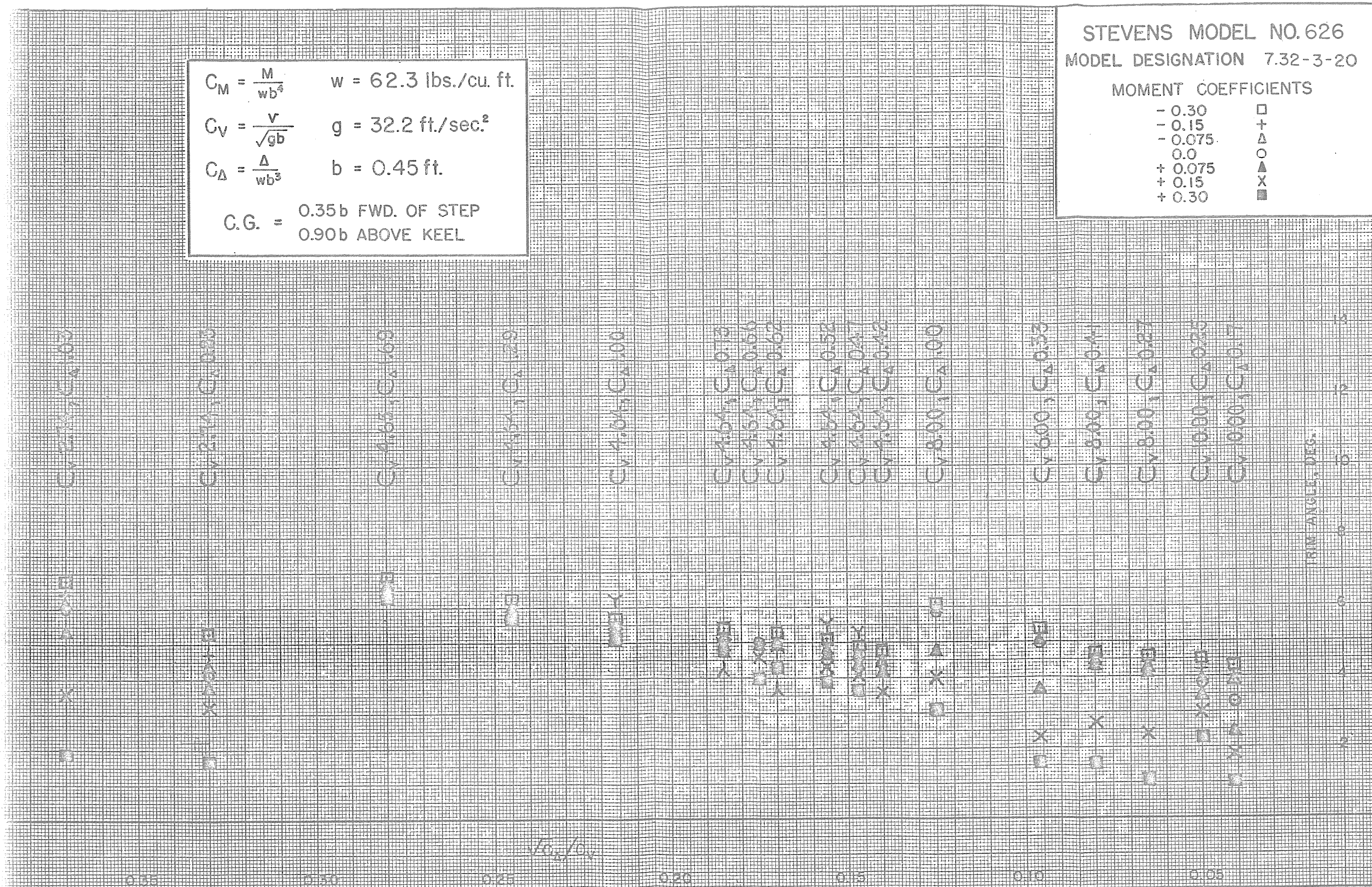

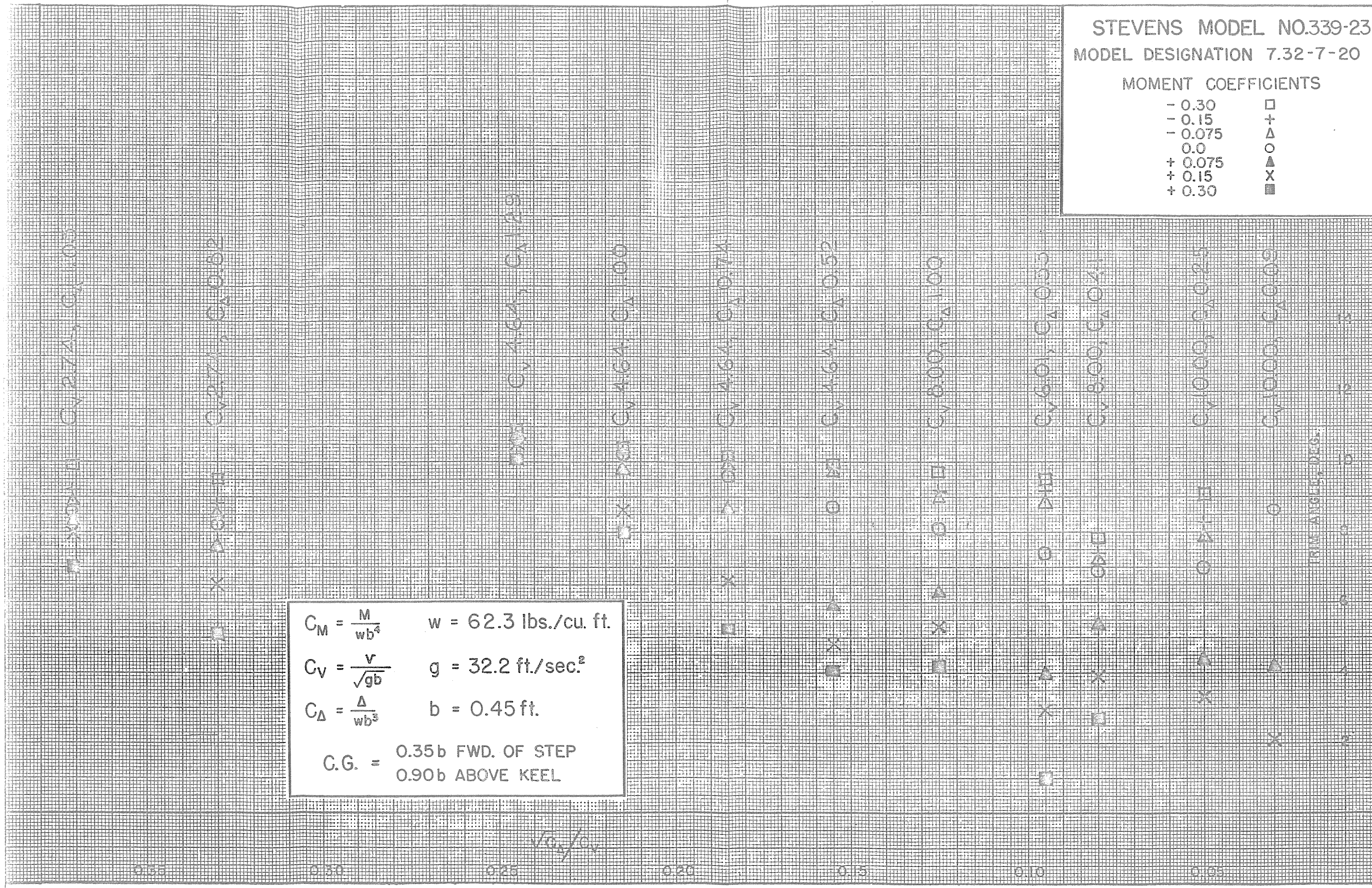
STEVENS MODEL NO.339-23
MODEL DESIGNATION 7.32-7-20
MOMENT COEFFICIENTS
− 0.30 □
− 0.15 +
− 0.075 Δ
0.0 O
+ 0.075 ▲
+ 0.15 X
+ 0.30 ■
$C_M = \frac{M}{wb^4}$
w = 62.3 lbs./cu. ft.
$C_V = \frac{v}{\sqrt{gb}}$
g = 32.2 ft./sec.^{2}
$C_\Delta = \frac{\Delta}{wb^3}$
b = 0.45 ft.
C.G. = 0.35 b FWD. OF STEP
0.90 b ABOVE KEEL
TRIM ANGLE, DEG.
$\sqrt{C_\Delta}/C_V$
0.35
0.30
0.25
0.20
0.15
0.10
0.05
0

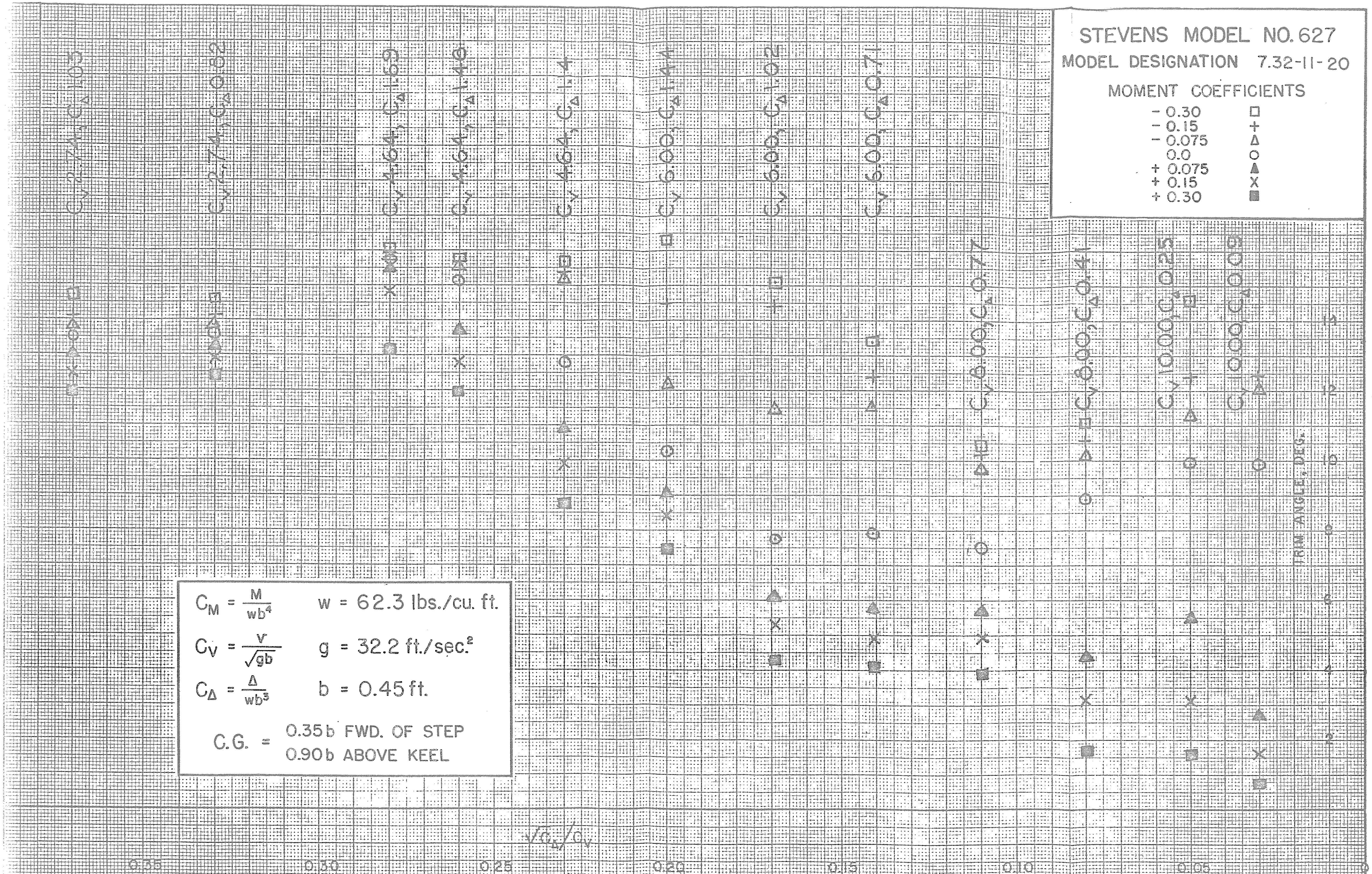
STEVENS MODEL NO. 627
MODEL DESIGNATION 7.32-11-20
MOMENT COEFFICIENTS
− 0.30 □
− 0.15 +
− 0.075 Δ
0.0 ○
+ 0.075 ▲
+ 0.15 X
+ 0.30 ■
C_V 2.74, C_Δ 1.03
C_V 2.74, C_Δ 0.82
C_V 4.64, C_Δ 1.69
C_V 4.64, C_Δ 1.46
C_V 4.64, C_Δ 1.4
C_V 6.00, C_Δ 1.44
C_V 6.00, C_Δ 1.02
C_V 6.00, C_Δ 0.71
C_V 6.00, C_Δ 0.77
C_V 8.00, C_Δ 0.41
C_V 10.00, C_Δ 0.25
C_V 10.00, C_Δ 0.09
TRIM ANGLE, DEG.
$\sqrt{C_\Delta}/C_V$
0.35
0.30
0.25
0.20
0.15
0.10
0.05
0
$C_M = \frac{M}{wb^4}$ w = 62.3 lbs./cu. ft.
$C_V = \frac{V}{\sqrt{gb}}$ g = 32.2 ft./sec.²
$C_\Delta = \frac{\Delta}{wb^3}$ b = 0.45 ft.
C.G. = 0.35 b FWD. OF STEP
0.90 b ABOVE KEEL

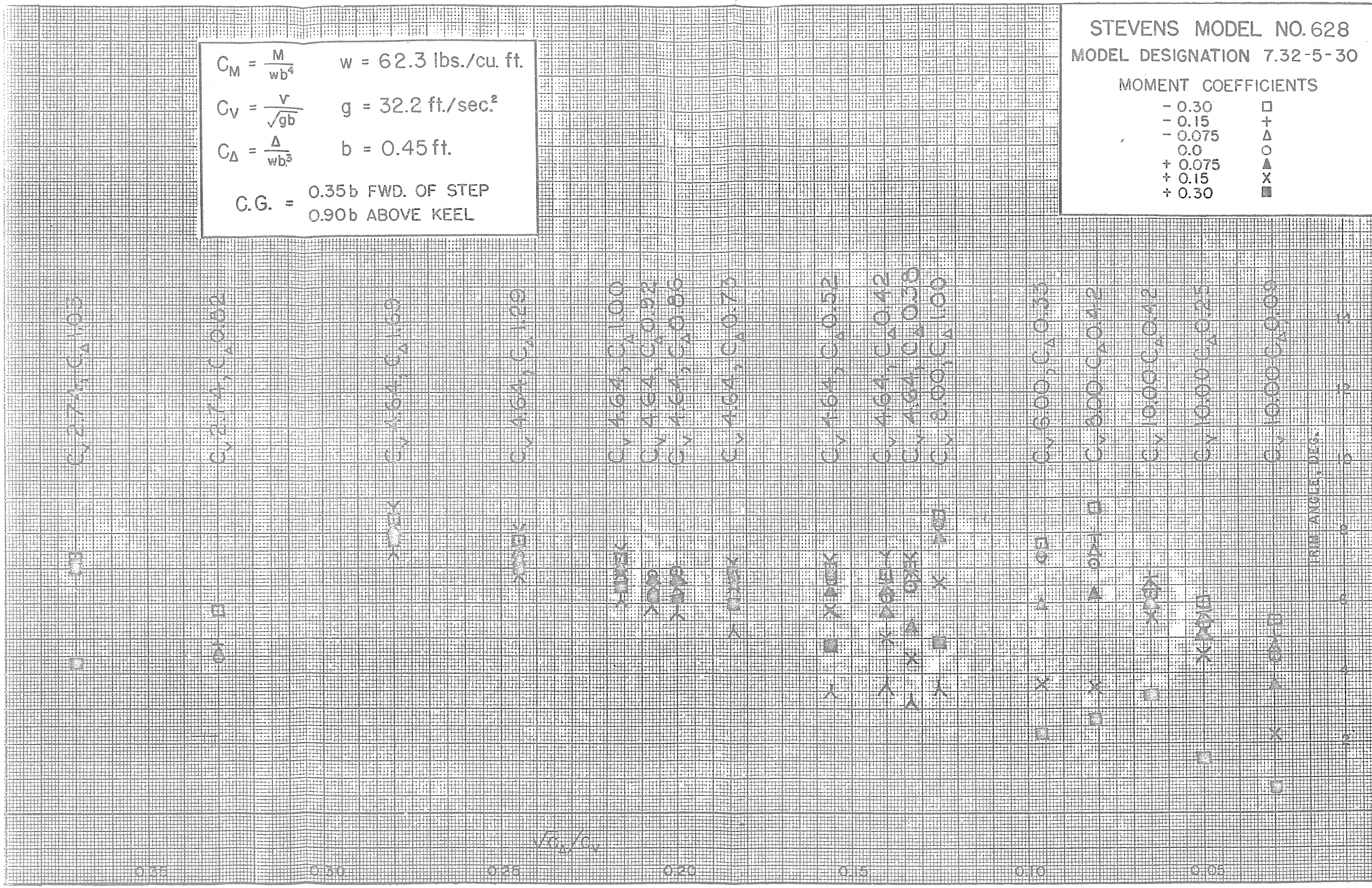
$C_M = \frac{M}{wb^4}$
$C_V = \frac{V}{\sqrt{gb}}$
$C_\Delta = \frac{\Delta}{wb^3}$
w = 62.3 lbs./cu. ft.
g = 32.2 ft./sec.²
b = 0.45 ft.
C.G. = 0.35 b FWD. OF STEP
0.90 b ABOVE KEEL
STEVENS MODEL NO. 628
MODEL DESIGNATION 7.32-5-30
MOMENT COEFFICIENTS
- 0.30
- 0.15
- 0.075
0.0
+ 0.075
+ 0.15
+ 0.30
TRIM ANGLE, DEG.
$\sqrt{C_\Delta}/C_V$
0.35
0.30
0.25
0.20
0.15
0.10
0.05
0

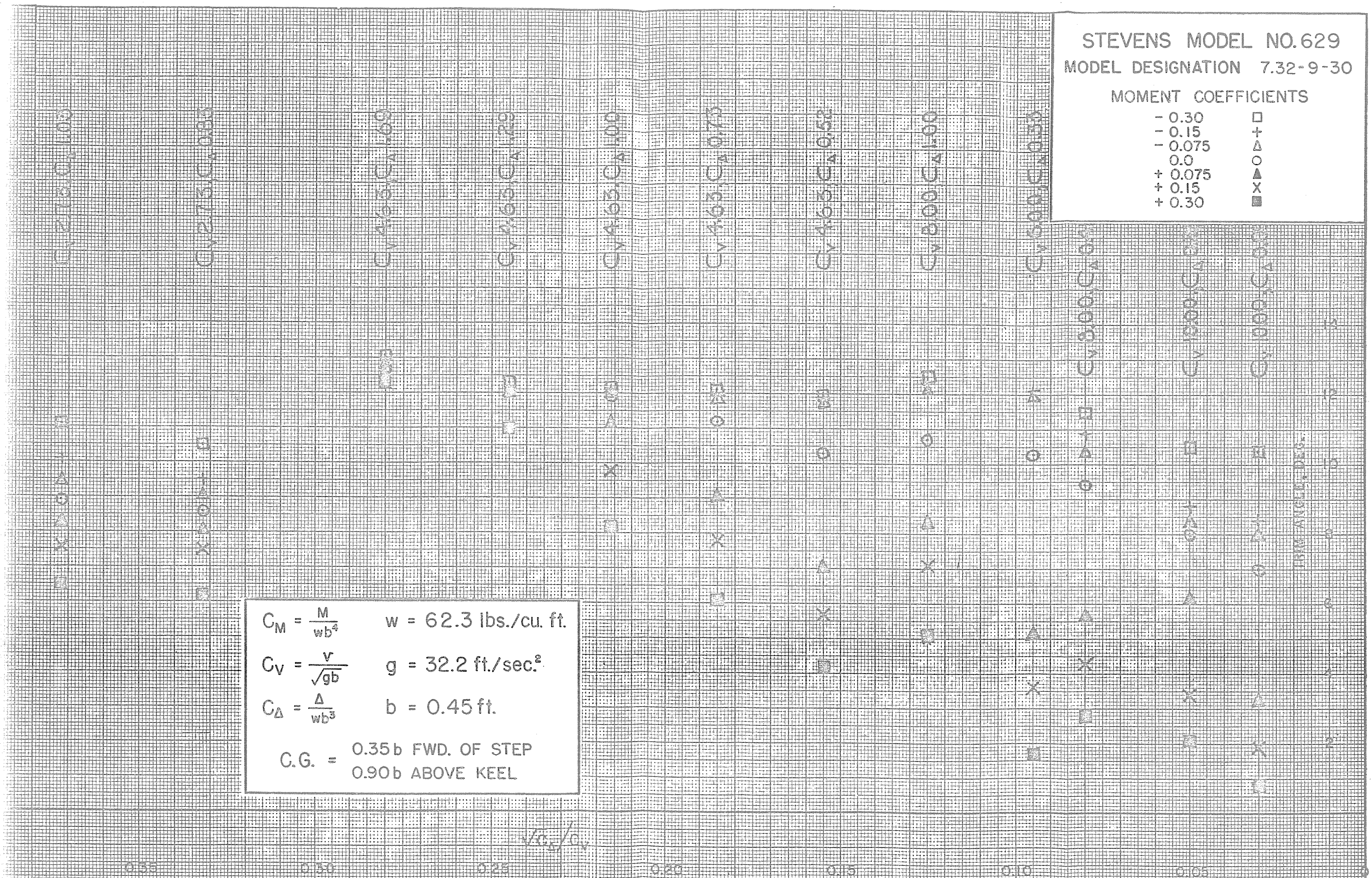
STEVENS MODEL NO. 629
MODEL DESIGNATION 7.32-9-30
MOMENT COEFFICIENTS
- 0.30 □
- 0.15 +
- 0.075 △
0.0 ○
+ 0.075 ▲
+ 0.15 X
+ 0.30 ■
$C_M = \frac{M}{wb^4}$ w = 62.3 lbs./cu. ft.
$C_V = \frac{V}{\sqrt{gb}}$ g = 32.2 ft./sec.^{2}
$C_\Delta = \frac{\Delta}{wb^3}$ b = 0.45 ft.
C.G. = 0.35 b FWD. OF STEP
0.90 b ABOVE KEEL
$\sqrt{C_\Delta}/C_V$
TRIM ANGLE, DEG.

MOMENT DATA CHARTS

FOR LENGTH-BEAM RATIO 8.45 HULLS

Pages 126 through 132

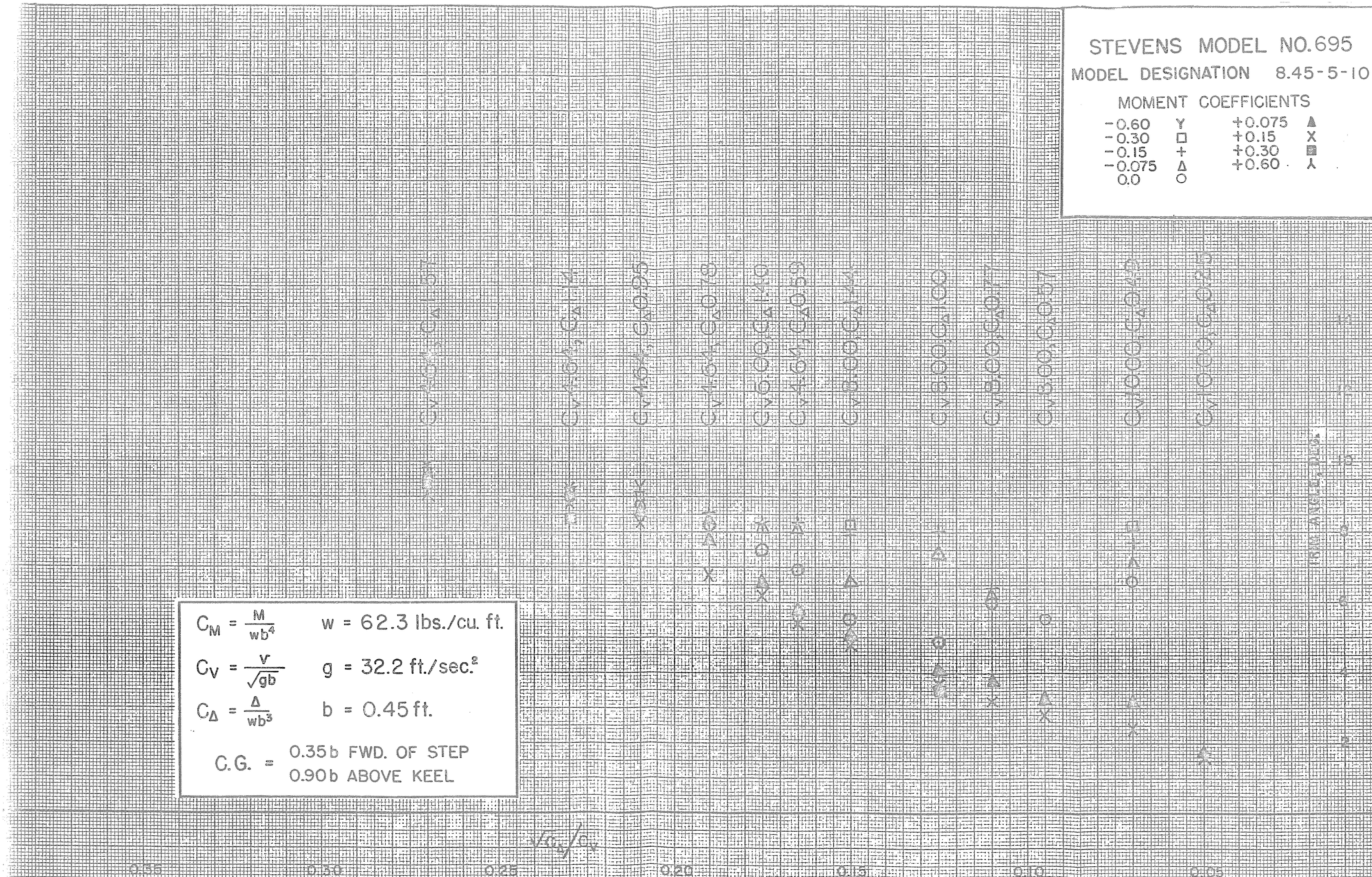
STEVENS MODEL NO.695
MODEL DESIGNATION 8.45-5-10
MOMENT COEFFICIENTS
-0.60 Y
-0.30 □
-0.15 +
-0.075 Δ
0.0 O
+0.075 ▲
+0.15 X
+0.30 ■
+0.60 ⅄
$C_M = \frac{M}{wb^4}$ w = 62.3 lbs./cu. ft.
$C_V = \frac{V}{\sqrt{gb}}$ g = 32.2 ft./sec.^{2}
$C_\Delta = \frac{\Delta}{wb^3}$ b = 0.45 ft.
C.G. = 0.35 b FWD. OF STEP
0.90 b ABOVE KEEL
$\sqrt{C_\Delta}/C_V$
0.35
0.30
0.25
0.20
0.15
0.10
0.05
0
TRIM ANGLE, DEG.

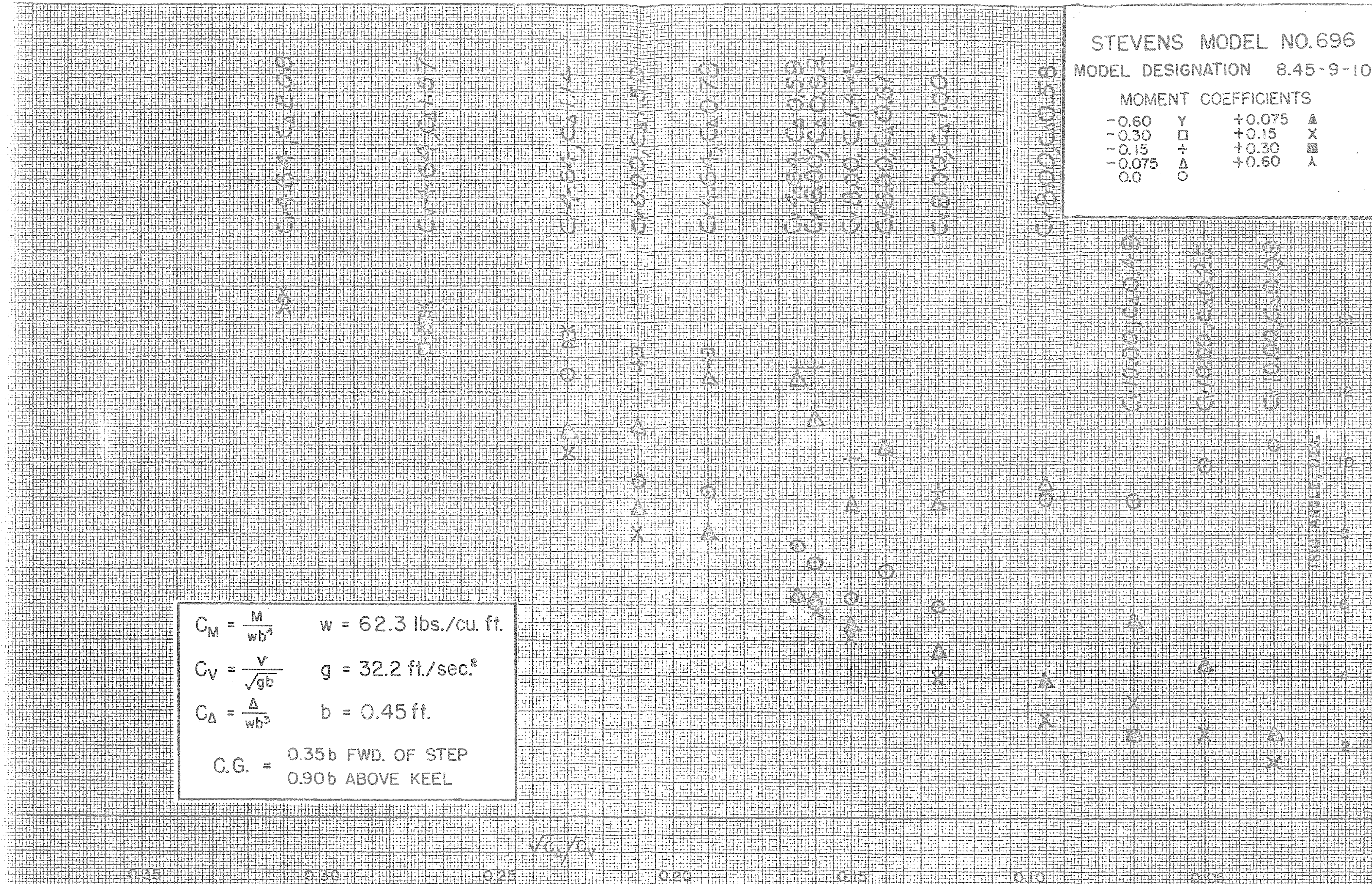
STEVENS MODEL NO. 696
MODEL DESIGNATION 8.45-9-10
MOMENT COEFFICIENTS
-0.60 Y
-0.30 □
-0.15 +
-0.075 Δ
0.0 O
+0.075 ▲
+0.15 X
+0.30 ■
+0.60 ⅄
$C_M = \frac{M}{wb^4}$
w = 62.3 lbs./cu. ft.
$C_V = \frac{V}{\sqrt{gb}}$
g = 32.2 ft./sec.^{2}
$C_\Delta = \frac{\Delta}{wb^3}$
b = 0.45 ft.
C.G. = 0.35 b FWD. OF STEP
0.90 b ABOVE KEEL
$\sqrt{C_\Delta}/C_V$
0.35
0.30
0.25
0.20
0.15
0.10
0.05
0
TRIM ANGLE, DEG.

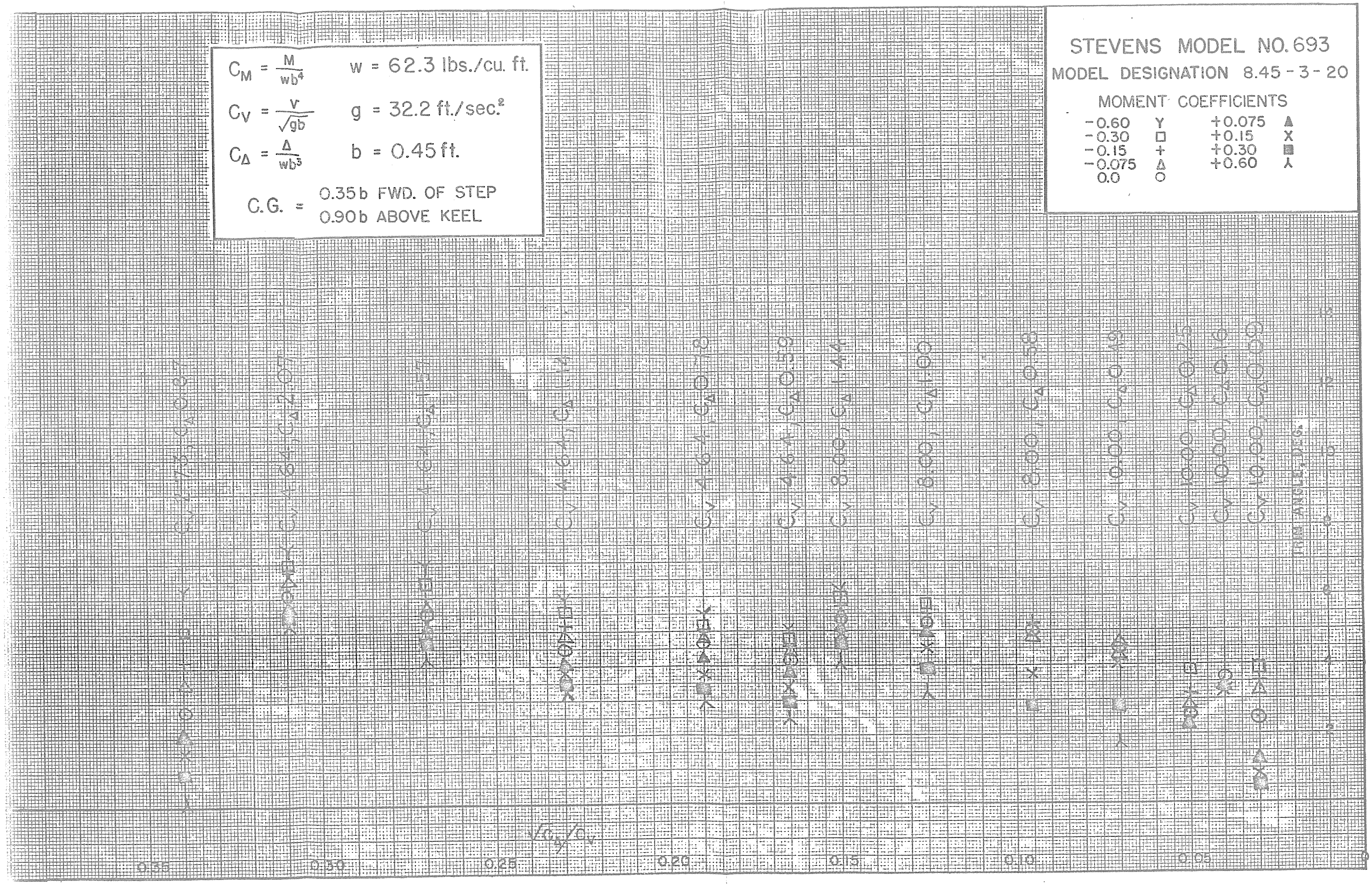
$C_M = \frac{M}{wb^4}$
w = 62.3 lbs./cu. ft.
$C_V = \frac{V}{\sqrt{gb}}$
g = 32.2 ft./sec.^{2}
$C_\Delta = \frac{\Delta}{wb^3}$
b = 0.45 ft.
C.G. = 0.35 b FWD. OF STEP
0.90 b ABOVE KEEL
STEVENS MODEL NO. 693
MODEL DESIGNATION 8.45 - 3 - 20
MOMENT COEFFICIENTS
-0.60 Y
-0.30 □
-0.15 +
-0.075 Δ
0.0 ○
+0.075 ▲
+0.15 X
+0.30 ■
+0.60 ⅄
TRIM ANGLE, DEG.
$\sqrt{C_\Delta}/C_V$
0.35
0.30
0.25
0.20
0.15
0.10
0.05
0

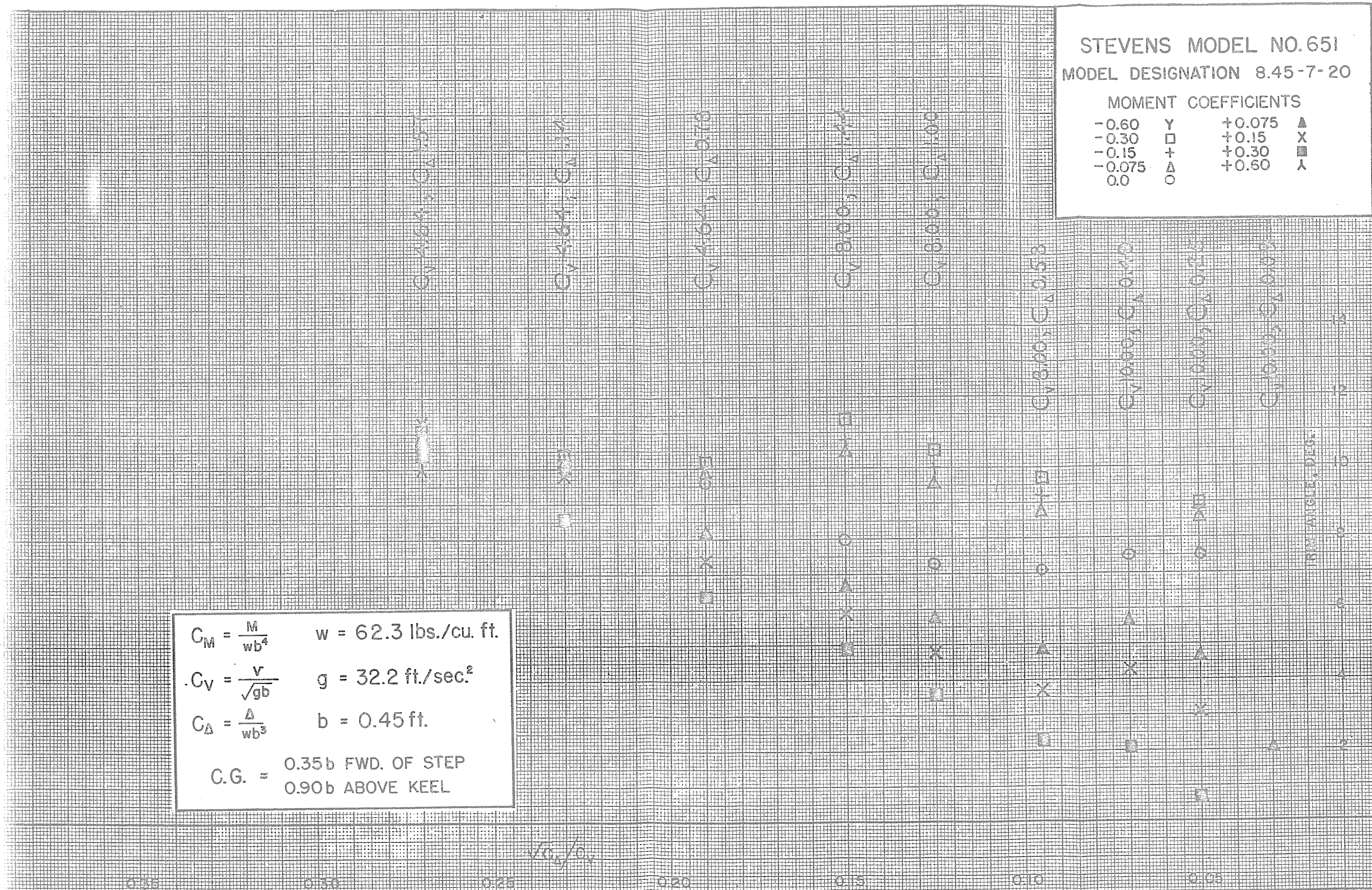
STEVENS MODEL NO. 651
MODEL DESIGNATION 8.45-7-20
MOMENT COEFFICIENTS
−0.60 Y
−0.30 □
−0.15 +
−0.075 Δ
0.0 ○
+0.075 ▲
+0.15 X
+0.30 ■
+0.60 ⅄
$C_M = \frac{M}{wb^4}$
w = 62.3 lbs./cu. ft.
$C_V = \frac{V}{\sqrt{gb}}$
g = 32.2 ft./sec.^{2}
$C_\Delta = \frac{\Delta}{wb^3}$
b = 0.45 ft.
C.G. = 0.35 b FWD. OF STEP
0.90 b ABOVE KEEL
$\sqrt{C_\Delta}/C_V$
TRIM ANGLE, DEG.

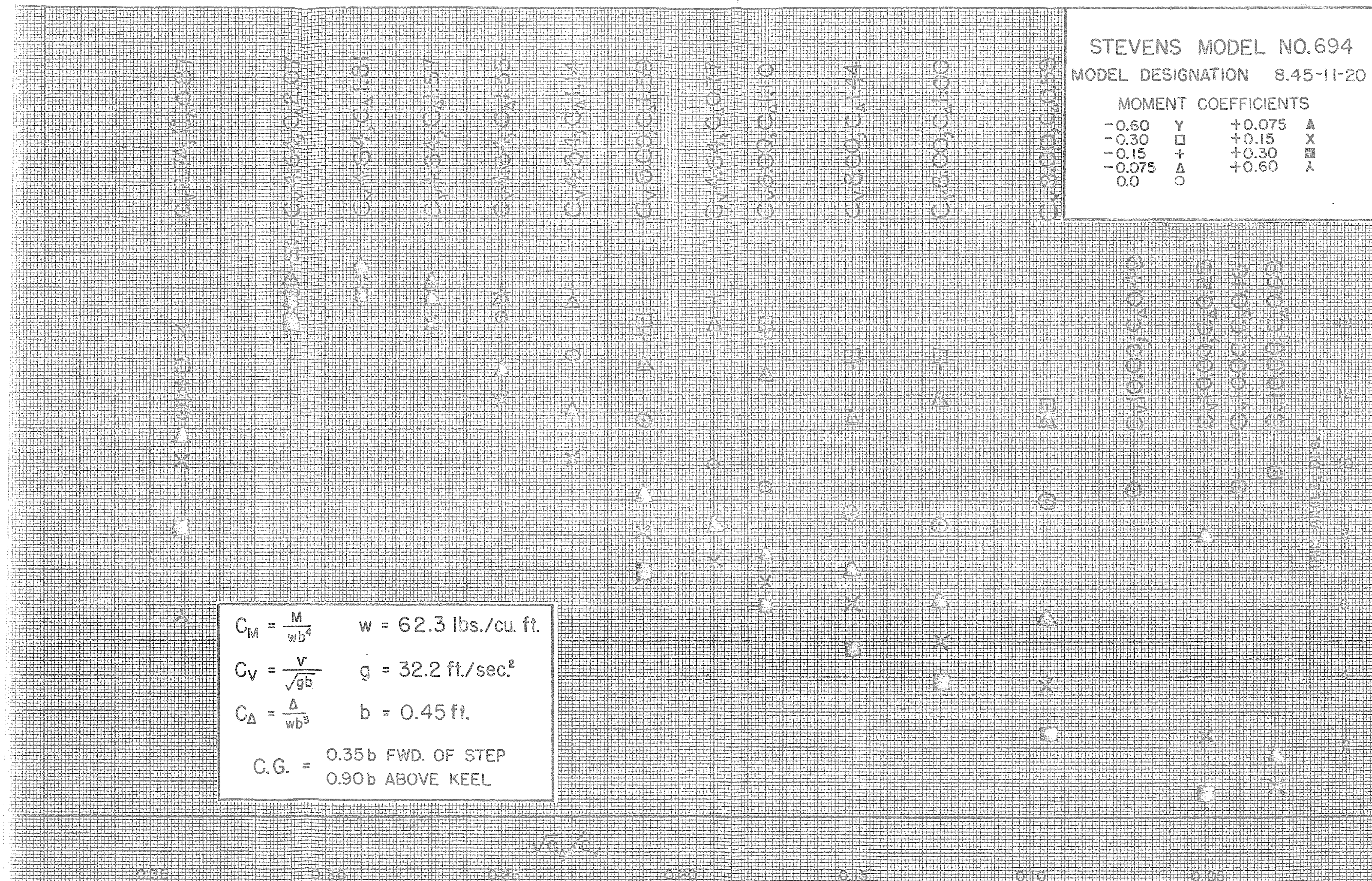
STEVENS MODEL NO. 694
MODEL DESIGNATION 8.45-11-20
MOMENT COEFFICIENTS
−0.60 Y
−0.30 □
−0.15 +
−0.075 Δ
0.0 ○
+0.075 ▲
+0.15 X
+0.30 ■
+0.60 ⅄
$C_M = \frac{M}{wb^4}$ w = 62.3 lbs./cu. ft.
$C_V = \frac{V}{\sqrt{gb}}$ g = 32.2 ft./sec.²
$C_\Delta = \frac{\Delta}{wb^3}$ b = 0.45 ft.
C.G. = 0.35 b FWD. OF STEP
0.90 b ABOVE KEEL

EXPERIMENTAL TOWING TANK
STEVENS INSTITUTE OF TECHNOLOGY
HOBOKEN, NEW JERSEY

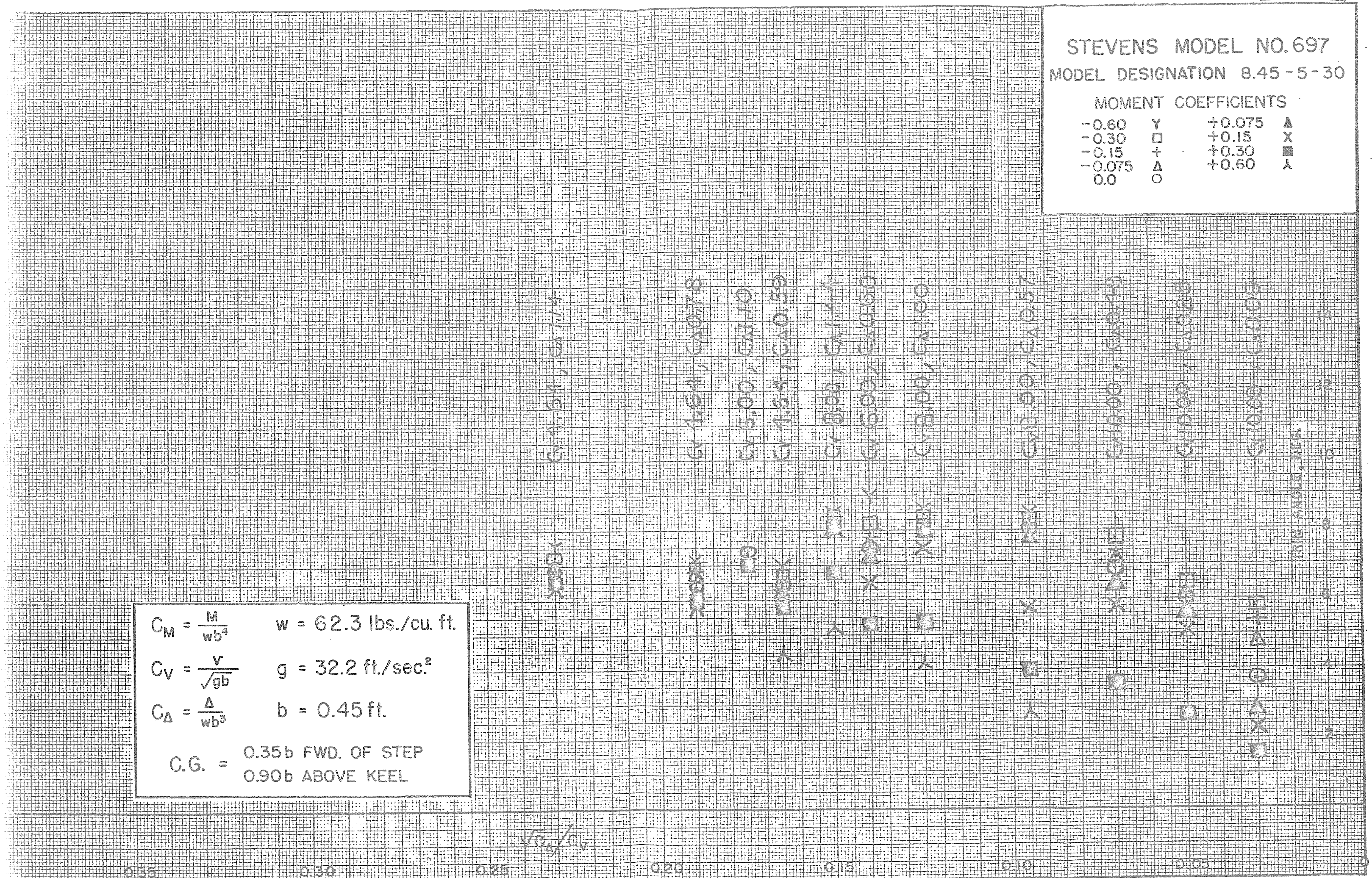

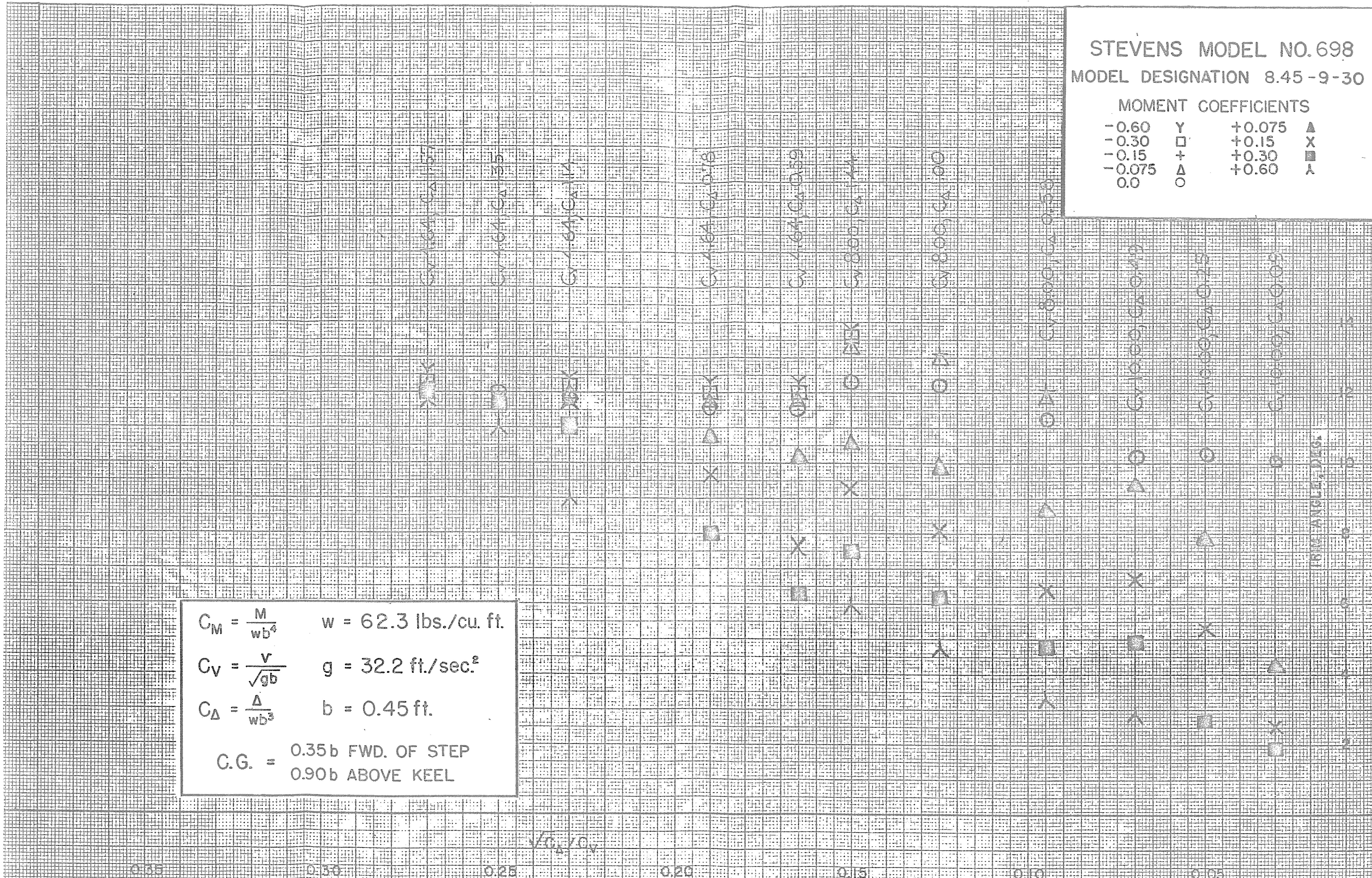
STEVENS MODEL NO. 698
MODEL DESIGNATION 8.45-9-30
MOMENT COEFFICIENTS
-0.60 Y
-0.30 □
-0.15 +
-0.075 Δ
0.0 O
+0.075 ▲
+0.15 X
+0.30 ■
+0.60 ⅄
Cv 4.64, CΔ 1.57
Cv 4.64, CΔ 1.35
Cv 4.64, CΔ 1.14
Cv 4.64, CΔ 0.78
Cv 4.64, CΔ 0.59
Cv 8.00, CΔ 1.44
Cv 8.00, CΔ 1.00
Cv 8.00, CΔ 0.58
Cv 16.00, CΔ 0.49
Cv 16.00, CΔ 0.25
Cv 16.00, CΔ 0.09
TRIM ANGLE, DEG.
14
12
10
8
6
4
2
$C_M = \frac{M}{wb^4}$
w = 62.3 lbs./cu. ft.
$C_V = \frac{V}{\sqrt{gb}}$
g = 32.2 ft./sec.²
$C_\Delta = \frac{\Delta}{wb^3}$
b = 0.45 ft.
C.G. = 0.35 b FWD. OF STEP
0.90 b ABOVE KEEL
$\sqrt{C_\Delta}/C_V$
0.35
0.30
0.25
0.20
0.15
0.10
0.05
0

STATIC PROPERTIES CHARTS

FOR LENGTH-BEAM RATIO 5.07 HULLS

Pages 133 through 139

STEVENS MODEL NO. 610
MODEL DESIGNATION 5.07-5-10
STATIC PROPERTIES
AND
MODEL LINES

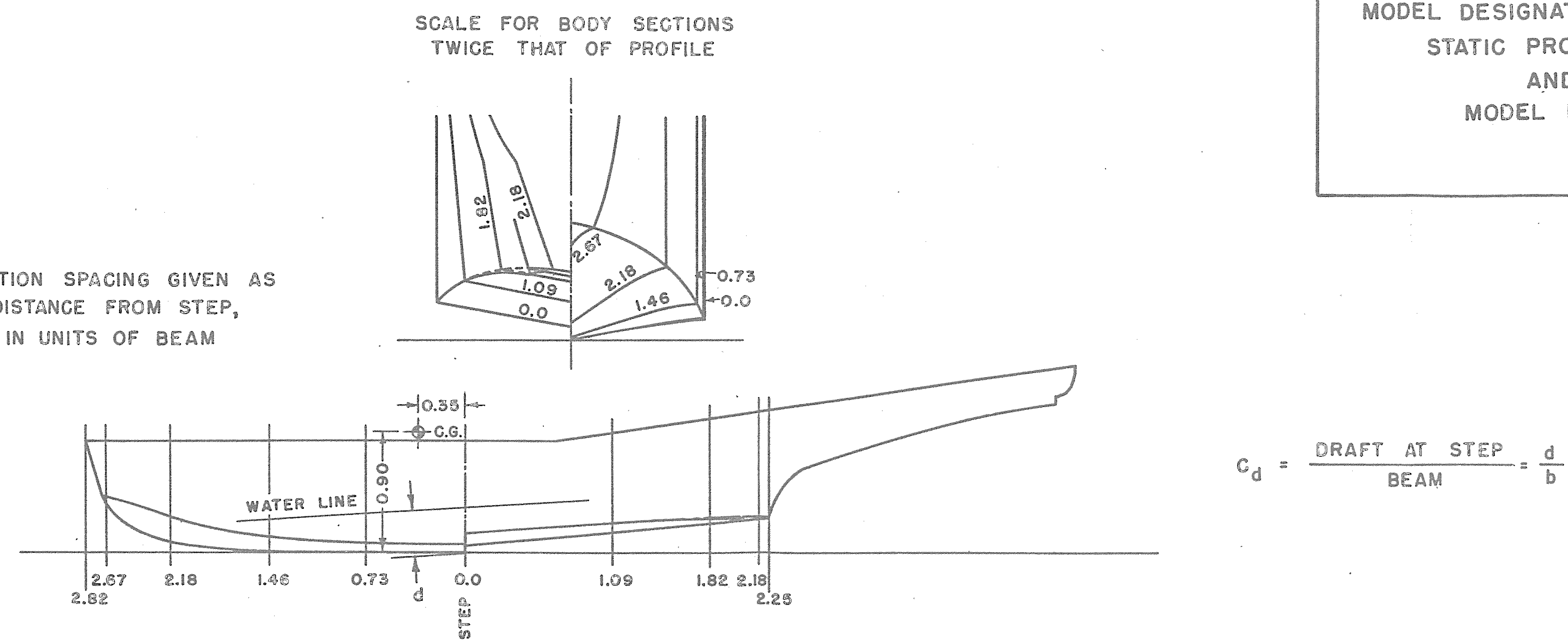

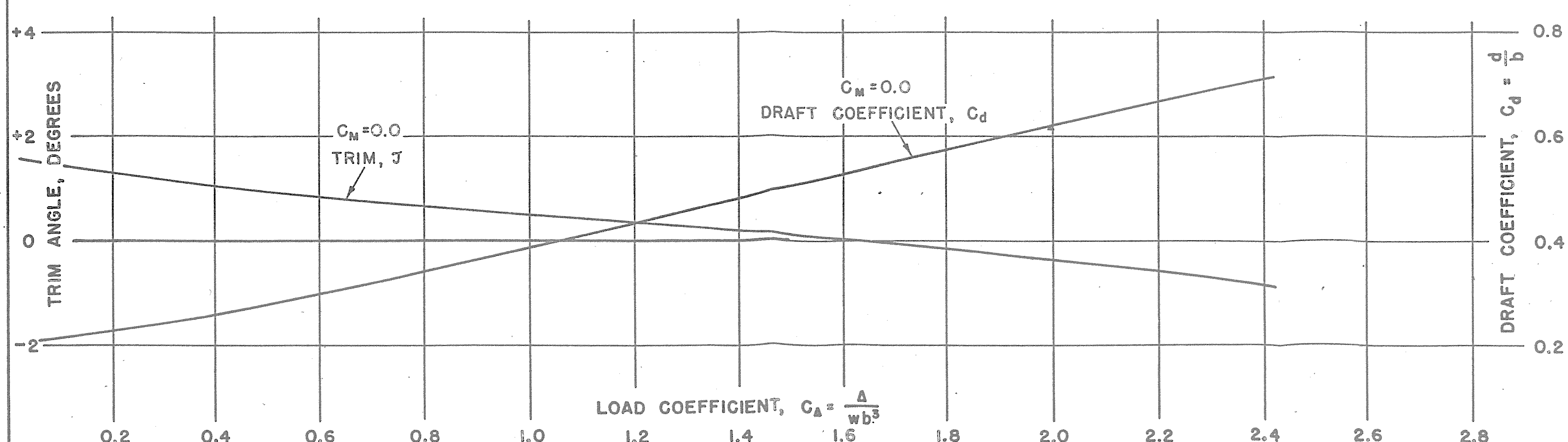

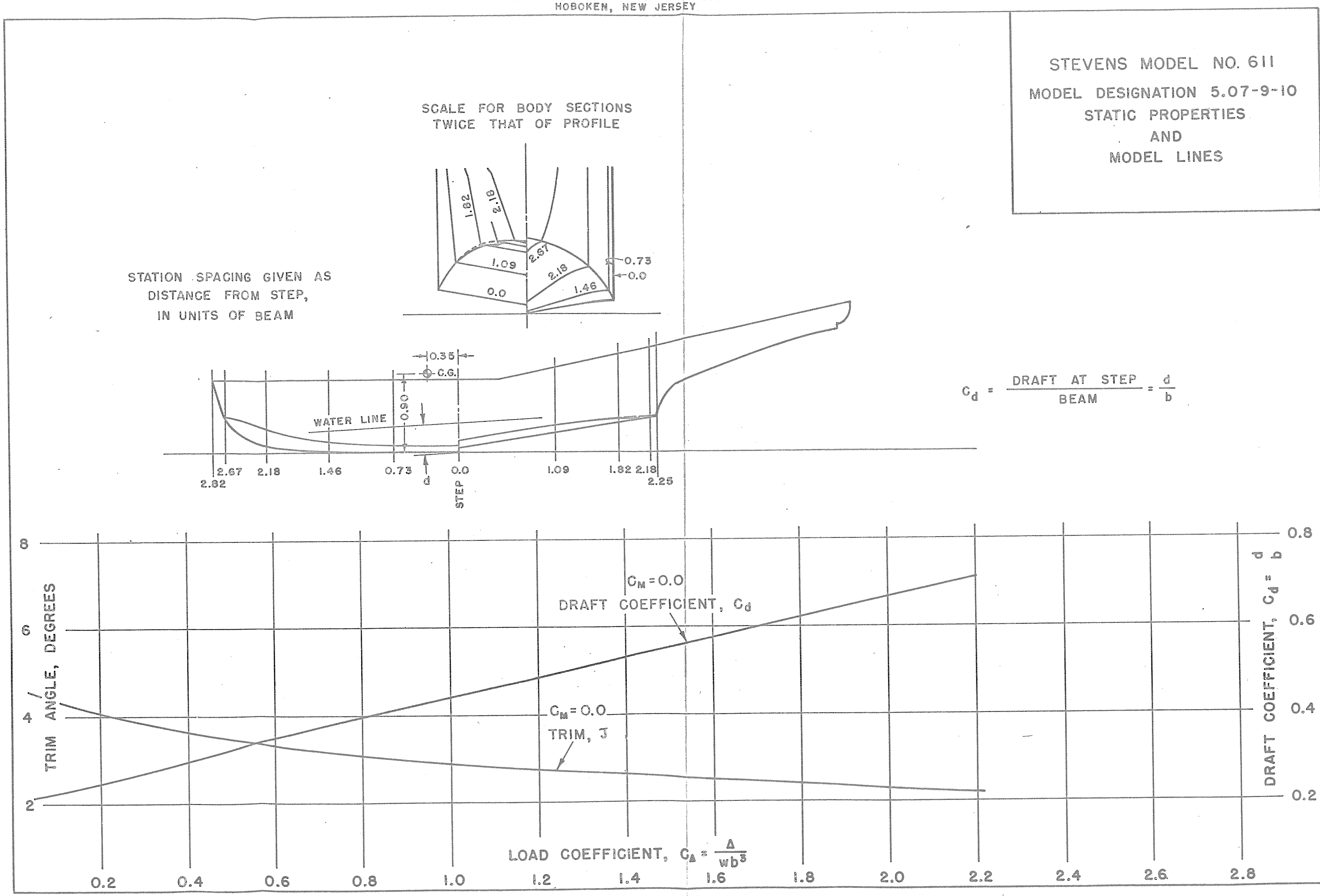
STEVENS MODEL NO. 611
MODEL DESIGNATION 5.07-9-10
STATIC PROPERTIES
AND
MODEL LINES
SCALE FOR BODY SECTIONS
TWICE THAT OF PROFILE
STATION SPACING GIVEN AS
DISTANCE FROM STEP,
IN UNITS OF BEAM
1.82
2.18
2.67
1.09
2.18
1.46
0.0
0.73
0.0
0.35
C.G.
0.90
WATER LINE
2.82
2.67
2.18
1.46
0.73
d
0.0
STEP
1.09
1.82
2.18
2.25
$C_d = \frac{\text{DRAFT AT STEP}}{\text{BEAM}} = \frac{d}{b}$
$C_M = 0.0$
DRAFT COEFFICIENT, C_d
$C_M = 0.0$
TRIM, τ
TRIM ANGLE, DEGREES
DRAFT COEFFICIENT, $C_d = \frac{d}{b}$
LOAD COEFFICIENT, $C_\Delta = \frac{\Delta}{wb^3}$
2
4
6
8
0.2
0.4
0.6
0.8
0.2
0.4
0.6
0.8
1.0
1.2
1.4
1.6
1.8
2.0
2.2
2.4
2.6
2.8

EXPERIMENTAL TOWING TANK
STEVENS INSTITUTE OF TECHNOLOGY
HOBOKEN, NEW JERSEY

R 325
-135-

STEVENS MODEL NO. 573

MODEL DESIGNATION 5.07-3-20

STATIC PROPERTIES
AND
MODEL LINES

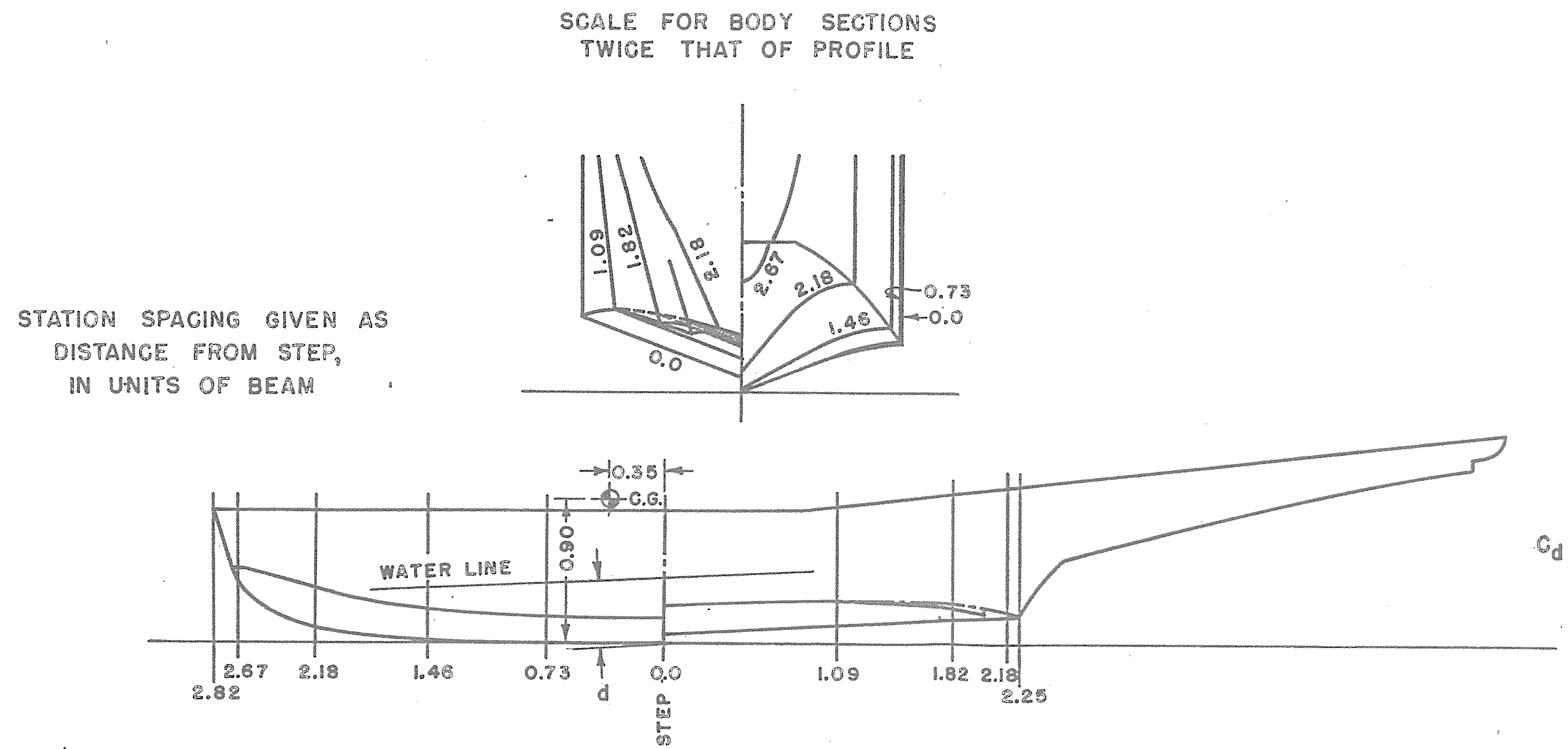

$C_d = \frac{\text{DRAFT AT STEP}}{\text{BEAM}} = \frac{d}{b}$

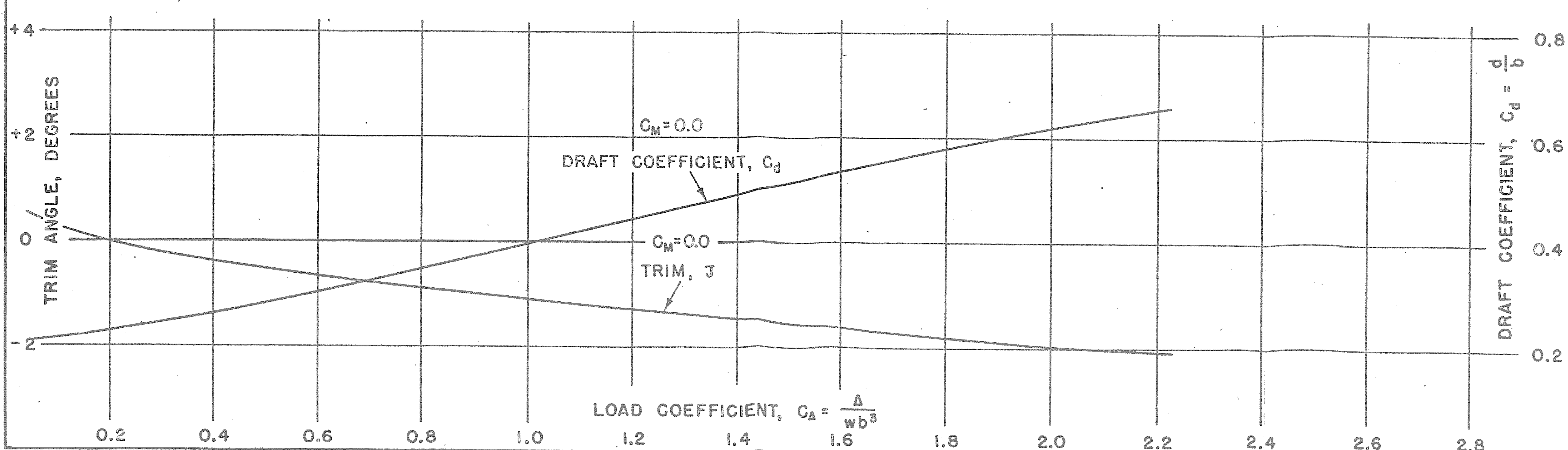

STEVENS MODEL NO. 339-22

MODEL DESIGNATION 5.07-7-20

STATIC PROPERTIES
AND
MODEL LINES

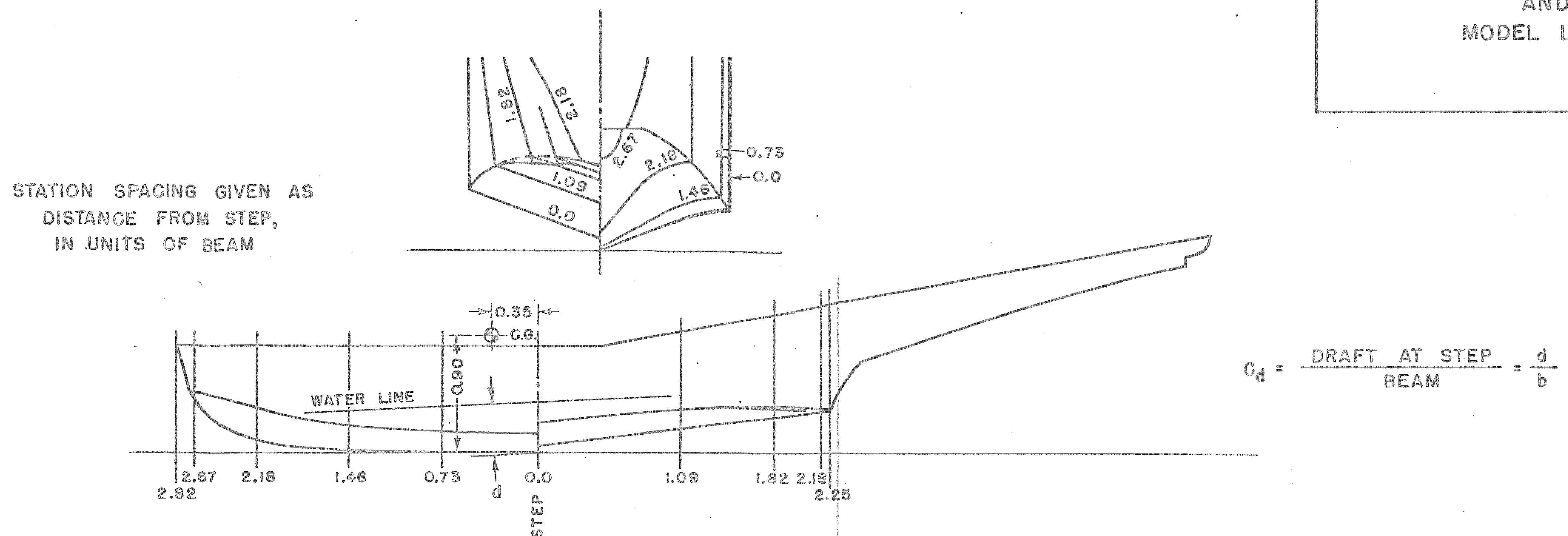

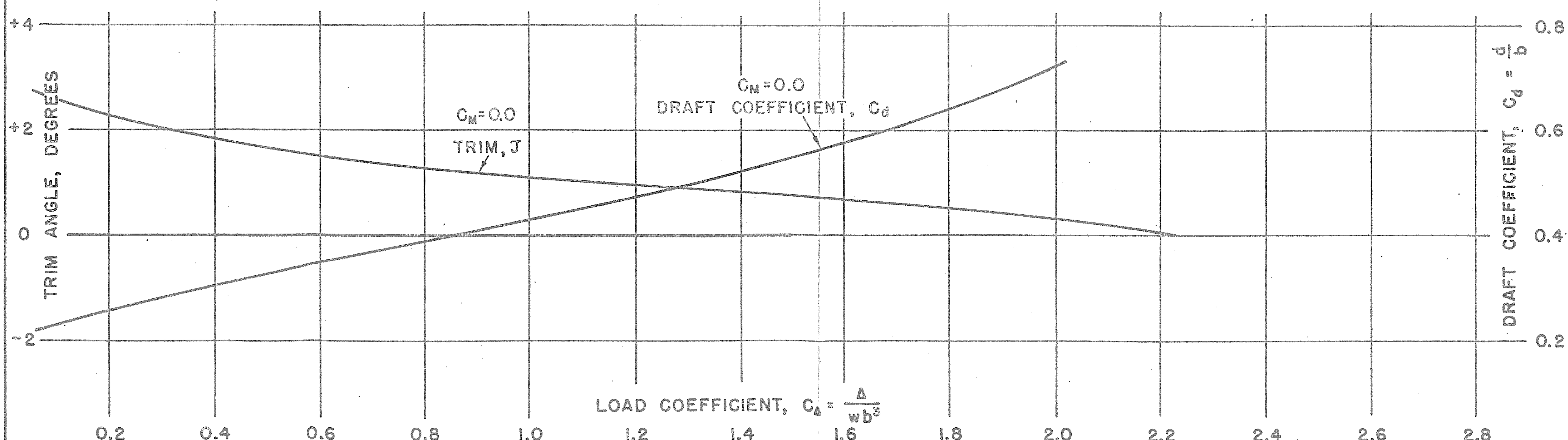

EXPERIMENTAL TOWING TANK
STEVENS INSTITUTE OF TECHNOLOGY
HOBOKEN, NEW JERSEY

STEVENS MODEL NO. 574
MODEL DESIGNATION 5.07-11-20
STATIC PROPERTIES
AND
MODEL LINES

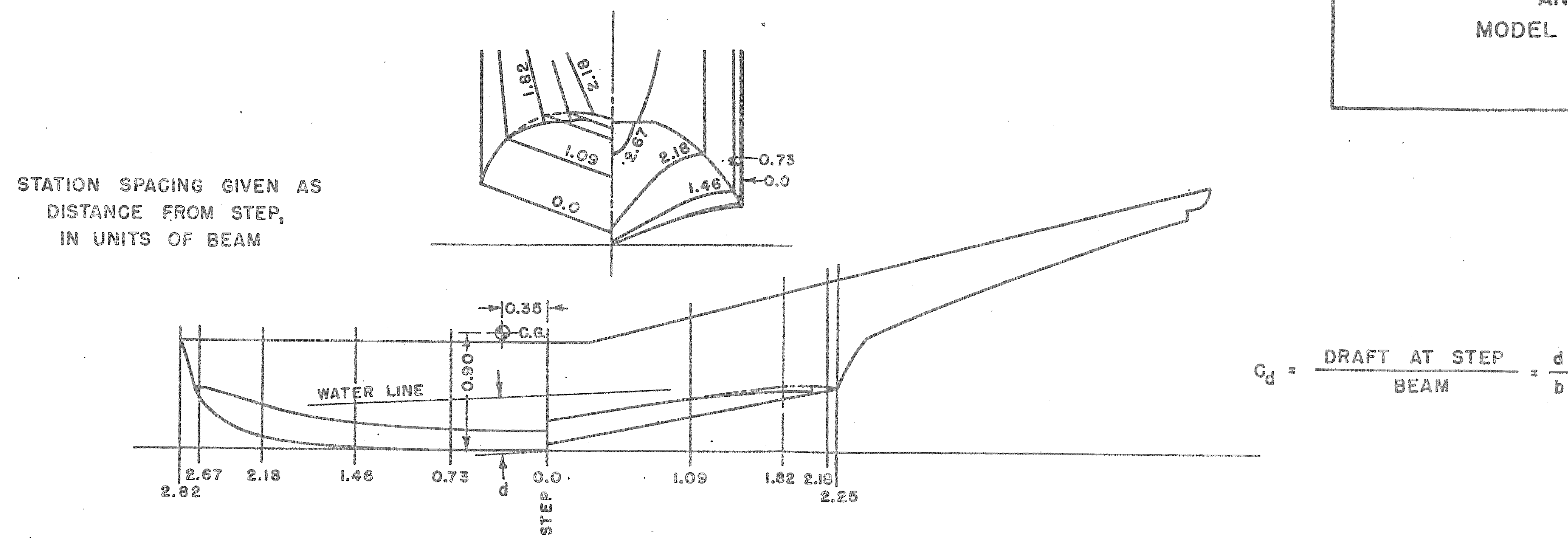

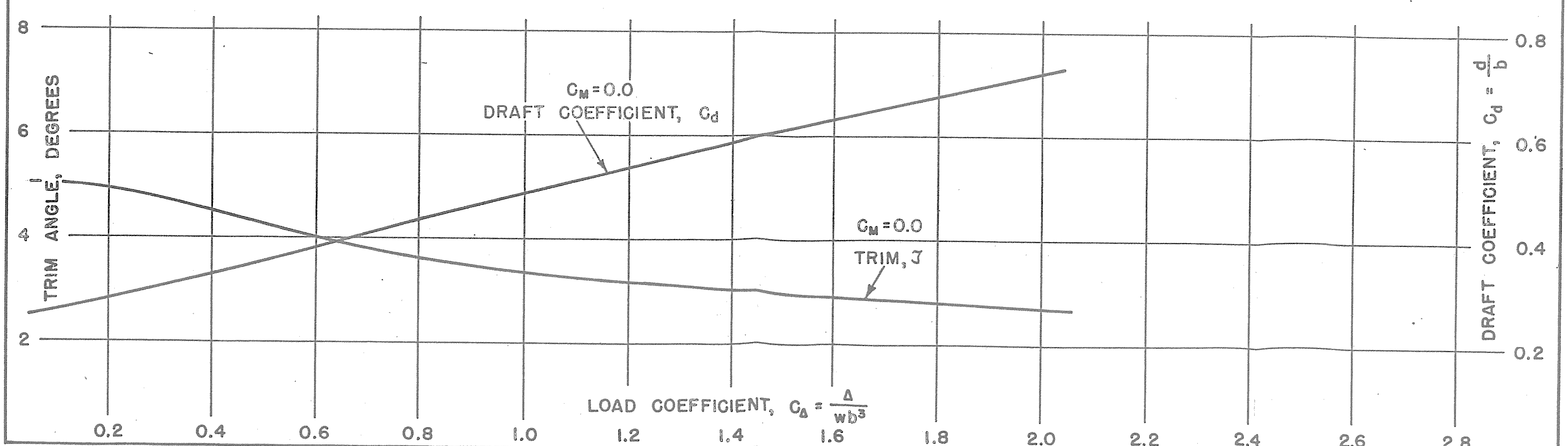

STEVENS MODEL NO. 612
MODEL DESIGNATION 5.07-5-30
STATIC PROPERTIES
AND
MODEL LINES

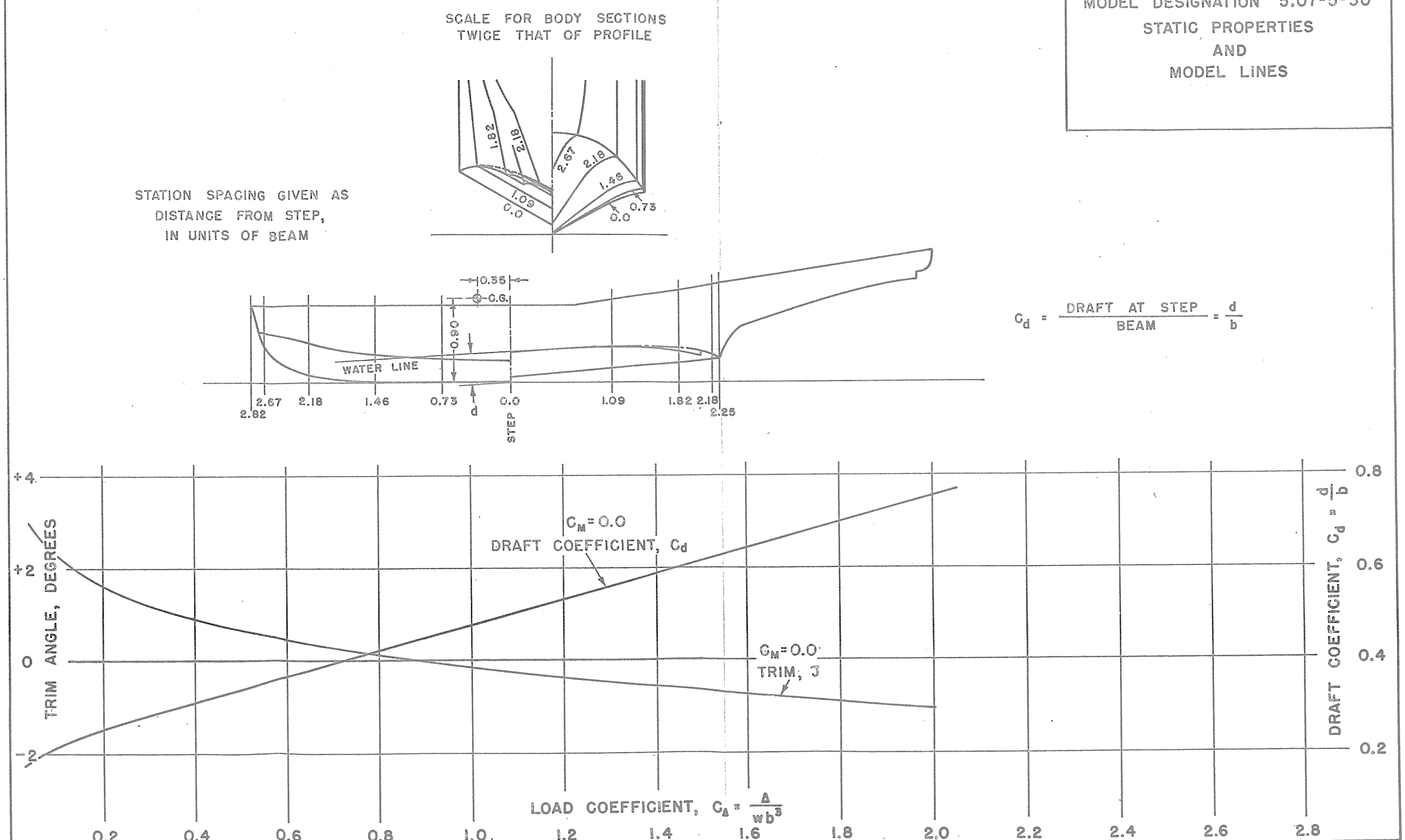

STEVENS MODEL NO. 613

MODEL DESIGNATION 5.07-9-30

STATIC PROPERTIES
AND
MODEL LINES

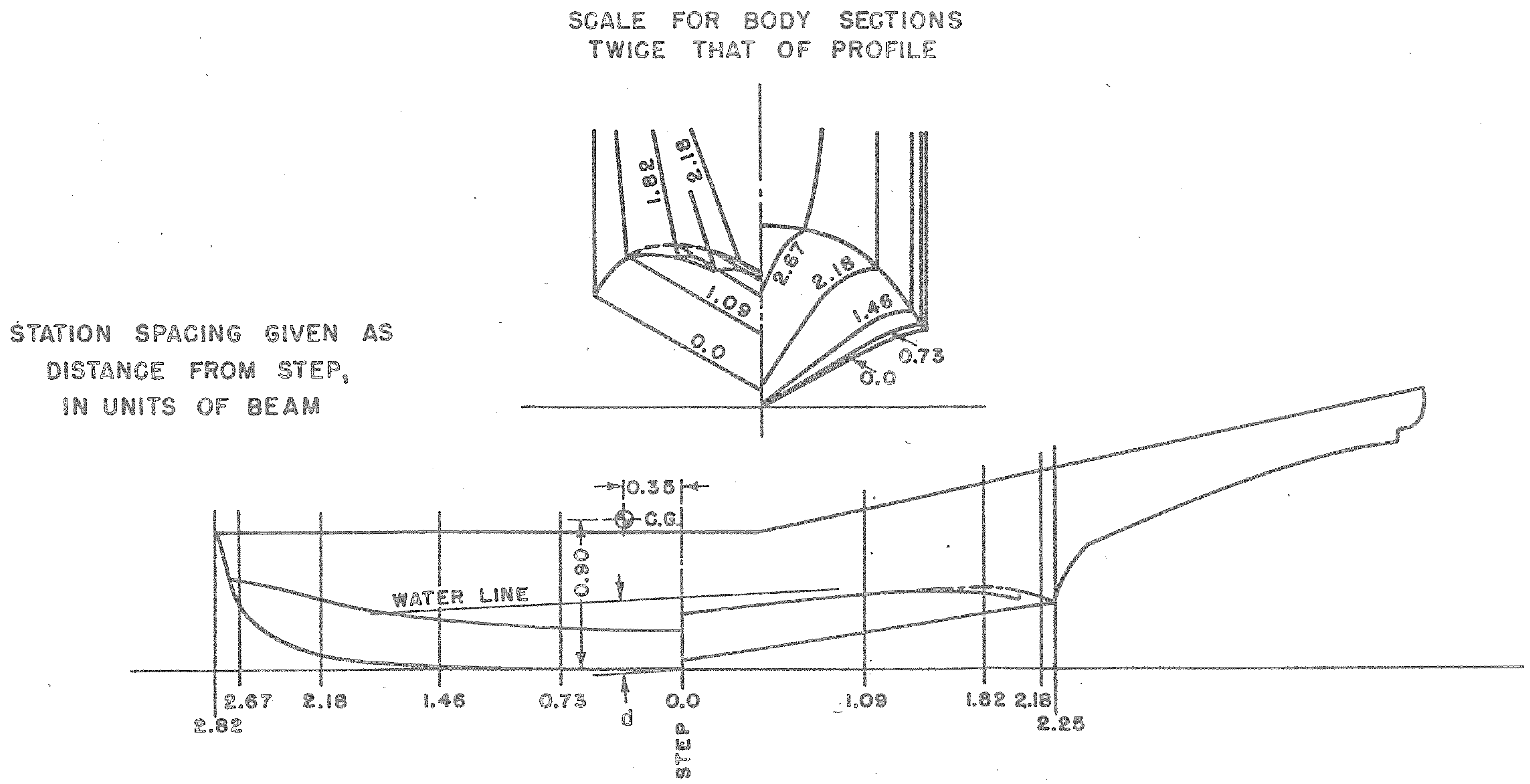

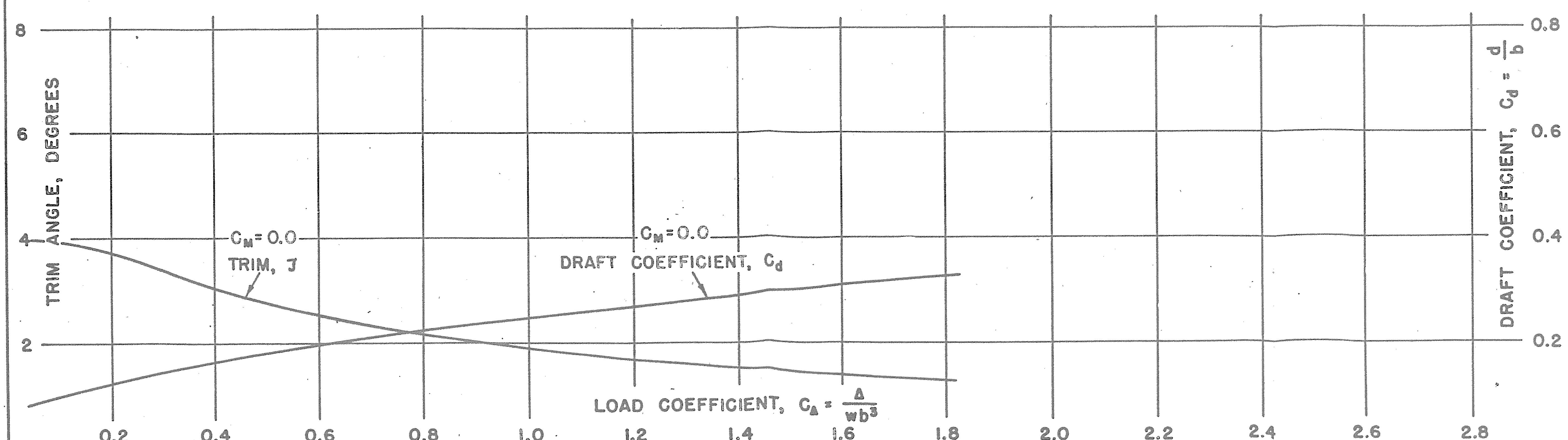

STATIC PROPERTIES CHARTS

FOR LENGTH-BEAM RATIO 6.19 HULLS

Pages 140 through 156

STEVENS MODEL NO. 556

MODEL DESIGNATION 6.19-3-0

STATIC PROPERTIES

AND

MODEL LINES

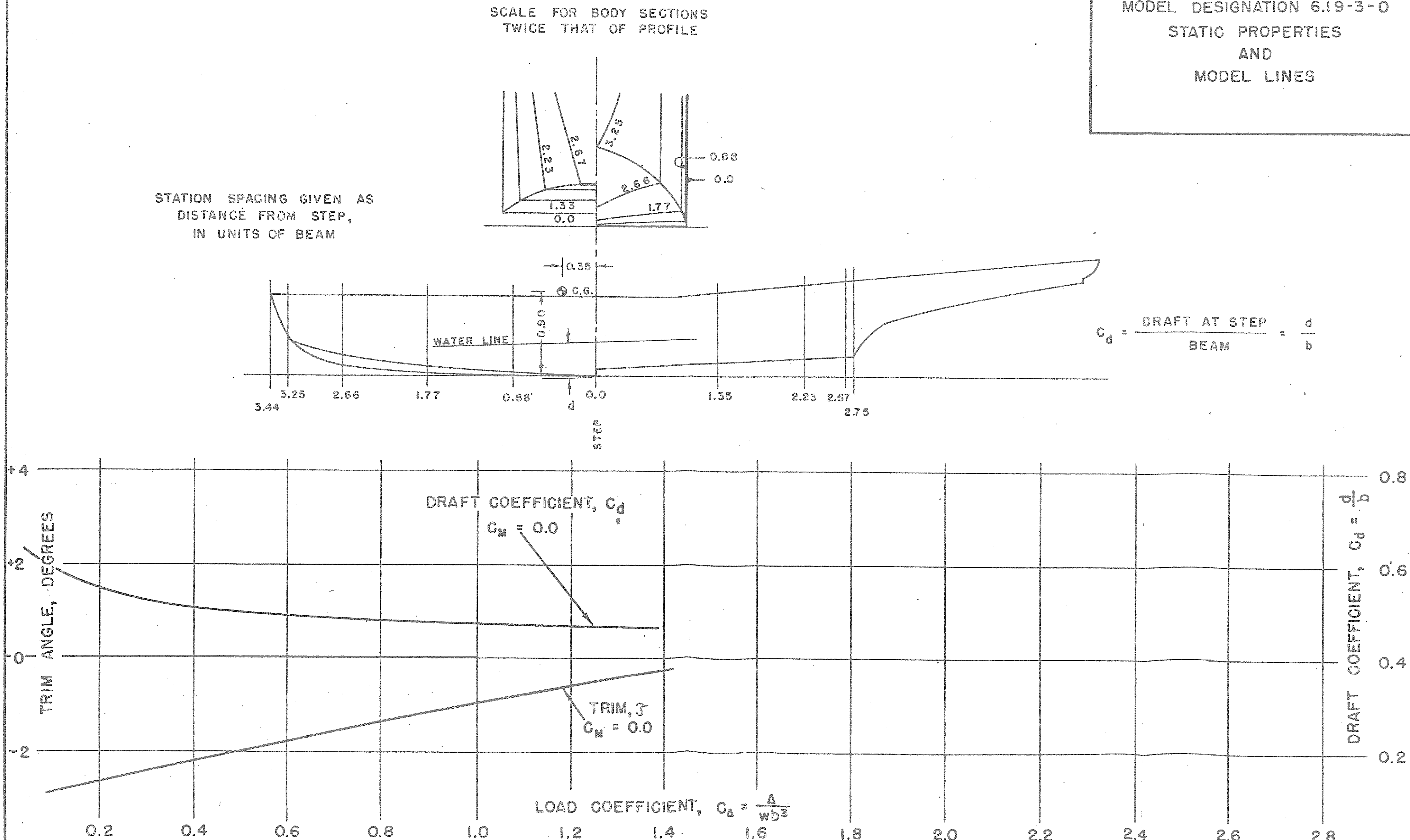

STEVENS MODEL NO. 532

MODEL DESIGNATION 6.19-7-0

STATIC PROPERTIES

AND

MODEL LINES

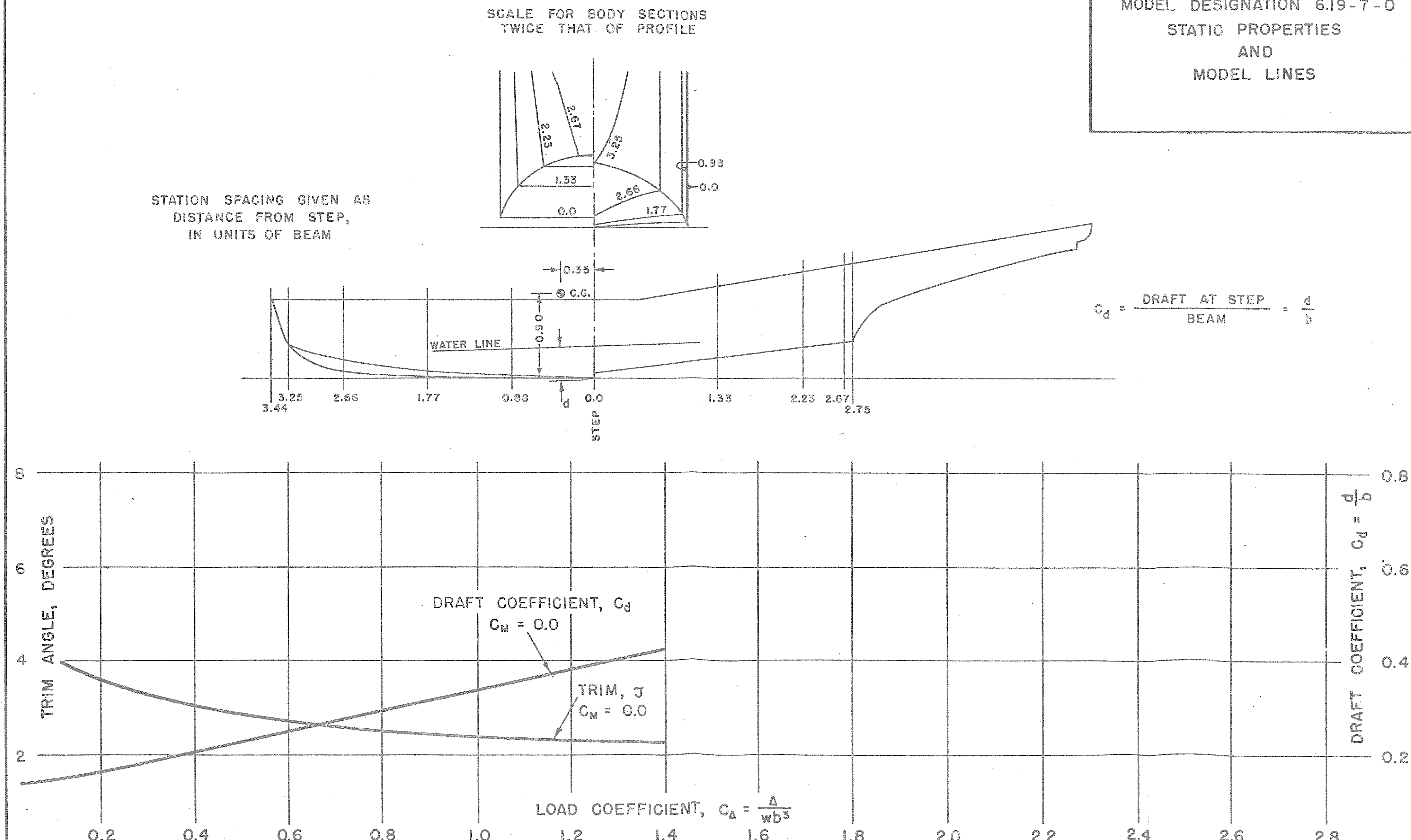

STEVENS MODEL NO. 557

MODEL DESIGNATION 6.19-11-0

STATIC PROPERTIES

AND

MODEL LINES

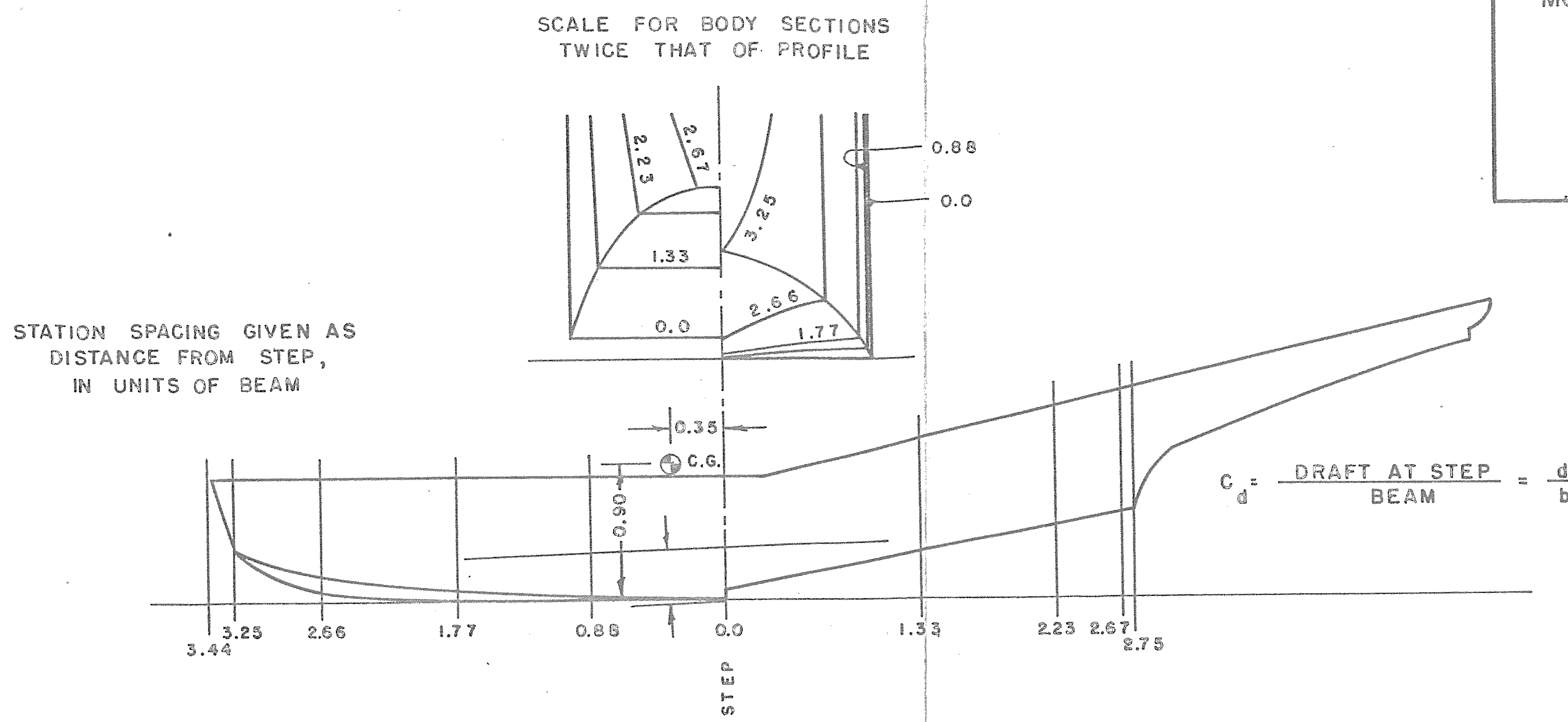

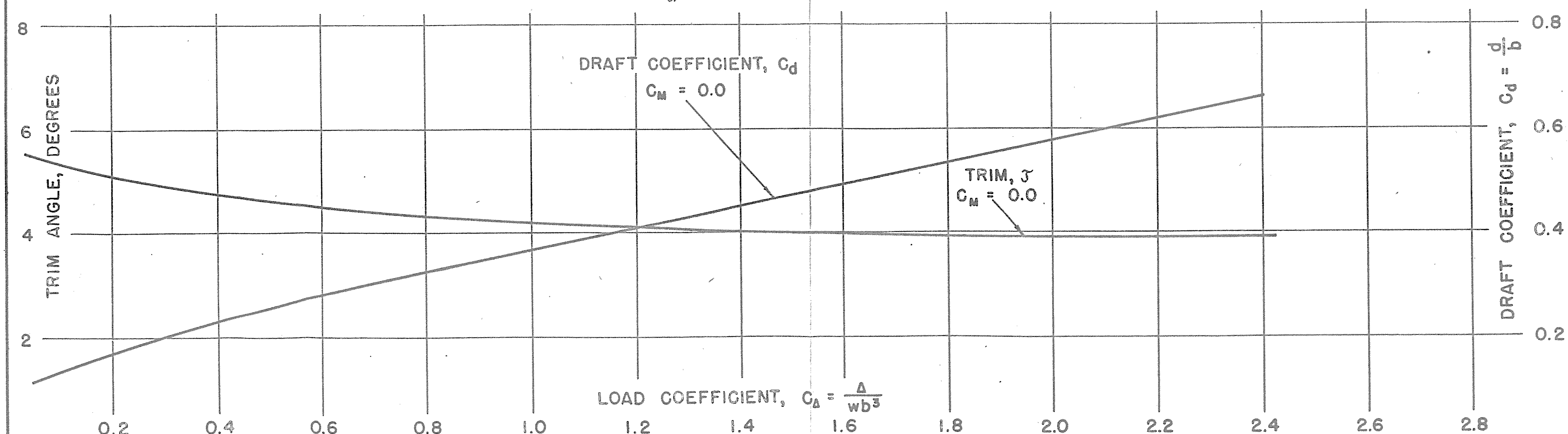

STEVENS MODEL NO. 604

MODEL DESIGNATION 6.19-5-10

STATIC PROPERTIES
AND
MODEL LINES

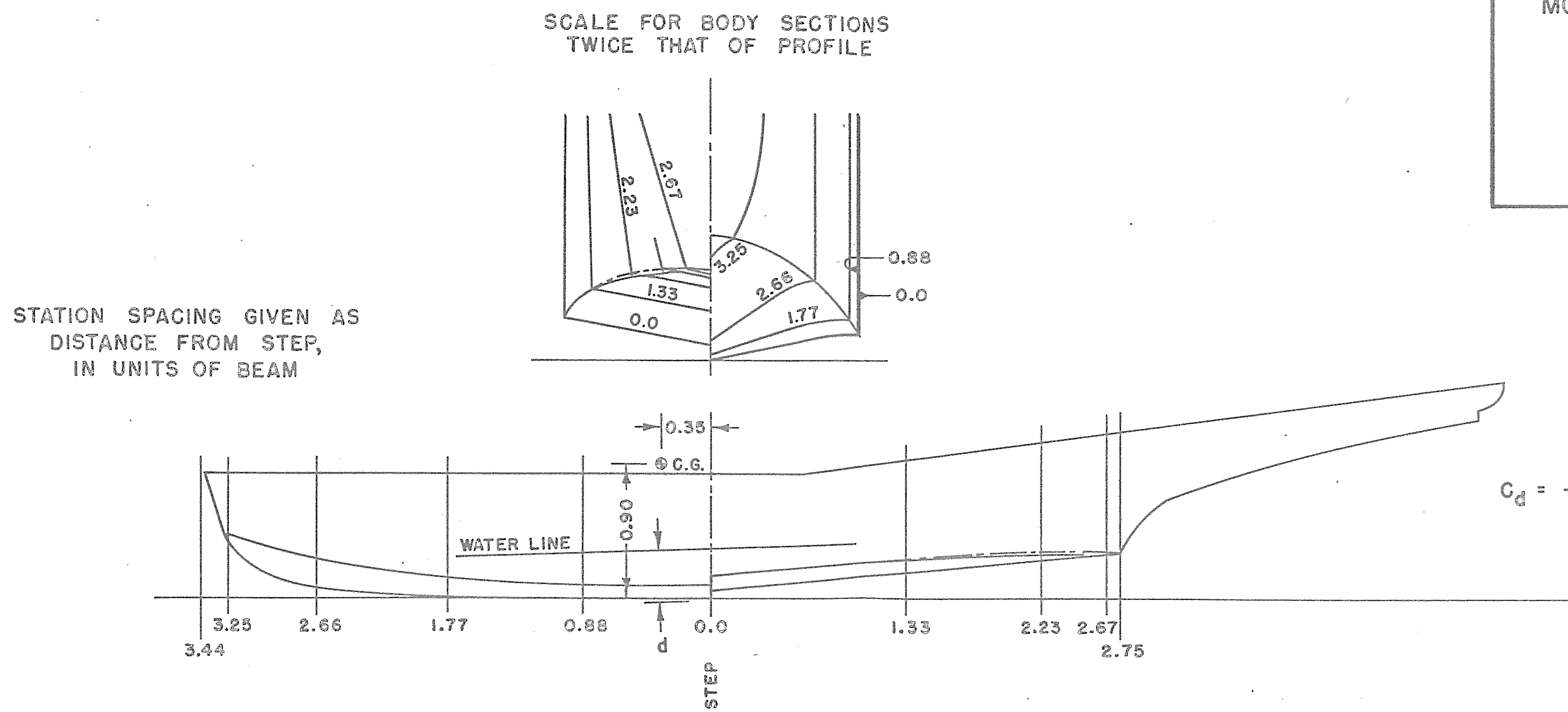

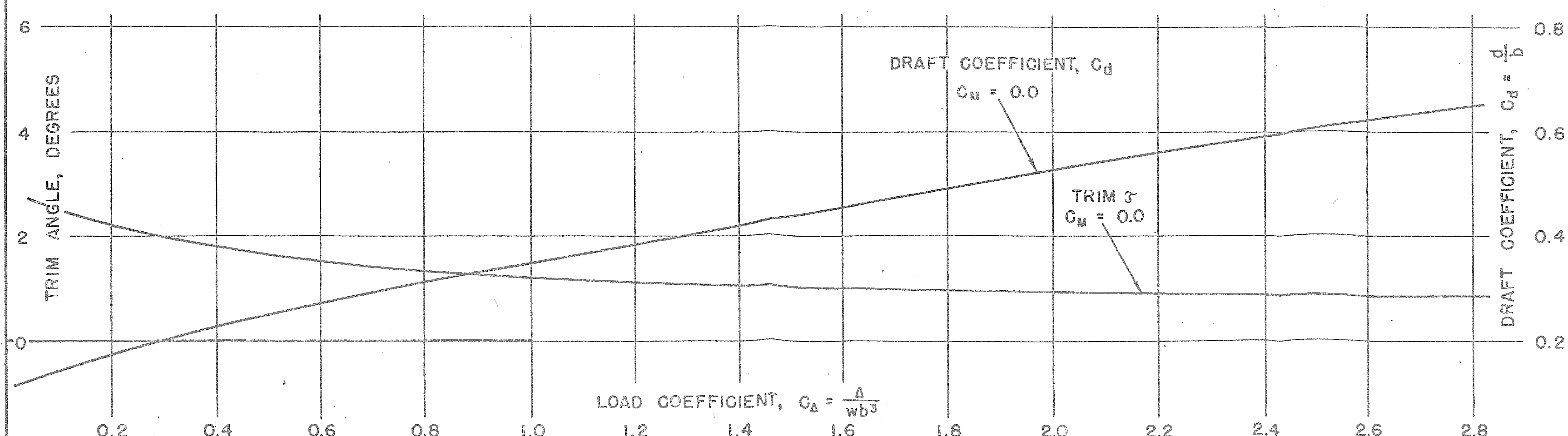

STEVENS MODEL NO. 533

MODEL DESIGNATION 6.19-7-10

STATIC PROPERTIES

AND

MODEL LINES

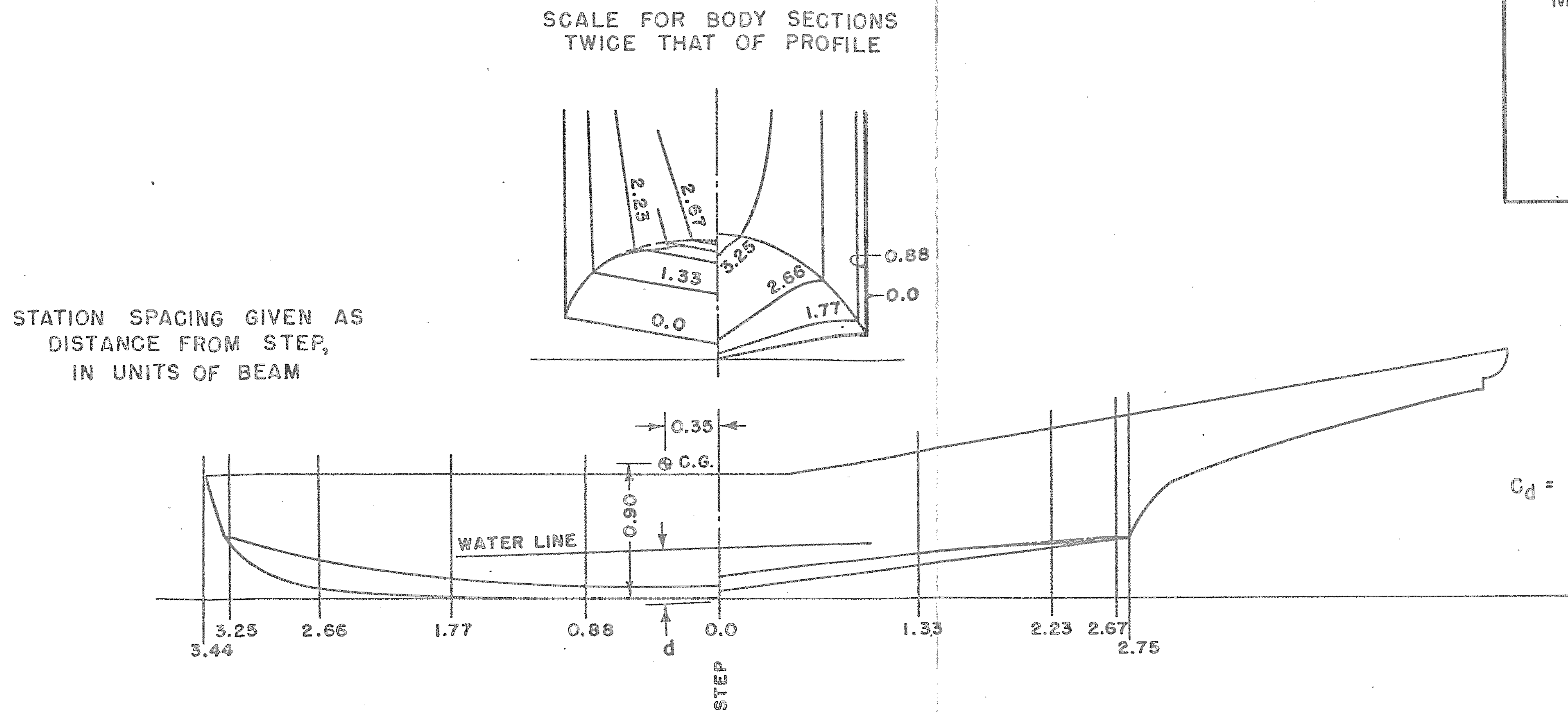

$C_d = \dfrac{\text{DRAFT AT STEP}}{\text{BEAM}} = \dfrac{d}{b}$

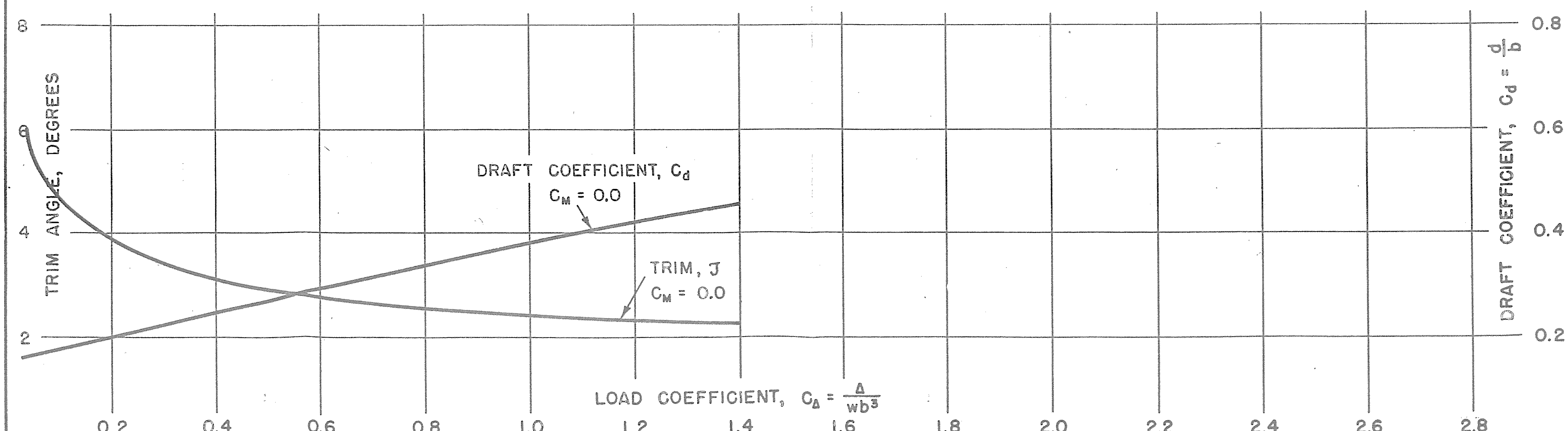

STEVENS MODEL NO. 605

MODEL DESIGNATION 6.19-9-10

STATIC PROPERTIES AND MODEL LINES

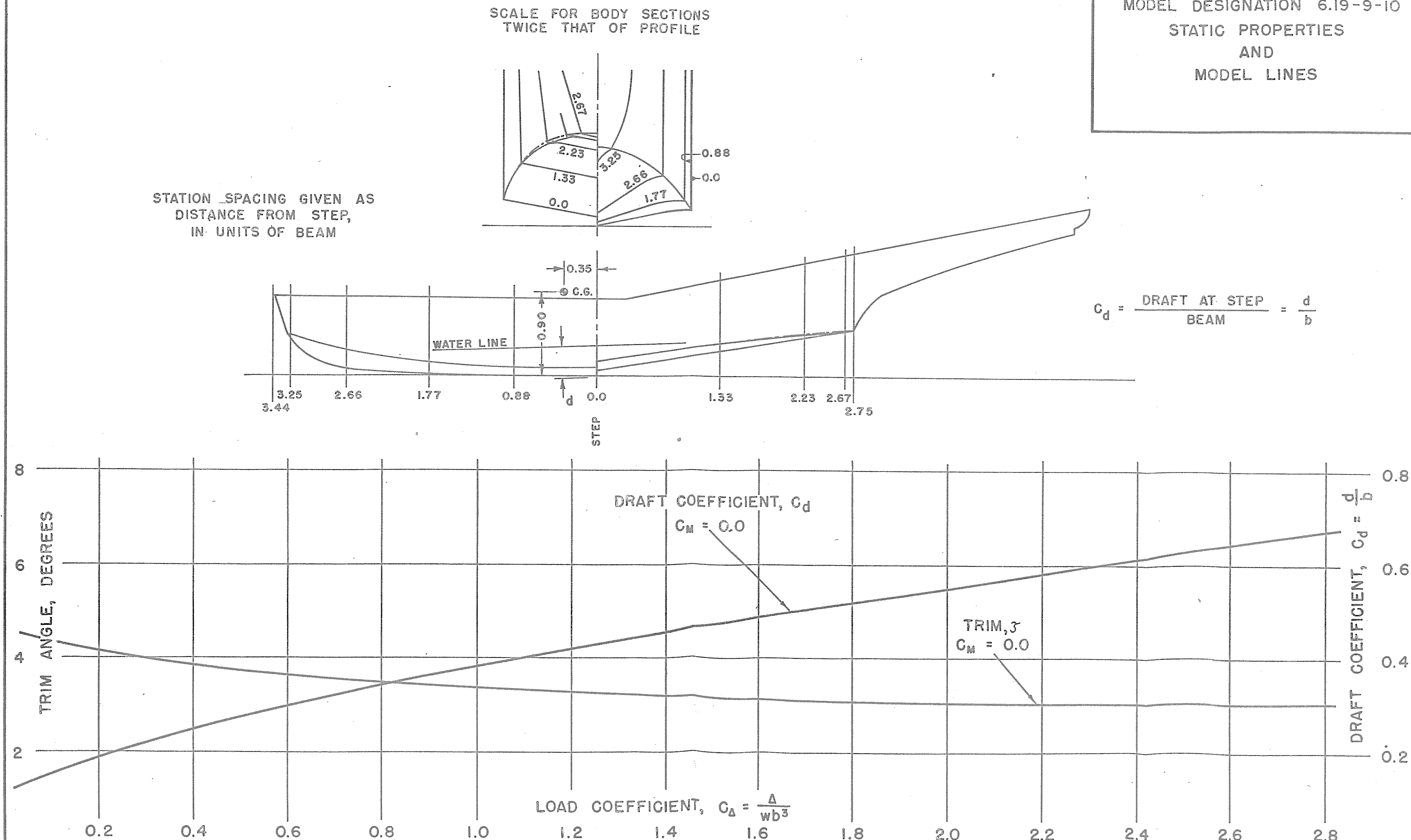

STEVENS MODEL NO. 536

MODEL DESIGNATION 6.19-3-20

STATIC PROPERTIES

AND

MODEL LINES

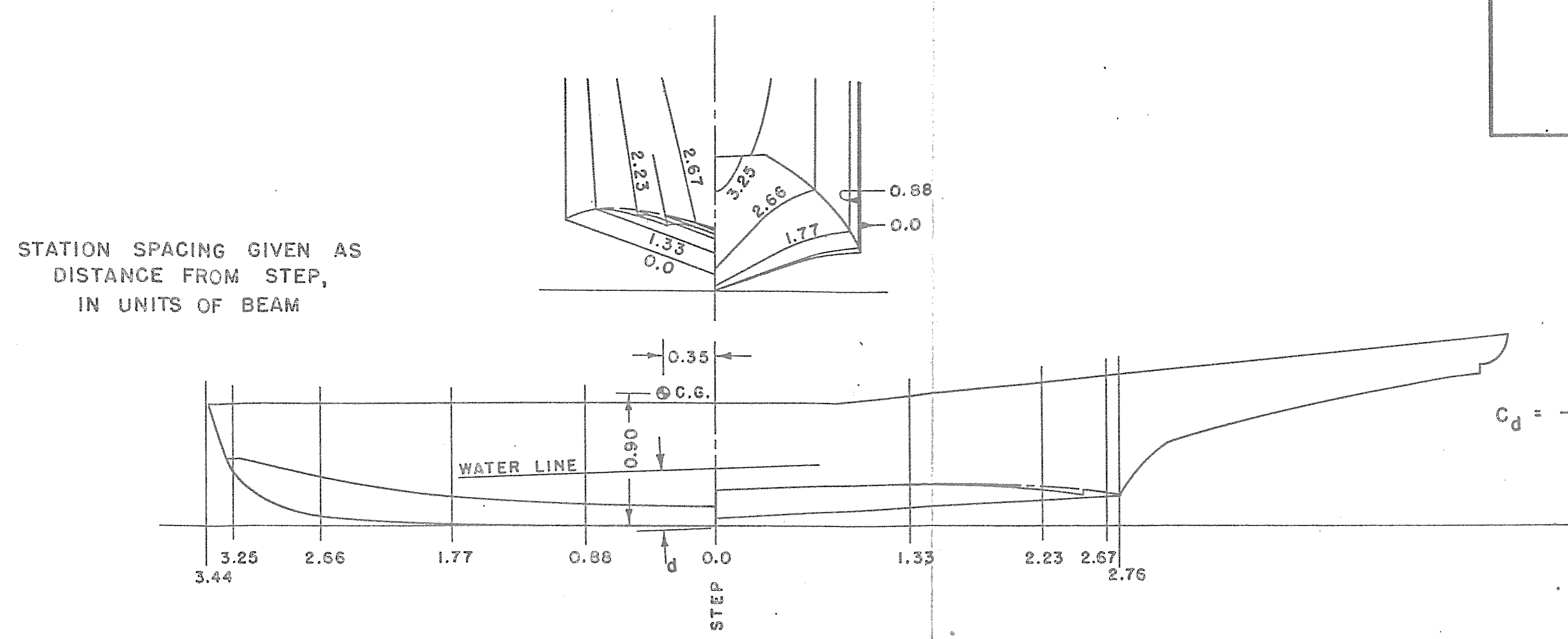

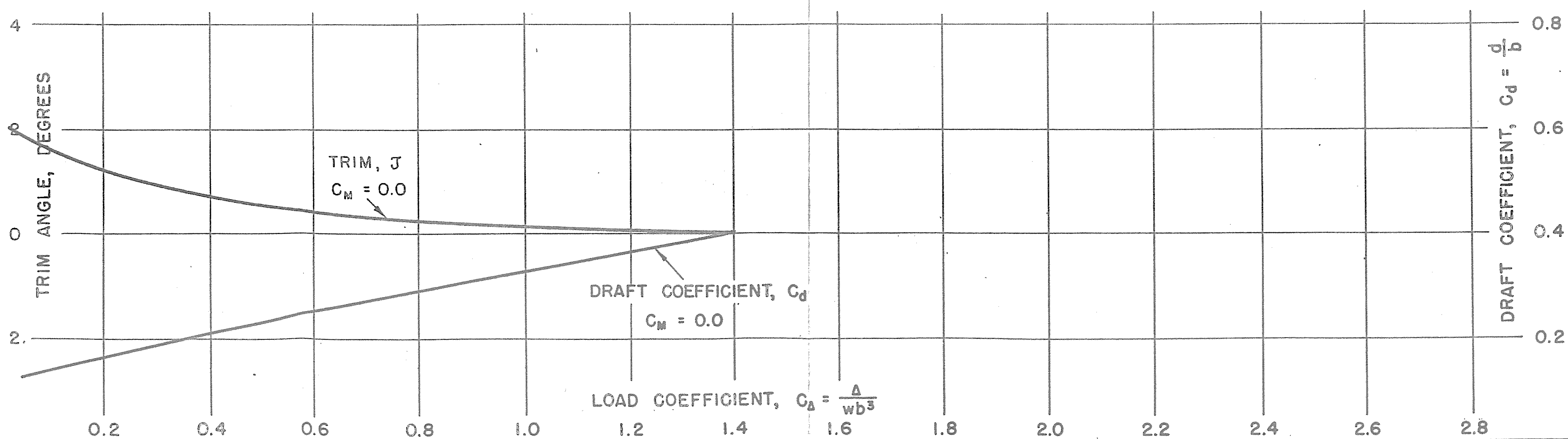

STEVENS MODEL NO. 537

MODEL DESIGNATION 6.19-5-20

STATIC PROPERTIES

AND

MODEL LINES

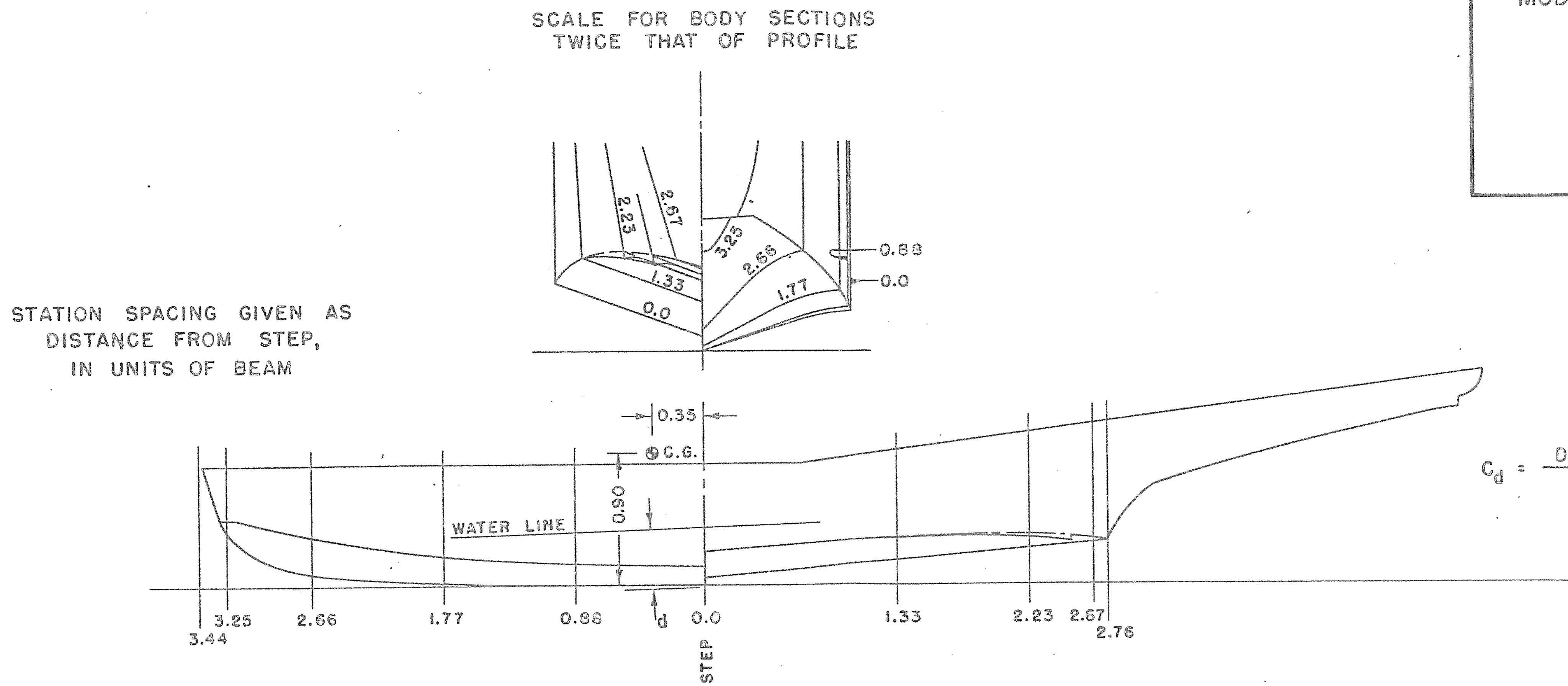

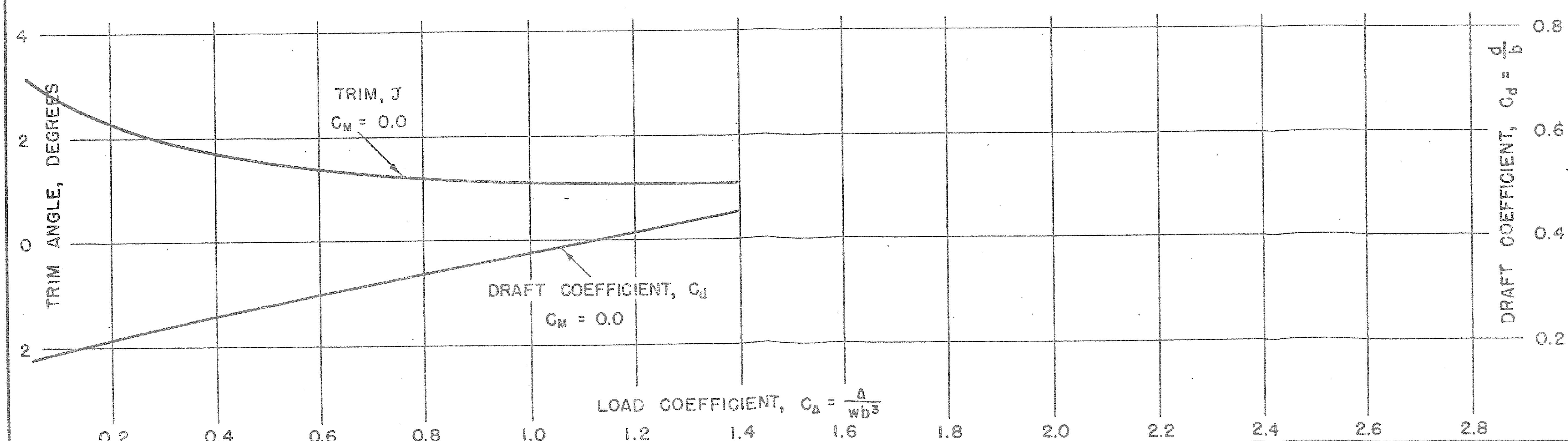

STEVENS MODEL NO. 591

MODEL DESIGNATION 6.19-7-20

STATIC PROPERTIES

AND

MODEL LINES

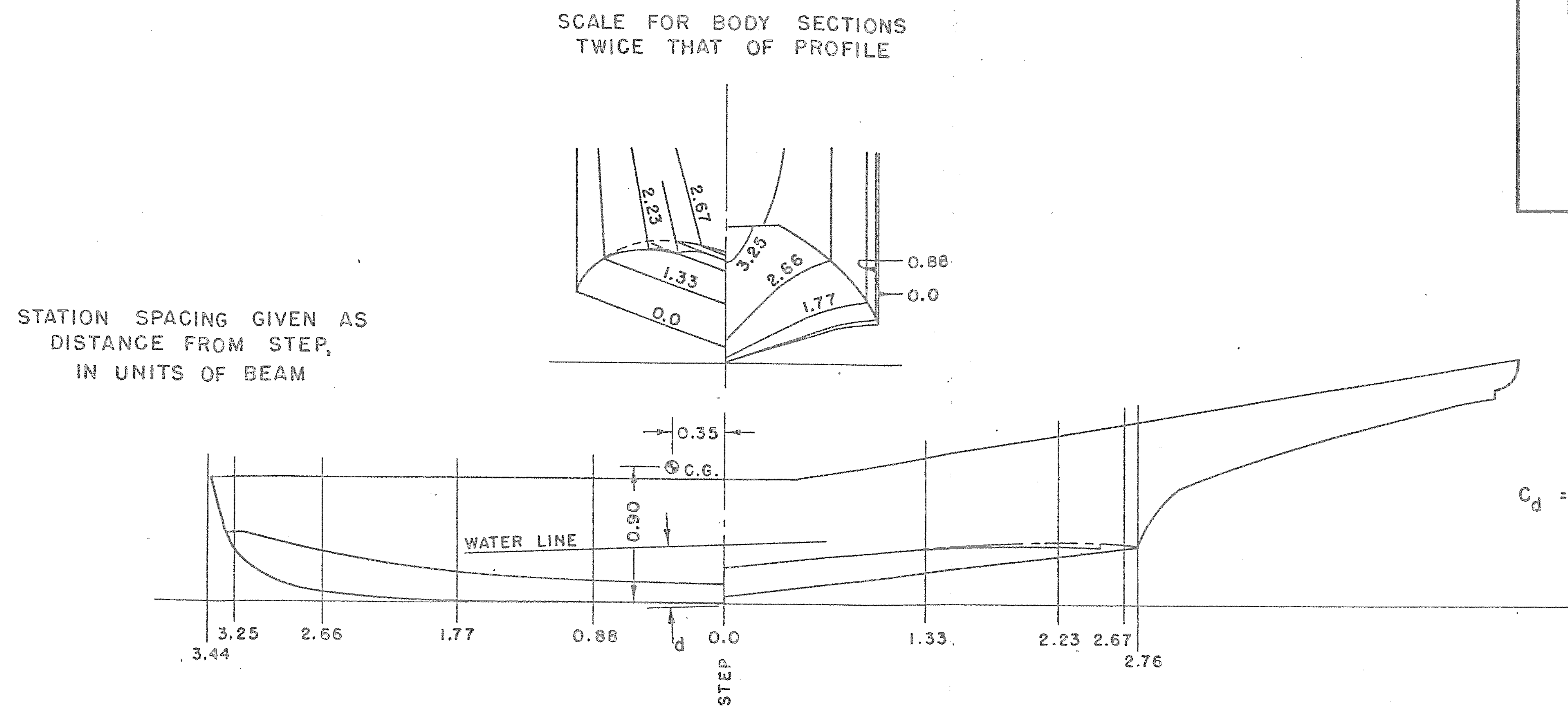

$C_d = \frac{\text{DRAFT AT STEP}}{\text{BEAM}} = \frac{d}{b}$

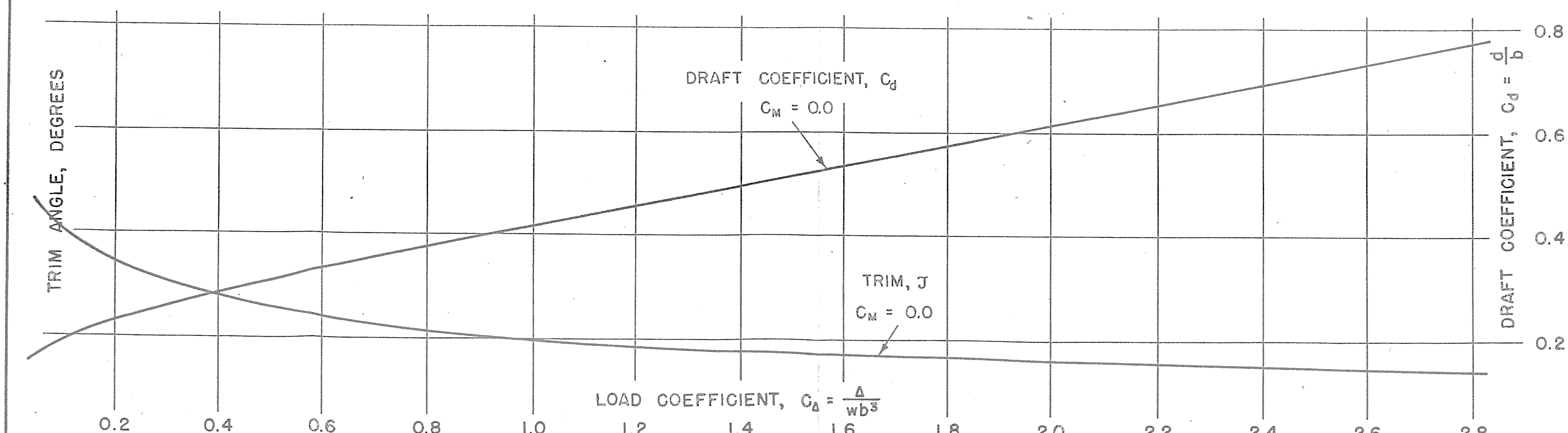

STEVENS MODEL NO. 538

MODEL DESIGNATION 6.19-9-20

STATIC PROPERTIES
AND
MODEL LINES

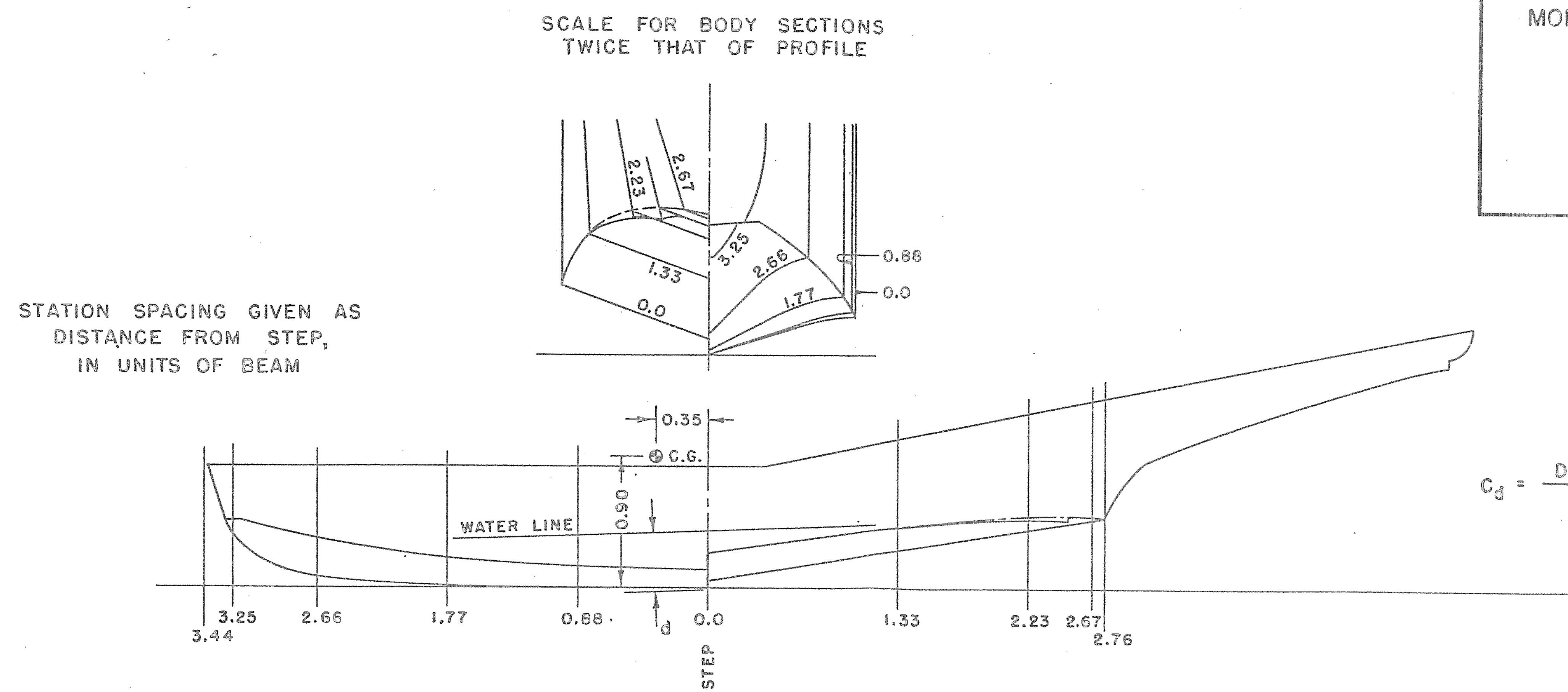

$C_d = \frac{\text{DRAFT AT STEP}}{\text{BEAM}} = \frac{d}{b}$

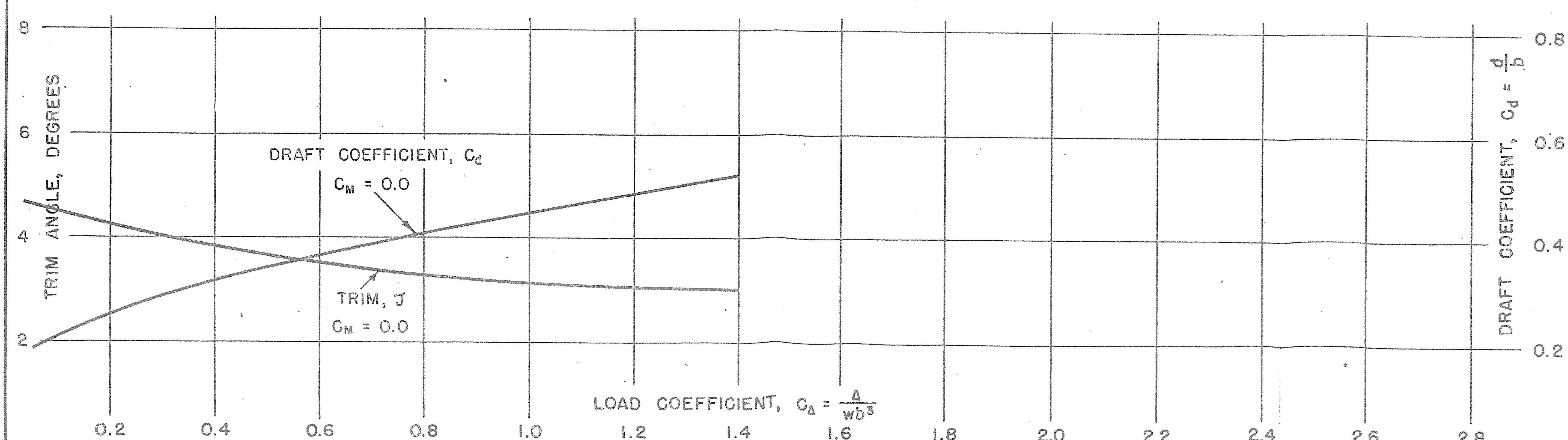

STEVENS MODEL NO. 539

MODEL DESIGNATION 6.19-11-20

STATIC PROPERTIES
AND
MODEL LINES

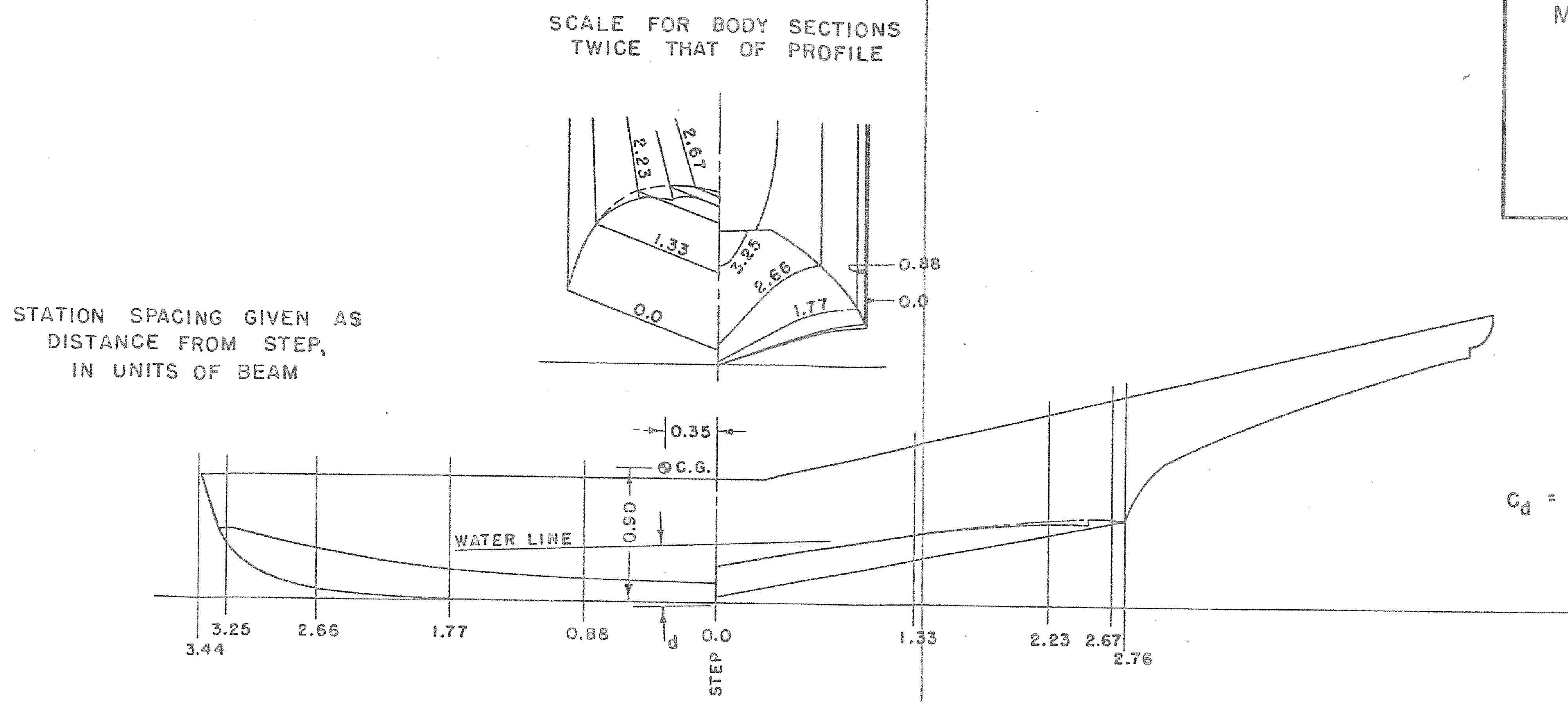

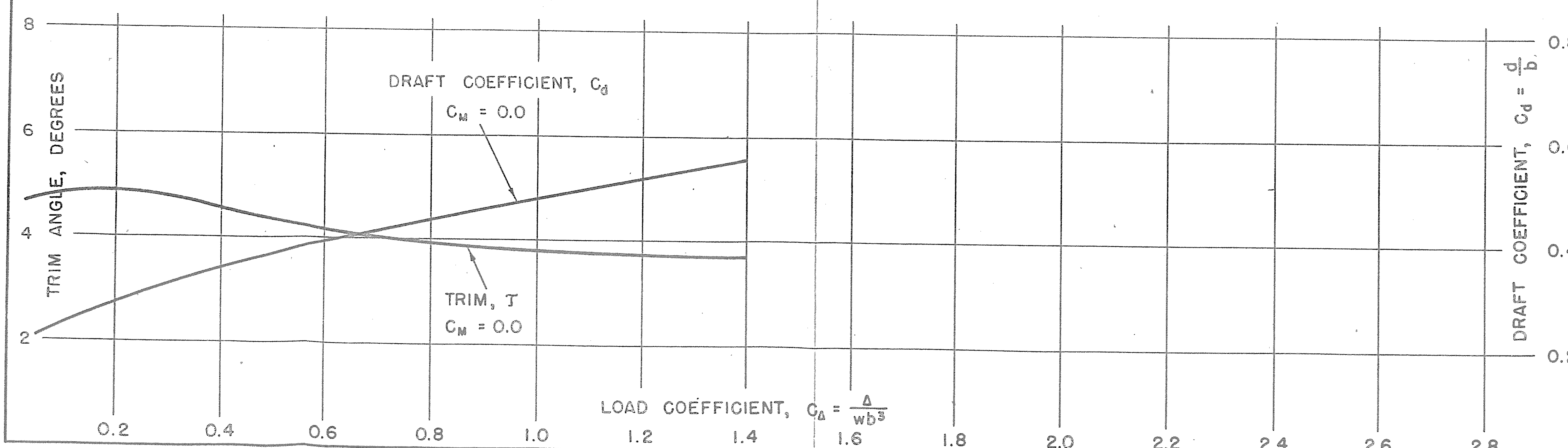

STEVENS MODEL NO. 606

MODEL DESIGNATION 6.19-5-30

STATIC PROPERTIES AND MODEL LINES

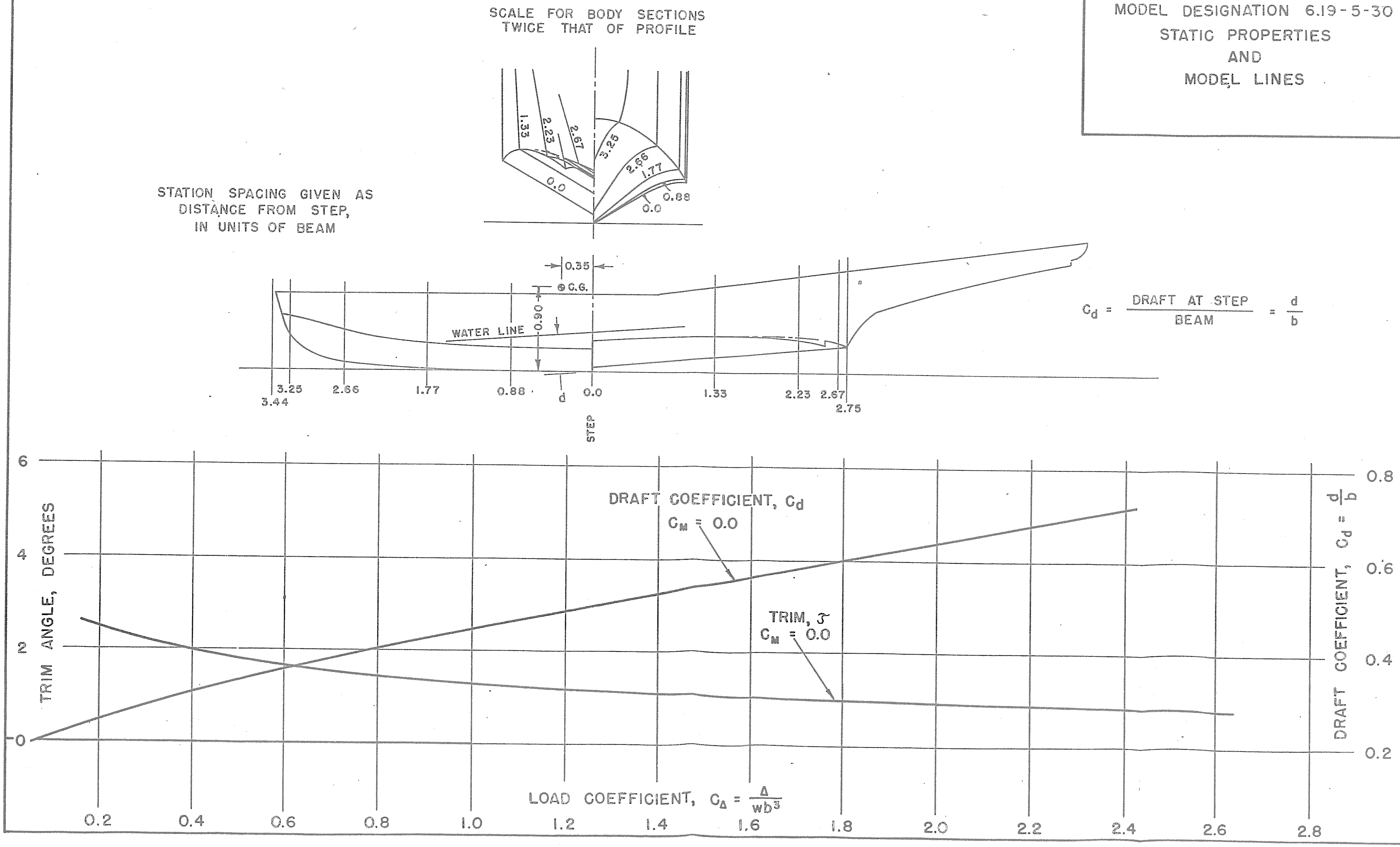

STEVENS MODEL NO. 534

MODEL DESIGNATION 6.19-7-30

STATIC PROPERTIES

AND

MODEL LINES

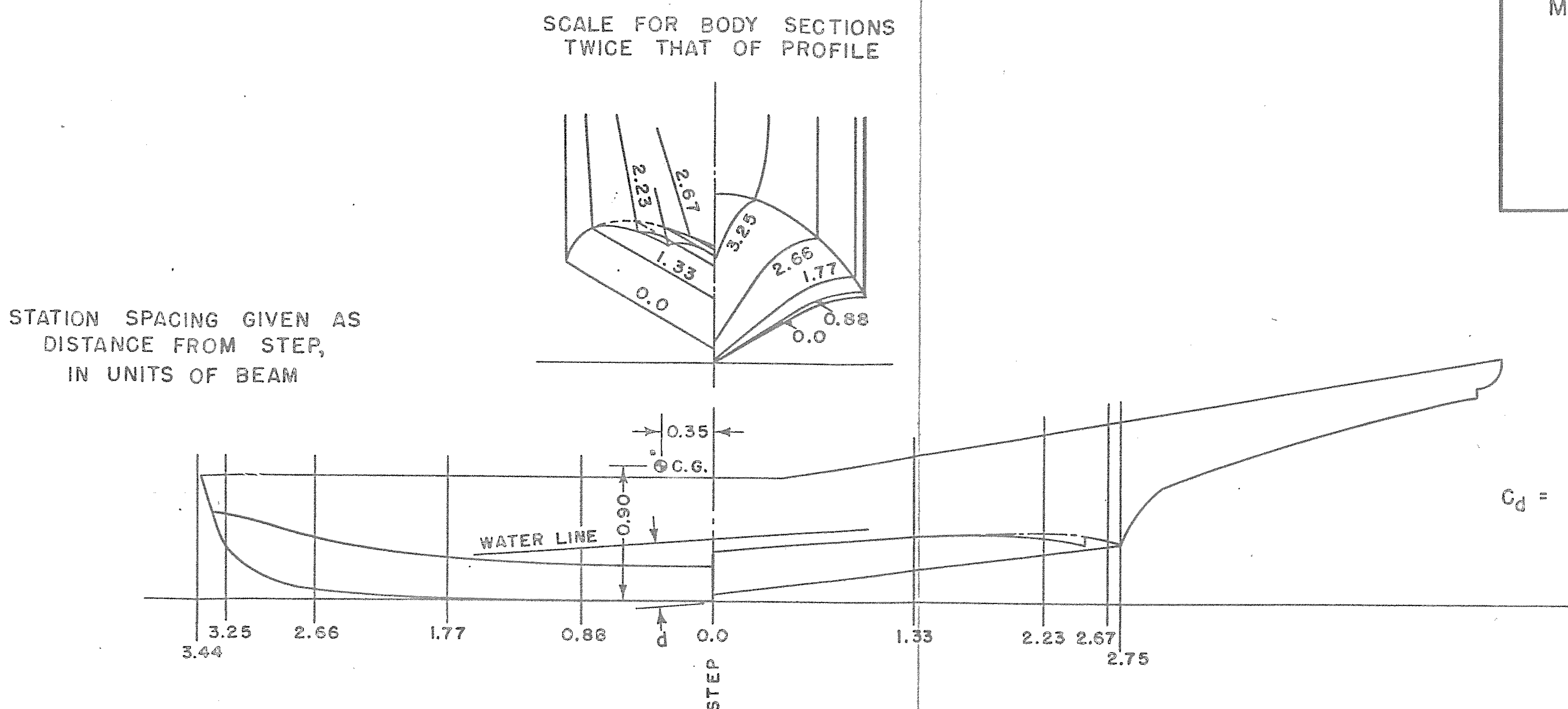

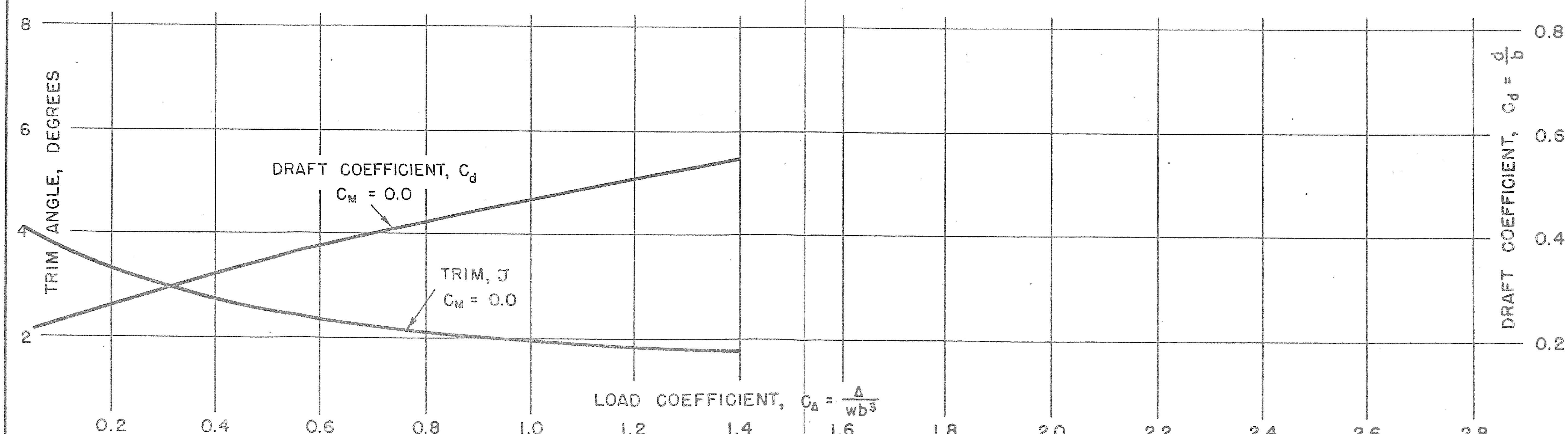

STEVENS MODEL NO. 607

MODEL DESIGNATION 6.19-9-30

STATIC PROPERTIES
AND
MODEL LINES

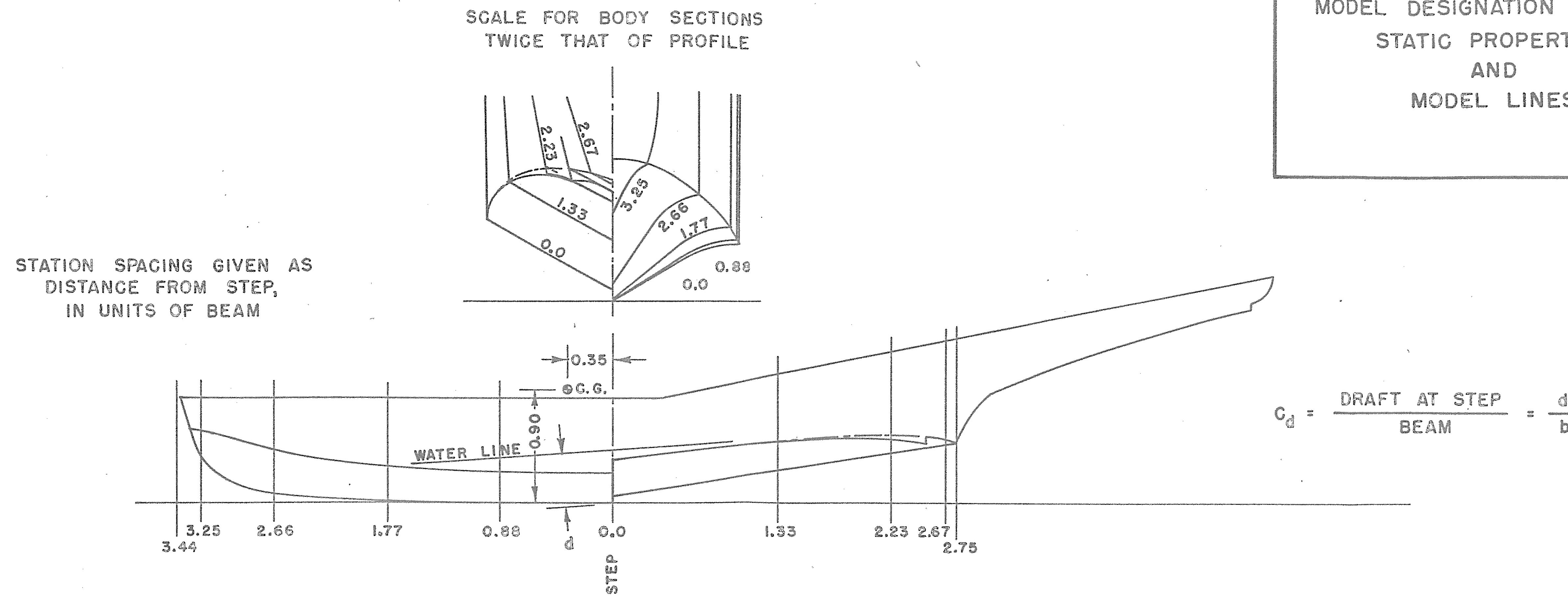

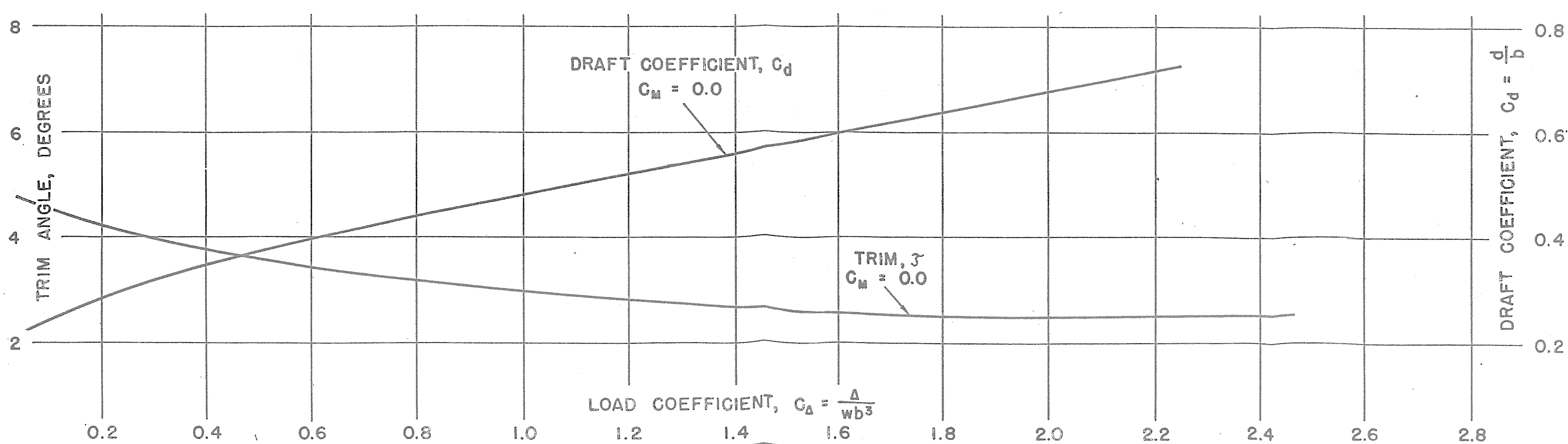

STEVENS MODEL NO. 558

MODEL DESIGNATION 6.19-3-40

STATIC PROPERTIES
AND
MODEL LINES

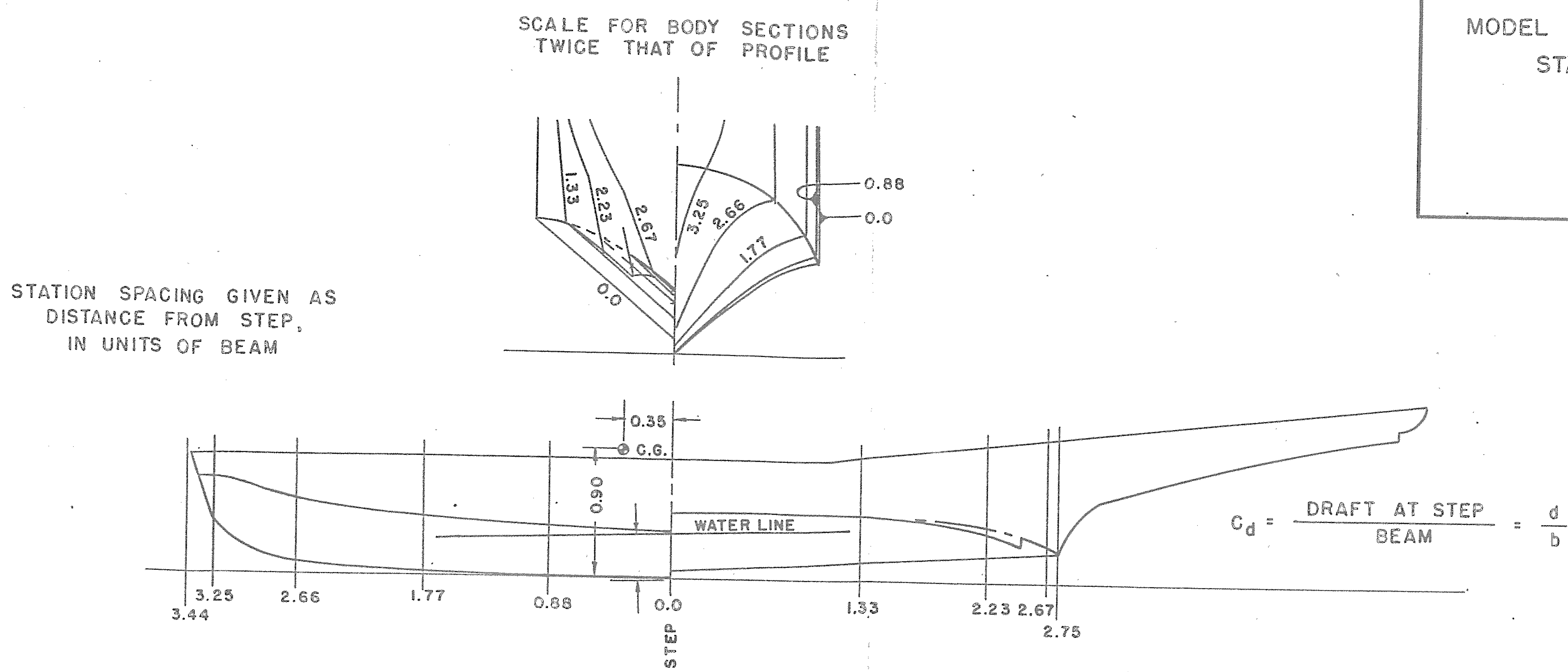

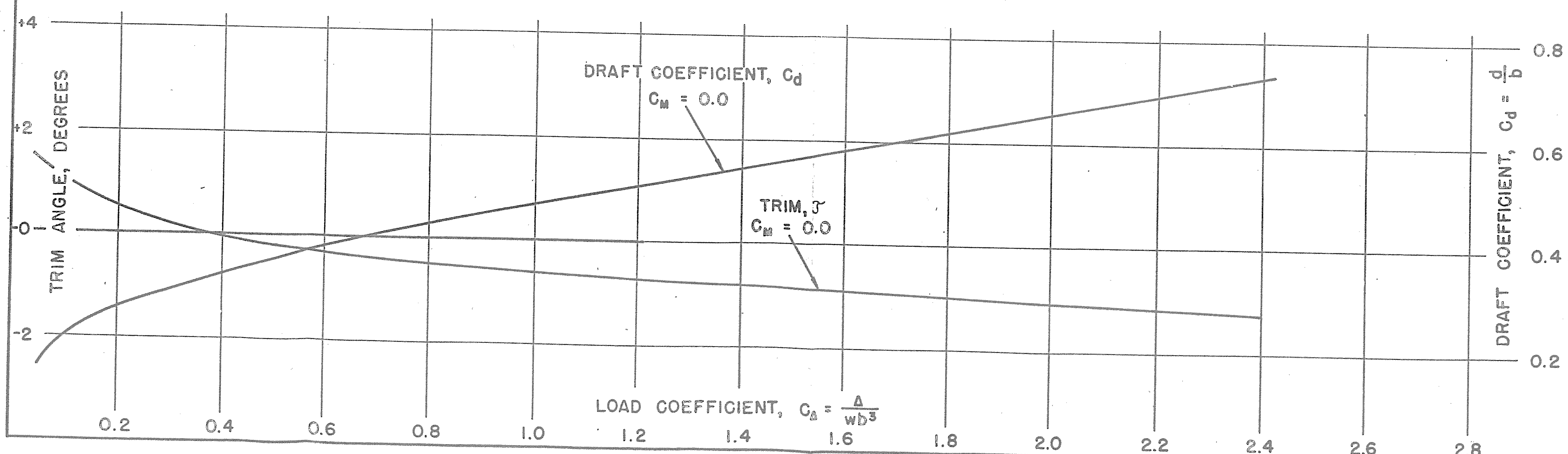

STEVENS MODEL NO. 535

MODEL DESIGNATION 6.19-7-40

STATIC PROPERTIES

AND

MODEL LINES

SCALE FOR BODY SECTIONS
TWICE THAT OF PROFILE

STATION SPACING GIVEN AS
DISTANCE FROM STEP,
IN UNITS OF BEAM

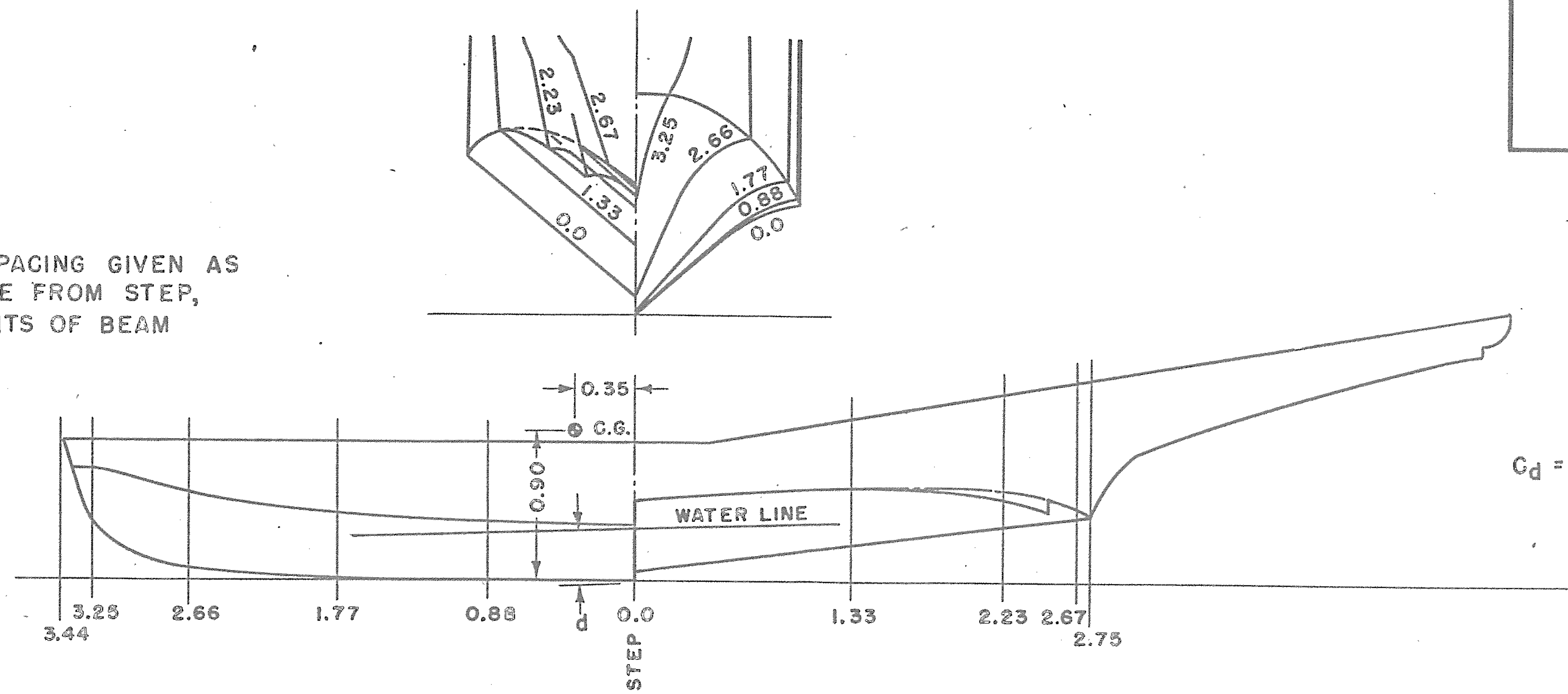

$C_d = \frac{\text{DRAFT AT STEP}}{\text{BEAM}} = \frac{d}{b}$

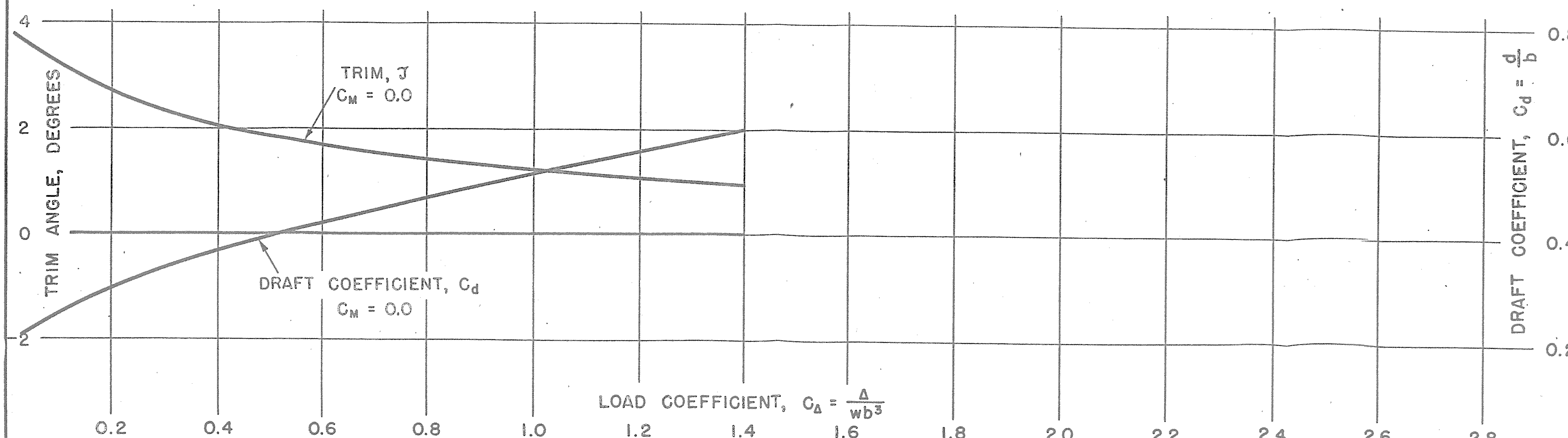

STEVENS MODEL NO. 559

MODEL DESIGNATION 6.19-11-40

STATIC PROPERTIES
AND
MODEL LINES

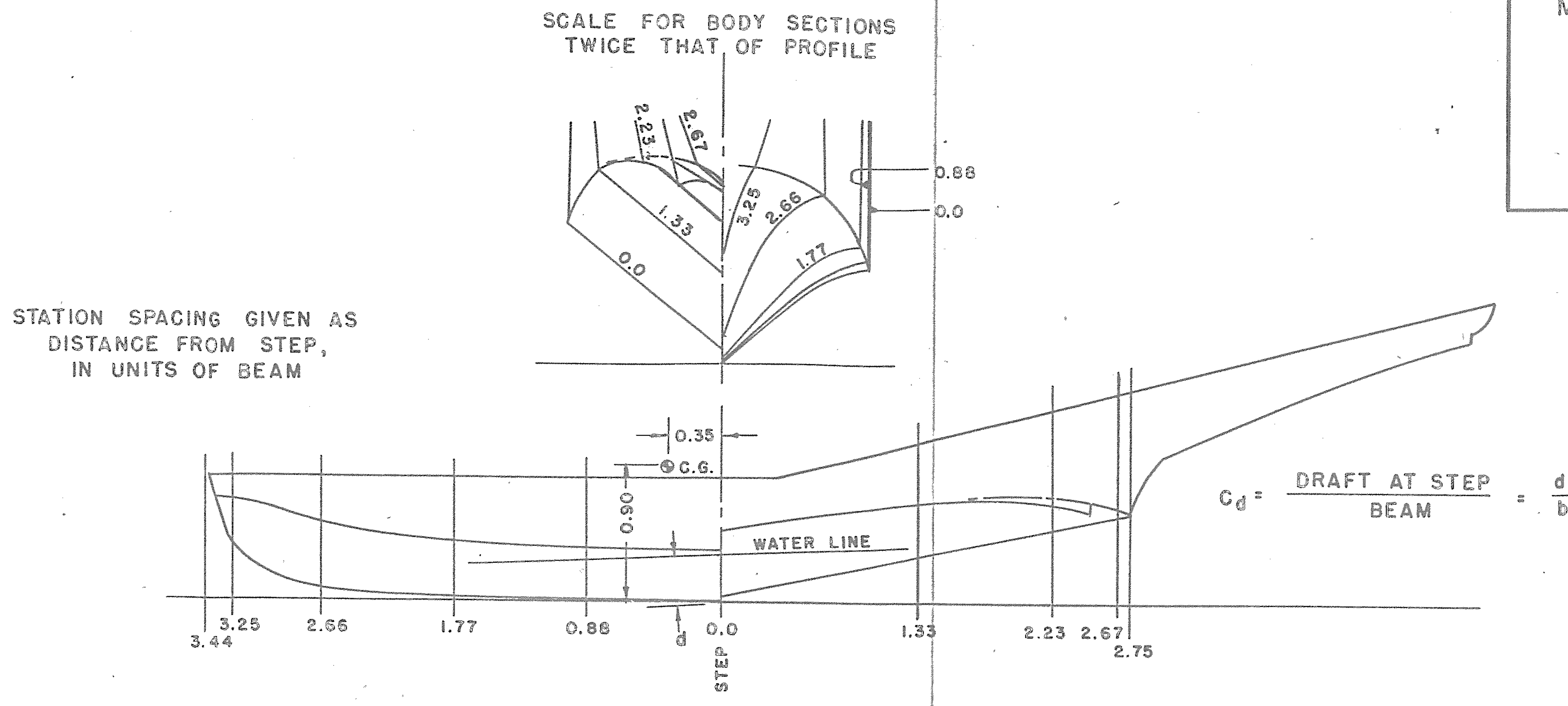

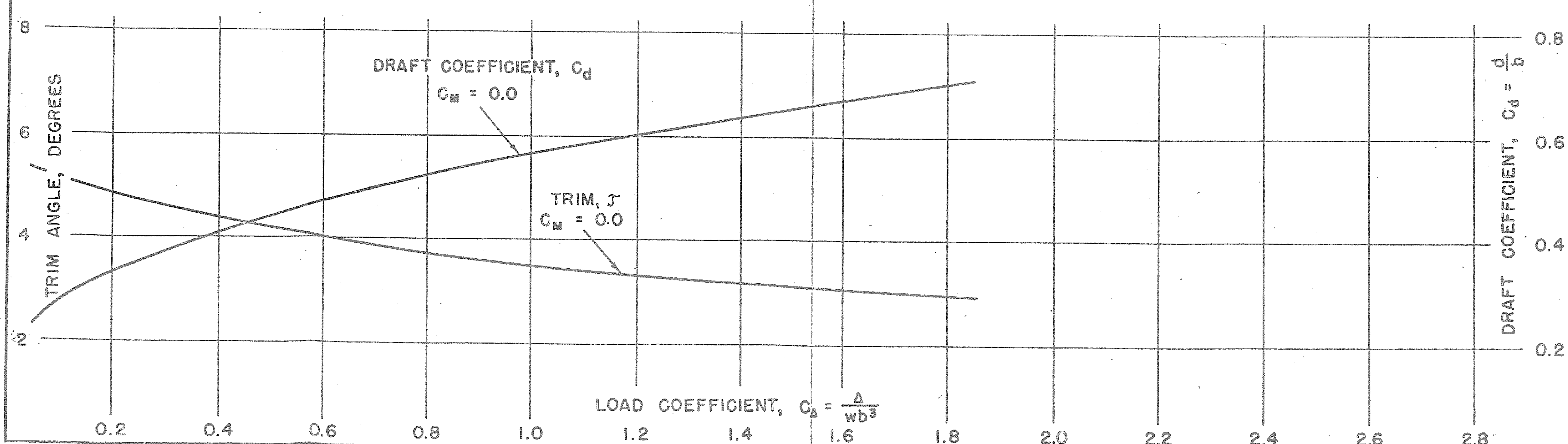

STATIC PROPERTIES CHARTS

FOR LENGTH-BEAM RATIO 7.32 HULLS

Pages 157 through 163

STEVENS MODEL NO. 624
MODEL DESIGNATION 7.32-5-10
STATIC PROPERTIES
AND
MODEL LINES

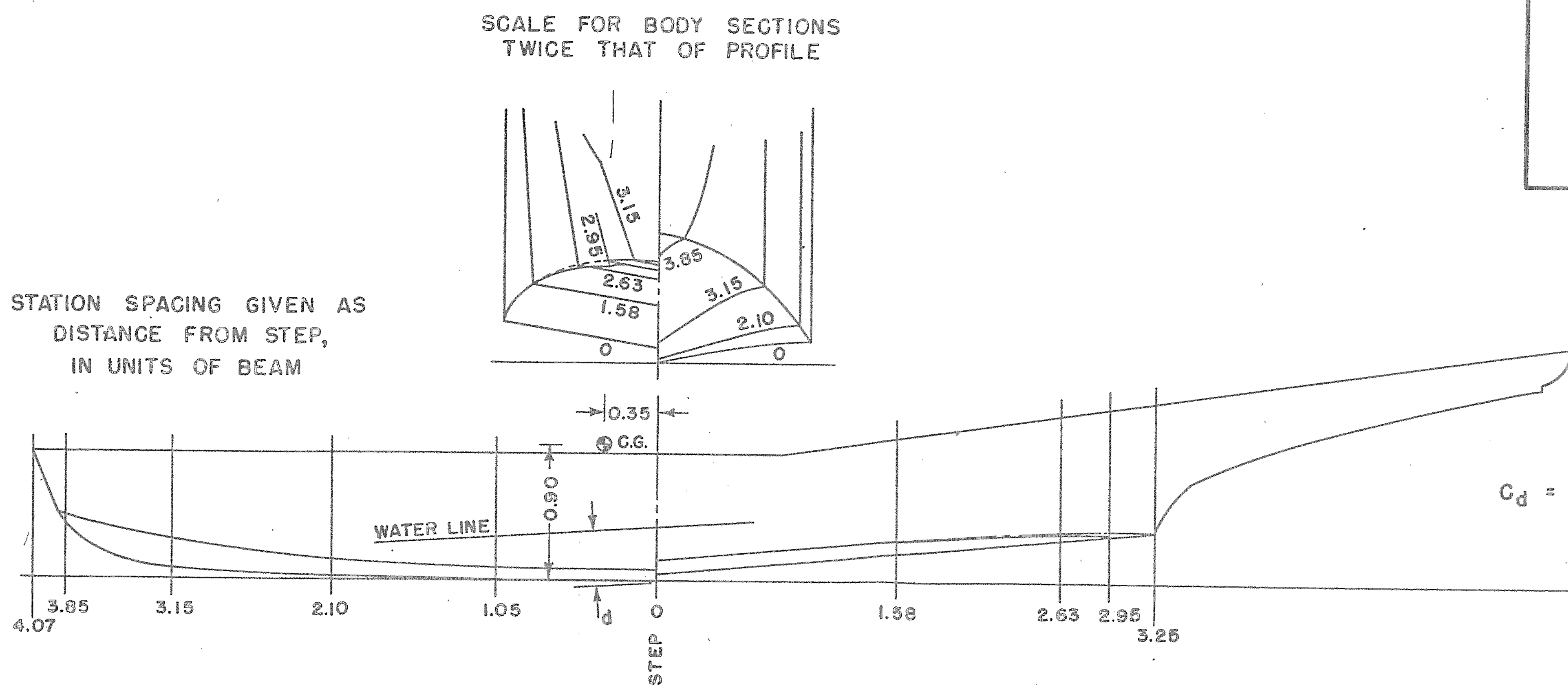

$C_d = \frac{\text{DRAFT AT STEP}}{\text{BEAM}} = \frac{d}{b}$

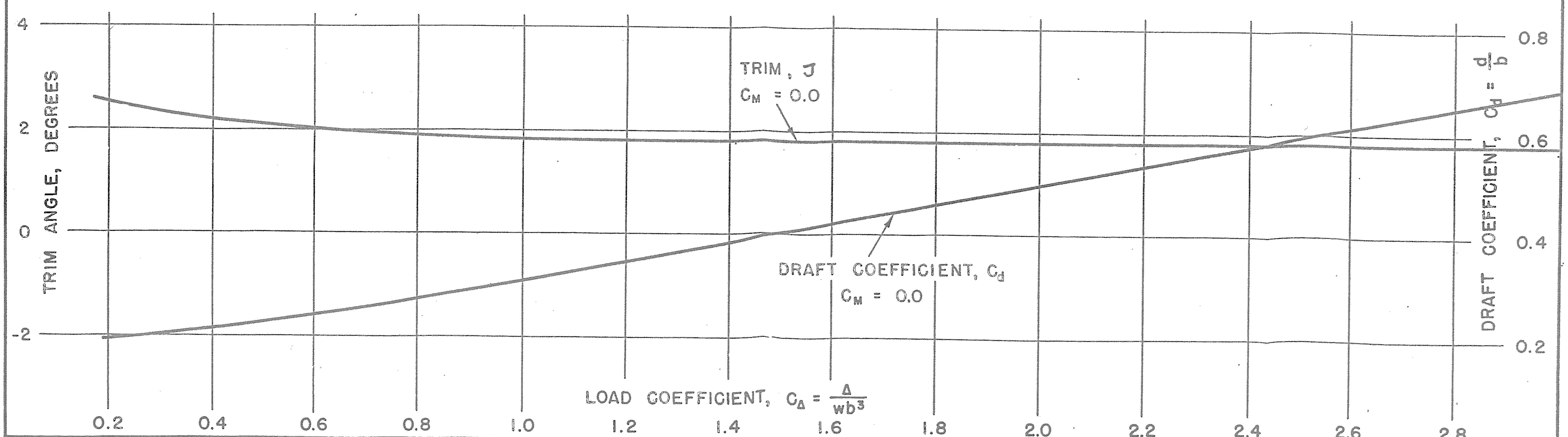

STEVENS MODEL NO. 625
MODEL DESIGNATION 7.32-9-10
STATIC PROPERTIES
AND
MODEL LINES

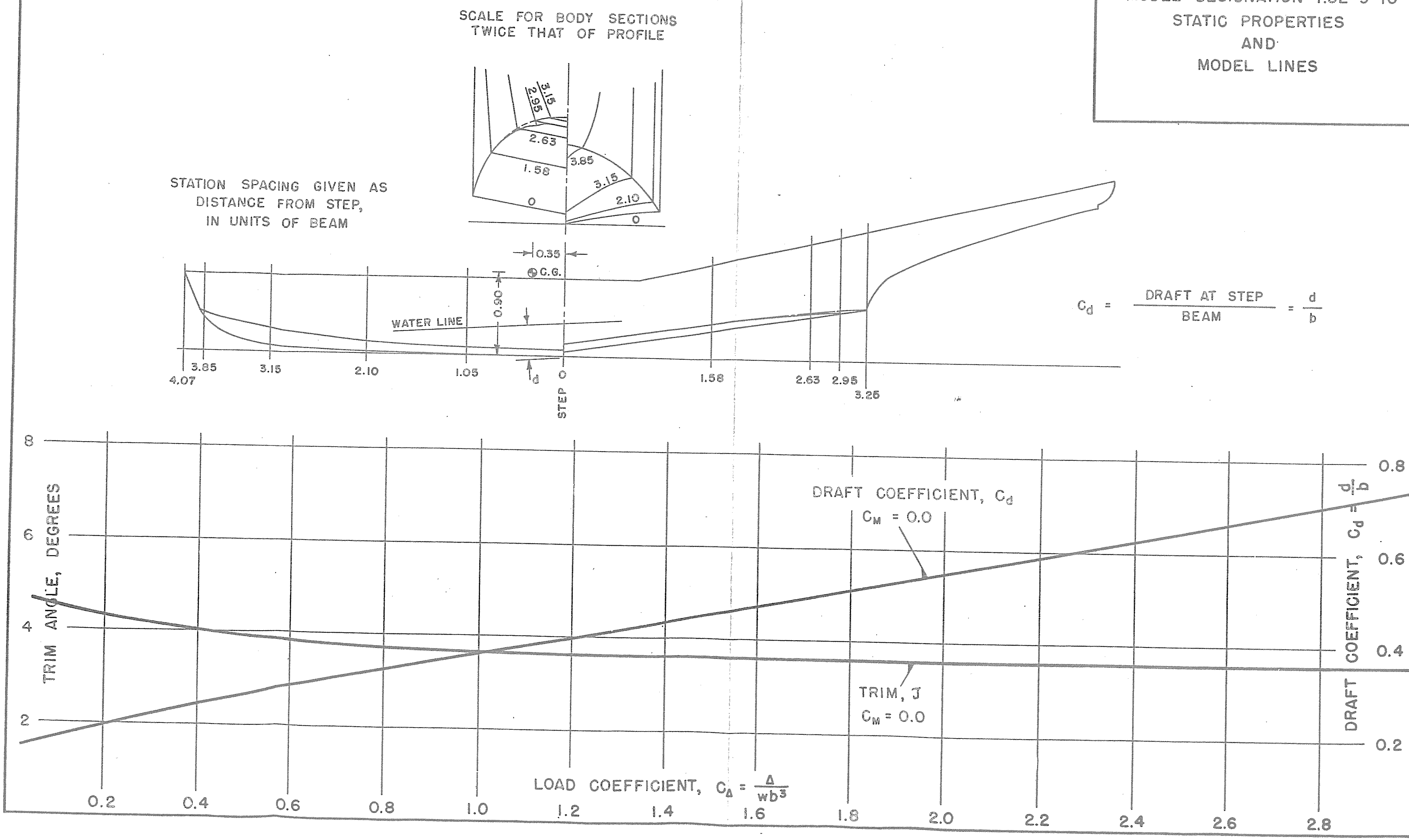

STEVENS MODEL NO. 626
MODEL DESIGNATION 7.32-3-20
STATIC PROPERTIES
AND
MODEL LINES

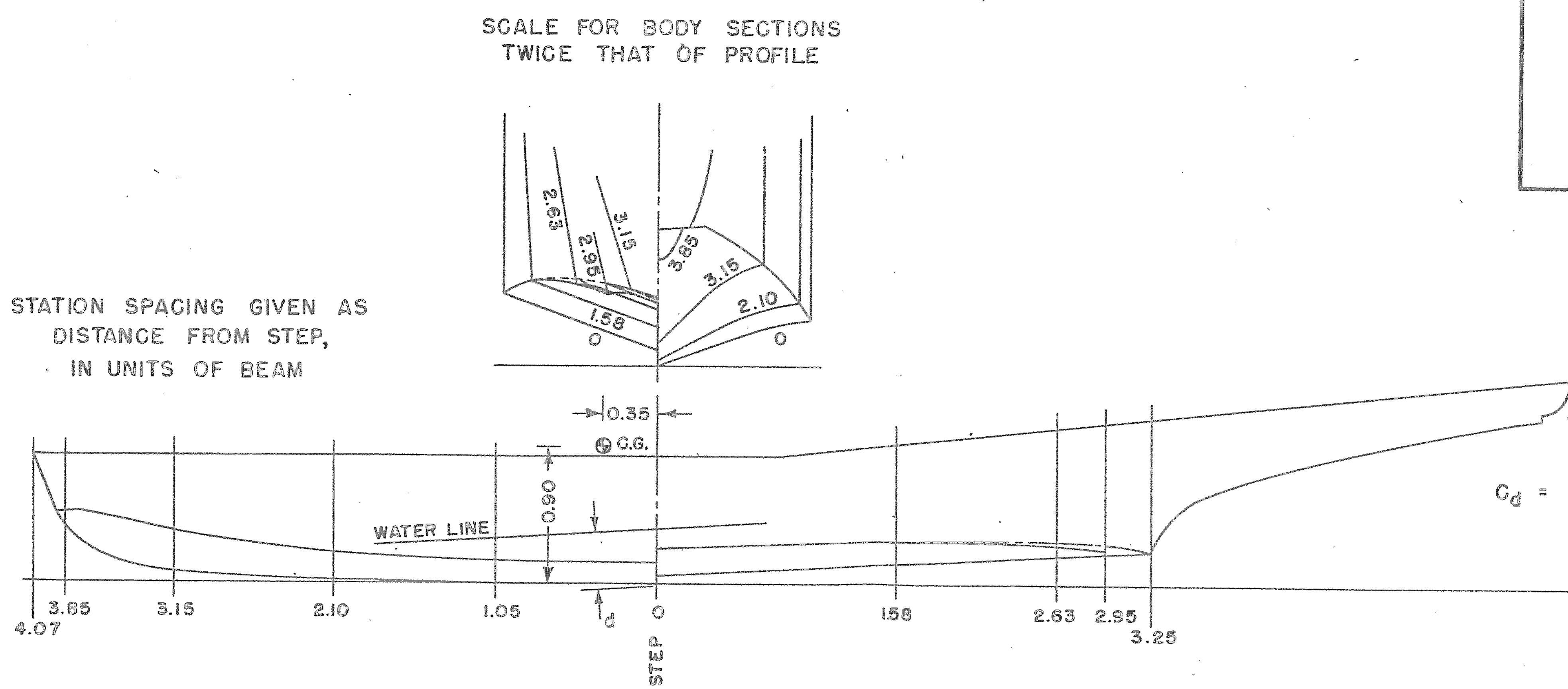

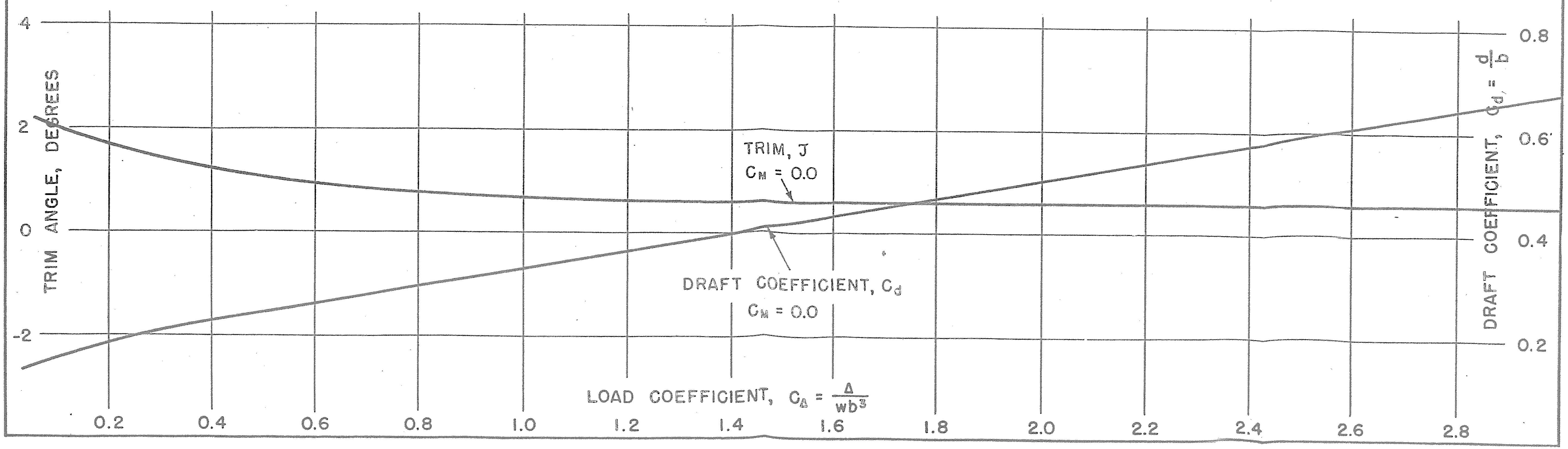

STEVENS MODEL NO.339-23

MODEL DESIGNATION 7.32-7-20

STATIC PROPERTIES
AND
MODEL LINES

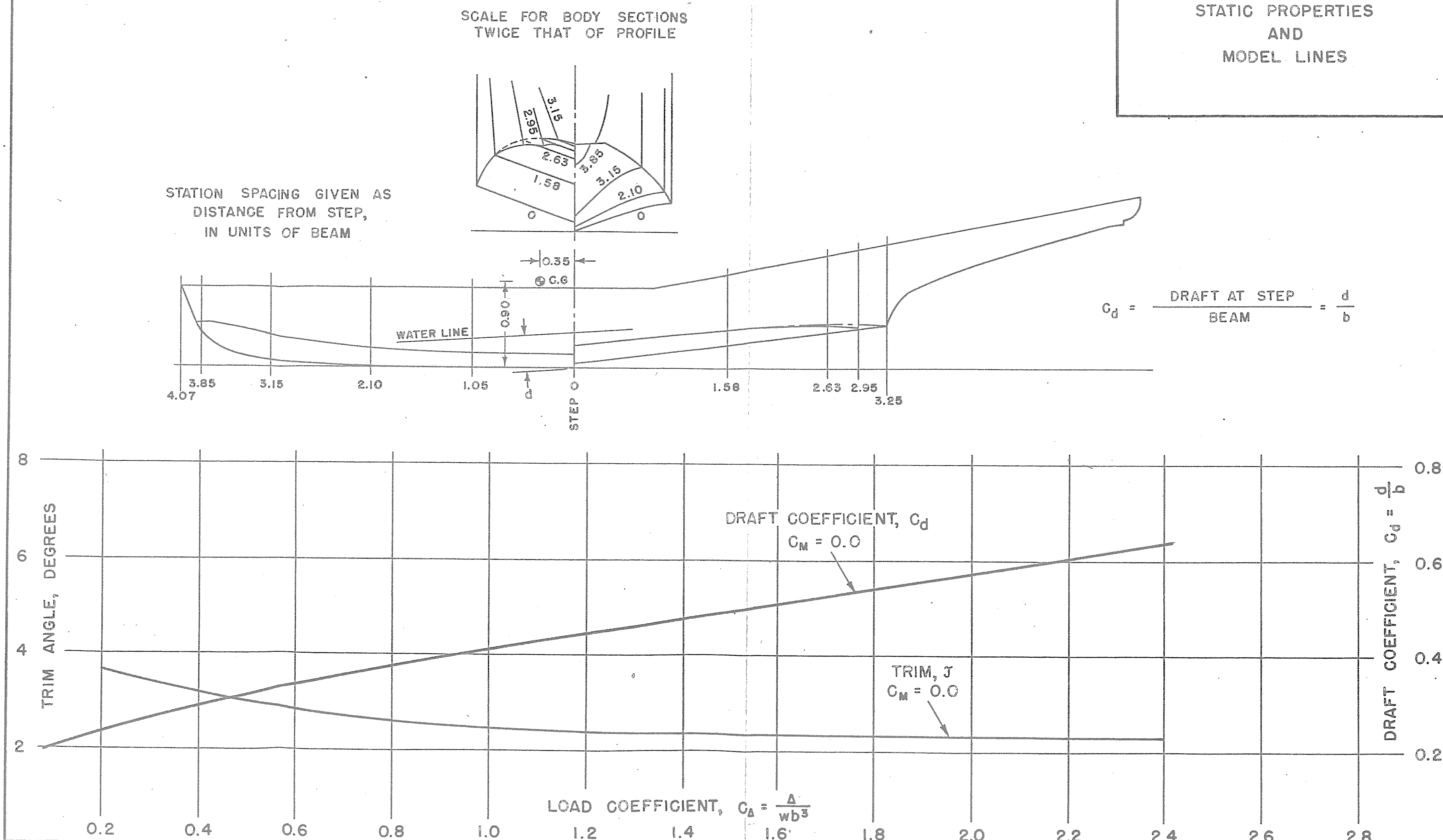

STEVENS MODEL NO. 627

MODEL DESIGNATION 7.32-11-20

STATIC PROPERTIES

AND

MODEL LINES

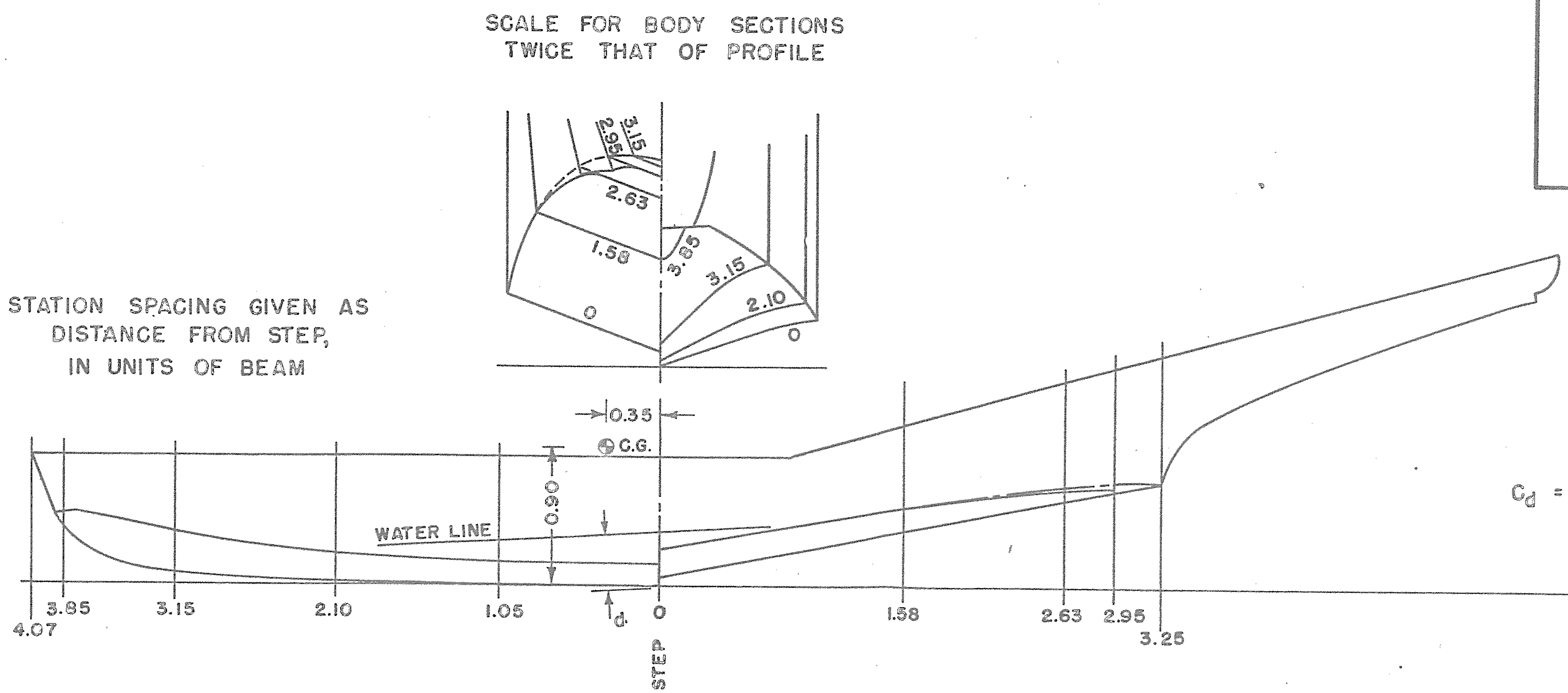

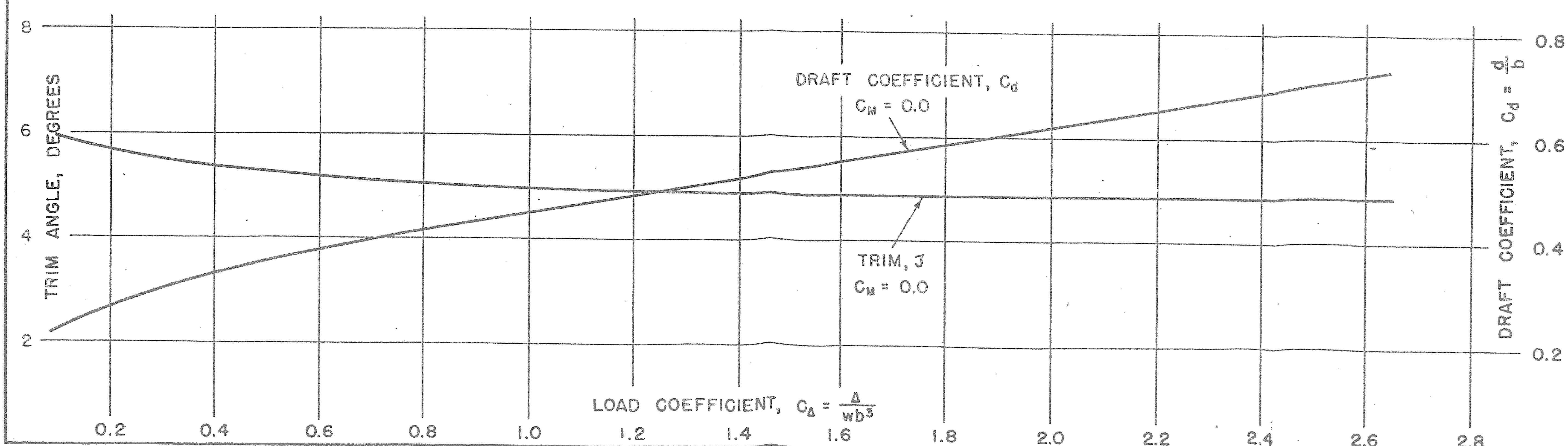

STEVENS MODEL NO. 628

MODEL DESIGNATION: 7.32-5-30

STATIC PROPERTIES

AND

MODEL LINES

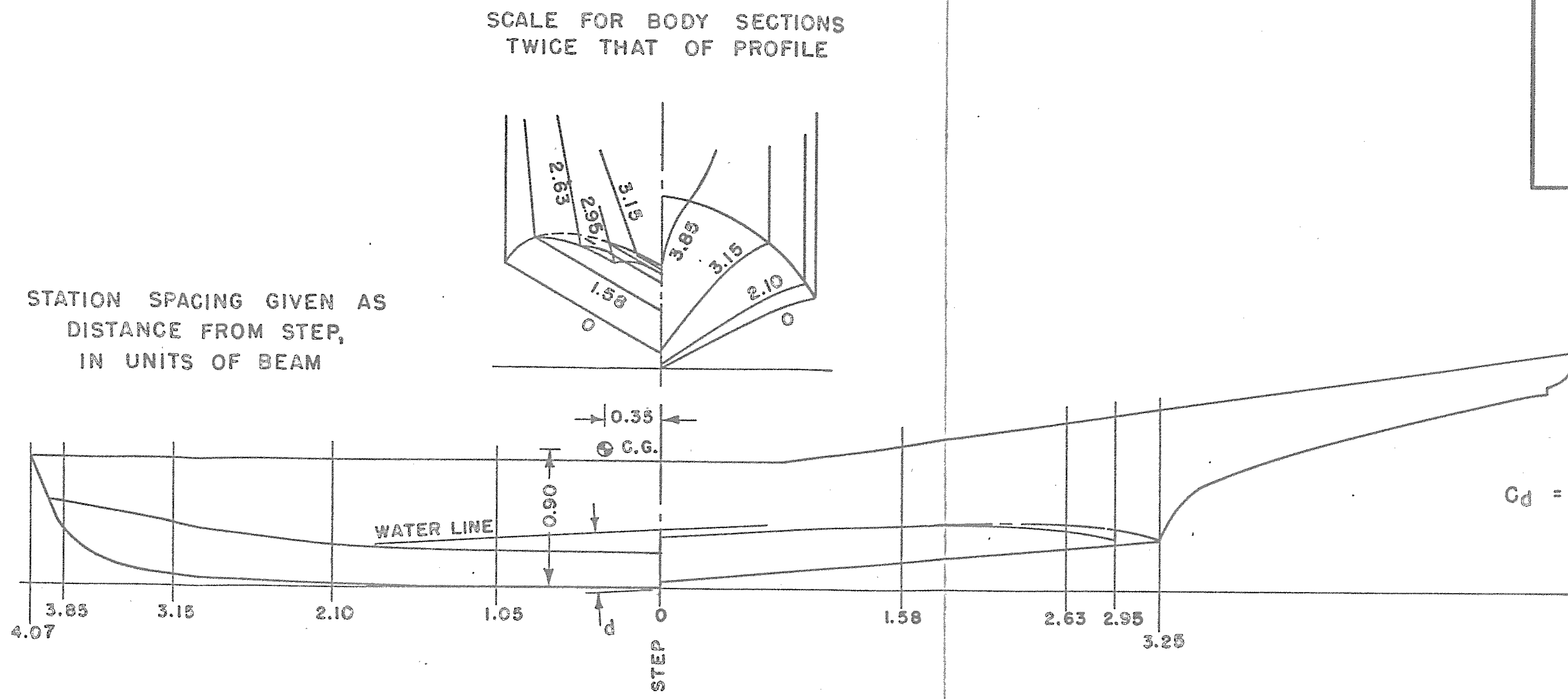

$$C_d = \frac{\text{DRAFT AT STEP}}{\text{BEAM}} = \frac{d}{b}$$

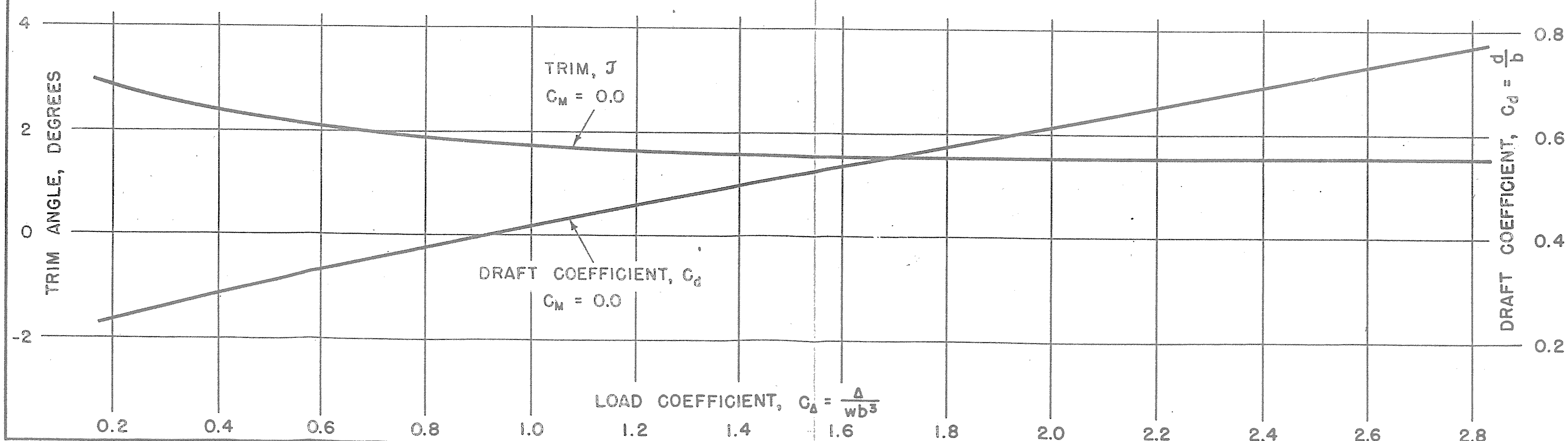

STEVENS MODEL NO. 629

MODEL DESIGNATION: 7.32-9-30

STATIC PROPERTIES
AND
MODEL LINES

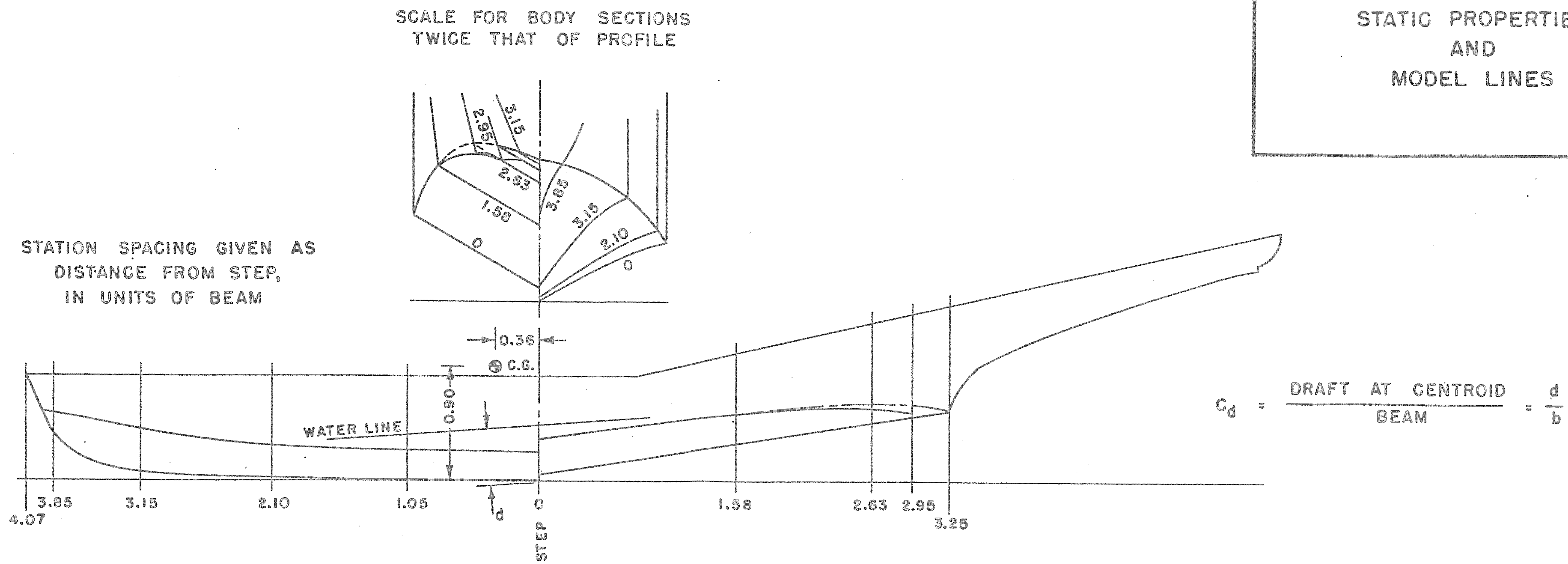

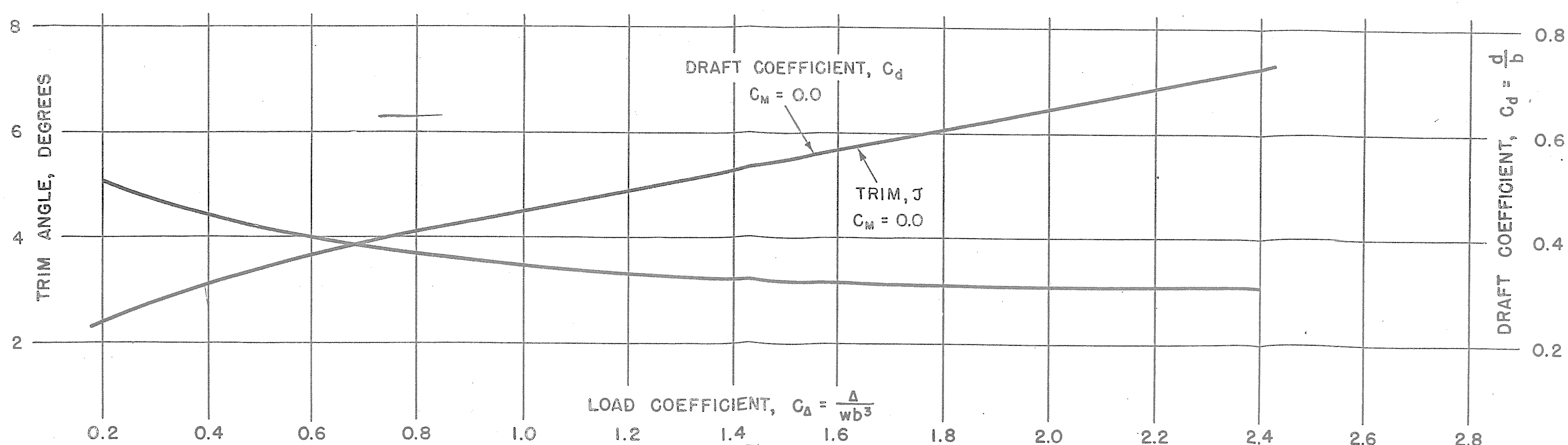

STATIC PROPERTIES CHARTS

FOR LENGTH-BEAM RATIO 8.45 HULLS

Pages 164 through 170

EXPERIMENTAL TOWING TANK
STEVENS INSTITUTE OF TECHNOLOGY
HOBOKEN, NEW JERSEY

R 32
-164

STEVENS MODEL NO. 695
MODEL DESIGNATION 8.45-5-10
STATIC PROPERTIES
AND
MODEL LINES

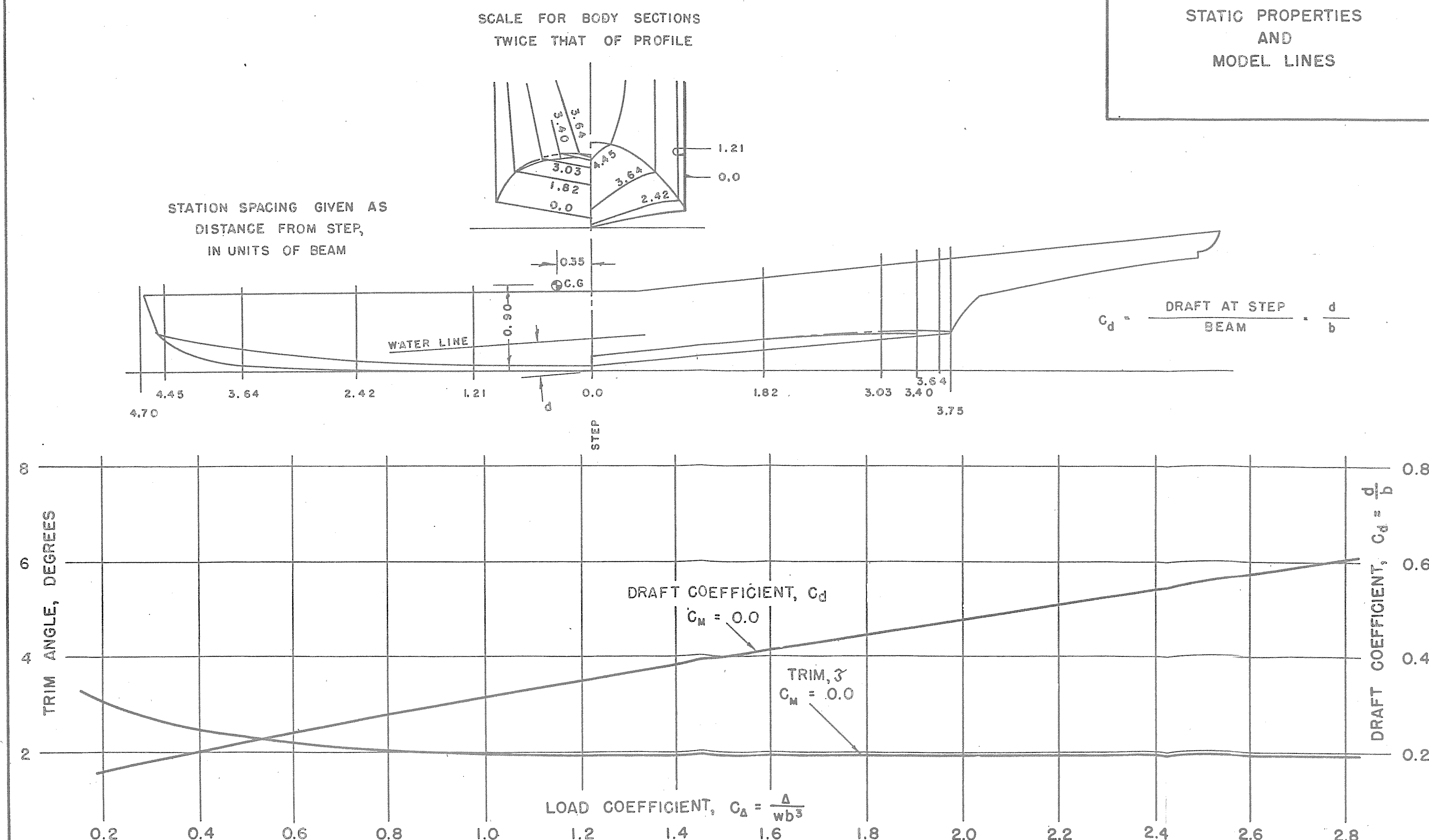

EXPERIMENTAL TOWING TANK
STEVENS INSTITUTE OF TECHNOLOGY
HOBOKEN, NEW JERSEY

R 32
-165

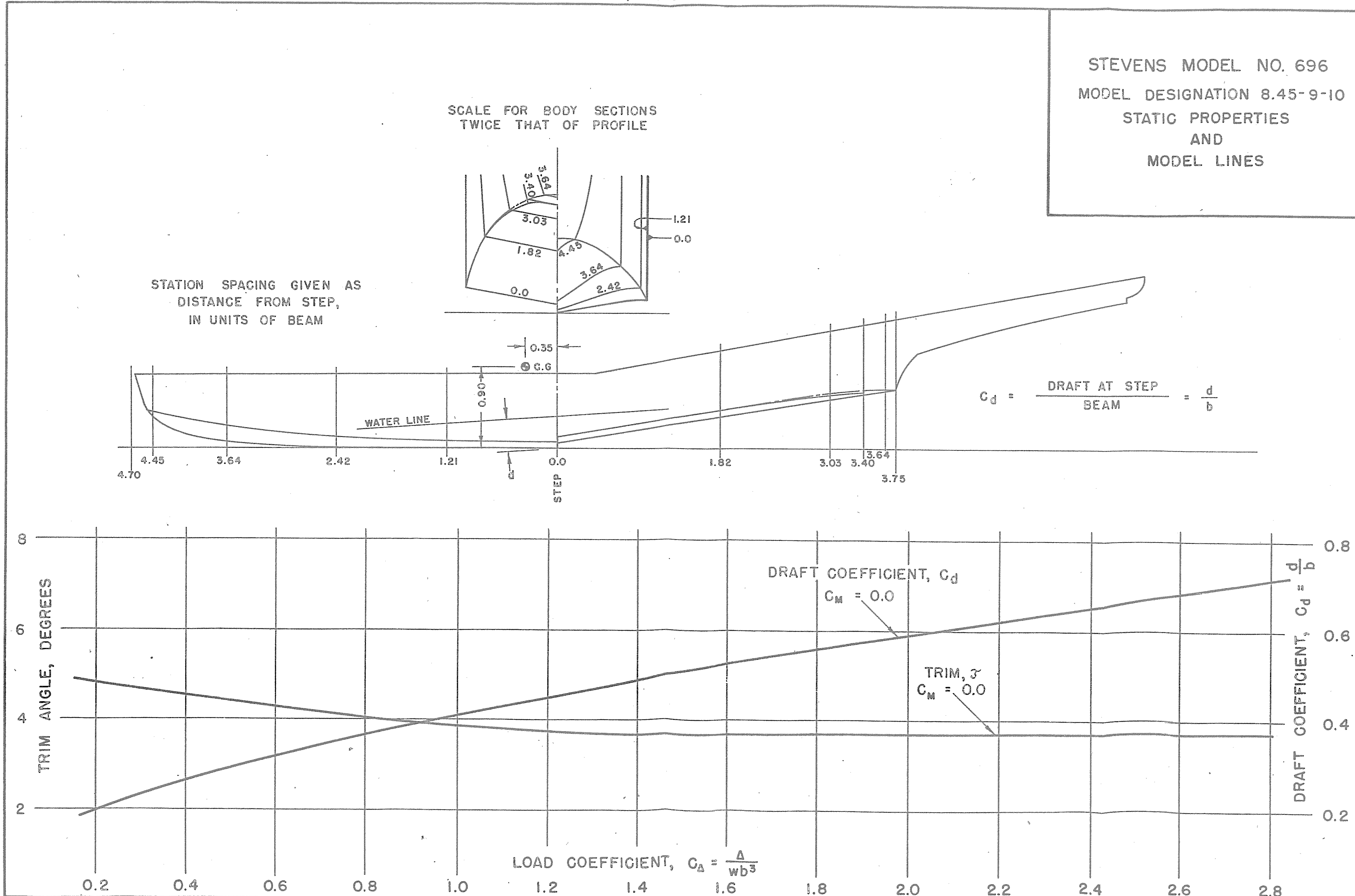

STEVENS MODEL NO. 693

MODEL DESIGNATION 8.45-3-20

STATIC PROPERTIES
AND
MODEL LINES

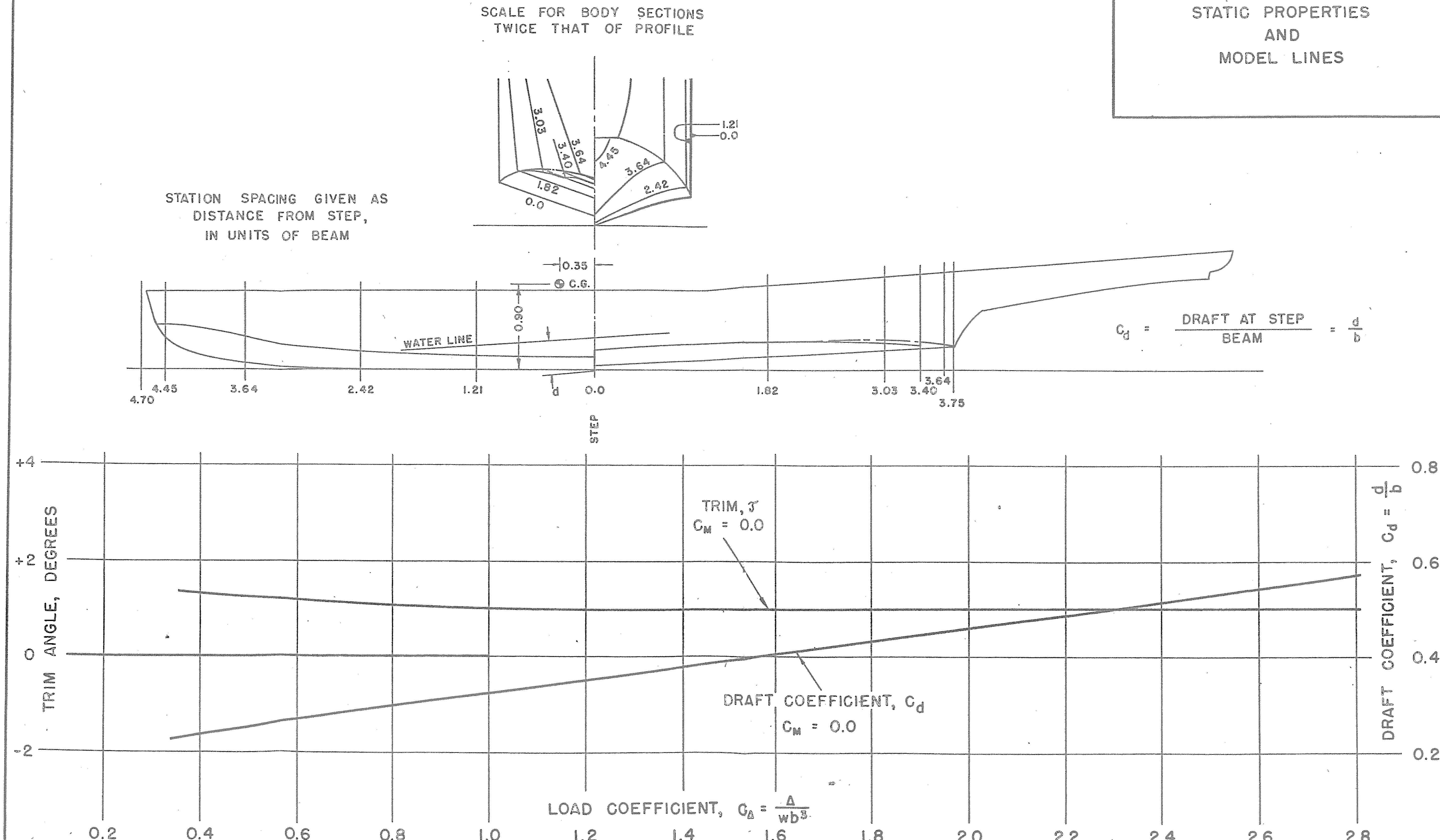

STEVENS MODEL NO. 651
MODEL DESIGNATION 8.45-7-20
STATIC PROPERTIES
AND
MODEL LINES

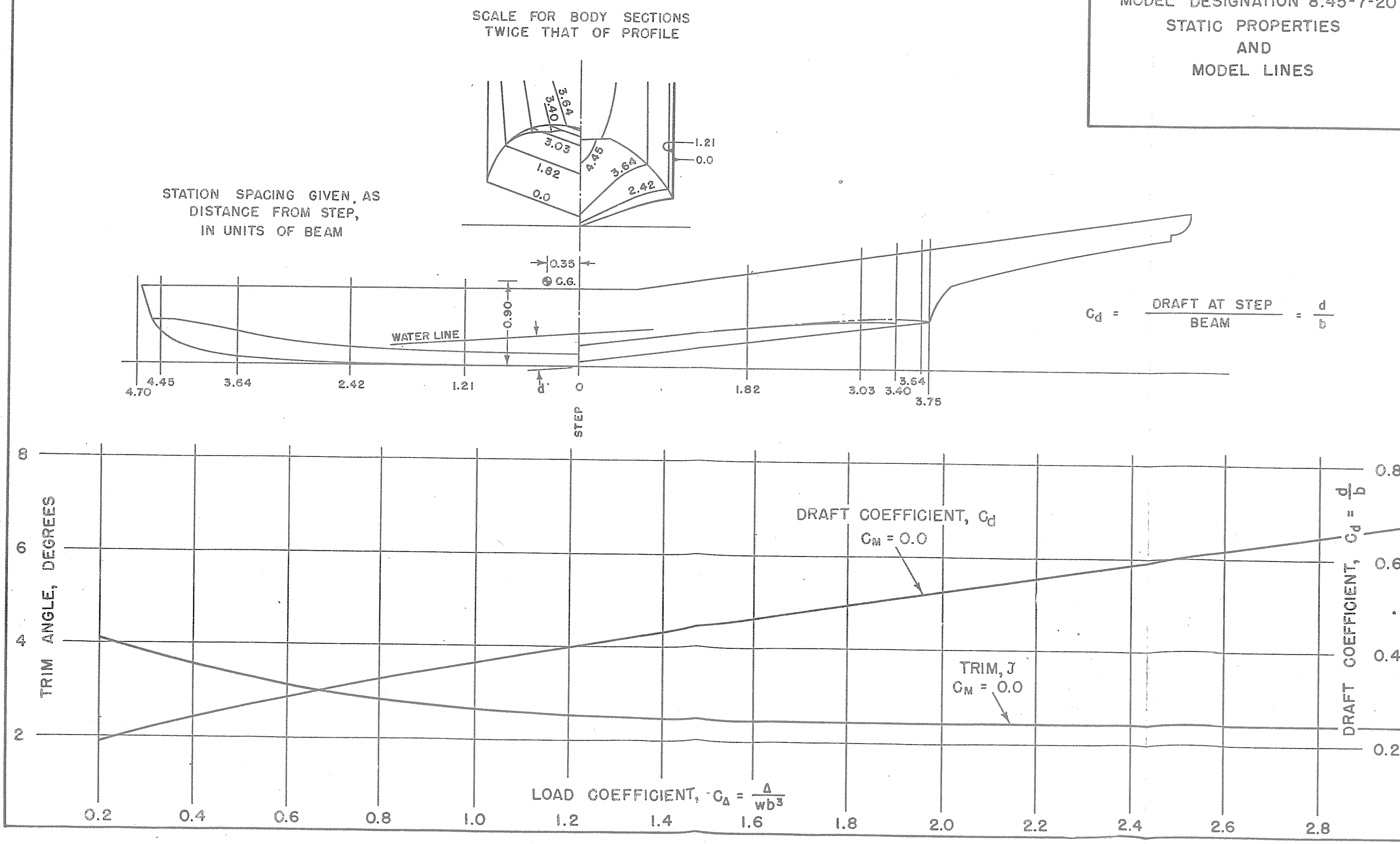

STEVENS MODEL NO. 694

MODEL DESIGNATION 8.45-11-20

STATIC PROPERTIES

AND

MODEL LINES

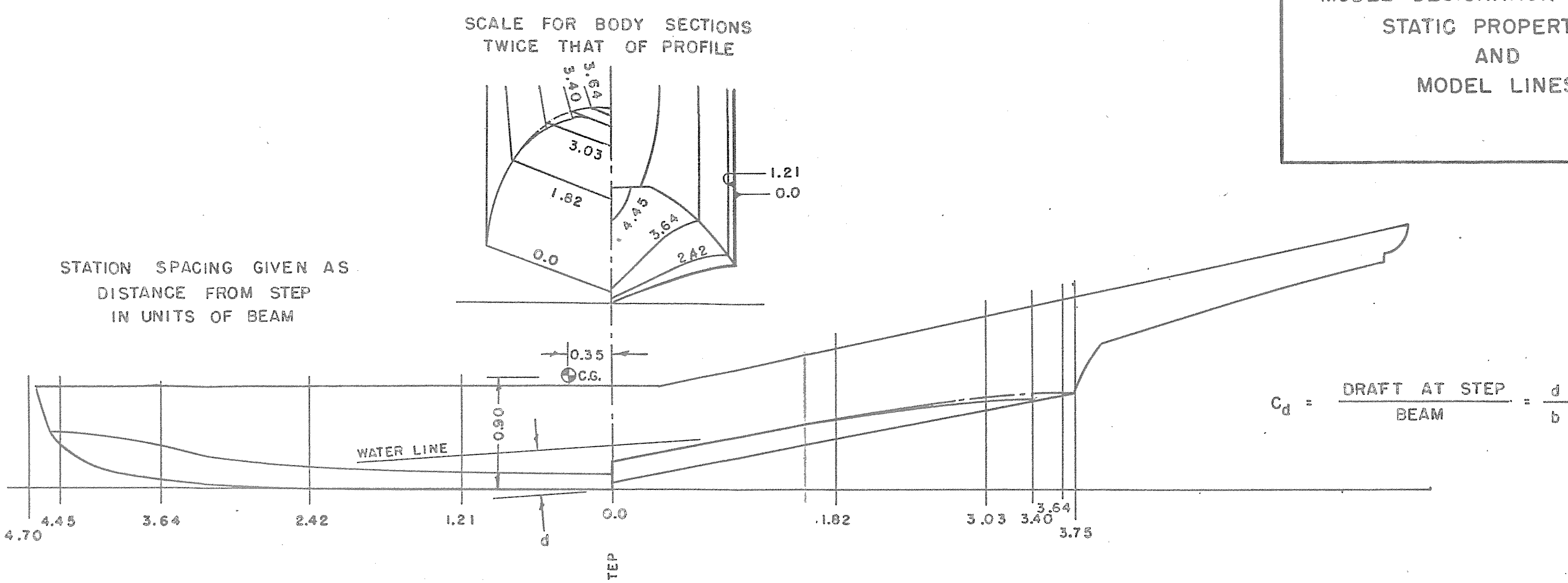

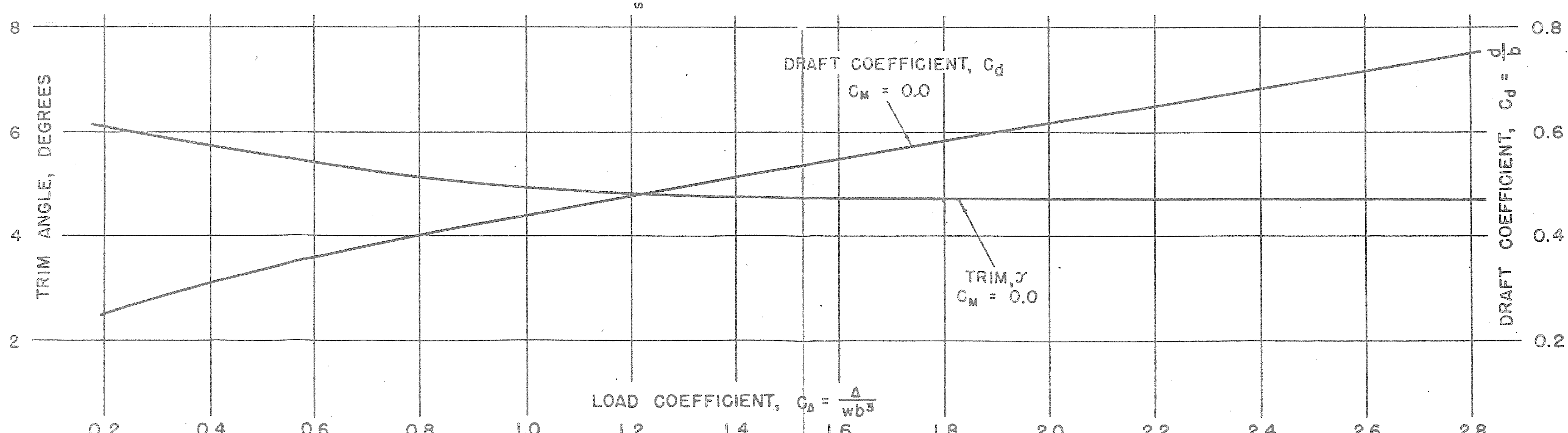

STEVENS MODEL NO. 697

MODEL DESIGNATION 8.45-5-30

STATIC PROPERTIES AND MODEL LINES

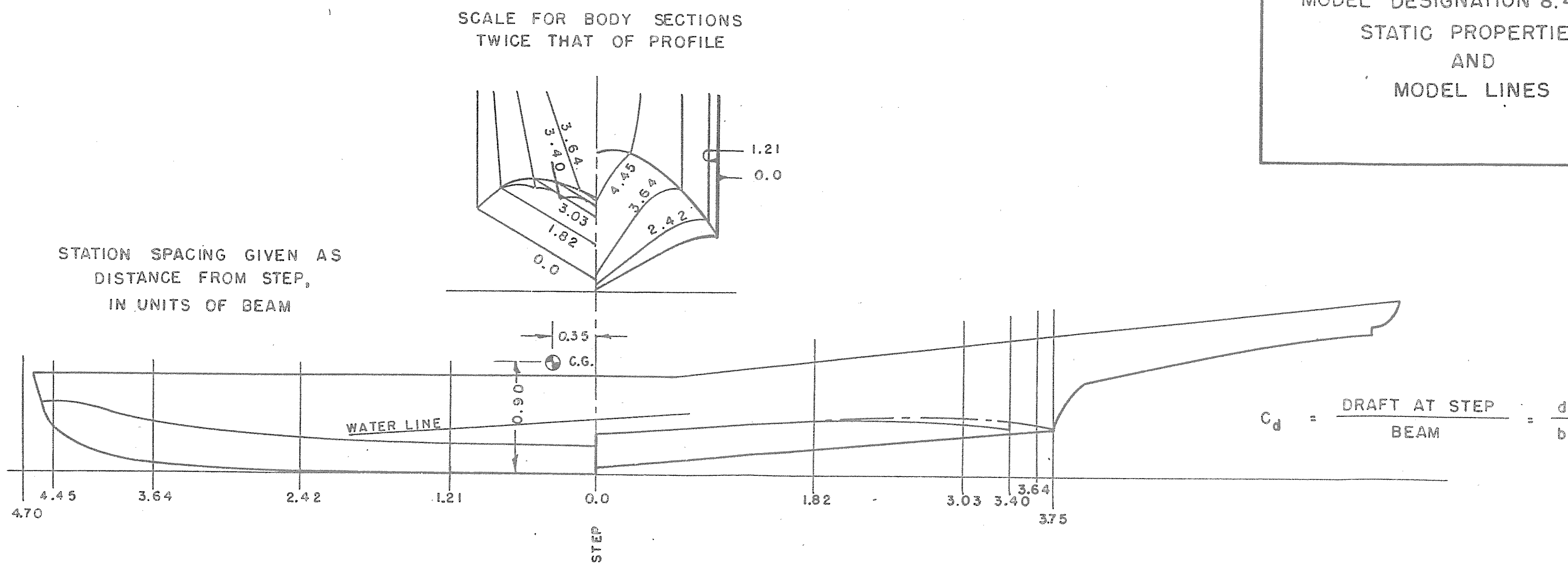

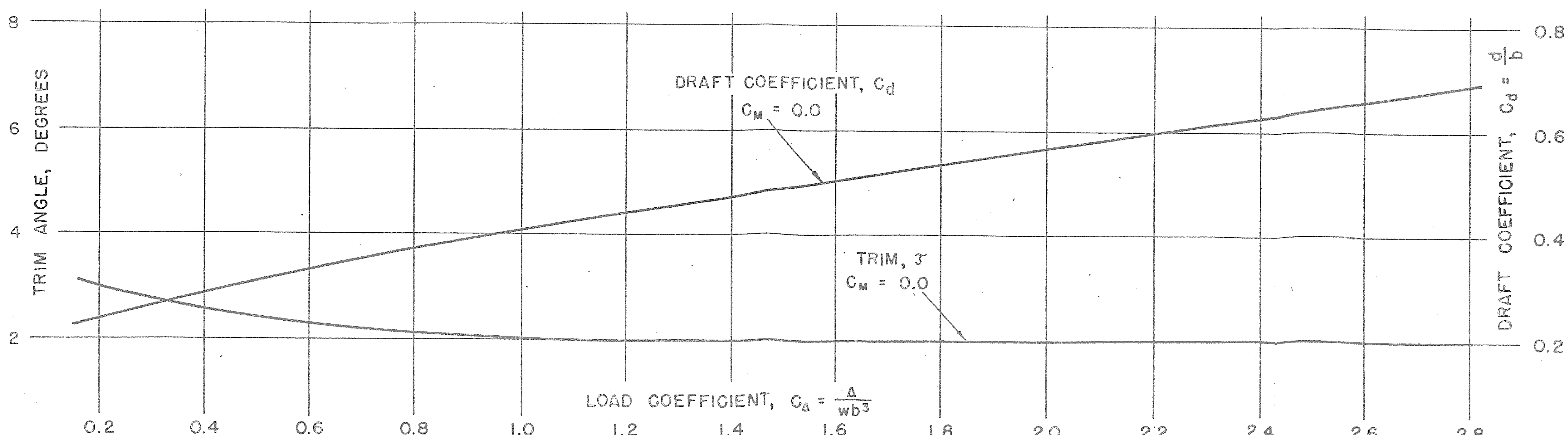

EXPERIMENTAL TOWING TANK
STEVENS INSTITUTE OF TECHNOLOGY
HOBOKEN, NEW JERSEY

R 325
-170-

STEVENS MODEL NO. 698

MODEL DESIGNATION 8.45-9-30

STATIC PROPERTIES
AND
MODEL LINES